BIOSYNTHESIS OF THE ANTIBIOTIC MUPIROCIN BY *PSEUDOMONAS FLUORESCENS* NCIMB 10586

by

RACHEL GURNEY

A thesis submitted to The University of Birmingham for the degree of DOCTOR OF PHILOSOPHY

School of Biosciences
College of Life and Environmental Sciences
The University of Birmingham
September 2012

ABSTRACT

The mupirocin biosynthetic pathway belongs to the *trans*-AT group in which acyltransferase (AT) activity is provided by a separate polypeptide (MmpC) rather than in *cis* as found in the typical type I polyketide synthases. AT docking domains have been documented in *trans*-AT PKS clusters for ten years yet little functional evidence is available. The cluster shows many interesting features that must be understood to create novel products.

Specificity studies demonstrated that AT2 performs the typical AT function of loading malonyl-CoA to ACPs throughout the cluster. Mutagenesis studies demonstrated the importance of AT active site residues for protein structural integrity, acquisition and transfer of malonate and propose an alternate role for AT1 as a proofreading enzyme responsible for hydrolysing truncated intermediates from the pathway. Consequently an edit, reload, reduce model for MmpC is proposed. Mutagenesis of docking domains led to a halt in mupirocin production and suggested that docking domains are required for structural integrity of the Mmps or for guiding the ACPs into the correct position for interactions with their respective partners. Studies involving a mutated ACP3 protein confirmed the importance of Trp^{55}, as demonstrated by structural changes and the inability of the protein to accept malonate from AT2.

ACKNOWLEDGEMENTS

I would like to thank my supervisor, Chris Thomas, for giving me the opportunity to study for my PhD and for his unwavering support, guidance and knowledge over the last four years. Thank you to my co-supervisor, Jo Hothersall, for her advice, patience and friendship. Thank you to the BBSRC for funding my research, to our collaborators at Bristol for their invaluable input and contributions, and to all the behind the scenes technicians and cleaners that make media and keep us in a constant supply of glass wear while at the same time providing cheerful banter.

Thank you to everyone in S101, past and present. In particular Yui, for saving my sanity and becoming a great friend; Yusra for 'very good' and for always paying me back when she borrowed from the bank of Rach; Tony for persistently inviting me for coffee despite the fact I don't like it; Elton, for always being there and for knowing absolutely everything; Claire for being a cheerful presence during my last nine months; Daisuke for showing me the joys of SDS-PAGE; Jenny, for starting what I was able to continue; Harry for his amazing effort and golden touch when it came to lab work.

Thanks to The Geeks for our lunchtime laughs – I really wouldn't have made it without you. We should write that book.

My parents have been a constant support throughout all of my years in education. Thank you - it would not have been possible without you, I hope I've done you proud! Finally I would like to thank my husband Nigel for continually supporting me. I couldn't have done it without you, and I promise to get a job.

TABLE OF CONTENTS

LIST OF FIGURES

LIST OF TABLES

LIST OF ABBREVIATIONS

3D	3 dimensional
3-HP	3-hydroxypropionate
3-O-C10-HSL	*N*-(3-oxodecanoyl) homoserine lactone
6-MSA	6-methylsalicyclic acid
9-HN	9-Hydroxynonanoic acid
A	Adenylation domain
A_{340}/A_{412}	Absorbance
aa	Amino acids
aa-AMP	Aminoacyl-adenylate
ACP	Type I acyl carrier protein
ACV	δ-(1-α-aminoadipyl)-1-cysteinyl-d-valine
AFM	Antifungal metabolite
AH	Acyl hydrolase
Ala/A	Alanine
Amp^R	Ampicillin resistance
Ap	Apical domain
APS	Ammonium persulphate
Arg/R	Arginine
ARMRL	Antimicrobial Resistance Monitoring Reference Laboratory
Asn/N	Asparagine
Asp/D	Aspartic acid
AT	Acyltransferase
ATP	Adenosine triphosphate
BLAST	Basic Local Alignment Search Tool
BSA	Bovine serum albumin
C	Condensation domain
CD	Circular dichroism
CDC	The Centres for Disease Control and Prevention
Chl^R	Chloramphenicol resistance
CHS	Chalcone synthase
CLF	Chain length factor
CoA	Coenzyme A
CR	Crotonase
Cys/C	Cysteine
DAPG	2,4 diacetylphloroglucinol
DD	Docking domain
DEBS	6-deoxyerythronolide B synthase
DH	Dehydratase
DM	Dimerisation module
DMSO	Dimethyl sulfoxide
DNA	Deoxyribonucleic acid
dNTP	Deoxyribonucleotide triphosphate
DRL	Deoxyxylulose-5-phosphate reductisomerase-like
DTNB	5, 5'-dithiobis-(2-nitrobenzoic acid)
DTT	Dithiothreitol
ECDC	The European Centre for Disease Prevention and Control
ECH	Enoyl-CoA hydratase
EDTA	Ethylenediamine-tetra-acetic-acid

Eq	Equatorial domain
ER/OR	Enoyl reductase/Oxidoreductase
Erm	Erythromycin-resistant-methylase
ERR	Edit Reload Reduce
EU	European Union
FAS	Fatty acid synthase
FDA	Food and Drug Administration
$FMNH_2$	Reduced flavin mononucleotide
Gln/Q	Glutamine
Gly/G	Glycine
GNAT	GCN5-related N-acetyltransferase
GSH	Reduced glutathione
GSSH	Oxidised glutathione
GST	Glutathione-S-transferase
HCS	Hydroxymethylglutaryl-CoA synthase
HEPES	4-(2-hydroxyethyl)piperazin-1-ethanesulfonic acid
His/H	Histidine
HPA	Health Protection Agency
HPLC	High performance liquid chromatography
HSL	Homoserine lactone
ID	Interdomain
Ile/I	Isoleucine
IleS	Isoleucyl-tRNA synthase
IleS2	Isoleucyl-tRNA synthase encoded by *mupA*
Int	Intermediate domain
IPTG	Isopropyl-β-D-thiogalactoside
Kan^S	Kanamycin sensitive
KDH	α-ketoglutarate dehydrogenase
KR	Ketoreductase
KS	Ketosynthase
L agar	Luria-Bertani agar
L broth	Luria-Bertani broth
LCMS	Liquid chromatography mass spectroscopy
LD	Linker domain
Leu/L	Leucine
Lys/K	Lysine
m/z	Mass to charge ratio
MA	Monic acid
mAcp	Type II acyl carrier protein
MAT	Malonyl-acetyl transferase
MBP	Maltose binding protein
MCAT	Malonyl-CoA-ACP transferase
MDR TB	Multidrug-resistant TB
MES	2-(N-morphino) ethanesulfonic acid
Met/M	Methionine
Mmp	Mupirocin multifunctional protein
MPT	Malonyl/palmitoyl transferase
MRSA	Methicillin-resistant *Staphylococcus aureus*
MSAS	6-methylsalicylic acid synthase
MT/ME	Methyltransferase

NAD^+	Nicotinamide adenine dinucleotide
NADH	Reduced NAD
NADPH	Reduced nictotinamide adenine dinucleotide phosphate
NCIMB	The National Collection of Industrial, food and Marine Bacteria
NDM-1	New Delhi metallo-beta-lactamase-1
NEB	New England Biolabs
NI	Negative ion
Ni-NTA	Nickel-nitriloacetic acid
NMR	Nuclear Magnetic Resonance
NRPS	Non-ribosomal peptide synthase
OD	Optical density
OPPF	Oxford Protein Production Facility
ORF	Open reading frame
PA	Pseudomonic acid
PBP	Penicillin binding protein
PCA	Phenazine-1-carboxylic acid
PCN	Phenazine-1-carboxamide acid
PCP	Peptidyl carrier protein
PCR	Polymerase chain reaction
PDB	Protein Data Bank
PDHC	Pyruvate dehydrogenase complex
PEG	Polyethylene glycol
PGPR	Plant growth-promoting rhizobacteria
Phe/F	Phenylalanine
PI	Positive ion
PKS	Polyketide synthase
Pro/P	Proline
PSIPRED	Protein Structure Prediction Server
PT	Phosphopantetheinyl transferase
PTFE	Polytetrafluoroethylene
RNA	Ribonucleic acid
SAM	S-adenosyl methionine
SANK	Daiichi Sankyo
SCC*mec*	*Staphylococcal* cassette chromosome *mec*
sdH_2O	Sterile distilled water
SDS	Sodium dodecyl sulphate
SDS-PAGE	SDS polyacrylamide gel electrophoresis
Ser/S	Serine
SIM	Selective ion monitoring
SMA	Styrene maleic acid
SMALP	SMA lipid particle
SNAC	N-acetylcysteamine
SSM	Secondary stage medium
Suc	Sucrose
TATFAR	Trans-Atlantic Task Force on Antimicrobial Resistance
TB	Tuberculosis
TCC	2, 3, 5-triphenyltetrazolium chloride
TCEP	tris(2-carboxyethyl)phosphine
TDR TB	Totally drug-resistant tuberculosis
TE	Thioesterase

TEMED	N, N, N', N'-tetramethylethylene diamine
Temp	Temperature
Tet^R	Tetracycline resistance
Thr/T	Threonine
TIM	Triose phosphate isomerase
T_m	Melting temperature
Tml	Thiomarinol
Tmp	Thiomarinol multifunctional protein
TNB	2-nitro-5-thiobenzoic acid
Tris	Tris(hydroxymethyl)aminomethane
Tri-X	Triton-X
Trp/W	Tryptophan
Tyr/Y	Tyrosine
UV	Ultraviolet
Val/V	Valine
VRE	Vancomycin-resistant *Enterococcus*
VRSA	Vancomycin-resistant *Staphylococcus aureus*
WHO	The World Health Organisation
WT	Wild type
XDR TB	Extensively drug-resistant TB
Ψ	Domains similar too

UNITS AND PREFIXES

A	Amps
Å	Angstrom
bp	Base pairs
Da	Daltons
deg	Degrees
g	Grams
h	Hours
kb	Kilobases
l	Litres
M	Molar
min	Minutes
^oC	Degrees Celsius
rpm	Revolutions per minute
s	Seconds
S	Svedberg
V	Volts
w/v	Weight per final volume

k	Kilo
m	Milli
µ	Micro
n	Nano

ADDENDUM

It should be noted that some material from Sections 1.2 and 1.3 (including subsections) was written as part of a published review on mupirocin by Gurney and Thomas (2011). For the full reference see References page 290.

CHAPTER 1

1 INTRODUCTION

1.1 Antibiotics

Every living organism has evolved methods to promote survival and reproductive fitness. Microbes produce metabolites such as siderophores, surfactants and antibiotics designed to increase the availability of nutrients in the immediate environment and aid their survival (Redfield, 2002; Brown and Balkwill, 2009). Humanity has been aware of antimicrobial properties of certain compounds for millennia; some of these may have been mystic and superstitious, while some compounds have been shown to have healing properties. Ancient Egyptians often utilised honey, lard, tree resin, green copper or mercury in wound healing, while ancient Greeks opted for oil extract of St. John's wort, wine or vinegar, and honey (Forrest, 1982; Lindblad, 2008). Galen documented use of cobwebs, writing ink, clay, dove faeces and aloe vera in his medical texts in approximately 179AD and Paulus Aegineta documented cleansing wounds with pine resin, radish, and honey as well as the more unusual lizard dung and ox blood between 607 and 690AD (Forrest, 1982; Lindblad, 2008). Countries such as India, Nigeria and Japan have also contributed to documentation of the use of plant extracts and compounds towards wound healing. In China during the period 1046 to 1600BC wine was utilised, in 400AD badger oil and honey were popular, and from the late 12th century until early 20th century sesame oil and mercury sulphide were more common (Lindblad, 2008). Honey appears regularly in texts detailing ancient and medieval medical history, and is one of the few compounds to have been investigated and proven to be beneficial in both artificial and animal models of healing (Lindblad, 2008). More recently (1877)

the antagonistic effects of bacteria were demonstrated by Louis Pasteur when he showed that aerobic bacteria had the power to rid anthrax cultures of their virulence (Foster and Raoult, 1974; Van Epps, 2006).

The start of what was to be termed 'the modern era of chemotherapy' came when Paul Ehrlich discovered that trypan red could be used therapeutically for the treatment of African sleeping sickness, and arsphenamine was active against syphilis (Bosch and Rosich, 2008). During the late 1920's-early 1930's a systematic search for antimicrobials from soil yielded an agent that destroyed the polysaccharide capsule of type III pneumococci bacteria, and led to the discovery of gramicidin, the first antibiotic to be tested clinically, by René Dubos (Van Epps, 2006). Howard Florey stated that had René Dubos not undertaken this work, he may never have decided to take up further investigation of penicillin. Although the discovery of penicillin is attributed to Alexander Fleming in 1928, history has documented several occasions where *Penicillium* moulds have been investigated. The name *Penicillium* was put forward in 1809 after the characteristic brush appearance of the sporangia of members belonging to this genus (Foster and Raoult, 1974). In 1874 William Roberts determined bacteria did not grow as well when media was covered with *Penicillium glaucum*, and in 1876 and 1881 John Tyndall determined the bacteriolytic properties of *Penicillium* moulds (Landsberg, 1949; Foster and Raoult, 1974). The serendipitous 're-discovery' of penicillin by Alexander Fleming in 1928 is one of the most documented and well-known stories of antibiotics. The exact circumstances surrounding this discovery are unknown, but it is thought a *Penicillium notatum* spore landed on an exposed *Staphylococcal* petri dish and upon returning from a holiday Fleming noticed the *Penicillium* colony and the clear lysis of some of the

Staphylococcal colonies on the plate (Fleming, 1945). After extensive work by Fleming, Howard Florey and Ernst Chain, penicillin went into clinical development in 1944 by Pfizer (Fleming, 1929; Chain *et al*., 1940; Pfizer, 2002). In the subsequent years a number of clinically important antibiotics were discovered and developed for chemotherapeutic use.

1.1.1 Major targets of antibiotics

Antibiotics can be classified according to four main targets: inhibition of cell wall, protein, folic acid, or nucleic acid synthesis (Figure 1.1) (Walsh, 2003). The bacterial cell wall is comprised of various components, including peptidoglycan (thicker in Gram-positive bacteria), membrane proteins (such as internalins and peptidases), and lipopolysaccharides (Gram-negative bacteria) or teichoic acids (Gram-positive bacteria) (Walsh, 2003). Antibiotics can attack various aspects of cell wall synthesis, for example β-lactams, which are analogues of a peptidoglycan subunit, act as substrates for the penicillin binding proteins (PBPs) thus blocking the transpeptidations that led to a strong peptidoglycan layer (Tomaz, 1979; Josephine *et al*., 2004). Fosfomycin binds to MurA, one of the first proteins involved in peptidoglycan synthesis, preventing catalytic turnover and consequently preventing synthesis of peptidoglycan (Skarzynski *et al*., 1998). Vancomycin is a glycopeptide antibiotic that inhibits cell wall synthesis by binding peptidoglycan subunits (Kahne *et al*., 2005). Daptomycin, a lipopeptide antibiotic, is one of the most recent antibiotics to be available clinically, and acts by inserting into the membrane disrupting integrity; ions escape and the membrane is depolarised, and consequently transport processes can no longer be carried out (Allen *et al*., 1987; Larkin, 2003).

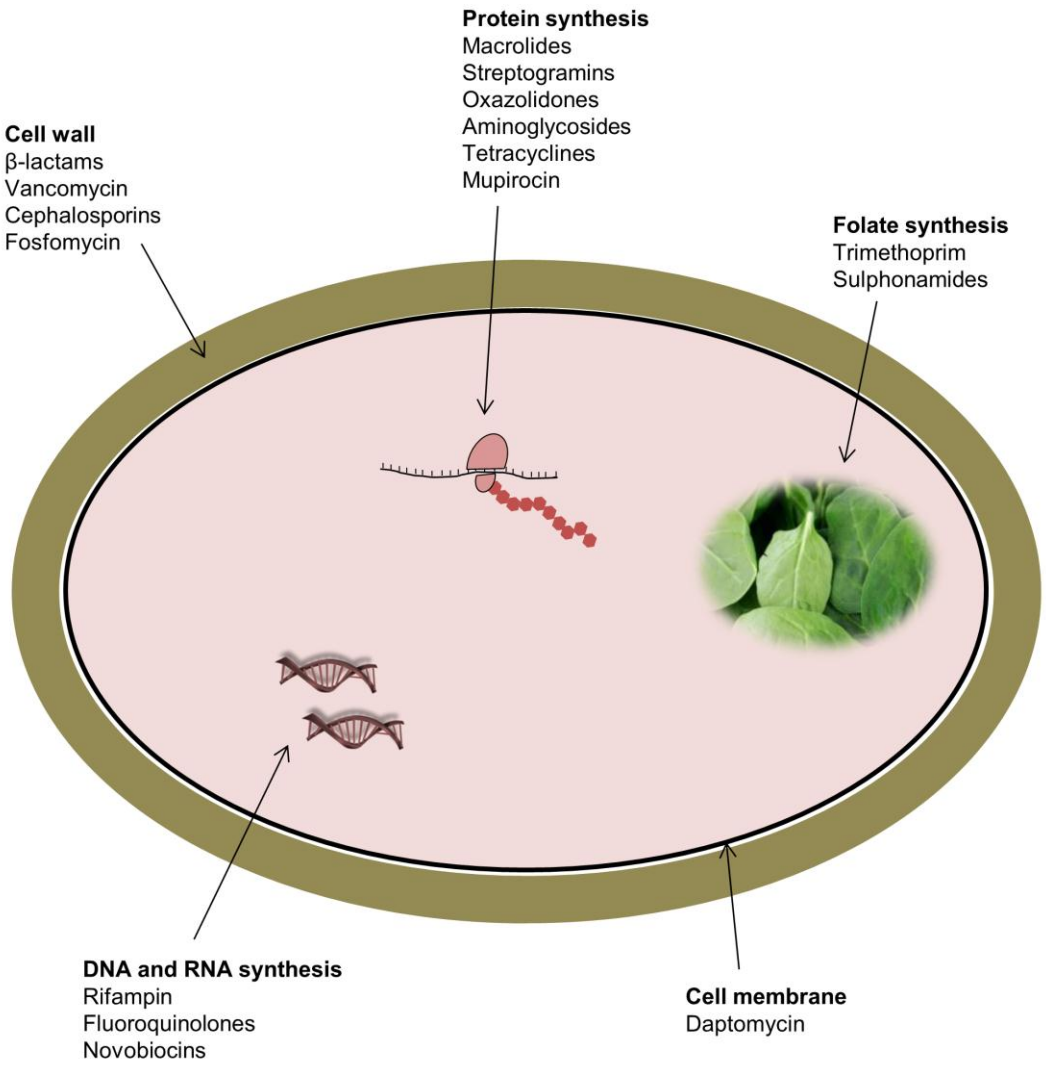

Figure 1.1. Principle targets of antibiotics. (Walsh, 2003b; Wright, 2010).

Antibiotics that inhibit protein synthesis are split into two subgroups: those which inhibit the 50S ribosomal subunit and those which inhibit the 30S ribosomal subunit. Erythromycin, chloramphenicol and pristinamycin all target the 50S subunit affecting the elongation stage of protein synthesis, while in addition erythromycin and pristinamycin also inhibit the translocation stage and availability of free tRNA (Kohanski *et al*., 2010). Aminoglycosides such as gentamycin and streptomycin target the 30S subunit, causing misincorporation of amino acids, resulting in a misfolded protein being incorporated into the cell envelope, while tetracycline inhibits aminoacyl-tRNA binding to the ribosome (Kohanski *et al*., 2010). The quinolones bind to DNA-topoisomerase complexes at the DNA cleavage stage preventing strand rejoining. Double-stranded breaks are introduced into the DNA, thereby blocking DNA replication, affecting cell division and ATP generation (Yoshida *et al*., 1990; Heddle and Maxwell, 2002). The rifamycins are RNA synthesis inhibitors that bind to the β-subunit of an actively transcribing RNA polymerase, and ultimately terminate transcription and as a consequence they also block DNA replication (Kohanski *et al*., 2010). Folic acid metabolism in bacteria occurs *de novo* (as opposed to eukaryotes which can transport necessary folate into cells from nutritional sources), so antibiotics that target part of the pathway for folic acid metabolism ultimately kill the bacteria. The sulfa drugs block different steps in folic acid metabolism, resulting in disruption of nucleic acid synthesis. Sulfamethoxazole blocks dihydropteroate synthase, inhibiting folic acid synthesis, while trimethoprim targets dihydrofolate reductase which inhibits tetrahydrofolic acid synthesis, and ultimately thymidine triphosphate synthesis which is required for DNA replication (Walsh, 2003).

Fatty acid synthesis is emerging as an additional target of antibiotics with several steps in the pathway being targeted: platensimycin targets condensing enzymes such as FabF and FabB; isoniazid has been used as a first line treatment for TB for years, however it is only recently that its target of β-keto-ACP-synthase has been elucidated; triclosan binds to enoyl-ACP reductase FabI thereby inhibiting fatty acid synthesis (Mdluli *et al*., 1998; Heath *et al*., 1999; Wang *et al*., 2006).

1.1.2 Antibiotic resistance

Antibiotic resistance is generally thought of as a modern phenomenon arising as a consequence of the 'golden era of antibiotics' (Hughes and Datta, 1983; Bhullar *et al*., 2012). However, studies have now shown that resistance is likely to be as old as antibiotics themselves, which is logical when considering that bacteria would have been exposed to antibiotics for millions of years. β-lactamases are predicted to have evolved over 2 billion years ago, and the resistance genes to have been located on plasmids for over a million years (Hall and Barlow, 2004). In accordance with this theory a β-lactamase was isolated from a bacterium found in sediment 1050m below the surface of the Pacific Ocean (Toth *et al*., 2010). Thought to have evolved in complete isolation from modern chemotherapy this was the first antibiotic resistance enzyme to be characterised from an organism inhabiting the deep-sea. A study analysing samples taken from 173-185m below land surface in Washington, USA, where the sediment had been sheltered completely from modern life for approximately 3 million years determined that 86% of bacteria isolated were resistant to at least one antibiotic (Brown and Balkwill, 2009). Over 60% of the strains analysed were resistant to more than one antibiotic and one was resistant to eight antibiotics (strain G880). Resistance to nalidixic acid and mupirocin were the most frequently observed (Brown and Balkwill, 2009). The Wright group at McMaster University in Canada have been instrumental in investigating the occurrence of antibiotic resistance in habitats that have been isolated from humanity. Analysis of DNA sequences from permafrost sediments in Alaska thought to have been completely isolated from the surface since the Pleistocene period (2.5 million – 11,700 years ago), identified mammals associated with the period (e.g. mammoth)

and none that were associated with the following period (D'Costa *et al*., 2011). Sequencing of bacterial rRNA established there was no contamination from modern bacteria and uncovered resistances to tetracycline, vancomycin and β-lactamases (D'Costa *et al*., 2011). A second study by the Wright group focussed on a cave in New Mexico that had been isolated from the modern world for over 4 million years - even surface water had not penetrated the sampling sites (Bhullar *et al*., 2012). Over 500 isolates were collected in the cave, 93 of which were carried forward for antibiotic susceptibility testing. Over 60% of the isolates were resistant to 3 or 4 antibiotics, with 3 being resistant to 14 different antibiotics, including the recently approved natural antibiotic daptomycin (Raja *et al*., 2003; Bhullar *et al*., 2012). Collectively these studies have shown that antibiotic resistance pre-dates our modern use of antibiotics, although it is highly likely that increase use of antibiotics and misprescribing is contributing to the increase in resistance we are seeing today (Bush *et al*., 2011).

There are several forms of resistance a bacterium could have towards an antibiotic: a producer must be able to protect itself from the antibiotic it is producing, there are 'physical' resistance mechanisms such as efflux pumps or enzymes that inactivate the antibiotic, and a resistance gene could be acquired by genetic mutation, or by acquisition of a plasmid or genetic material from another bacterium (Figure 1.2). Biofilms can also provide some protection for bacteria from antibiotics, and it has recently been shown that aggregating *Klebsiella pneumoniae* in the bloodstream can survive treatment by antibiotics (Anderl *et al*., 2000; Thornton *et al*., 2012). Autoimmunity of bacteria to the antibiotics they produce is paramount to their survival and it is thought that resistance mechanisms must have evolved with

antibiotic-producers before being transposed to/acquired by other bacteria (Walsh, 2003a).

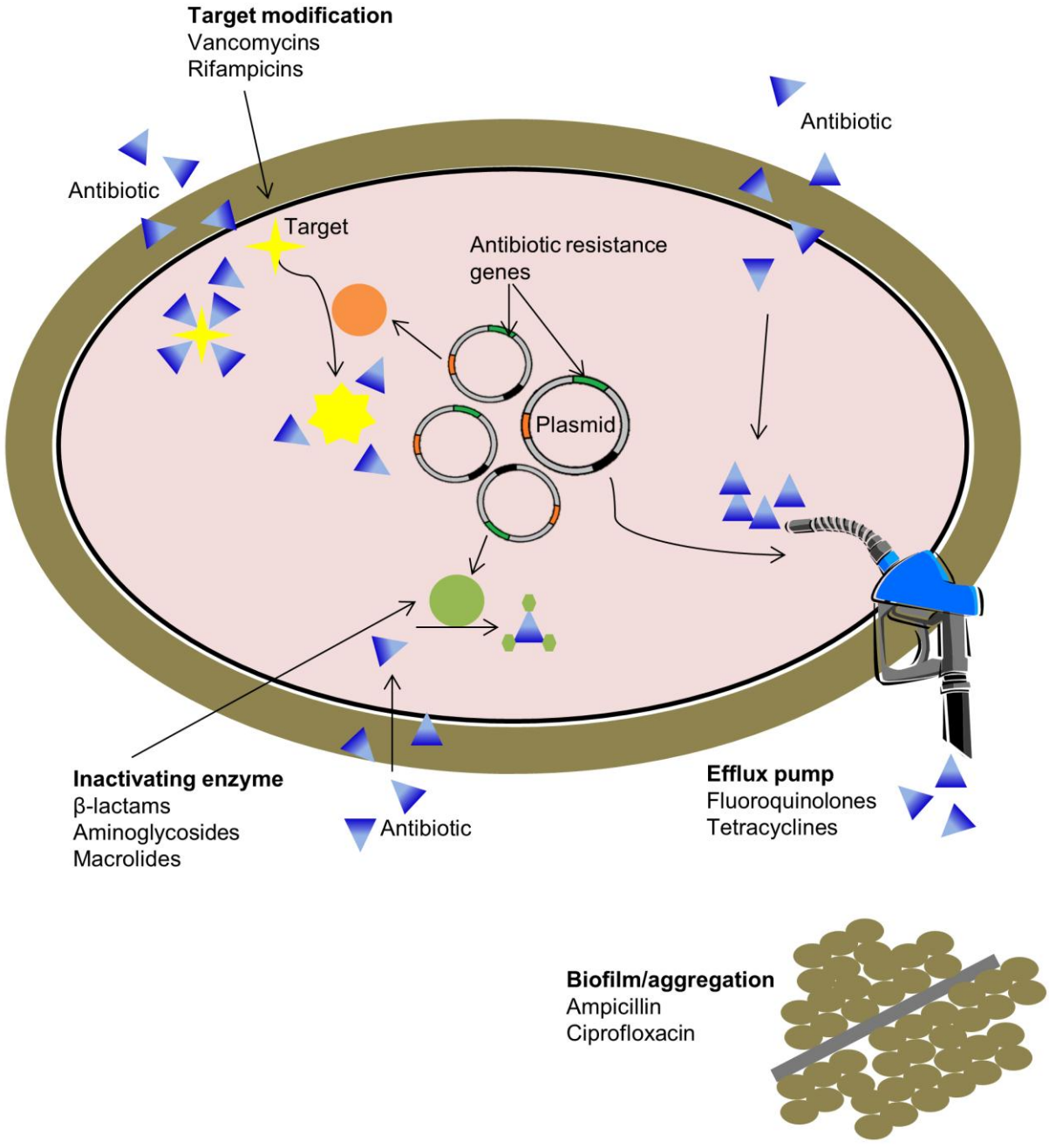

Figure 1.2. Mechanisms of antibiotic resistance. Microbes can evade antibiotics by modifying targets, producing inactivating enzymes that interfere with antibiotic function, producing efflux pumps to remove the antibiotic from the cell before any damage can be done, and by forming biofilms. (Anderl *et al*., 2000; Walsh, 2003a, Wright, 2010).

Autoimmunity in macrolide producers, such as erythromycin, can take several forms: modification by an erythromycin-resistant-methylase (Erm) so the antibiotic cannot bind to the 50S ribosomal subunit and production of transport proteins to efficiently remove erythromycin from the cell (Skinner and Cundliffe, 1982; Skinner *et al*., 1983). Aminocoumarin producers protect themselves by modifying the target of the antibiotic (ATP-binding site of the GyrB subunit of DNA gyrase) by mutation so it cannot bind (Tsai *et al*., 1997). Autoimmunity in vancomycin producers is enforced by three enzymes, VanH, VanA, and VanX, which collectively alter the peptidoglycan precursor, thereby reducing affinity of the antibiotic for peptidoglycan and conferring resistance (Walsh *et al*., 1996).

Bacterial immunity to antibiotics may be innate, as in the case of the opportunistic pathogen *Pseudomonas aeruginosa* which has 71 outer membrane porins and 30 efflux pumps. Alternatively, immunity may be acquired, as in the case of methicillin-resistant *Staphylococcus aureus* (MRSA) and vancomycin-resistant *Staphylococcus aureus* (VRSA), which have several mobile genetic elements and pathogenicity islands that contribute to resistance to several antibiotics (Hiramatsu *et al*., 2001; Walsh, 2003a). The mechanisms of resistance in bacteria towards antibiotics produced by other organisms are often similar to the self-resistance mechanisms described previously: mutation; inactivation or degradation of antibiotics by enzymes; efflux mechanisms; weakened permeability; increased synthesis of an affected metabolite; and acquisition of a modified target (Walsh, 2003a). β-lactamases hydrolyse the β-lactam ring in this class of antibiotics (e.g. penicillin and cephalosporin) thus rendering it ineffective against the target (Thomson and Moland, 2000). β-lactam-resistant *Streptococcus pneumonia* produces five mutated PBPs,

ultimately reducing the PBP affinity for the β-lactam (Nagai *et al*., 2002). Transmembrane proteins can act as pumps, actively exporting foreign substances from the bacterial cell. These efflux pumps can have a narrow or broad range of specificity, but each bacterial cell will have many, as already mentioned with regards to *P. aeruginosa* (Paulsen *et al*., 1996). Bacterial replication occurs rapidly; consequently there is a high chance of mutation which could lead to the development of resistance over a relatively short period of time if an antibiotic is naturally present in the environment (Walsh, 2003a). Alongside the high mutation rate in bacteria, resistance genes are often located on mobile genetic elements such as transposons or plasmids, leading to a very efficient method of transfer between organisms. For example, the VanA resistance genes are located on a transposon within a plasmid in vancomycin-resistant *Enterococcus faecalis* (VRE) (Walsh, 2003a). The genome of *Salmonella enterica* serovar Typhimurium DT104 has evolved to include an antibiotic resistance island containing resistance genes to many clinically important antibiotics – streptomycin, sulphonamides, chloramphenicol, tetracycline and ampicillin (Kim *et al*., 2009).

1.1.3 Implications of antibiotic resistance

Since the discovery of penicillin the development of antibiotics has revolutionised the treatment of infectious diseases. However, even in his original work on penicillin, Fleming noted that some bacteria were completely insensitive to the antibiotic, and further investigation by his colleagues attributed this resistance to an enzyme which was present in several different bacteria (1929; Abraham and Chain, 1940). In his Nobel lecture Fleming warned about the consequences of

resistance to penicillin occurring and suggested prudent use of penicillin to preserve its use (1945). As discussed previously, it is highly likely that some bacteria were resistant to penicillin long before scientists discovered the full potential of this antibiotic, but from a clinical perspective resistance was observed immediately, with occurrence rising steeply after mass-production (Bellamy and Klimek, 1948; Klimek *et al*., 1948; Gould, 1958). Throughout history resistance to antibiotics has been documented anywhere from immediately to tens of years after development, but this can vary greatly. While penicillin resistance was known at the time of development, resistance to erythromycin was not observed until 35 years after initial clinical development (Walsh, 2003a). Between the 1940s and 1970s many clinically important antibiotics were discovered and developed, but in the 21st century less than ten have been approved for clinical use (Figure 1.3) (Patel *et al*., 2001; Larkin, 2003; Higgins *et al*., 2005; Kasbekar, 2006; Colson, 2008; Keam, 2008). In the last two years the U.S. Food and Drug Administration (FDA) has approved only three antibiotics – ceftaroline fosamil in October 2010 for bacterial infections such as MRSA; fidaxomicin in September 2011 for use against *Clostridium difficile*; and levofloxacin in April 2012 for use against *Yersinia pestis* (Morrissey *et al*., 1996; Ikeda *et al*., 2008; Louie *et al*., 2009; FDA, 2012).

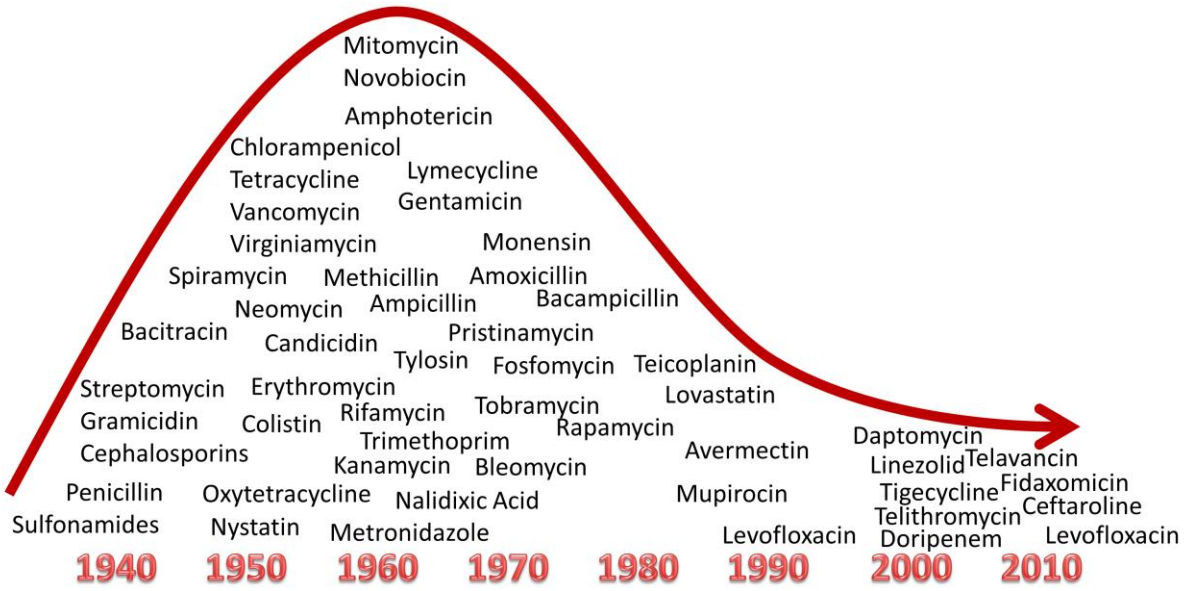

Figure 1.3. Timeline of antibiotic development.

Development of resistance has not ceased during the recent lag of antibiotic development – resistance to new antibiotics is still occurring, yet no new antibiotics are being developed, something which could lead to a very dire situation in the future (Clatworthy *et al*., 2007; Frabbretti *et al*., 2011). With the emergence of so called 'superbugs' like totally drug-resistant tuberculosis (TDR TB), *C. difficile*, *Enterococcus*, New Delhi metallo-beta-lactamase 1 (NDM-1) producing bacteria, MRSA and VRSA, new therapies and antibiotics are vitally important for the future of humanity.

The situation with TB has declined rapidly since the 1990's when multidrug-resistant TB (MDR TB) was first described, to extensively drug-resistant TB (XDR TB) in 2006 and now TDR TB (Migliori *et al*., 2007a; Udwadia, 2012). The first cases of TDR TB were reportedly in 2007 in Italy (Migliori *et al*., 2007b). Fifteen patients in Iran were diagnosed with TDR TB in 2009, and there have been several cases in

India in 2012 that were resistant to all first line and second line TB drugs (Velayati *et al*., 2009; Udwadia *et al*., 2012).

C. difficile is resistant to clindamycin, and newer antibiotics such as levofloxacin and moxifloxacin. It is thought to be hyper-virulent, with spores surviving treatment by detergents and cleaning agents (Taubes, 2008). *C. difficile* is a major problem in terms of hospital-acquired infections, however the rate of mortality rate is reducing each year – so much so that the rate dropped by 31% from 2009 to 2010, and a further 24% from 2010 to 2011 in England and Wales (Kyte, 2011; Pegler, 2012).

Enterococcus species have emerged over the last decade as another threatening nosocomial infection. Often displaying resistances to lipopeptides, aminoglycosides, streptogramins, β-lactams or glycopeptides, the Gram-positive *Enterococcus* can thrive in a situation where antibiotics have targeted Gram-negative organisms (Arias and Murray, 2012). Of particular concern is VRE which can only be treated with daptomycin - however daptomycin resistance is also starting to emerge in these bacteria causing a very worrying situation for the future (Kelesidis *et al*., 2011).

The most recent superbugs to hit the media headlines worldwide are those that carry the NDM-1 gene. First isolated from a strain of *K. pneumonia* originating in New Delhi, this gene conveys the potential to protect its host from all antibiotics known to man, with the exceptions of fluoroquinolones and colistin (Yong *et al*., 2009). This readily transmissible element has also been isolated from *E. coli* and *K. pneumonia* from various locations in the UK (Figure 1.4) (Kumarasamy *et al*., 2010).

Figure 1.4. Distribution of NDM-1 producing Enterobacteriaceae strains in the UK. (Kumarasamy *et al*., 2010).

There may however be some light at the end of the tunnel with researchers investigating new targets and methods to eradicate resistance genes from bacteria, but it is time consuming and costly. Due to the short-course nature of antibiotics and the need to restrict use of new antibiotics to reduce selection of resistant strains, the development of novel antibiotics by pharmaceutical companies is not financially rewarding (GlaxoSmithKline, 2012). Despite this however, private companies and academic research institutes world-wide are working towards developing new drugs and alternative therapies. A study analysing new antibiotic treatments in development

discovered that 66 new active substances were being researched (Freire-Moran *et al*., 2011). Of those 66 new agents, 27 were thought to have a new mechanism of action, and 8 had activity against Gram-negative bacteria (Freire-Moran *et al*., 2011). Researchers are tapping into the vast resources provided by marine organisms - in 2009 over 1000 novel compounds were found to have been isolated from marine organisms (Blunt *et al*., 2011). Another untapped resource is that of uncultured symbiotic organisms – some antimicrobial compounds that have already been characterised are thought to originate from symbiotic organisms (for example, pederin, bacillaene and bryostatin), yet there remains uncharacterised a potential natural product treasure trove (Piel, 2009). Potential new targets for antibiotics are being uncovered, such as the deoxyxylulose-5-phosphate reductisomerase-like (DRL) enzyme involved in isoprenoid biosynthesis in *Brucella abortus*, and the bacterial pyruvate dehydrogenase complex (PDHC) (Birkenstock *et al*., 2012; Perez-Gil *et al*., 2012). Alternative therapies, such as plasmid displacement are being investigated as a method to expel resistance genes located on plasmids from the gut microbiome (Hale *et al*., 2010).

Several taskforces have been put into place on both sides of the Atlantic in an effort to solve the current antibiotic resistance crisis. The World Health Organisation (WHO) has formulated a strategic action plan for antibiotic resistance in Europe; the Department of Health in the UK is supporting research into antibiotic resistance with an injection of funding; the TransAtlantic Task Force on Antimicrobial Resistance (TATFAR) was instigated in 2009 with the aim of encouraging research collaborations between the USA and EU and has launched the 10x20 initiative (10 novel antibacterial drugs by 2020) (Anon, 2012a; Rodier, 2011; Department of

Health, 2012). The Centres for Disease Control and prevention (CDC) and European Centre for Disease prevention and Control (ECDC) both have action plans and surveillance systems in place for monitoring and coping with antibiotic resistance (CDC, 2011; ECDC, 2012). In the UK, specifically, there is the Health Protection Agency (HPA) and its Antimicrobial Resistance Monitoring Reference Laboratory (ARMRL) monitoring resistance and performing susceptibility tests, and the Antibiotic-Action movement highlighting the issues relating to resistance (Antibiotic-Action, 2011; Health Protection Agency, 2012). These initiatives have led to the preparation of policies and guidelines for healthcare providers, clinicians, researchers, agriculturalists, governments and countries, as summarised below:

- Public education
- Improved public health and sanitation
- Control of antibiotic use/correct prescribing
- Ban on antibiotics as agricultural growth promoters in Europe, fading out in the USA
- Surveillance to track use and resistance to antibiotics
- Enforcing regulation
- Development of new antibiotics
- Development of alternative therapies
- Encouragement of transatlantic collaborative chemotherapy research (Reynolds, 2009; Enne, 2010; Bush *et al*., 2011; Laxminarayan and Powers, 2011; Anon 2012b; Alcorn, 2012).

With the worldwide media putting the spotlight on antibiotic resistance, consequently ensuring everyone understands the impact; researchers can focus on finding novel and alternative therapies.

1.1.4 Methicillin-resistant *Staphylococcus aureus*

The discovery of penicillin caused an explosion of investigation for other such substances. In 1960 researchers at the Beecham Research Laboratories developed a new penicillin antibiotic, methicillin (celbenin) that was effective against 22 strains of penicillin-resistant *S. pyogenes* (Rolinson *et al.,* 1960). Just a few months later methicillin resistance was reported in the British Medical Journal (Jevons, 1961). Resistance has escalated and MRSA has become a world-wide problem, particularly within hospitals, but community acquired MRSA infections are becoming increasingly more frequent (Jevons *et al*., 1963; Kriebs, 2008). The map in Figure 1.5 (A) shows the severity of the MRSA problem across Europe, with many countries having recorded incidences of 10-50% of *S. aureus* isolates being resistant to methicillin. As shown in Figure 1.5 (B) the proportion of MRSA isolates in the UK has been gradually reducing from 2006. It is interesting to note that Scandinavia, The Netherlands and Estonia have a percentage resistance of less than five per cent. This success has been mainly attributed to a 'search and destroy' policy and restrictive prescribing of antibiotics (Cars *et al*., 2001; Wertheim *et al*., 2004; van Rijen *et al*., 2008). The 'search and destroy' policy includes strict guidelines to screen patients being admitted to hospital for treatment as well as hospital staff, and isolation of MRSA positive individuals until tests prove negative or until discharge from hospital (van Trijp *et al*., 2007). When this policy was trialled at a hospital in

Ireland between 2007 and 2008, it was found that single-bed isolation was the most effective method of quashing nosocomial MRSA (Higgins *et al*., 2010). It may be that more countries can learn from the 'search and destroy' policy implemented in Northern Europe.

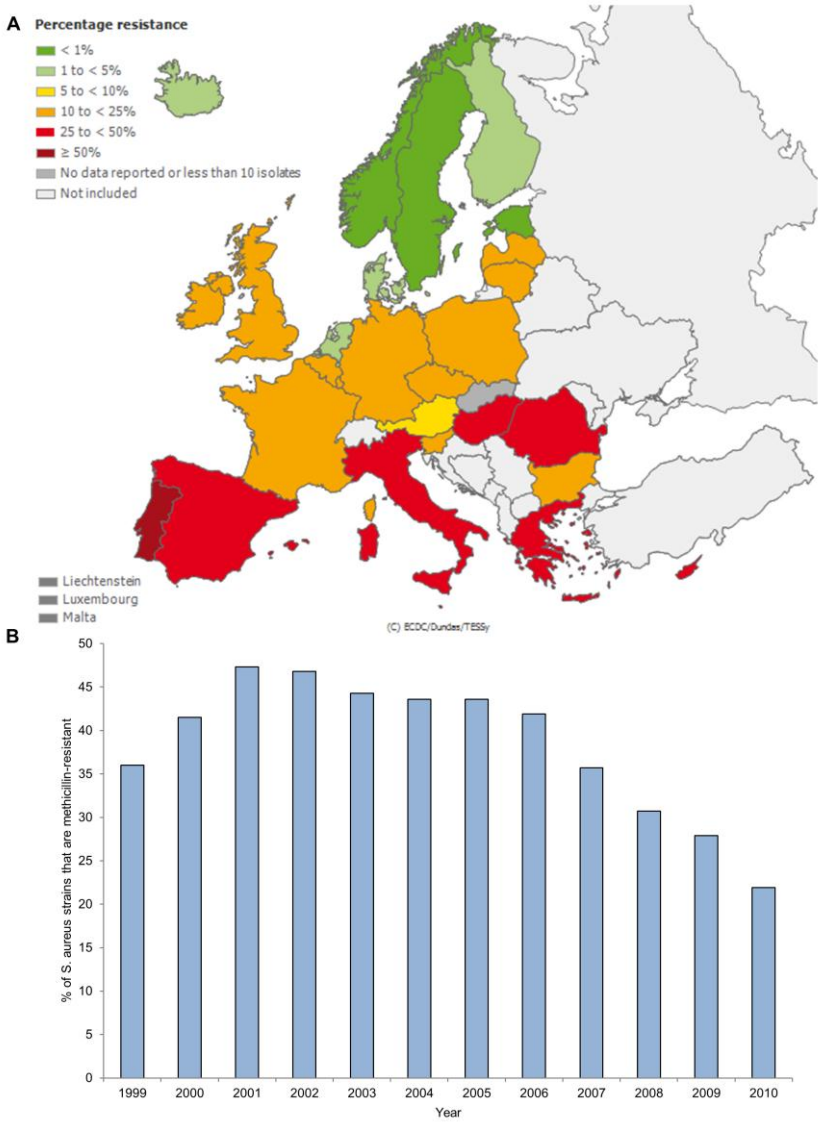

Figure 1.5. MRSA spread in Europe and the UK. (A) Proportion of MRSA isolates in participating countries in 2009. Report generated by data submitted to The European Surveillance System up to 24-08-2012. **(B)** Proportion of *S. aureus* isolates that are methicillin-resistant in the UK from 1999-2010. (European Centre for Disease Prevention and Control, 2012).

The antibiotic resistance capabilities of MRSA are integrated within a large antibiotic resistance island known as the *Staphylococcal* cassette chromosome *mec* (SCC*mec*), which incorporates *mecA* – the methicillin-resistance gene (Ito *et al*., 1999; Katayama *et al*., 2000). There are 5 different forms of SCC*mec* within MRSA species and up to 17 variants of these types. All SCC*mec* types give resistance to β-lactams, while types II and III also provide multi-resistance on integrated plasmids and a transposon - including kanamycin, tobramycin, bleomycin, penicillins, heavy metals, tetracycline, macrolides, lincosamide and streptogramin (Deurenberg *et al*., 2007). While types I-III are mainly associated with nosocomial MRSA infections, types IV and V are associated with community-acquired MRSA (Deurenberg *et al*., 2007). Within the SCC*mec* island there are two recombinase genes, *ccrA* and *ccrB*, that are involved in integrating SCC*mec* into and excision of SCC*mec* from the *S. aureus* chromosome, and as a consequence have been involved in the evolution of MRSA (Katayama *et al*., 2000). One of the key antibiotics in treating and overcoming MRSA has been mupirocin, a polyketide antibiotic first introduced in the UK in 1985 (Cookson, 1990).

1.2 Polyketides

Polyketides are secondary metabolites produced by bacteria, fungi and some plants that display a wide range of biological activities that are increasingly exploited as therapeutic tools. For example: antibiotics (erythromycin and mupirocin), anti-cancer agents (daunomycin) and immunosuppressants (rapamycin) (McDaniel *et al*., 1993). Type I and II polyketide synthases (PKSs) are closely related to fatty acid synthases (FASs) (Figure 1.6) and are classified according to their protein architecture: when clustered as a large multifunctional polypeptide they are denoted as type I, when mono-functional proteins form multi-enzyme complexes they are classed as type II (Walsh, 2003a; Ridley *et al*., 2008). Type III PKSs are quite different from FASs and can be found in plants and some bacteria. There is great interest in the diversity of PKS systems since they provide a growing source of genetic building blocks for synthetic biology which aims to generate novel biologically active molecules.

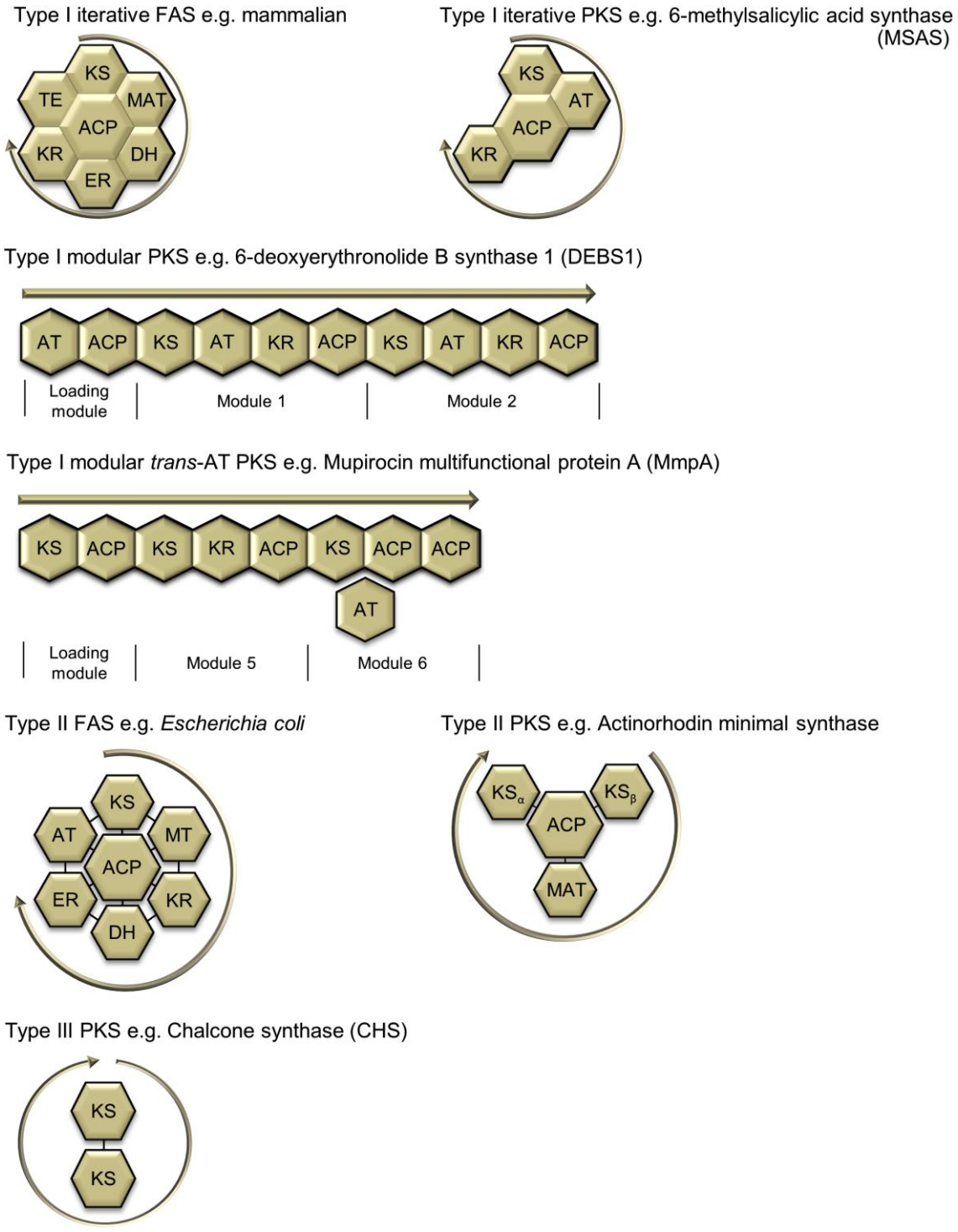

Figure 1.6. The similarity of domain arrangement between FASs and PKSs.
Different enzymatic functions are indicated by labelled hexagons: MAT, malonyl-acetyl transferase; DH, dehydratase; KR, ketoreductase; ER, enoyl reductase; ACP, acyl carrier protein; TE, thioesterase. Where hexagon sides touch they are part of the same polypeptide, where there is a gap and hexagons are connected by a short line they represent different polypeptides that are part of a multi-protein complex. (Richardson *et al*., 1999; Austin and Noel, 2003; Mercer and Burkart, 2007).

1.2.1 Fatty acid biosynthesis

In all organisms fatty acid biosynthesis is carried out by fatty acid synthases (FAS). The large multifunctional mammalian FAS is denoted as type I – a single protein carries all of the enzymatic domains required. In plants, protozoa and bacteria the type II FAS is characterised as a multi-enzyme complex comprised of mono-functional proteins, each of which is responsible for one step within the pathway (Schujman and de Mendoza, 2008). Although the enzyme structure differs between mammals and bacteria, the process of fatty acid biosynthesis is the same. Malonyl- and acetyl-CoA are loaded to an acyl carrier protein (ACP), prior to a four-step process (condensation, reduction, dehydration and reduction) to develop a saturated acyl group that becomes the substrate for the subsequent repeated cycles. Each cycle extends the fatty acid chain by two carbons – contributed by malonate.

For bacteria *E. coli* has become a model organism, providing valuable information about the processes that take place during fatty acid synthesis (Magnuson *et al*., 1993). The FAS II of *E. coli* is comprised of seven core polypeptides (encoded by the *fab* genes) that work together to catalyse fatty acid synthesis (Maier *et al*., 2008). This process starts with acetyl-CoA (starter) and malonyl-CoA (extender) which are both activated by acyltransferases (AT). The starter and the extender units are then condensed by the ketosynthase (KS) to form acetoacetyl-ACP (the acetoacetyl group is bound to the phosphopantetheine arm of the ACP), which then undergoes reduction via ketoreductase (KR) to form D-β-hydroxybutyryl-ACP. Next a dehydratase (DH) removes water with the formation of a double bond, before an enoyl reductase (ER) reduces the double bond to form butyryl-ACP (Nelson and Cox, 2005). This cycle is then repeated to elongate the

chain before release of the complete intermediate by a thioesterase (TE). The main difference between PKS and FAS systems is that FASs invariably catalyse reductive cycles on the condensation products, whereas PKSs occasionally omit the reductive stage after the condensation leading to a greater variety of products (McDaniel *et al*., 1993; Crosby *et al*., 1995).

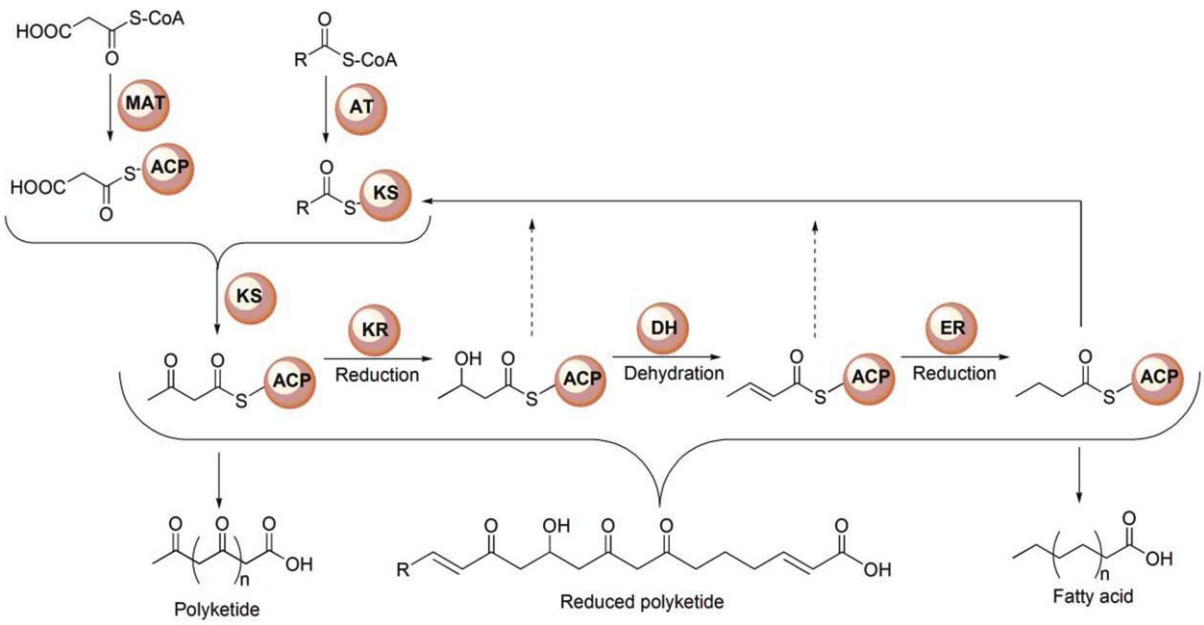

Figure 1.7. Scheme depicting the chemical steps involved in fatty acid and polyketide synthesis. The β-ketoacyl moiety produced in fatty acid synthesis is always fully reduced, whereas in polyketide synthesis it can either be partially or fully reduced. (MAT, malonyl-CoA-ACP transferase; AT, acyltransferase; ACP, acyl carrier protein; KS, ketosynthase; KR, Ketoreductase; DH, Dehydratase; ER, enoyl reductase (Smith and Tsai, 2007).

1.2.2 Type I polyketides

Type I PKSs consist of large multifunctional enzymes with domains joined covalently (Figure 1.6) (Cane, 2010; Hill and Staunton, 2010). Iterative fungal type-I PKSs use the functional domains repeatedly; for example 6-methylsalicylic acid synthase (MSAS) during the production of methylsalicylic acid, a precursor to the antibiotic patulin (Richardson *et al*., 1999; Moore and Hopke, 2001). Modular bacterial type-I PKSs use each set of catalytic sites once within a cycle, such as in the case of 6-deoxyerythronolide B synthase (DEBS) during the production of erythromycin (Moore and Hopke, 2001; Chopra *et al*., 2008). There are exceptions to the co-linearity ruling, such as the slipping and stuttering of modules. Module skipping has been observed during polyketide engineering and occurs naturally in some clusters, such as the pikromycin PKS where module 6 is not necessarily required, and the Stigmatellin PKS where module 4 is likely skipped (Xue and Sherman, 2000; Rowe *et al*., 2001; Thomas *et al*., 2002; Moss *et al*., 2004; Wenzel *et al*., 2005). Aberrant stuttering occurs when modules operate in an iterative matter, as in the case of the aureothin and borrelidin PKSs and engineered DEBS derivatives (Wilkinson *et al*., 2000; Moss *et al*., 2004; He and Hertweck, 2005).

1.2.2.1 Erythromycin biosynthesis pathway

Erythromycin is a polyketide antibiotic that blocks protein synthesis by acting on the ribosome – the binding of erythromycin releases peptidyl-tRNA prematurely, thereby blocking polypeptide translation; it also binds to the polypeptide export tunnel of the 50S ribosomal subunit, causing a build-up of oligopeptidyl-tRNA which concurrently terminates polypeptide elongation (Walsh, 2003a).

The erythromycin gene cluster of *Saccharopolyspora erythraea* is a typical modular type-I PKS (Donadio *et al*., 1993; Marsden *et al*., 1994; Cortes *et al*., 1995; Ruan *et al*., 1997; Marsden *et al*., 1998; Stassi *et al*., 1998; Lal *et al*., 2000). The polyketide synthase involved in the erythromycin biosynthesis pathway is DEBS, which consists of three multifunctional enzymes, DEBS1, DEBS2 and DEBS3 (Caffrey *et al*., 1992; Marsden *et al*., 1994; Lal *et al*., 2000). Each enzyme is encoded by a separate gene (*eryAI*, *eryAII*, and *eryAIII*, respectively) and contains two modules – therefore six modules together catalyse the addition of starter and extension units (Figure 1.8) (Lal *et al*., 2000). The N-terminus of DEBS1 contains an additional loading domain incorporating two additional catalytic sites, an AT and an ACP, thought to provide the propionyl-CoA starter unit to the first module, prior to transfer to the active site of the KS on module 1 (Lau *et al*., 2000). Six decarboxylative condensations between a propionyl-CoA starter unit and methylmalonyl-CoA extender units form a heptaketide which is then cyclised to form the product 6-deoxyerythronolide B (Lal *et al*., 2000; Walsh, 2003a). The cyclisation is catalysed by the TE domain of module 6, at the C-terminal of DEBS3 (Lal *et al*., 2000). Each module of the DEBS system has a KS, ACP and methylmalonyl-specific AT domain; in addition modules one, two, four, five and six also contain a KR domain, while the fourth module also contains DH and ER domains (Walsh, 2003a).

The DEBS system has become a model system for polyketides of all types and research has allowed several aspects of polyketide production to be investigated. Crystal structures of portions of modules 3 and 5 demonstrated for the first time the topology and 3D organisation of a modular PKS, and the crystal structure of the DH domain in module 4 elucidated how a polyketide substrate

interacts with the cognate DH domain (Tang *et al*., 2006; Tang *et al*., 2007; Keatinge-Clay, 2008; Cane, 2010). Many studies have contributed to the information base of AT specificity within PKS clusters by altering extender unit specificity to produce novel metabolites (Ruan *et al*. 1997; Marsden *et al*. 1998; Reeves *et al*. 2001; Long *et al*., 2002; Del Vecchio *et al*., 2003). Novel metabolites were also produced when the whole loading module from the avermectin PKS was swapped into the erythromycin PKS (Marsden *et al*., 1998). The Khosla group have highlighted the importance of the linkers that flank the modular AT domains in the DEBS system, hypothesising that they are important for ACP recognition or position and potentially for catalysing acyl group transfer (Wong *et al*., 2010). More recently the Khosla group demonstrated the specificity of ACP domains for their cognate KS domain, and again highlighted the importance of inter-domain linkers for aligning domains correctly for polyketide synthesis (Kapur *et al*., 2012).

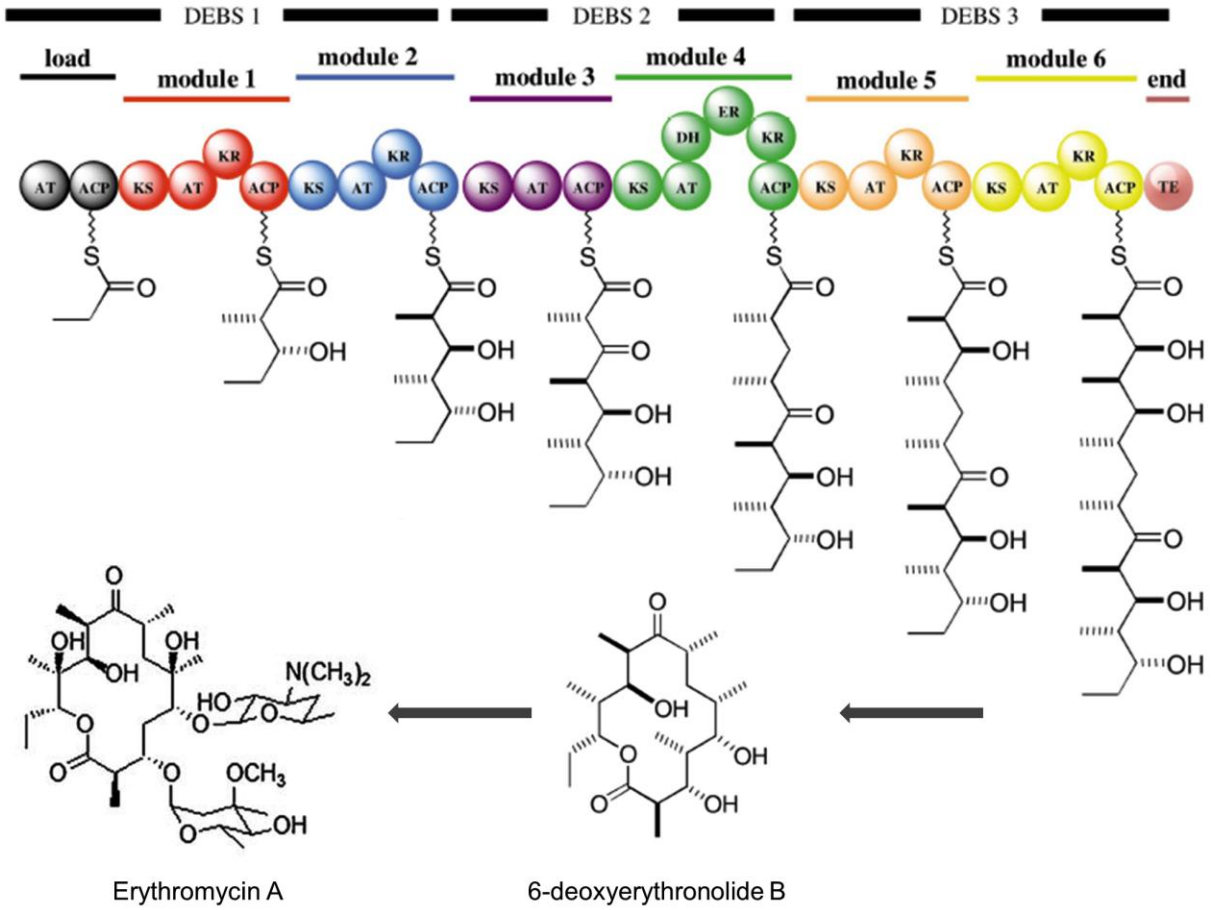

Figure 1.8. Organisation of the polyketide synthase DEBS, responsible for erythromycin biosynthesis. The complete DEBS comprises of three polypeptides, DEBS1, DEBS2 and DEBS3, which encompass the six condensation modules required for production of the erythromycin precursor 6-deoxyerythronolide. Domains are acyltransferase (AT), acyl carrier protein (ACP), ketosynthase (KS), ketoreductase (KR), dehydratase (DH), enoyl reductase (ER), and thioesterase (TE) (Staunton and Weissman, 2001).

1.2.3 Type II polyketides

Type II PKSs, found in bacteria and plants, assemble an iterative multienzyme complex by encoding distinct proteins (Lal *et al*., 2000; Moore and Hopke, 2001; Chopra *et al*., 2008). The minimal type II PKS is comprised of three subunits: KS_{α}, KS_{β} (also known as chain length factor – CLF) and an ACP. This minimal PKS can synthesize a full-length polyketide chain: the KS_{β} catalyses the decarboxylation of malonyl-ACP to acetyl-ACP (the ACP can be loaded by the actions of a malonyl-acetyl transferase (MAT) or can self-load), second, the KS_{α} catalyses the iterative extension of the chain (McDaniel *et al*., 1993; Crosby *et al*., 1995; McDaniel *et al*., 1993; Crump *et al*., 1996; Dreier *et al*., 1999; Tang *et al*., 2003; Beltran-Alvarez *et al*., 2007). The chain is then cyclised and released from the protein. Figure 1.9 shows the processes involved in producing actinorhodin and the novel products SEK4 and SEK4b. In this case the minimal PKS has synthesised the C_{16} chain and, in the absence of auxiliary tailoring enzymes, spontaneous cyclisation of the individual octaketides has formed products SEK4 and SEK4b (Dreier *et al*., 1999; Beltran-Alvarez *et al*., 2007). Interestingly it has been hypothesized that the same MAT is utilised not only by the minimal PKS, but also by fatty acid synthesis within the polyketide-producing cell (Tang *et al*., 2004a; Wesener *et al*., 2011).

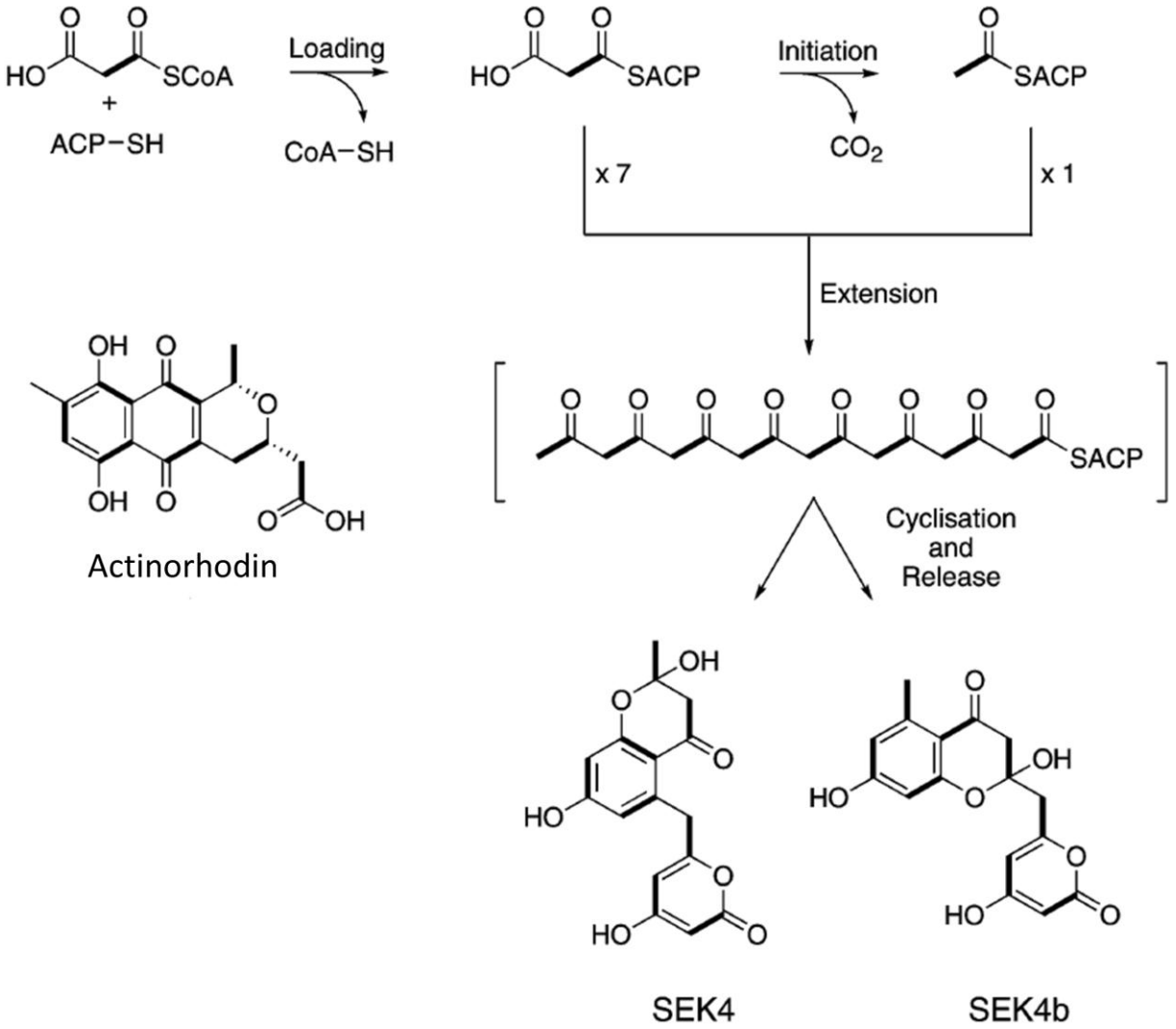

Figure 1.9. Biosynthesis of octaketides by the actinorhodin minimal PKS.
Actinorhodin is synthesised by seven rounds of condensation with malonyl-CoA. Ketoreductases, aromatases, cyclases, oxygenases and methylases interact with and modify the emerging polyketide to produce the final products (Dreier *et al*., 1999; Beltran-Alvarez *et al*., 2007).

1.2.4 Type III polyketides

Until the characterisation of the bacterial type III PKSs RppA and PhlD in 1999 it was thought that type III PKSs only occurred in plants (Bangera and Thomashow, 1999; Funa *et al*., 1999). Type III PKSs consist of a homodimer (Figure 1.6), working independently of ACPs to utilise a wide variety of CoA thioesters as substrates, resulting in extraordinary product diversity; such as aloesone, a secondary metabolite involved in chromone synthesis in rhubarb; plant flavonoid synthesis; bacterial melanin biosynthesis; and resveratrol, an antimicrobial produced by some plants in response to bacterial or fungal attack that is also thought to be the beneficial compound of red wine and has anti-cancer properties (Schröder *et al*., 1998; Moore and Hopke, 2001; Abe *et al*., 2004; Austin *et al*., 2004; Gross *et al*., 2006; Flores-Sanchez and Verpoorte, 2009). The chalcone/stilbene synthase superfamily is one of the most widely studied type III PKSs. Decarboxylative condensations add acetate to an acyl-CoA starter unit, prior to cyclisation, aromatisation and downstream modifications (Austin and Noel, 2003). Compound diversity comes from the wide variety of starter and extender units that can be used during biosynthesis, for example: naringenin chalcone is synthesised from *p*-coumaroyl-CoA and 3 malonyl-CoA units; while aloesone is synthesised from acetyl-CoA and 6 malonyl-CoA units (Flores-Sanchez and Verpoorte, 2009).

1.3 Mupirocin - pseudomonic acid

Mupirocin is a polyketide antibiotic produced by the soil bacterium *Pseudomonas fluorescens* NCIMB 10586, isolated from Hampstead Heath in London (Fuller *et al.*, 1971; LGC Standards, 2010). *Pseudomonas* spp. are Gram-negative, aerobic (yet can utilise nitrogen as the electron acceptor under anaerobic conditions), rod-shaped bacteria found in a variety of habitats including soils, water, and on the surfaces of plant roots and leaves (Palleroni and Moore, 2004; Remold *et al*., 2011). Fluorescent pseudomonads are particularly important as plant growth-promoting rhizobacteria (PGPR), as they colonise plant roots and are thought to promote the growth of the plant by producing substances which protect it from pathogens (Haas and Défago, 2005). The substances produced include antifungal metabolites (AFMs) (for example, 2,4 diacetylphloroglucinol (DAPG), phenazine-1-carboxamide acid (PCN), oomycin A and fusaric acid) and secondary metabolites (for example, hydrogen cyanide, pyoverdin and pseudobactin) (Lugtenberg and Bloemberg, 2004). Pseudomonads (including fluorescent strains) are important biocontrol agents in the preservation of agricultural crops and progress has been made to improve the biocontrol activity of these strains by introducing extra copies of the required genes, and by creating new strains for use in agriculture (Morrissey *et al*., 2004; Haas and Défago, 2005). Examples of AFM-producing *P. fluorescens* strains are CHA0 which produces hydrogen cyanide, 2-79 which produces phenazine-1-carboxylic acid (PCA), and Q2-87 which produces DAPG. In addition Pseudomonads produce several polyketide metabolites (Table 1.1). Of particular importance in this case is *P. fluorescens* NCIMB 10586, which produces mupirocin.

Table 1.1. Polyketide metabolites produced by species of *Pseudomonas*.

Pseudomonad	Polyketide
P. fluorescens Pf-5	Pyoluteorin
P. aeruginosa[*]	Pederin
P. syringae pathovars	Coronatine
P. fluorescens Q2-87	DAPG
P. fluorescens NCIMB 10586	Mupirocin

*Thought to be the bacterial symbiont responsible for pederin biosynthesis (Kellner, 2002). DAPG, 2,4 diacetylphloroglucinol. (Hothersall and Thomas, 2004).

In 1887 the Swiss scientist C. Garré carried out work on a strain of *P. fluorescens* that exhibited antibiotic activity, aside from pioneering the streak method used today for assessing activity, he was the first scientist to record the antibiotic activity of this strain of bacteria (Brunel, 1951; Florey, 1945). The substance responsible for this antibiotic activity was finally isolated almost a century later and was identified as pseudomonic acid (PA) (Fuller *et al*., 1971). Subsequent investigations revealed a mixture of four pseudomonic acids (A-D), collectively named mupirocin, with extensive antibacterial activity. The structure of mupirocin, shown in Figure 1.10, comprises a monic acid (MA, a heptaketide) containing a pyran ring, attached to 9-hydroxynonanoic acid (9-HN) via an ester linkage (Fuller *et al*., 1971; Chain and Mellows 1974, 1977a; Alexander *et al*., 1978; Whatling *et al*., 1995). Pseudomonic acid A (PA-A) accounts for 90% of mupirocin. Pseudomonic acid B (PA-B) has a hydroxide group replacing the hydrogen at C8, pseudomonic acid C (PA-C) has an alkene group replacing the epoxide at C10-C11, and pseudomonic acid D (PA-D) has an alkene group replacing the alkane at C4'-C5' (Chain and Mellows, 1977b; Clayton *et al*., 1980, 1982; O'Hanlon *et al*., 1983; El-Sayed *et al*.,

2003). Mupirocin targets bacterial isoleucyl-tRNA synthase (IleS) (for more detail see Section 1.3.5) competitively inhibiting the formation of Ile tRNA, and ultimately blocking protein synthesis (Hughes and Mellows, 1978).

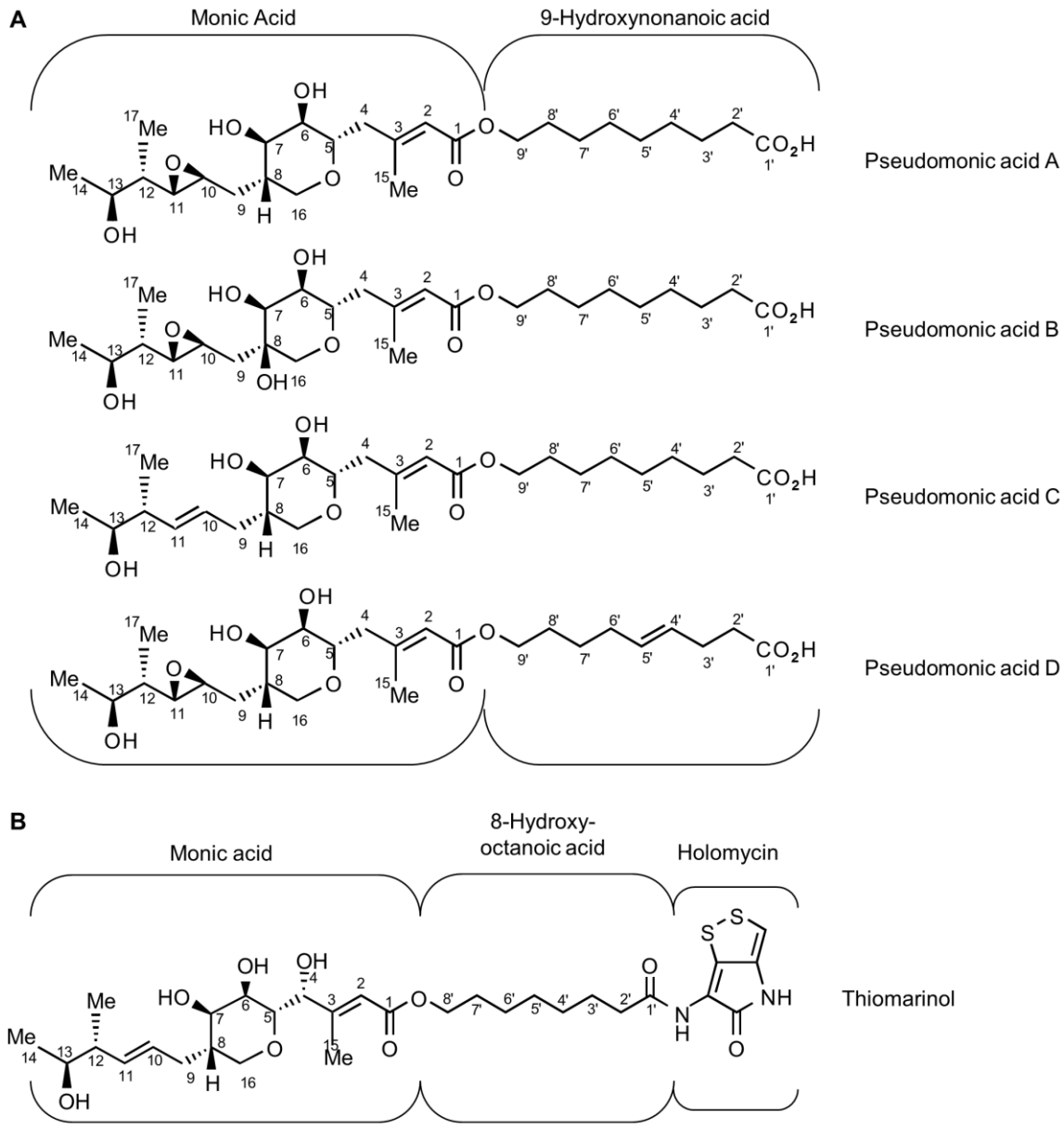

Figure 1.10. The structure of mupirocin and thiomarinol. (A) The structure of mupirocin, showing the monic acid and 9-HN moieties. Mupirocin is a mixture of four pseudomonic acids: PA-A (~ 90%), PA-B (~ 8%), PA-C (<2%), PA-D (<2%). **(B)** Structure of thiomarinol A, showing the marinolic acid (equivalent to pseudomonic acid/mupirocin) and holomycin moieties.

1.3.1 Mupirocin biosynthetic cluster

A 75kb region of the *P. fluorescens* NCIMB 10586 chromosome involved in mupirocin biosynthesis was identified by transposon mutagenesis and subsequently analysed by DNA sequencing, gene knock-outs and complementation studies (Whatling *et al*., 1995; El-Sayed *et al*., 2003). The cluster can be conveniently split into 2 sections: the first section comprising primarily of genes encoding 3 large multifunctional PKSs (MmpA, B and D) and a smaller multifunctional PKS (MmpC), plus at least 2 single function polypeptides, and the other section comprising genes encoding 2 small PKSs (MmpE and F) in addition to 29 individual "tailoring" proteins. Table 1.2 shows all of the genes involved in mupirocin biosynthesis and their putative functions. The cluster is unusual in that the order of the genes does not match the order of biosynthetic steps – biosynthesis starts with MmpD (Figures 1.11 and 1.12). The multifunctional genes *mmpD* and *A* together encode the first four and last two elongating modules respectively and one putative transfer/non-elongating/processing module. They comprise appropriate KS, ACP, KR, DH and methyltransferase (MT) functions for monic acid backbone synthesis while *mmpC* encodes two AT domains and a putative ER domain. The *mmpB* gene encoding single KS, KR and DH domains and triple ACP domains is proposed to be responsible for synthesis of the 9-HN moiety, but also encodes the only TE suggesting that it controls the final steps of the pathway and release of products. Resistance to mupirocin is encoded within the cluster by MupM which shows significant similarity to other IleS proteins (for more detail go to Section 1.3.6) (El-Sayed *et al*., 2003).

Table 1.2. Gene functions of the mupirocin biosynthetic cluster.

ORF	Proposed function
mupA	Reduced flavin mononucleotide ($FMNH_2$) oxygenase
mmpA	PKS: load/transfer KS, ACP; module 5 KS, KR, ACP; module 6 KS, ACP, ACP
mupB	3-Oxo-ACP synthase
mmpB	PKS: KS, DH, KR, ACP, ACP, ACP, TE
mmpC	Dual AT and putative ER
mmpD	PKS: module 1 KS, DH, KR, MT, ACP; module 2 KS, DH, KR, ACP; module 3 KS, DH, KR, MT, ACP; module 4 KS, KR, ACP
mupC	Dienoyl CoA reductase
mAcpA	ACP
mupD	3-Oxo-ACP synthase
mupE	ER
mAcpB	ACP
mupF	KR
mAcpC	ACP
mupG	3-Oxo-ACP synthase
mupH	β-hydroxyl-β-methyl glutarate (HMG) CoA synthase
mupJ	Enoyl CoA hydratase
mupK	Enoyl CoA hydratase
mmpE	PKS: KS, hydroxylase
mupL	Hydrolase
mupM	Isoleucyl-tRNA synthetase
mupN	Phosphopantetheinyl transferase
mupO	Cytochrome P450
mupP	Unknown
mupQ	Acyl CoA synthase
mupS	3-Oxo-ACP reductase
mAcpD	ACP
mmpF	PKS: KS
mAcpE	ACP
mupT	Ferrodoxin dioxygenase
mupU	Acyl CoA synthase
mupV	Oxidoreductase
mupW	Dioxygenase
mupR	Transcriptional activator
mupX	Amidase
mupI	N-Acyl homoserine lactone synthase

Abbreviations: *mmp*, mupirocin multifunctional polypeptide gene; PKS, polyketide synthase; KS, ketosynthase; DH, dehydratase; KR, ketoreductase; ACP, acyl carrier protein; TE, thioesterase; AT, acyltransferase; ER, enoyl reductase; MT, methyltransferase; mAcp mupirocin acyl carrier protein; ORF, open reading frame (El-Sayed *et al*., 2003; Hothersall *et al.*, 2007).

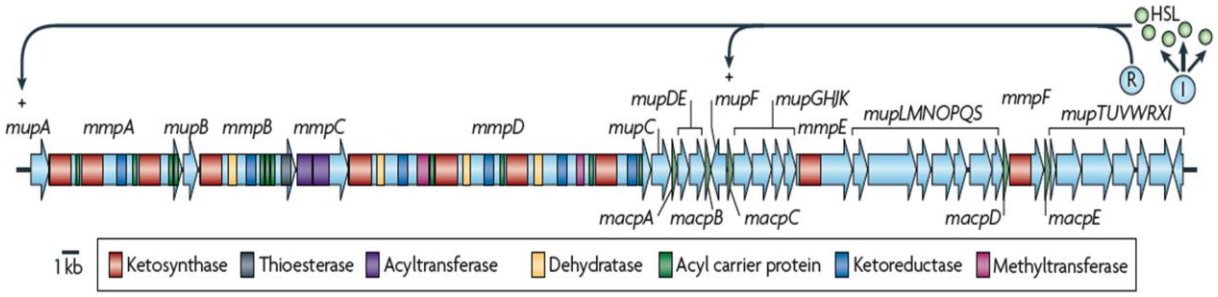

Figure 1.11. Genetic organisation of the mupirocin cluster. The control circuits emanating from MupR are indicated by arrows. R, MupR; I, MupI, HSL, homoserine lactone (Thomas *et al*., 2010).

1.3.2 Mupirocin biosynthesis

Mupirocin biosynthesis occurs in a very similar manner to that of fatty acids: the condensation of carboxylic acid starter units is catalysed by a KS and a dicarboxylic acid extender unit is transferred to the phosphopantetheine arm of an ACP; the KS then catalyses a condensation reaction to join the starter and extender units; the product is either left unreduced or is partially or fully reduced by the actions of KR, DH and ERs; further rounds of elongation can be undertaken until the polyketide has reached the designated length (El-Sayed *et al*., 2003; Walsh, 2003a; Hothersall, *et al*., 2007). Throughout this process two ATs are proposed to act in *trans* to catalyse the transfer of starter and extender units to KS and ACPs respectfully, via acyl-CoA-activated intermediates between condensation modules (Hothersall, *et al*., 2007; Wu *et al*., 2008).

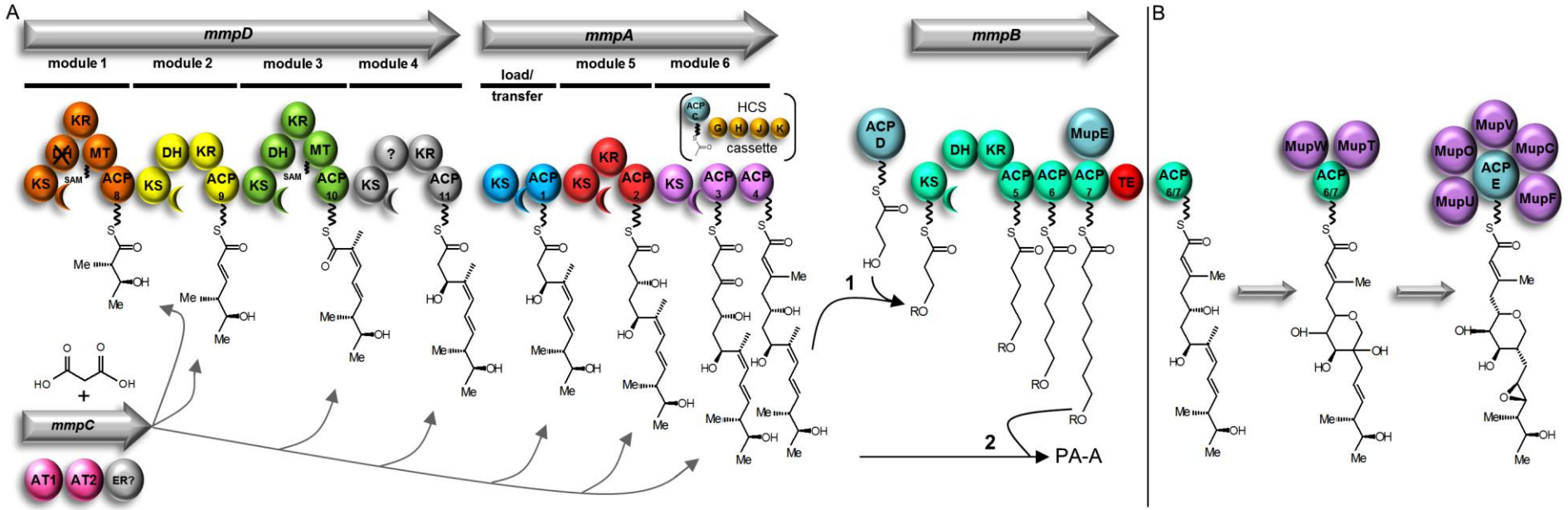

Figure 1.12. Scheme for biosynthesis of mupirocin. **(A)** The monic acid (MA) backbone is synthesised by condensation of extender units and further modifications by the six modules of MmpD and MmpA. 9-hydroxynonanoic acid (9-HN) is synthesised by the iterative condensations and further ketoreduction and dehydration catalysed by MmpB on a proposed 3-hydroxypropionate (3-HP) starter unit. Two possible pathways for the addition of 9-HN to the MA backbone: continued extension onto MA that is already esterified to 3-HP (pathway 1, R = monic acid); or, separate synthesis followed by esterification (pathway 2, R=H). **(B)** The MA structure is modified by tailoring enzymes, such as MupW, T, O, U, V, C and F, which function to form the pyran ring and the epoxide group at C-10,-11. Whether this happens before or after joining to 9-HN, or on ACP6 or 7 is not known. Crescents depict docking domains. ACPs are numbered in gene order; mAcpA and B are omitted from this schematic on the basis of their undetermined functions (Gurney and Thomas, 2011)

1.3.2.1 Monic acid biosynthesis

The heptaketide chain that comprises the backbone of monic acid is synthesised by six condensation reactions of acetate-derived units catalysed by MmpD (modules 1 to 4) and MmpA (modules 5 and 6) as shown in Figure 1.12, A (Martin and Simpson, 1989; El-Sayed *et al*., 2003). Synthesis of mupirocin is thought to begin on MmpD despite MmpA being one of the first proteins to be transcribed – a mutant that knocked-out the activity of the KR of MmpD module 4 prevented PA-A from being produced. Instead a tetraketide, mupiric acid (Figure 1.13, C), was produced as it was unable to continue down the assembly line to form the fully complete monic acid product of MmpD and MmpA (Wu *et al*., 2008).

Synthesis could begin with one of the *trans*-acting ATs (located on MmpC) transferring an activated starter unit (acetyl-Coenzyme A intermediate) to the 4'-phosphopantetheine arm of ACP8 and then to the thiol group of the active Cys of KS5. An activated extender unit (malonyl-CoA) could then be transferred by one of the ATs to the vacant ACP8, prior to decarboxylative (Claisen) condensation catalysed by KS5. Alternatively an activated starter unit could be transferred directly to the KS5. The first module could then carry out ketoreduction and α-methylation to create the structure that mimics the isoleucine side chain. Synthesis continues through three further rounds of condensation and modification on successive modules of MmpD (KS/ACP modules 2, 3 and 4), including a second α-methylation by the MT in module 3, before the acyl intermediate is passed to MmpA. Two further elongation modules on MmpA extend the chain to give the C_{17} precursor to monic acid. The first module of MmpA is likely to act as a transfer or processing module due to the presence of an atypical KS (KS^0) domain. A typical KS domain has an active

motif consisting of CHH, where C is the active site Cys, and the H's represent His residues at positions 135 and 173 (Aparicio *et al*., 1996). The mupirocin KS1 has the motif CQH, indicating an unusual role or an inactive domain – it can bind the intermediate but cannot catalyse a condensation (El-Sayed *et al*., 2003). The mupirocin system is not the only system to demonstrate this unusual motif – occurrences have also been documented in chivosazol, pederin and myxovirescin PKS systems (Piel, 2002; Perlova *et al*., 2006; Simunovic *et al*., 2006). Another form of KS has also been documented, those where the active site Cys has been replaced by Gln – KS^{Q} domains. These domains are thought to be very similar to the KS_{β}/CLF of type II FAS and PKS systems, where the active site Gln has a role in decarboxylation catalysis (Bisang *et al*., 1999). In many systems it has been hypothesised that these KS^{Q} domains are responsible for the loading and decarboxylase function required for system initiation (Kakavas *et al*., 1997; Xue *et al*., 1998; Bisang *et al*., 1999; Kopp *et al*., 2005; Schneider *et al*., 2007). Due to the location of the KS^{0} domain within the mupirocin cluster it seems unlikely to be responsible for system initiation, but perhaps it performs an alternative function. Deletion (as well as mutation of active site residues) of the domains of the loading module resulted in a loss of antibiotic production, indicating their importance for mupirocin production, however more research is required to fully understand the presence and roles of these domains within the cluster (El-Sayed *et al*. 2003).

1.3.2.2 Tailoring the monic acid backbone

The mupirocin cluster contains many genes that are needed to modify ("tailor") the PKS-bound intermediate to form the final PA structure. The modifications involve incorporation of a methyl group at C15, hydroxylation at C6, epoxidation at C10-11 and formation of the pyran ring (Figure 1.12, B) (Cooper *et al*., 2005a; Hothersall *et al.*, 2007). Bioinformatics can often predict both biochemical function and partner genes which work together (based on being found together in other genomes). In the mupirocin cluster these include the hydroxymethylglutaryl-CoA Synthase (HCS) cassette genes *mAcpC*, *mupG, H, J, K* (for function see below) as well as two other blocks *mAcpD, mupS, Q, mmpF* (function currently unknown) and *mupD* and *mupE* (an ER responsible for the C6'-7' reduction). However, gene knock-outs and product analysis are essential since other gene sets such as *mupW, T* (pyran ring formation) and *mAcpE*, *mupO, U, V, C* and *F* (further reduction around the pyran ring) seem to have functions currently unique to this cluster. While it is clear at what stage in the pathway some of them work, for example the HCS cassette that functions at module 6, for others it is either flexible or still unclear. Gene functions relating to double bond reduction in 9-HN, C6-hydroxylation and C-10,-11 epoxidation are currently under investigation, although it is predicted the hydroxylase domain of MmpE performs the epoxidation (Hothersall, unpublished data, 2012).

Gene knock-outs have been particularly instrumental in indicating a possible pathway for pyran ring formation and PA-A synthesis (Figure 1.13, A). In this scheme MupW and MupT catalyse the epoxidation of the C-8,-16 double bond (essential for formation of the tetrahydropyran ring) which makes the C-16 more receptive to attack by the C-5 hydroxyl group. Esterification with 9-HN and C-10,-11 epoxidation, which

may occur before or after this, result in PA-B. Mutation of *mupW* and *mupT* resulted in accumulation of a novel metabolite, mupirocin W, lacking the tetrahydropyran ring but having the attached 9-HN confirming the role of MupW/T in mupirocin biosynthesis but not defining when it normally occurs (Cooper *et al*., 2005a). To produce PA-A, MupU is proposed to mediate the transfer of the intermediate to mAcpE before MupO, a cytochrome P_{450} may catalyse oxidation of the C-7 hydroxyl to the ketone, while subsequent dehydration by MupV generates a C-8,-9 enoyl bond. MupC is proposed to reduce the C-8,-9 bond, before MupF catalyses ketoreduction at C-7 and the resultant product is released as PA-A (Cooper *et al*., 2005a; Cooper *et al*., 2005b; Hothersall *et al.*, 2007; Wu *et al*., 2007). Gene knock-outs of MupW, MupF and MupC have yielded mupirocin W, mupirocin F and mupirocin C respectively (Figure 1.13, C) and contributed to the above scheme for pyran ring formation. As stated previously, along with PA-A there are several other intermediates released, most notably PA-B. It was hypothesised that over expression of mAcpE, MupO, U, V, C, and F would increase the conversion of PA-B to the more biologically active PA-A. However, while introducing these proteins in *trans* in the wild type (WT) strain did increase the production of PA-A by over twofold, it also increased the production of PA-B (Macioszek, 2009). The increase in PA-A production was determined to be due to the actions of mAcpE, MupU, MupV and MupC. Work is currently underway to investigate the roles of MupU and mAcpE further as it is predicted MupU transports the intermediate from MmpB to mAcpE, where dehydration would take place.

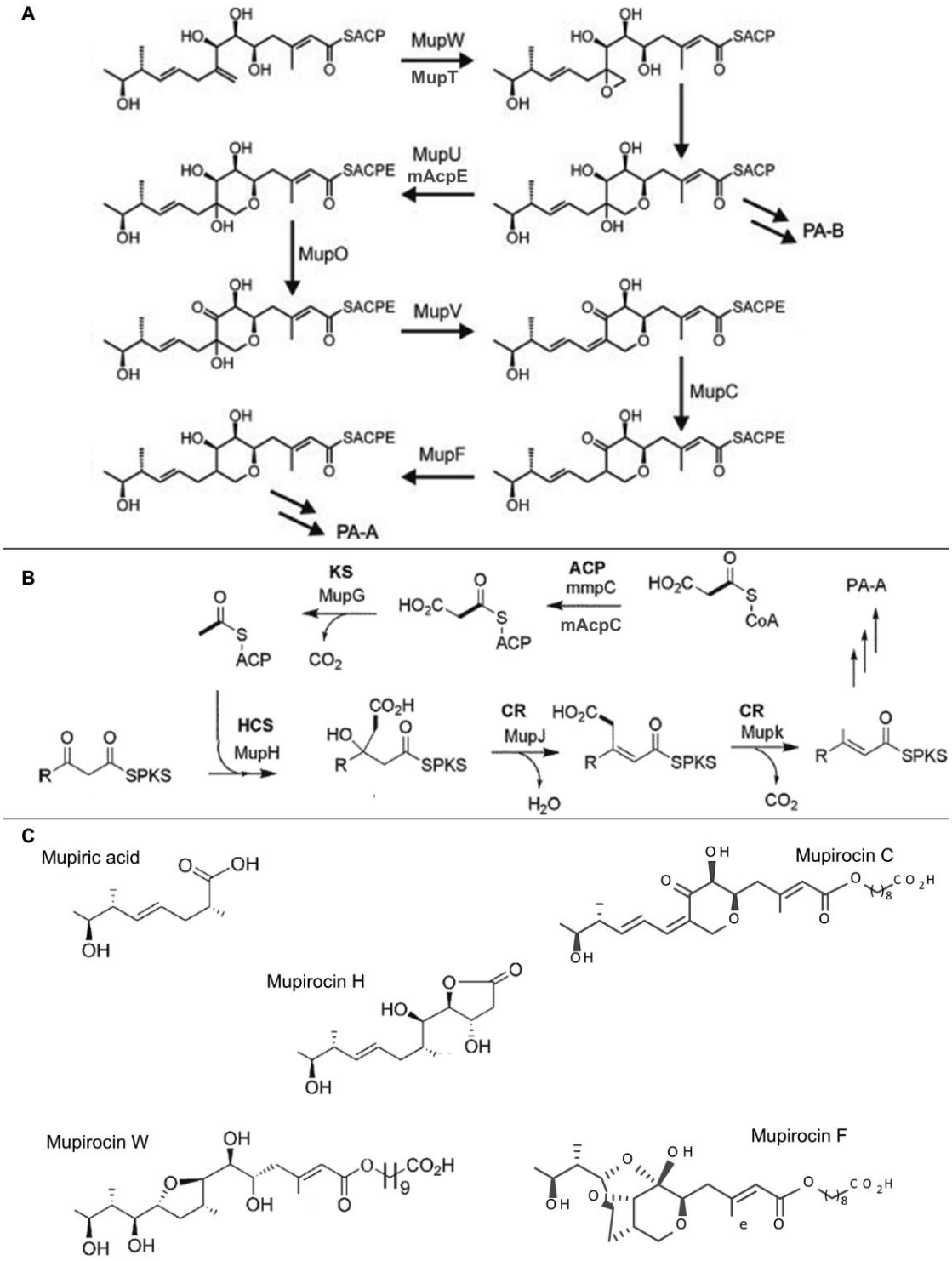

Figure 1.13. Tailoring steps from the mupirocin pathway and intermediates released. (A) Formation of the pyran ring. **(B)** Actions of the HCS cassette. **(C)** Intermediates released from gene knock-outs: mupiric acid is produced by ΔKR-D4, mupirocin H by Δ*mupH*, mupirocin W by Δ*mupW/mupT*, mupirocin C by Δ*mupC*, and mupirocin F by Δ*mupF*. PA-B, pseudomonic acid B; PA-A, pseudomonic acid A; ACP, acyl carrier protein; KS, ketosynthase; HCS, hydroxymethylglutaryl-CoA synthase; CR, crotonase. (Hothersall *et al*., 2007; Wu *et al*., 2007)

The HCS cassette, comprised of MupG, H, J, K and mAcpC, is responsible for the incorporation of the β-methyl group at C-15 while the growing intermediate is tethered to ACP4 (Figure 1.12, B): MupG catalyses the decarboxylation of acetate from a malonate bound to mAcpC; MupH catalyses the condensation to produce a gluconate intermediate; dehydration, catalysed by MupJ is finally followed by decarboxylation mediated by MupK to produce the β-methylthioester (Rahman *et al*., 2005; Wu *et al*., 2007; Wu *et al*., 2008). The functions of related HCS cassettes have been proposed by a number of groups and experimental evidence supporting these hypotheses have been provided from studies on myxovirescin (Simunovic *et al*., 2006), jamaicamide (Edwards *et al*., 2004), leinamycin (Tang *et al*., 2004b), bacillaene (Butcher *et al*., 2007) and curacin A (Chang *et al*., 2004).

1.3.2.3 9-hydroxynonanoic acid biosynthesis

Since there are strong indications for the role of MmpD and MmpA in MA synthesis it seems logical that MmpB, the third type I PKS, is responsible for 9-HN synthesis although as yet there is no direct evidence for this. However, 9-HN is proposed to be derived from a 3-hydroxypropionate (3-HP) starter unit with MmpB iteratively catalysing three rounds of condensation with malonate as the extender unit (Figure 1.12, A). MmpB does not contain an ER domain but an in-frame deletion of MupE results in a 6'-7' enoyl bond suggesting that it, possibly in conjunction with MupD, is responsible for at least part of the required ER activity (Hothersall *et al*., 2007; Macioszek, 2009; Hothersall and Wu, unpublished data). Since mutagenesis of *mupE* resulted in the formation of only a partially saturated fatty acid chain, an additional enzyme must be responsible for reduction of the fatty acid chain to give 9-

HN. There is a third domain in MmpC which has predicted ER activity, that could function during the formation of 9-HN. Work by Calderone group at Harvard University demonstrated that PksE, an enzyme from the dihydrobacillaene PKS consisting of AT and ER domains, provided ER activity in *trans* (Bumpus *et al*., 2008). The terminal TE domain of MmpB could then either catalyse the release of the saturated 9-HN, or provide a means of esterification with MA (Figure 1.12) (El-Sayed *et al*., 2003; Hothersall *et al*., 2007). The order in which events occur is still under investigation. It is possible either that 9-HN and monic acid are synthesized separately and then joined together to complete the mupirocin structure, or that 9-HN is elongated on a starter unit (3-HP) esterified with the product of MmpD/MmpA. Currently the latter appears more likely due to the release of PA-A and PA-B with C_7 side chains in place of C_9 side chains – indicating MmpB works on monic acid to add the fatty acid prior to release by the TE (Hothersall *et al*., 2011).

1.3.3 Regulation of mupirocin production

A quorum sensing mechanism controls expression of the mupirocin biosynthetic genes. This involves the constitutive production of diffusible signal molecules (auto inducers, in this case N-acyl homoserine lactones) that accumulate in the environment of the bacteria and, when the population reaches a critical density (quorum), switch on target gene transcription via an activator protein. In theory this means that in the case of producing substances such as antibiotics, the concentration produced will be sufficient enough to kill the competing bacteria.

Based on sequence alignments with the *Vibrio harveyi* Lux system, the genes *mupR* and *mupI* were predicted to mediate quorum-regulated expression of the

mupirocin cluster (El-Sayed *et al*., 2001). MupI is required to produce *N*-(3-oxodecanoyl) homoserine lactone (3-O-C10-HSL) which by analogy to other systems is predicted to bind to MupR, which can then bind to the promoter to activate it (El-Sayed *et al*., 2001; Hothersall *et al*., 2011). Thus the MupR-MupI system activates transcription of the *mup* operon upon binding to the *lux* box promoter regions of *mupA*, *mAcpC* and *mupF*, while surprisingly *mupI* does not appear to have a *lux* box region or any obvious promoter (Fuqua *et al*., 1994; El-Sayed *et al*., 2001; Hothersall *et al*., 2007). In an attempt to upregulate mupirocin production, 3-O-C10-HSL was added to the production media, and separately *mupI* was expressed in *trans* to the WT producer; however neither approach was successful (Hothersall *et al*., 2011). An alternative approach was to express *mupR* in *trans*, and this resulted in a fivefold increase in PA-A production in the WT, as well as detection of early intermediates such as mupiric acid, mupirocin H and fatty-acid-truncated versions of PA-A and PA-B (Hothersall *et al*., 2011). The same investigation also highlighted a potential regulatory role for the product of *mupX*, which is located in between *mupR* and *mupI* in the cluster.

1.3.4 Special features of the mupirocin cluster

The mupirocin cluster contains various features that distinguish it from typical PKSs such as the DEBS system and whose activities may be useful in the generation of novel pathways. Refer to Appendix for a summary of *trans*-AT PKS traits and figures of select clusters.

1.3.4.1 Dependence on in *trans* ATs

The mupirocin PKSs differ from those of the well studied erythromycin biosynthetic system from *S. erythraea* (Lal *et al*., 2000) in that the AT domains are absent from each module and are encoded by a separate gene, *mmpC* (El-Sayed *et al*., 2003). They thus belong to the group of PKS systems termed 'in *trans*' AT PKSs, of which a growing number have been described and analysed including those that produce myxovirescin, virginiamycin, leinamycin, lankacidin, pederin, rhizoxin, bryostatin, kirromycin, mycosubtilin, bacillaene, difficidin, macrolactin, chivosazol, disorazol and thiomarinol (Piel, 2002; Cheng *et al*., 2003; Chen *et al*., 2006; Kopp *et al*., 2005; Mochizuki *et al*., 2003; Perlova *et al*., 2006; Simunovic *et al*., 2006; Aron *et al*., 2007; Partida-Martinez and Hertweck, 2007; Pulsawat *et al*., 2007; Schneider *et al*., 2007; Sudek *et al*., 2007; Weber *et al*., 2008; Piel, 2010). For more details please refer to Chapter 4.

1.3.4.2. No integrated ER domains

The *trans*-acting AT PKSs either completely lack ER domains or have them in unusual positions. For example, in the myxovirescin biosynthetic cluster it has been proposed that the ER domain of TaO is shared between modules 7 and 8, encoded

on Ta-1 and TaO respectively (Simunovic *et al*., 2006). In the mupirocin cluster one of the tailoring proteins, MupE, provides ER activity in *trans*. ER domains are also thought to be located on discrete proteins, with *trans*-acting ATs, such as LnmG and MmpC (Cheng *et al*., 2003; El-Sayed *et al*., 2003). There are five distinct architectures of the AT-encoding genes (Figure 4.4): single ATs, tandem AT-domains, single AT with single TE domain, single AT with single ER domain, tandem ATs with a single ER domain (Gurney and Thomas, 2011; Jensen *et al*., 2012; Musiol and Weber, 2012). These architectures are distributed throughout two evolutionary pathways. Their functionality and relevance is yet to be determined. Control of enoyl reduction in the mupirocin pathway is currently under investigation.

1.3.4.3 Methyl group incorporation

In type I systems with modular AT domains each module can specify the nature of the extender unit, for example choosing methylmalonate rather than malonate. When all modules share one or two *trans*-acting ATs incorporation of α-methyl groups can be specified by MT domains in a module. These occur in the *mup* cluster and all other *trans*-AT PKSs mentioned previously, with the exceptions of FK228, macrolactin, mycosubtilin, neocarzillin and zwittermicin (Duitman *et al*., 1999; Otsuka *et al*., 2004; Cheng *et al*., 2007; Schneider *et al*., 2007; Kevany *et al*., 2009). However, this is not obligatory because some systems employ a mixture of *trans*- and *cis*-acting ATs (Otsuka *et al*., 2004; Weber *et al*., 2008; Kevany *et al*., 2009). In mupirocin the MT domains in modules one and three are responsible for the methyl groups at positions C-17 and C-16 in the final structure, which are incorporated from S-adenosyl methionine (SAM) (El-Sayed *et al*., 2003; Feline *et al*., 1977; Wu *et al*.,

2008). In addition, many of the *trans*-AT group of PKS contain β-branches to the polyketide backbone that are incorporated under the actions of an HCS cassette (Chen *et al*., 2006; Cheng *et al*., 2003; Partida-Martinez and Hertweck, 2007; Pulsawat *et al*., 2007; Simunovic *et al*., 2006; Sudek *et al*., 2007). As detailed in Section 1.3.2.2, the mupirocin HCS cassette catalyses the incorporation of the methyl group at C-15. Studies on mupirocin have also provided evidence of the functions of the HCS cassette – mutation of *mupH* produced a new metabolite, mupirocin H (Figure 1.12, C), which appeared to be a truncated version of MA incorporating a 3-hydroxy-γ-lactone ring (Wu *et al*., 2007).

1.3.4.4 Duplicated acyl carrier proteins

The multifunctional proteins MmpA and MmpB contain tandem doublet and triplet ACPs respectfully (El-Sayed *et al*., 2003). There are several other *trans*-AT PKSs with similar unusual domain architecture: leinamycin, lankacidin, bacillaene, difficidin, chivosazol, virginiamycin, and macrolactin (Chen *et al*., 2006; Cheng *et al*., 2003; Mochizuki *et al*., 2003; Perlova *et al*., 2006; Pulsawat *et al*., 2007; Schneider *et al*., 2007). The ACPs of the mupirocin doublet (ACP3 and 4) and triplet (ACP5, 6 and 7) are more closely related to each other than any other ACPs within the cluster, indicating they may have arisen from gene duplication events. Another unusual feature of the tandem ACPs is the unusually short linker regions between the individual domains – the spacers between domains on the Mmps are usually approximately 100 amino acids in length, but ACP3 and 4 are separated by just 12 amino acids and ACP5, 6 and 7 by only 3. Rahman et al. (2005) produced various mutants to determine the roles of these tandem ACPs: mutants of ACP3 and 4, and

ACP5, 6, and 7 resulted in loss of mupirocin production when analysed by bioassay and high performance liquid chromatography (HPLC). Pairwise mutants of ACP5/6, 6/7 and 5/7 reduced mupirocin production to less than 20% of WT, while individual mutants of ACP3 and 4, and ACP5, 6, and 7 resulted in approximately 60% and 25-36% of production when compared to WT, respectively. The authors concluded that while any one ACP from the cognate doublet and triplet clusters is sufficient for mupirocin biosynthesis, production was significantly improved by an increase in numbers, indicating that the doublet and triplet set of ACPs are functionally redundant (Rahman *et al*., 2005). Reducing the tandem ACPs to a single ACP would be rate-limiting. The results indicated that the doublet ACPs (3/4) work in parallel, while ACP5 physically blocks access of other ACPs to some part of the machinery if it is inactivated by a point mutation (Rahman *et al*., 2005).

1.3.5 Clinical significance

Mupirocin competitively inhibits IleS, blocking the formation of Ile tRNA and thus inhibiting protein synthesis (Hughes and Mellows, 1978). IleS catalyses the transfer of isoleucine onto tRNA via the formation of aminoacyl-adenylate (aa-AMP). The C-14 to C-11 terminus of MA resembles the side-chain structure of Ile and interacts with the Ile-specific binding pocket of IleS (Figure 1.14) (Yanagisawa *et al*., 1994). The pyran ring interacts with the ATP binding site of IleS, and it is thought the 9-HN moiety may stabilise the binding by its affinity for a hydrophobic groove (Nakama *et al*., 2001). Mupirocin has a remarkably broad spectrum of activity; it is active against both Gram-positive and Gram-negative organisms, and particularly effective against those *Staphylococcal* and *Streptococcal* species most commonly

responsible for infections of the skin (Sutherland *et al*., 1985). Mupirocin cannot be used systemically due to its high affinity for serum and rapid metabolism in body fluids (it is hydrolysed at the ester joining monic acid to 9-HN), but has been successfully used topically for many years (Basker *et al*., 1980; Sutherland *et al*., 1985).

Pseudomonic acid was tentatively used as a potential therapeutic agent for skin infections and nasal carriage of antibiotic-resistant strains of *Staphylococcus aureus* in 1983 (Wuite *et al*., 1983; Dacre *et al*., 1983). In 1985 it was introduced for the treatment of bacterial skin infections, and in 1988 for nasal carriage of *Staphylococci*, including MRSA (Cookson *et al*., 1990). MRSA colonising the skin and nose can easily be transferred to other areas of the body or wounds, thus causing particular concern during surgical procedures and when exposed cuts or burns are present (Neu, 1992). Marketed globally, mupirocin is now used world-wide for topical treatment of impetigo, infected skin lesions and for decolonisation of patients with nasal carriage of *Staphylococcus*, including MRSA (GlaxoSmithKlein, 2010; Medimetriks, 2008; TEVA, 2003). In fact, mupirocin is effective in infiltrating *S. aureus* and *P. aeruginosa* biofilms on the surface of burns, demonstrating the full potential of this antibiotic in a clinical setting (Hammond *et al*., 2011). Decolonisation of patients that carry MRSA can reduce the risk of infection in patients and decrease transmission to other patients (Gilpin *et al*., 2010).

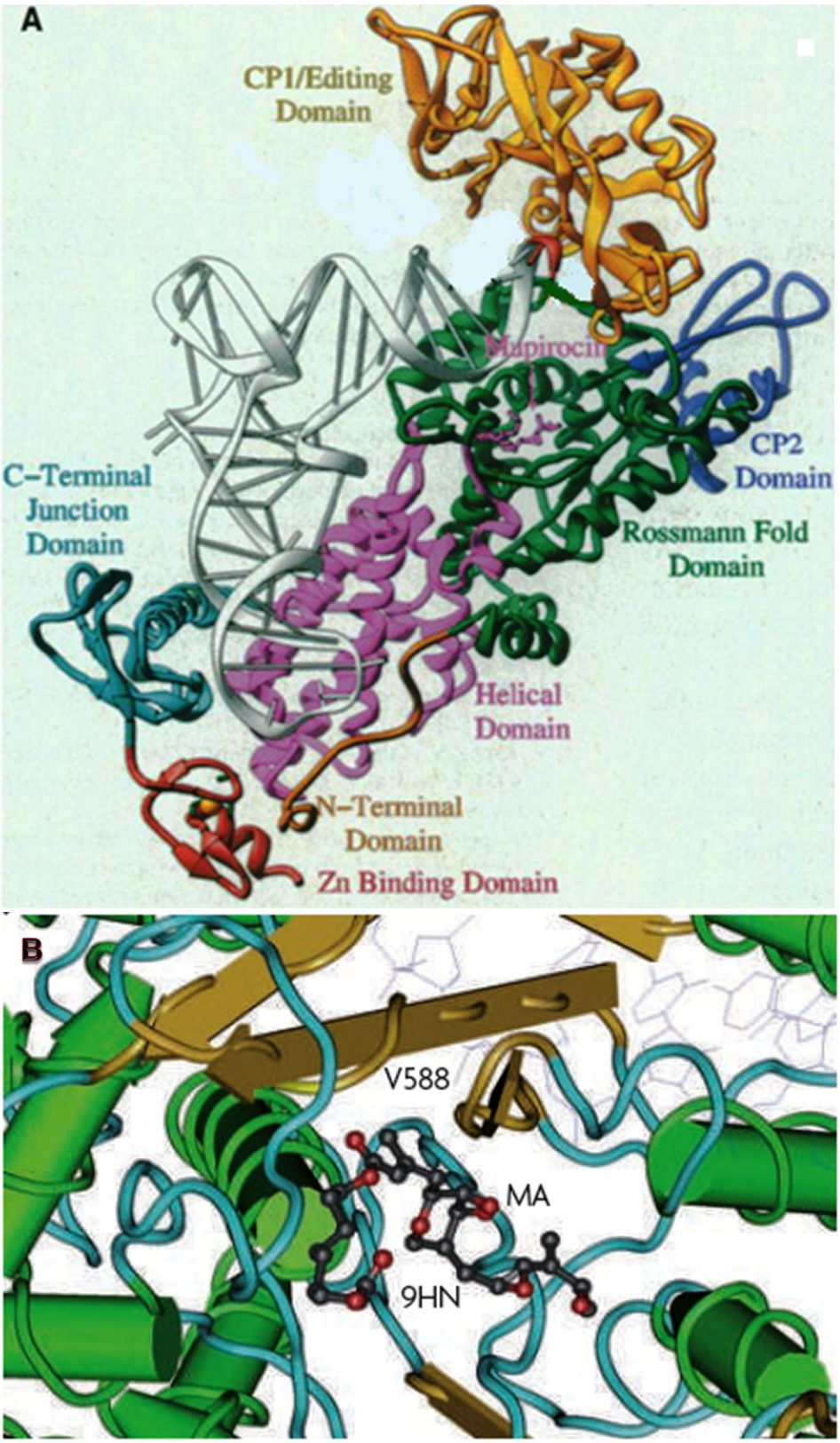

Figure 1.14. Mupirocin binding to isoleucyl-tRNA synthase. (A) Structure of isoleucyl-tRNA complex with isoleucyl-tRNA and mupirocin. The protein is coloured by domain, mupirocin is shown in pink (Silvian *et al*., 1999). **(B)** Mupirocin binding in the synthetic site of isoleucyl-tRNA synthase, mupirocin is shown in grey (Thomas *et al*., 2010).

1.3.6 Resistance to mupirocin

The initial widespread use of mupirocin to treat MRSA led to resistance first being recorded in 1987 (Rahman *et al*., 1987). Resistance to mupirocin has two distinct levels: high level resistance >500µg/ml, and the more common low level between 8-256µg/ml (Ramsey *et al*., 1996). Low level resistance normally arises from spontaneous mutations in the chromosomally encoded IleS, in particular V558F and V631F, which distort the hydrophobic pocket of the Rossman fold to the point where mupirocin binding is impeded (Yanagisawa *et al*., 1994; Antonio *et al*., 2002; Hurdle *et al*., 2004). These mutations tend to be non-transferable and generally of little clinical significance (Eltringham, 1997; Slocombe and Perry, 1991).

High level resistance has a more substantial effect on clinical treatments and involves the presence of an IleS similar to the eukaryotic versions, which are known to be more resistant to mupirocin (Racher *et al*., 1991; Yanagisawa and Kawakami, 2003). The gene responsible for producing this highly mupirocin-resistant IleS2 is the plasmid-encoded *mupA* (*mupM* or *tmlM* in the mupirocin and thiomarinol producers) (Dyke *et al*., 1991; Eltringham, 1997; Farmer *et al*., 1992; Gilbart *et al*., 1993; Hodgson *et al*., 1994; Rahman *et al*., 1987). The *mupA* gene is associated with transposable elements as part of different plasmids, often self-transmissible, that also confer resistance to other antibiotics, such as gentamicin, tetracycline and trimethoprim (Patel *et al*., 2009; Perez-Roth *et al*., 2010). Comparison of sequences surrounding *mupA* genes from self-transmissible plasmids in *S. aureus* indicates apparently multiple gene capture events with varying amounts of the same flanking sequences as if the gene comes from the chromosome of an as yet unidentified organism (Perez-Roth *et al*., 2010). Further analysis of the growing wealth of

bacterial genome sequences also reveals that many bacteria carry two IleS proteins – the second (IleS2) belonging to this eukaryote-like mupirocin resistance type correlating with a mupirocin resistant phenotype. The reasons for carriage of a second IleS are at present unclear, but it seems quite likely that it is one such IleS2 gene in an as yet unidentified bacterium that is the source of *mupA* in *S. aureus*. *Bifidobacteria* spp. are highly resistant to mupirocin and the antibiotic is often used to select for them. The high level of resistance (>1,800µg/ml) in these organisms has been traced to a single amino acid mutation within an amino acid motif thought to be involved in binding mupirocin – HIGH (Serafini *et al*., 2011). In highly resistant organisms such as *Bifidobacteria* spp., *S. aureus* and *P. fluorescens* NCIMB 10586 the Ile in this motif is replaced with the bulkier Tyr preventing mupirocin from binding (Figure 1.15) (Serafini *et al*., 2011).

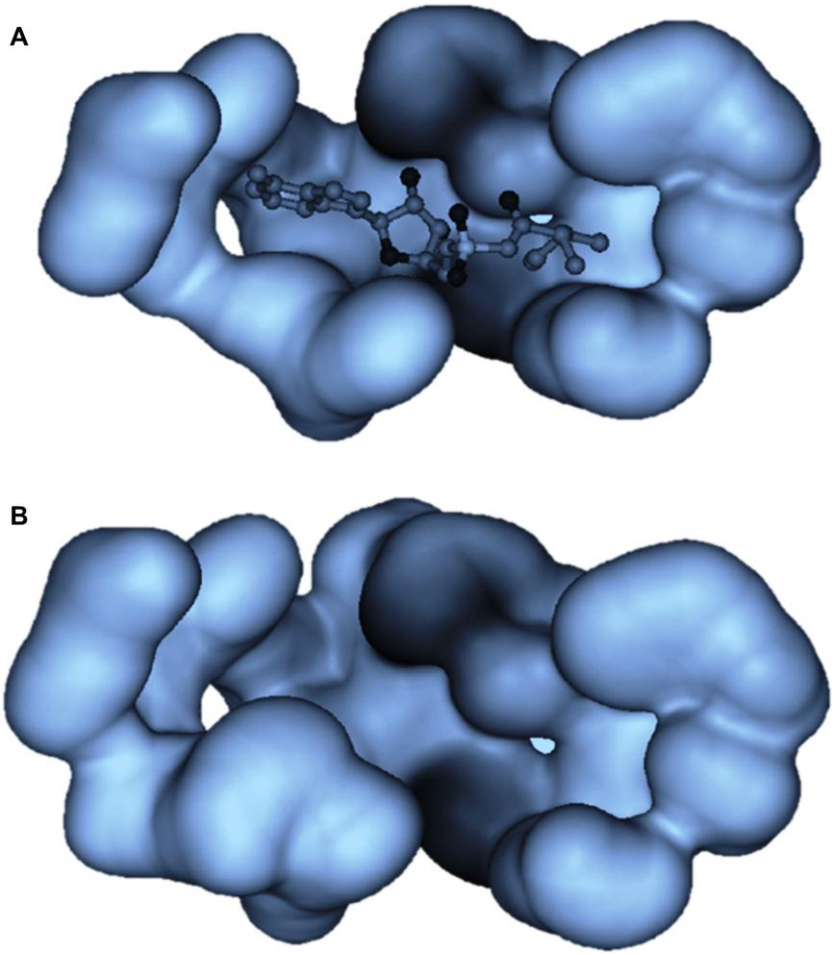

Figure 1.15. 3D structural model of the mupirocin binding site of isoleucyl-tRNA. (A) The binding site from the mupirocin-sensitive *Thermus thermophilus*. **(B)** The binding site from the mupirocin-resistant *Bifidobacterium bifidum* PRL2010 (Serafini *et al*., 2011).

Mupirocin resistance is increasing globally, and there are many examples of this. A study in Kuwait which sampled 53 MRSA isolates (74% of which expressed high level mupirocin resistance) reported a significant increase in the number of high level mupirocin-resistant MRSA isolates between 1993 and 1995; over the total study period (1990 to 1995) 42% of the isolates demonstrated high-level resistance (Udo *et al*., 1999; Vasquez *et al*., 2000). Between 1994 and 1995 at two closely situated hospitals in Brazil, resistance to mupirocin was >50% in one and approximately 6% in the other – the difference being that mupirocin was used far more frequently in the first hospital (Orrett, 2008). A recent study showed that high level mupirocin resistance was detected in 17% of patients involved, and this led to decolonisation failure (Gilpin *et al*., 2010).

In areas where mupirocin is readily available the occurrence of resistance is high: in New Zealand mupirocin became available over the counter in 1991 and by 1999 up to 28% of *S. aureus* isolates were mupirocin-resistant (Upton *et al*., 2003). After increased mupirocin use in Western Australia high level mupirocin resistance reached 15% but subsequent government issued guidance on limiting use reduced these levels to 0.3% after four years (Torvaldsen *et al*., 1999). In the Netherlands mupirocin use increased from 3.6kg/year in 2006 to 13.3kg/year in 2010, and concurrently mupirocin resistance detected in *Staphylococci* isolates increased from 8% in 2006 to 22% in 2011 (Bathoorn *et al*., 2012). Surveillance of mupirocin-resistant MRSA in 32 Canadian hospitals demonstrated that out of 4980 isolates, the prevalence of high level mupirocin resistance increased from 1.6% to 7% between 1995 and 2004 (Simor *et al*., 2007). Highly mupirocin-resistant strains of MRSA are not restricted to the clinical setting as they have been detected in community-

acquired strains, nor are they restricted to patients where prior use of mupirocin was documented (Udo and Sarkhoo, 2010; Nakajima *et al*., 2011). While it has been demonstrated that increased use of mupirocin is related to the increase in mupirocin-resistant MRSA occurrence (Caffrey *et al*., 2010), a study in France determined that a decrease in prevalence (10% in 2004 down to 3% in 2009) was not necessarily due to the parallel decreased volume of mupirocin used. The investigators postulated that it could instead be due to the way mupirocin was used, for example a controlled prescription for a period of time and refraining from using mupirocin if additional MRSA infection sites are known or if decolonisation fails (Talon *et al*., 2011).

Rather worryingly a new mupirocin resistance mechanism has been discovered in MRSA strains isolated in Canada. Encoded on a non-conjugative plasmid, the *mupB* gene is thought to be responsible for high level mupirocin resistance seen in cases where *mupA* was not present (Patel *et al*., 2009; Swenson *et al*., 2010; Seah *et al*., 2012). This newly identified gene encodes an IleS that shares 41.8% similarity and contains conserved motifs found in IleSs.

Among these studies a recurring conclusion is evident – surveillance and prudent use of mupirocin is vitally important and can reduce the levels of resistance. As a last line of defence against MRSA it is essential we preserve the use of mupirocin (Park *et al*., 2012). Again, continued research is required to find suitable alternatives should MRSA one day become totally mupirocin resistant. Already this research is producing novel ideas - REP8839 is a compound that inhibits methionyl-tRNA synthase and has been found to be effective against mupirocin-resistant MRSA (Critchley and Ochsner, 2008).

1.4 Non-ribosomal peptide synthases

The organisation of non-ribosomal peptide synthases (NRPSs) into modules within protein subunits is analogous to that of the organisation of PKS type I gene clusters and FASs. These multi-domain enzymes utilise the assembly line-like organisation in the catalytic reactions that produce structurally diverse antibiotics such as the penicillin precursor δ-(1-α-aminoadipyl)-1-cysteinyl-d-valine (ACV), tyrocidine, vancomycin and bactracin (Mootz *et al*., 2002; Walsh, 2003a; Schaffer and Otten, 2009). An initiation module, followed by elongation modules and a termination module comprise this assembly line. Domains of the elongation modules are condensation (C), adenylation (A), and the ACP equivalent peptidyl carrier protein (PCP) (Walsh, 2003a). The process begins by selection of an amino acid from a pool of substrates by the initiation A domain: aminoacyl adenylate is formed and transferred to the adjoining PCP; peptide bonds form between activated substrates on neighbouring PCPs by the actions of C domains; finally deacylation of the PCP results in the growing peptide chain being transferred to the next module (Figure 1.16) (Mootz *et al*., 2002; Schaffer and Otten, 2009). The single NRPS, ACV synthetase, is involved in the assembly of the precursor of the penicillins. Of the ten domains that make up the assembly line three are adenylation, each selecting for a different amino substrate. Consequently there are three PCP domains adjacent to the A domains. The C domain of module two catalyses the reaction to condense the first two amino acids, while the C domain of module 3 catalyses the condensation between the second and third amino acids. The enzyme also contains epimerisation and termination modules (Walsh, 2003a). The antibiotic bleomycin is a peptide-polyketide hybrid metabolite formed from a hybrid NRPS-PKS system. One PKS

gene containing KS, AT, MT, KR and ACP domains is sandwiched in between ten NRPS genes; during biosynthesis, one acetate and nine amino acids are incorporated into the bleomycin structure (Du *et al*., 2000).

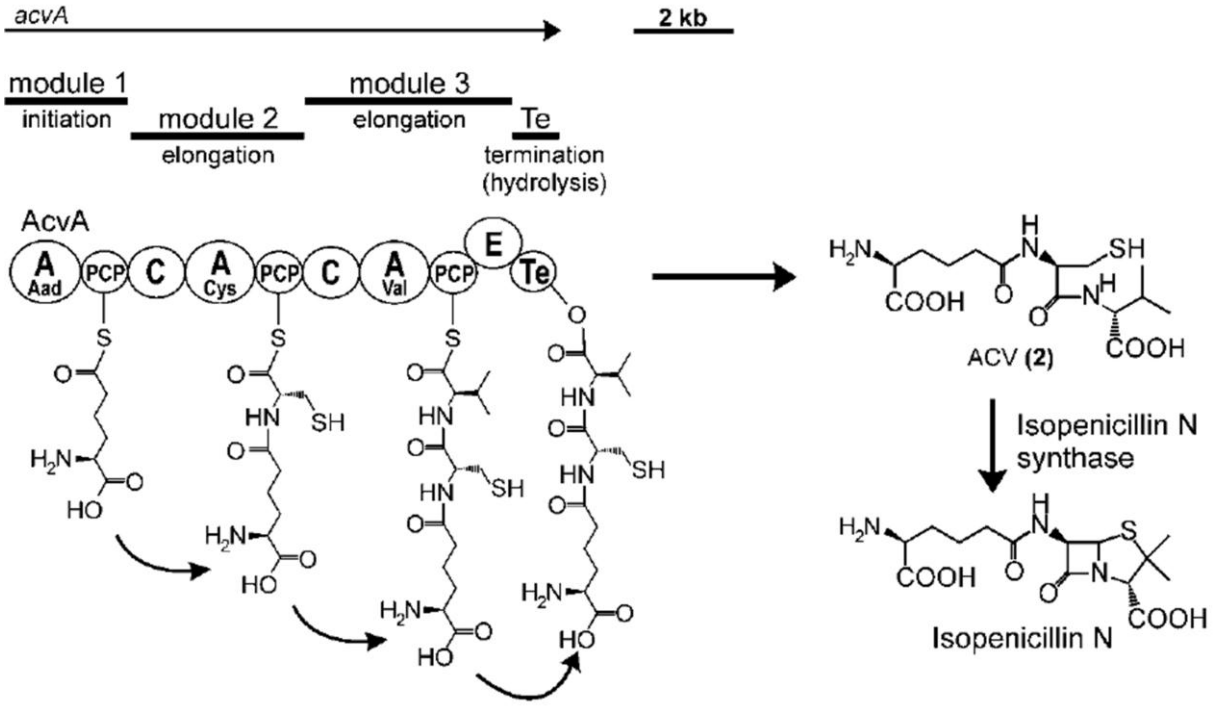

Figure 1.16. Biosynthesis scheme of the tripeptide penicillin precursor δ-(1-α-aminoadipyl)-1-cysteinyl-d-valine (ACV). The three core domains are arranged in the order A-C-PCP to add one amino acid to the growing chain. A, adenylation domain; C, condensation domain; PCP, peptidyl carrier protein; TE, thioesterase (Mootz *et al*., 2002).

1.4.1 The thiomarinols

The thiomarinols are antibiotics produced by the marine bacterium *Pseudoalteromonas* sp. SANK 73390. They have a chemical structure which is essentially a combination of two independent antibiotics, PA and holomycin (Figure 1.10, B). The pyrrothine moiety (holomycin) is attached to the marinolic acid portion (PA-like) via an amide bond (Shiozawa *et al*., 1993). With a broad range of activity

against both Gram-positive and Gram-negative bacteria, thiomarinol A displays far more potency than mupirocin; for example the activity is approximately twentyfold higher against organisms such as MRSA and *E. coli* (Shiozawa *et al*., 1993). The activity is also stronger than that of short chain pyrrothine antibiotics, such as holomycin, which displays tenfold less potent activity against *E. faecalis* (Oliva *et al*., 2001; Shiozawa *et al*., 1993). Thiomarinols B and E displayed excellent antimicrobial activity, similar to that of thiomarinol A, while thiomarinols C, D and F showed less potent activity (Shiozawa *et al*., 1995; 1997).

Recently, a 97kb plasmid encoding the hybrid PKS-NRPS thiomarinol production system from *Pseudoalteromonas* sp. SANK 73390 was identified (Figure 1.17). The plasmid included 27 PKS-encoding ORFs required for synthesis of the marinolic acid portion and 7 NRPS-encoding ORFs thought to be responsible for the pyrrothine moiety. Despite their similarity, there are several intriguing differences between the thiomarinol and mupirocin gene clusters: there are several extra ACPs throughout the cluster presumably increasing throughput (Rahman *et al*., 2005); there is an additional non-elongating KS (KS^0) on TmpB which forms an extra module with one of the additional ACPs; there is significant tailoring gene reorganisation; identification of possible operator sequences suggests five transcriptional units; and there is no evidence for regulatory genes such as the mupirocin quorum sensing system of *mupR/mupI* (Fukuda *et al*., 2011). The thiomarinol homologue of mup-mAcpE appears to be missing, and so it has been suggested that the late tailoring steps may occur on the extra module in TmpB, in particular removal of the C_8 hydroxyl group after pyran ring formation (completed by mupU/mAcpE in the mupirocin system) (Thomas, 2012). Recent research in the Thomas laboratory has

demonstrated that deleting the extra module from TmpB causes a reduced amount of thiomarinol A and B to be produced, but increased amount of thiomarinol G production (Omer-Bali, 2012).

During the elucidation of the thiomarinol production pathway several novel metabolites were generated, some of which were shown to have activity against *Bacillus subtilis* and MRSA (Murphy *et al*., 2011). This highlights the potential of using mutation and mutasynthesis to generate novel antibiotics with significant clinical applications in the future.

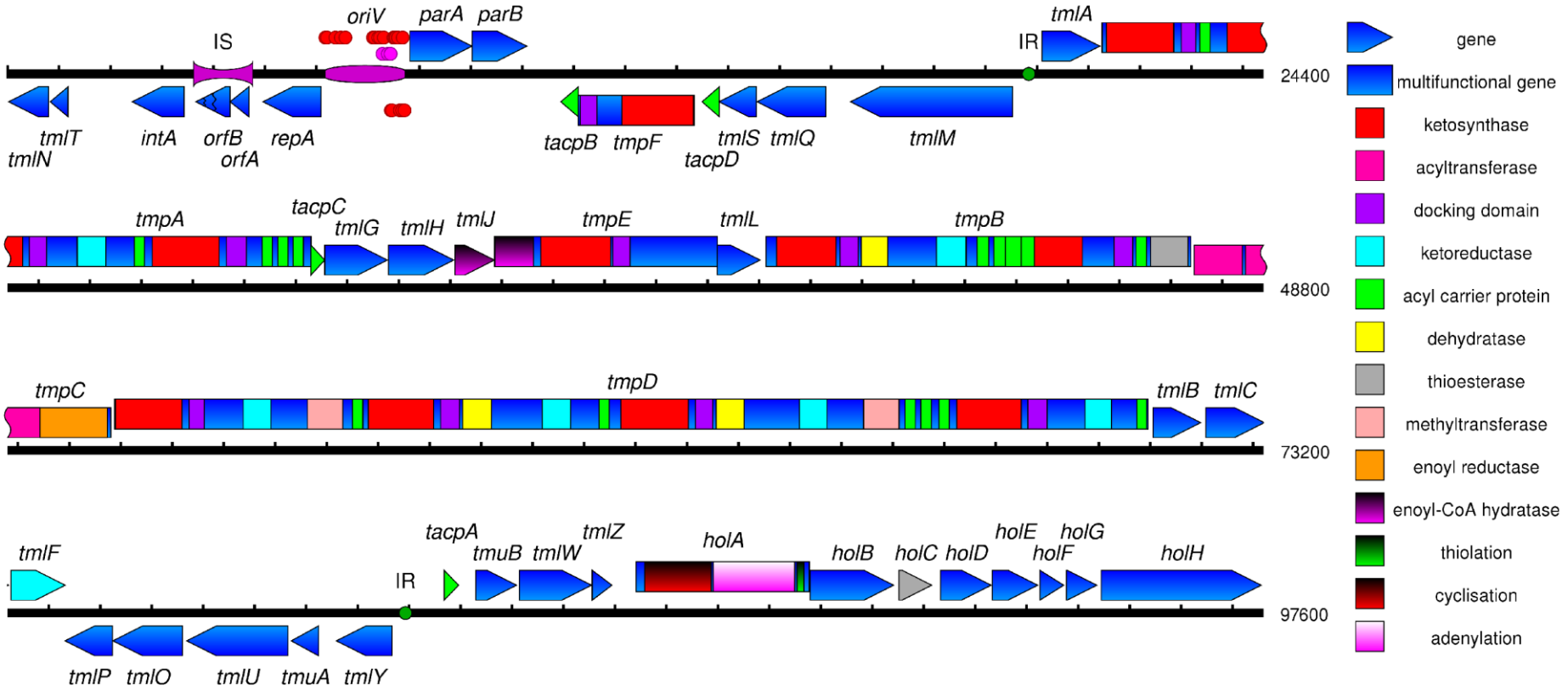

Figure 1.17. Map of pTML1. Predicted protein coding genes are shown, with predicted biosynthesis domains colour coded. Modules are identifiable by segments of megaproteins running from a ketosynthase (KS) (red) to an acyl carrier protein (ACP) (green). Like the mupirocin biosynthetic genes the thiomarinol genes belong to the *trans*-AT synthases that encode separate acyltransferases (AT). Linked to each KS domain is an adjacent docking domain. (Fukuda *et al.*, 2011)

1.5 Statement of objectives

Research in the Thomas laboratory at The University of Birmingham has focussed on mupirocin for nearly 13 years, and during that time much has been learnt about the pathway and the processes that are involved in synthesising this important antibiotic. Despite this, however, there remains much to be understood and there are many pathways the research could take in the future. The objectives of the project as a whole were to completely understand the mupirocin biosynthesis pathway, with the aim of producing novel compounds and concurrently contributing valuable information to the growing group of PKSs known as *trans*-AT PKSs.

The *trans*-AT group of PKSs is a rapidly growing group and more and more information is being elucidated each year. However one of the critical aspects of these pathways remains poorly understood – that of the functions of the ATs. Out of the 30 or so systems characterised that employ *trans*-ATs, only a few of the ATs have been fully characterised themselves. This study is particularly focussed on two of the domains of *mmpC* – the ATs. The immediate objectives were to purify the ATs to produce soluble protein and to determine the substrates they interact with by biochemical characterisation. The successful purification of AT2 led to characterisation, however, AT1 turned out to be more problematic, as described in Chapters 3 and 4.

An alternative method for the investigation of AT1 was developed – point mutations were introduced into the AT2-containing plasmid in an attempt to make it more AT1-like. Chapter 5 shows that mutant proteins were produced and characterised by enzyme assays and autoradiography, in addition to performing circular dichroism to analyse the structural changes caused by the mutations.

This method of investigating AT1 in turn led to a further method – introducing point mutations into the *P. fluorescens* NCIMB 10586 chromosome. This work was jointly planned by C. M. Thomas, myself and Harry Thorpe, an undergraduate project student I was supervising at the time. Harry designed the primers required for introducing the mutations and performed the molecular biology, bioassays and HPLC. Further analysis of the mutant strains by LCMS was performed at The University of Bristol by Zhongshu Song. The data was analysed and interpreted by myself and is presented in Chapter 6.

Docking domains have been documented in *trans*-AT systems for the last 10 years. Little was known about them, and very few functional studies had been performed. As they were thought to be remnants of once functional *cis*-acting ATs it seemed prudent that their investigation be included in this study. *P. fluorescens* NCIMB 10586 deletion mutants were designed to delete regions thought to be structural or functional and the subsequent mutant strains analysed by bioassay and HPLC. Again, further analysis of the mutant strains by LCMS was performed at The University of Bristol by Zhongshu Song. Chapter 7 describes the results and conclusions from this particular sub-project.

Research in the Thomas laboratory at The University of Birmingham was already underway investigating β-branching ACPs, which appear to be another common feature among *trans*-AT PKSs, although not restricted to this group. Bioinformatic studies by Dong *et al*., (manuscript in preparation, 2012) had identified a conserved Trp residue in ACPs thought to be important for HCS recognition. A W>L mutation was introduced into ACP3 and 4 and this was introduced into the *P. fluorescens* NCIMB 10586 chromosome. Results demonstrated the importance of

this residue as no PA-A was produced. In order to fully assess the phenotype of the mutated ACP a project was designed to purify ACP3 (ACP4 was tricky to work with). An undergraduate project student, Erika Yamada, designed primers to amplify the mutated ACP and performed the molecular biology. However the mutant displayed additional residues which required excising from the plasmid. Chapter 8 describes this work, along with the phenotypical characterisation which was performed by myself – phosphopantetheinylation of the ACP and subsequent malonylation by AT2.

There are many directions this work could take, and these are further described in later sections. It is hoped that the work described thereafter contributes not only to the field of polyketides but also to protein biology and antibiotic resistance.

CHAPTER 2

2 MATERIALS AND METHODS

2.1 Bacterial strains, culture conditions and plasmids

Bacterial strains used in this study are detailed in Table 2.1. *Pseudomonas fluorescens* NCIMB 10586 was grown in L broth or L agar, supplemented with 50 µg/ml ampicillin at 30ºC. Plasmids were initially transformed into *Escherichia coli* strain DH5α, ahead of transformations into strain BL21 (DE3) for working cultures. *E. coli* Lemo21 (DE3) was used for expression of clones prone to insolubility. *E. coli* S17-1 was utilised to mobilise vectors into *P. fluorescens* by conjugation. *E. coli* XL10-Gold ultra-competent cells were used for the transformation of mutant plasmids. *Bacillus subtilis* 1064 was used as an indicator strain in bioassays. *E. coli* and *B. subtilis* strains were grown in L broth or on L agar, supplemented with appropriate antibiotics at 37ºC overnight. Antibiotics used in this study are listed in Table 2.2. The pET vector system was used for the cloning and expression of recombinant proteins in *E. coli*; pGEM-T-Easy was used to clone polymerase chain reaction (PCR) products for sequencing; pSUEH was incorporated into various transformants to maximise the solubility of recombinant proteins; pAKE604 was the suicide vector used to introduce chromosomal deletions. Plasmids used and constructed in this study are detailed in Tables 2.3-2.8, according to the relevant chapter.

Table 2.1. Bacterial strains used in this study.

Bacterial strain	Genotype/phenotype	Source/ reference
B. subtilis 1064	*trpC2amyE::(spec* P_{xyl}*-gfp-lacI) chr::*pSG1196 *(rrnD-lacO cat)*	Moir *et al*., 1979
E. coli BL21 (DE3)	F^- *ompT hsd*SB *gal dcm* (DE3) All-purpose strain for high-level protein expression and easy induction. Contains the DE3 lysogen that carries the gene for T7 RNA polymerase under the control of the *lac*UV5 promoter.	Invitrogen
E. coli DH5α	*end*A1 *recA hsd*R17 *lac*ZΔM15 *supE44 gyrA96 thi-I rel*A1 F^- High transformation efficiency strain. Supports blue/white screening utilising the activity of β-galactosidase.	Gibco BRL
E. coli Lemo21 (DE3)	F^- *ompT hsd*SB *gal dcm* (DE3) *fhuA2 lysY p*Lemo Cm^R Contains the host features of BL21 (DE3) while allowing for tuneable expression of difficult clones. Tuneable expression is achieved by varying the level of lysozyme (*lysY)* the natural inhibitor of T7 RNA polymerase.	NEB
E. coli S17-1	*RecA pro hsdR RP4-2 Tc::Mu-Km::Tn7*	Simon *et al*., 1983
E. coli XL10-Gold	Tet^R Δ(*mcrA*)*183* Δ (*mcrCB-hsdSMR-mrr*)*173 endA1 supE44 thi-1 recA1 gyrA96 relA1 lac* Hte [F´ *proAB* $lacI^q$*ZΔM15* Tn*10* (Tet^R) Amy Chl^R]	Logan, 2012
P. fluorescens NCIMB 10586	Mupirocin-producer wild type (WT). Amp^R	G.T. Banks

Table 2.2. Antibiotics used in this study.

Antibiotic	Working concentration (µg/ml)	Medium
Ampicillin	50	H_2O
Carbenicillin	50	H_2O
Chloramphenicol	34	70% C_2H_6O
Kanamycin sulphate	50	H_2O
Tetracycline hydrochloride	15	70% C_2H_6O

Table 2.3. Plasmids used in Chapter 3.

Plasmid	Size (kb)	Properties	Source/ reference
pET28a	5.4	Kan^R, T7*lac* promoter, N-terminus His•Tag	Novagen
pET28b	5.4	Kan^R, T7*lac* promoter, C-terminus His•Tag	Novagen
pGBT340	5.3	Modified pET28a without T7 tag. Kan^R	Jagura-Burdzy *et al*., 1999
pGEM-T-Easy	3.0	Amp^R, *lacZα*. Linear T-tailed plasmid for cloning PCR products. Blue/white screening	Promega
pGEX-2t	4.9	Amp^R, *tac* `promoter, N-terminus GST•Tag	G. E. Healthcare
pJH10	14.5	IncQ. pOLE1 IncC1 deleted. Tet^R (from pDM1.2) *ori*T	El Sayed *et al*., 2001
pJHN11	15.4	851bp MupN fragment cloned into pJH10	Hothersall *et al*., 2007
pJS551	5.6	303bp *Eco*RI-*Hind*III mAcpA fragment cloned into pGBT340	Shields, 2008
pJS552	5.6	249bp *Eco*RI-*Hind*III mAcpB fragment cloned into pGBT340	Shields, 2008
pJS553	5.5	234bp *Eco*RI-*Hind*III mAcpC fragment cloned into pGBT340	Shields, 2008
pJS554	5.6	318bp *Eco*RI-*Hind*III mAcpD fragment cloned into pGBT340	Shields, 2008
pJS555	5.5	240bp *Eco*RI-*Sac*I mAcpE fragment cloned into pGBT340	Shields, 2008
pJS559	6.4	959bp *Eco*RI-*Sac*I AT1 fragment cloned into pET28a	Shields, 2008
pJS560	6.4	971bp *Eco*RI-*Sac*I AT2 fragment cloned into pET28a	Shields, 2008
pJS561	5.7	267bp *Bam*HI-*Eco*RI ACP1 fragment cloned into pET28a	Shields, 2008
pJS5610	5.7	273bp *Bam*HI-*Eco*RI ACP10 fragment cloned into pET28a	Shields, 2008
pJS5611	5.7	267bp *Bam*HI-*Eco*RI ACP11 fragment cloned into pET28a	Shields, 2008
pJS562	5.7	267bp *Bam*HI-*Eco*RI ACP2 fragment cloned into pET28a	Shields, 2008

pJS563	5.7	270bp *Eco*RI-*Sac*I ACP3 fragment cloned into pET28a	Shields, 2008
pJS564	5.7	267bp *Bam*HI-*Eco*RI ACP4 fragment cloned into pET28a	Shields, 2008
pJS565	5.7	273bp *Bam*HI-*Eco*RI ACP5 fragment cloned into pET28a	Shields, 2008
pJS566	5.7	273bp *Bam*HI-*Eco*RI ACP6 fragment cloned into pET28a	Shields, 2008
pJS567	5.7	273bp *Bam*HI-*Eco*RI ACP7 fragment cloned into pET28a	Shields, 2008
pJS568	5.7	270bp *Bam*HI-*Eco*RI ACP8 fragment cloned into pET28a	Shields, 2008
pJS569	5.7	279bp *Bam*HI-*Eco*RI ACP9 fragment cloned into pET28a	Shields, 2008
pRG300	4.0	1kb *Xho*I-*Nco*I fragment encoding linker-AT1 cloned into pGEM-T-Easy	This study
pRG301	6.4	959bp *Eco*RI-*Sac*I AT1 fragment cloned into pET28b with 10 residue linker	This study
pRG302	6.4	959bp *Eco*RI-*Sac*I AT1 fragment cloned into pET28b	This study
pRG303	6.4	959bp *Eco*RI-*Sac*I AT1 fragment cloned into pET28a with 15 residue linker	This study
pRG304	5.9	959bp *Eco*RI-*Sac*I AT1 fragment cloned into pGEX-2t	This study
pRG305	6.4	938bp *Eco*RI-*Sac*I tml-AT1 fragment cloned into pET28a	This study
pRG306	6.4	974bp *Eco*RI-*Sac*I tml-AT2 fragment cloned into pET28a	This study
pSUEH	4.5	Chl^R, *lac* and GroEL promoters	Lund, 1993

Table 2.4. Plasmids used in Chapter 4.

Plasmid	Size (kb)	Properties	Source/ reference
pET28a	5.4	Kan^R, T7*lac* promoter, N-terminus His•Tag	Novagen
pGBT340	5.3	Modified pET28a without T7 tag. Kan^R	Jagura-Burdzy *et al*., 1999
pJH10	14.5	IncQ. pOLE1 IncC1 deleted. Tet^R (from pDM1.2) *ori*T	El Sayed *et al*., 2001
pJHN11	15.4	851bp MupN fragment cloned into pJH10	Hothersall *et al*., 2007
pJS553	5.5	234bp *Eco*RI-*Hind*III mAcpC fragment cloned into pGBT340	Shields, 2008
pJS554	5.6	318bp *Eco*RI-*Hind*III mAcpD fragment cloned into pGBT340	Shields, 2008
pJS560	6.4	971bp *Eco*RI-*Sac*I AT2 fragment cloned into pET28a	Shields, 2008
pJS561	5.7	267bp *Bam*HI-*Eco*RI ACP1 fragment cloned into pET28a	Shields, 2008
pJS563	5.7	270bp *Eco*RI-*Sac*I ACP3 fragment cloned into pET28a	Shields, 2008
pJS565	5.7	273bp *Bam*HI-*Eco*RI ACP5 fragment cloned into pET28a	Shields, 2008
pJS568	5.7	270bp *Bam*HI-*Eco*RI ACP8 fragment cloned into pET28a	Shields, 2008

Table 2.5. Plasmids used in Chapter 5.

Plasmid	Size (kb)	Properties	Source/ reference
pET28a	5.4	Kan^R, T7*lac* promoter, N-terminus His•Tag	Novagen
pGBT340	5.3	Modified pET28a without T7 tag. Kan^R	Jagura-Burdzy *et al*., 1999
pJH10	14.5	IncQ. pOLE1 IncC1 deleted. Tet^R (from pDM1.2) *ori*T	El Sayed *et al*., 2001
pJHN11	15.4	851bp MupN fragment cloned into pJH10	Hothersall *et al*., 2007
pJS553	5.5	234bp *Eco*RI-*Hind*III mAcpC fragment cloned into pGBT340	Shields, 2008
pJS560	6.4	971bp *Eco*RI-*Sac*I AT2 fragment cloned into pET28a	Shields, 2008
pJS561	5.7	267bp *Bam*HI-*Eco*RI ACP1 fragment cloned into pET28a	Shields, 2008
pJS563	5.7	270bp *Eco*RI-*Sac*I ACP3 fragment cloned into pET28a	Shields, 2008
pJS565	5.7	273bp *Bam*HI-*Eco*RI ACP5 fragment cloned into pET28a	Shields, 2008
pRG501	6.4	971bp *Eco*RI-*Sac*I fragment encoding AT2 H89S cloned into pET28a	This study
pRG502	6.4	971bp *Eco*RI-*Sac*I fragment encoding AT2 R115Q cloned into pET28a	This study
pRG503	6.4	971bp *Eco*RI-*Sac*I fragment encoding AT2 M119F cloned into pET28a	This study
pRG504	6.4	971bp *Eco*RI-*Sac*I fragment encoding AT2 S190N cloned into pET28a	This study
pRG505	6.4	971bp *Eco*RI-*Sac*I fragment encoding AT2 A191R cloned into pET28a	This study
pRG506	6.4	971bp *Eco*RI-*Sac*I fragment encoding AT2 N224S cloned into pET28a	This study
pRG507	6.4	971bp *Eco*RI-*Sac*I fragment encoding AT2 Q242V cloned into pET28a	This study
pRG508	6.4	971bp *Eco*RI-*Sac*I fragment encoding AT2 V247L cloned into pET28a	This study
pRG509	6.4	971bp *Eco*RI-*Sac*I fragment encoding AT2 S190V and A191R cloned into pET28a	This study

pRG510	6.4	971bp *Eco*RI-*Sac*I fragment encoding AT2 R115Q and Q242V cloned into pET28a	This study
pRG511	6.4	971bp *Eco*RI-*Sac*I fragment encoding AT2 R115Q, Q242V, S190N and A191R cloned into pET28a	This study
pRG512	6.4	971bp *Eco*RI-*Sac*I fragment encoding AT2 H89S and Q242V cloned into pET28a	This study
pRG513	6.4	971bp *Eco*RI-*Sac*I fragment encoding AT2 H89S, Q242V and R115Q cloned into pET28a	This study
pRG514	6.4	971bp *Eco*RI-*Sac*I fragment encoding AT2 H89S, Q242V, R115Q and V247L cloned into pET28a	This study
pRG515	6.4	971bp *Eco*RI-*Sac*I fragment encoding AT2 S190N, A191R and M119F cloned into pET28a	This study
pRG516	6.4	971bp *Eco*RI-*Sac*I fragment encoding AT2 H89S and R115Q cloned into pET28a	This study
pRG517	6.4	971bp *Eco*RI-*Sac*I fragment encoding AT2 R115Q, Q242V, S190N, A191R and V247L cloned into pET28a	This study
pRG518	6.4	971bp *Eco*RI-*Sac*I fragment encoding AT2 R115Q, Q242V, S190N, A191R, V247L and M119F cloned into pET28a	This study

Table 2.6. Plasmids used in Chapter 6.

Plasmid	Size (kb)	Properties	Source/ reference
pAKE604	7.2	pMB1 replicon. Amp^R, Km^R, *oriT, lacZα, sacB*	El-Sayed *et al*., 2001
pET28a	5.4	Kan^R, T7*lac* promoter, N-terminus His•Tag	Novagen
pGEM-T-Easy	3.0	Amp^R, *lacZα*. Linear T-tailed plasmid for cloning PCR products. Blue/white screening	Promega
pHT601	4.0	1kb *Hind*III-*Xba*I fragment encoding AT1 S95H cloned into pGEM-T-Easy	This study/Harry Thorpe
pHT602	4.0	1kb *Pst*I-*Xba*I fragment encoding AT2 H89S cloned into pGEM-T-Easy	This study/Harry Thorpe
pHT603	8.2	1kb *Hind*III-*Xba*I fragment encoding AT1 S95H cloned into pAKE604	This study/Harry Thorpe
pHT604	8.2	1kb *Eco*RI-*Xba*I fragment encoding AT2 H89S cloned into pAKE604	This study/Harry Thorpe
pRG605	6.4	959bp *Eco*RI-*Sac*I fragment encoding AT1 S95H cloned into pET28a	This study

Table 2.7. Plasmids used in Chapter 7.

Plasmid	Size (kb)	Properties	Source/ reference
pAKE604	7.2	pMB1 replicon. Amp^R, Km^R, *oriT, lacZα, sacB*	El-Sayed *et al*., 2001
pGEM-T-Easy	3.0	Amp^R, *lacZα*. Linear T-tailed plasmid for cloning PCR products. Blue/white screening	Promega
pRG701	3.5	500bp *Eco*RI-*Sal*I fragment (*mmpA* region 1 upstream arm) cloned into pGEM-T-Easy	This study
pRG702	3.5	500bp *Sal*I-*Bam*HI fragment (*mmpA* region 1 downstream arm) cloned into pGEM-T-Easy	This study
pRG703	3.5	500bp *Eco*RI-*Sal*I fragment (*mmpA* region 2 upstream arm) cloned into pGEM-T-Easy	This study
pRG704	3.5	500bp *Sal*I-*Bam*HI fragment (*mmpA* region 2 downstream arm) cloned into pGEM-T-Easy	This study
pRG705	3.5	500bp *Eco*RI-*Hind*III fragment (*mmpD* region 1 upstream arm) cloned into pGEM-T-Easy	This study
pRG706	3.5	500bp *Hind*III-*Bam*HI fragment (*mmpD* region 1 downstream arm) cloned into pGEM-T-Easy	This study
pRG707	3.5	500bp *Eco*RI-*Hind*III fragment (*mmpD* region 2 upstream arm) cloned into pGEM-T-Easy	This study
pRG708	3.5	500bp *Hind*III-*Bam*HI fragment (*mmpD* region 2 downstream arm) cloned into pGEM-T-Easy	This study
pRG710	8.2	1kb *Eco*RI-*Bam*HI fragment (deletion of *mmpA* DD region 1 – ΔA1) cloned into pAKE604	This study
pRG711	8.2	1kb *Eco*RI-*Bam*HI fragment (deletion of *mmpA* DD region 2 – ΔA2) cloned into pAKE604	This study
pRG712	8.2	1kb *Eco*RI-*Bam*HI fragment (deletion of *mmpA* DD – ΔA3) cloned into pAKE604	This study
pRG713	8.2	1kb *Eco*RI-*Bam*HI fragment (deletion of *mmpD* DD region 1 – ΔD1) cloned into pAKE604	This study
pRG714	8.2	1kb *Eco*RI-*Bam*HI fragment (deletion of *mmpD* DD region 2 – ΔD2) cloned into pAKE604	This study
pRG715	8.2	1kb *Eco*RI-*Bam*HI fragment (deletion of *mmpD* DD – ΔD3) cloned into pAKE604	This study

Table 2.8. Plasmids used in Chapter 8.

Plasmid	Size (kb)	Properties	Source/ reference
pET28a	5.4	Kan^R, T7*lac* promoter, N-terminus His•Tag	Novagen
pEY801	3.3	270bp *Eco*RI-*Sac*I fragment encoding ACP3 W55L cloned into pGEM-T-Easy	This study/Erika Yamanda
pEY802	5.7	270bp *Eco*RI-*Sac*I fragment encoding ACP3 W55L cloned into pET28a	This study/Erika Yamanda
pGEM-T-Easy	3.0	Amp^R, *lacZα*. Linear T-tailed plasmid for cloning PCR products. Blue/white screening	Promega
pJH10	14.5	IncQ. pOLE1 IncC1 deleted. Tet^R (from pDM1.2) *ori*T	El Sayed *et al*., 2001
pJHN11	15.4	851bp MupN fragment cloned into pJH10	Hothersall *et al*., 2007
pJS562	6.4	971bp *Eco*RI-*Sac*I AT2 fragment cloned into pET28a	Shields, 2008
pJS563	5.7	270bp *Eco*RI-*Sac*I ACP3 fragment cloned into pET28a	Shields, 2008

2.2 Polymerase chain reaction

Polymerase chain reaction (PCR) was used to amplify segments of DNA from *P. fluorescens* NCIMB 10586. The bacterial chromosomal DNA template was prepared by adding one colony to 30µl of sdH_2O and boiling for 10min, before centrifugation. 20µl of the supernatant was transferred to a fresh tube and held on ice until required. If plasmid DNA was to be used as a template, dilutions were used to determine the optimal concentration of plasmid DNA to be used, i.e. 1/10 or 1/100 diluted with 1/10 TNE buffer (100mM Tris pH 8.0, 50mM NaCl, 5mM EDTA pH 8.0) and added to the reaction mixture. Primers were synthesised by Alta Bioscience of the University of Birmingham, and were diluted to 15pmole/µl prior to use (Table 2.9 – Table 2.13). Generally the BIO-X-ACT long DNA polymerase kit (Bioline) was used for amplification for DNA cloning. PCR for screening was performed with *Taq* polymerase (Invitrogen), if it was required. Annealing temperatures were calculated according to the melting temperature (T_m) of the primer. The melting temperature was calculated using the following equation:

$$T_m = 4\,(G + C) + 2\,(A + T)\ \ °C$$

Table 2.9. Primers used in Chapter 3.

Name	Template DNA	Sequence	Purpose	Restriction sites
AT1BF	*P. fluorescens* NCIMB 10586	CCATGGGCGTGTCCATTGTTTTCATGTTTTC	Clone AT1 and a 10 residue linker into pET28b	*Nco*I *Sal*I
AT1BR	*P. f.* 10586	CTCGAGCGCGCCCGCGCCCGCGCCCGCGCCCGCGCCGTCGACCGCGCTGACAACGCGCTGTGC		*Xho*I *Sal*I
LINKAF1	*P. f.* 10586	GGATCCGGCGCGGGCGCGGGCGCGGACGGCGCGTCGGCGCGGGCGCGGGCGCGG	Linker for pJS561	*Bam*HI *Ahd*I
LINKAR1	*P. f.* 10586	GCGCGCCCGCGCCCTGGCCCGCAGCGCGCCCGCGCCCGCGCGAATTC		*Ahd*I *Eco*RI
AT1pGEXF	*P. f.* 10586	CTCCCGGGGTGTCCATTGTTTTCATGTTT	Clone AT1 into pGEX-2t vector	*Sma*I
AT1pR	*P. f.* 10586	GCTGAATTCTCACGCGCTGACAACGCGC		*Eco*RI

Bases underlined correspond to restriction sites.

Table 2.10. Primers used in Chapter 5.

Name	Template DNA	Sequence	Purpose	Restriction sites
91F2	pET28a-AT2	GTGGTATGTGCTCGGGTCCAGCCTCGGCGAG	AT2 H89S mutation	-
91R2		CTCGCCGAGGCTGGACCCGAGCACATACCAC		-
117F3	pET28a-AT2	CTGGTCAAGCGGCAGGGCGAACTCATG	AT2 R115Q mutation	-
117R3		CATGAGTTCGCCCTGCCGCTTGACCAG		-
121F	pET28a-AT2	GGCGAACTCTTCTCCGAGGCCACC	AT2 M119F mutation	-
121R		GGTGGCCTCGGAGAAGAGTTCGCC		-
197F	pET28a-AT2	GCGTTGAATGTCAACGCGCCTTTCCAC	AT2 S190N mutation	-
197R3		GTGGAAAGGCGCGTTGACATTCAACGC		-
198F	pET28a-AT2	GCGTTGAATGTCAGCCGGCCTTTCCACTCC	AT2 A191R mutation	-
198R		GGAGTGGAAAGGCCGGCTGACATTCAACGC		-
231F	pET28a-AT2	CCGGTGATCGCCAGTGTCGACGCACGC	AT2 N224S mutation	-
231R		GCGTGCGTCGACACTGGCGATCACCGG		-
250F	pET28a-AT2	CAGTTGGCGCGGGTAATGACGTCATCG	AT2 Q242V mutation	-
250R		CGATGACGTCATTACCCGCGCCAACTG		-
255F	pET28a-AT2	GACGTCATCGCTGCAGTGGGTCG	AT2 V247L mutation	-
255R		CGACCCACTGCAGCGATGACGTC		-

17F	pET28a-AT2	GCGTTGAATGTCAACCGGCCTTTCCACTCC	AT2 S190N and A191R mutations	-
17R		GGAGTGGAAAGGCCGGTTGACATTCAACGC		-
250F	pET28a-AT2 R115Q	CAGTTGGCGCGGGTAATGACGTCATCG	AT2 R115Q and Q242V mutations	-
250R		CGATGACGTCATTACCCGCGCCAACTG		-
17F	pET28a-AT2 R115Q and Q242V	GCGTTGAATGTCAACCGGCCTTTCCACTCC	AT2 R115Q, Q242V, S190N and A191R mutations	-
17R		GGAGTGGAAAGGCCGGTTGACATTCAACGC		-
17F	pET28a-AT2 R115Q, Q242V, S190N, and A191R	GCGTTGAATGTCAACCGGCCTTTCCACTCC	AT2 R115Q, Q242V, S190N, A191R and V247L mutations	-
17R		GGAGTGGAAAGGCCGGTTGACATTCAACGC		-
121F	pET28a-AT2 R115Q, Q242V, S190N, A191R and V247L	GGCGAACTCTTCTCCGAGGCCACC	AT2 R115Q, Q242V, S190N, A191R, V247L and M119F mutations	-
121R		GGTGGCCTCGGAGAAGAGTTCGCC		-
121F	pET28a-AT2 S190N and A191R	GGCGAACTCTTCTCCGAGGCCACC	AT2 S190N, A191R and M119F mutations	-
121R		GGTGGCCTCGGAGAAGAGTTCGCC		-

117F3	pET28a-AT2 H89S	CTGGTCAAGCGGCAGGGCGAACTCATG	AT2 H89S and R115Q mutations	-
117R3		CATGAGTTCGCCCTGCCGCTTGACCAG		-
250F	pET28a-AT2 H89S	CAGTTGGCGCGGGTAATGACGTCATCG	AT2 H89S and Q242V mutations	-
250R		CGATGACGTCATTACCCGCGCCAACTG		-
117F3	pET28a-AT2 H89S and Q242V	CTGGTCAAGCGGCAGGGCGAACTCATG	AT2 H89S, Q242V and R115Q mutations	-
117R3		CATGAGTTCGCCCTGCCGCTTGACCAG		-
255F	pET28a-AT2 H89S, Q242V and R115Q	GACGTCATCGCTGCAGTGGGTCG	AT2 H89S, Q242V, R115Q and V247L mutations	-
255R		CGACCCACTGCAGCGATGACGTC		-

Table 2.11. Primers used in Chapter 6.

Name	Template DNA	Sequence	Purpose	Restriction sites
AT1F1	*P. fluorescens* NCIMB 10586	GCGAAGCTTCCATGTGGCCACGGTGGACG	AT1 S95H mutation	*Hind*III
AT1R1	*P. f.* 10586	CAGGCTATGGCCAAGTACATGGTCGGGGTATACACCG		*Msc*I
AT1F2	*P. f.* 10586	GTACTTGGCCATAGCCTGGGAGAAGTGGCTGCG		*Msc*I
AT1R2	*P. f.* 10586	CCCTCTAGAGGCCTTCAAGGTATTCAATGGCGG		*Xba*I
AT2F1	*P. f.* 10586	GCGCCATGGTGGTGCGCTCGACACTGCAG	AT2 H89S mutation	*Nco*I/*Pst*I
AT2R1	*P. f.* 10586	GAGGCTCGAGCCGAGCACATAGTCGGGGGGC		*Xho*I
AT2F2	*P. f.* 10586	GCTCGGCTCGAGCCTCGGCGAGTTCTGCGC		*Xho*I
AT2R2	*P. f.* 10586	GGCTCTAGACTCGATGCTTTCGACCCACTGC		*Xba*I
AT1MF	pET28a-AT1	CATGTACTCGGCCACAGCCTGGGAGAAGTG	AT1 S95H mutation	-
AT1MR	pET28a-AT1	CACTTCTCCCAGGCTGTGGCCGAGTACATG		-

Bases underlined correspond to restriction sites.

Table 2.12. Primers used in Chapter 7.

Name	Template DNA	Sequence	Purpose	Restriction sites
A1F1	*P. fluorescens* NCIMB 10586	CCGAATTCACCCCGTGGCAGATATCGCTG	Deletion of *mmpA* DD region 1 (arm 1)	*Eco*RI
A1R1	*P. f.* 10586	CCGTCGACGCACAGCGTCGGCTCATCGATC		*Sal*I
A1F2	*P. f.* 10586	CCGTCGACTTACACACGGGCGATCTTACGGGC	Deletion of *mmpA* DD region 1 (arm 2)	*Sal*I
A1R2	*P. f.* 10586	CCGGATCCTAAGGGGCGGCAATGCGCTGC		*Bam*HI
A2F1	*P. f.* 10586	CCGAATTCTTCATAAAATCCTCGACTTTGAACAGC	Deletion of *mmpA* DD region 2 (arm 1)	*Eco*RI
A2R1	*P. f.* 10586	CCGTCGACCTCGGCCCAAGGGTCAAGCGC		*Sal*I
A2F2	*P. f.* 10586	CCGTCGACTATGACGCGCCTGCACCCATG	Deletion of *mmpA* DD region 2 (arm 2)	*Sal*I
A2R2	*P. f.* 10586	CCGGATCCCGCTGGCGGTCCGCGTTAAAATGC		*Bam*HI
D1F1	*P. f.* 10586	CCGAATTCAAGCCCATGGCACCGGCACC	Deletion of *mmpD* DD region 1 (arm 1)	*Eco*RI
D1R1	*P. f.* 10586	CCAAGCTTGCTGGCAGATGCGCCGGCAC		*Hind*III
D1F2	*P. f.* 10586	CCAAGCTTGCCTCGCAGGCCGAGGTCCAG	Deletion of *mmpD* DD region 1 (arm 2)	*Hind*III
D1R2	*P. f.* 10586	CCGGATCCGCCCCGGCGCTTGCTGGTCG		*Bam*HI
D2F1	*P. f.* 10586	CCGAATTCTCTACCCGGTGACCCGCCTG	Deletion of *mmpD* DD region 2 (arm 1)	*Eco*RI
D2R1	*P. f.* 10586	CCAAGCTTCTCGGCCAGCGTTTGCAGGTG		*Hind*III
D2F2	*P. f.* 10586	CCAAGCTTTTGCCGACCGCGCCGACCGATC	Deletion of *mmpD* DD region 2 (arm 2)	*Hind*III
D2R2	*P. f.* 10586	CCGGATCCGGCACCACGACCAACGCCAGC		*Bam*HI
A2R3	*P. f.* 10586	CTTTTACCCTCTTGGATCGC	To check product of *mmpA* deletion	-

Bases underlined correspond to restriction sites.

Table 2.13. Primers used in Chapter 8.

Name	Template DNA	Sequence	Purpose	Restriction sites
ACP3 FP	pGEM-T-Easy ACP3 W55L, ACP4 W57L No. C (A. Haines)	CAGAATTCATGCCTTTAGCGGCCAAGGCGGC	Clone ACP3 W55L into pET28a	*Eco*RI
ACP3 RP		GTGAGCTCTCACTGAAGCTGGGTGCCCACCC		*Sac*I

Bases underlined correspond to restriction sites.

2.2.1 BIO-X-ACT long DNA polymerase kit

The BIO-X-ACT long kit (Bioline) provides high fidelity with proofreading ability, and is capable of amplifying DNA fragments up to 20kb. BIO-X-ACT long DNA polymerase provides a seventeenfold increase in fidelity than *Taq* polymerases, and has been optimised to achieve results from long templates. Reaction mixtures were set up as two solutions, detailed in Table 2.14. 24µl of solution A and 25µl of solution B was placed into to each reaction tube and 1µl of DNA added (H_2O was used as a control). PCR was carried out in a Sensoquest labcycler using the program detailed in Table 2.15.

Table 2.14. BIO-X-ACT long DNA polymerase kit reaction conditions.

Solution A		
Component	**Total volume (µl)**	**Volume/reaction (µl)**
Sample DNA	-	1
dNTP (2.5mM)	16	4
Primer F (15pmole/µl)	4	1
Primer R (15pmole/µl)	4	1
H_2O	72	18
Solution B		
Components	**Total volume (µl)**	**Volume/reaction (µl)**
Enzyme (4U/µl)	1.5	0.375
Buffer (10x)	20	5
$MgCl_2$ (50mM)	6	1.5
Spec Factor (5x)	40	10
H_2O	32.5	8.125

Table 2.15. BIO-X-ACT PCR program details.

Stage	Description	Length	Temp (°C)	Cycles
1	Denaturation	2min	94	1
2	Denaturation	15s	94	10
	Annealing	30s	(T_m-4)	
	Elongation	1min	70	
3	Denaturation	15s	94	20
	Annealing	30s	(T_m-4)	
	Elongation (plus 5s increment each cycle)	1min	70	
4	Final elongation	7min	70	1

2.2.2 Invitrogen *Taq* polymerase

Taq is a heat-stable polymerase isolated from *Thermus aquaticus*, and lacks proofreading activity. PCR for screening was performed with the Invitrogen PCR kit and each reaction was set up as detailed in Table 2.16 and performed as described in Table 2.17:

Table 2.16. *Taq* polymerase PCR reaction conditions.

Component	Volume/reaction (µl)
Template DNA	1
10x Buffer	5
dNTPs (2.5mM)	4
Taq polymerase	0.6
50% glycerol	10
Primer F (15pmole/µl)	0.3
Primer R (15pmole/µl)	0.3
MgCl (50mM)	1
H_2O	27.8

Table 2.17. *Taq* polymerase PCR program details.

Stage	Description	Length	Temp (°C)	Cycles
1	Denaturation	2min	94	1
2	Denaturation	15s	94	30
	Annealing	30s	(T_m-4)	
	Elongation	1min	72	
3	Final elongation	7min	72	1

2.2.3 QuikChange® site-directed mutagenesis PCR

Based on the QuikChange® site-directed mutagenesis kit by Stratagene, this method involves amplification of template plasmid DNA incorporating a point mutation at the same time. The template plasmid DNA is then digested to remove it from the sample. Mutagenic PCR was performed with the high fidelity *Pfu* DNA polymerase kit (Promega) and each reaction was set up as detailed in Table 2.18 and performed using the conditions described in Table 2.19. A primer mix was prepared by adding 100pmole/µl of each to sdH_2O to reach a final concentration of 10pmole/µl. A dNTP mix was prepared by combining 100mM of each nucleotide with sdH_2O to a final concentration of 10mM. A control was included that omitted the primers (replaced by sdH_2O).

Table 2.18. *Pfu* polymerase PCR reaction conditions.

Component	Volume/reaction (µl)
Template DNA	1
Pfu 10x Buffer	5
dNTPs (10mM)	2
Pfu DNA polymerase (2-3U/µl)	1
Primer mix (10pmole/µl)	2
H_2O	39

Table 2.19. *Pfu* polymerase PCR program details.

Stage	Description	Length	Temp (°C)	Cycles
1	Denaturation	1min	95	1
2	Denaturation	30s	95	12
	Annealing	1min	55	
	Elongation	14min	68	

An agarose gel was run to check for the presence of template and amplified DNA. Methylated template DNA was digested with *Dpn*I at 37°C for 1h.

2.2.4 Velocity DNA polymerase

Velocity is a fast high-fidelity polymerase that generates blunt ended products. PCR for chromosomal deletion mutants was performed with the Velocity PCR kit (Bioline) and each reaction was set up as detailed in Table 2.20 and performed as described in Table 2.21:

Table 2.20. Velocity polymerase PCR reaction conditions.

Component	Volume/reaction (µl)
Template DNA	2
5x Buffer	10
dNTPs (2.5mM)	5
Velocity *Taq* polymerase	0.5
Primer F (15pmole/µl)	2
Primer R (15pmole/µl)	2
DMSO	1.5
H_2O	27

Table 2.21. Velocity polymerase PCR program details.

Stage	Description	Length	Temp (°C)	Cycles
1	Denaturation	2 min	98	1
2	Denaturation	30s	98	30
	Annealing	30s	(T_m-4)	
	Elongation	20s	72	
3	Final elongation	7 min	72	1

2.3 DNA manipulation

2.3.1 Plasmid extraction

Plasmid DNA was extracted by alkaline SDS lysis method of Birnboim and Doly (1979) or using Bioneer Accuprep® plasmid extraction kit.

2.3.1.1 Birnboim and Doly alkaline SDS method

Bacteria carrying plasmids were grown overnight in L broth supplemented with appropriate antibiotics. 1ml of the overnight culture was spun for 1min at 14,000rpm in a microfuge. The bacterial pellet was re-suspended in 100µl of ice cold lysis solution 1 (25mM Tris pH8.5, 10mM EDTA pH 8.0, 50mM glucose). 200µl of freshly prepared solution 2 (0.4M sodium hydroxide and 2% SDS) was added and the tube inverted several times before incubation on ice for 5min. 150µl of neutralising solution (3M sodium acetate pH 5.0) was added and the tube inverted several times before incubation on ice for 5min. Proteins and cell debris were pelleted by centrifugation for 10min at 14,000rpm at 4ºC. The supernatant was poured into a new tube and plasmid DNA precipitated by addition of 400µl of isopropanol, prior to repeating the centrifugation step. The supernatant was discarded and the DNA washed with 70% ethanol followed by centrifugation for 10min at 14,000rpm. The supernatant was discarded and the DNA dried for 20min at 48ºC, prior to dissolving in 1/10 diluted TNE buffer. The plasmid DNA was stored at -20ºC until required.

2.3.1.2 Bioneer Accuprep® plasmid extraction kit

All solutions were provided by Bioneer and the method carried out according to the manufacturer's protocol. 1.5ml of an overnight culture was centrifuged at room temperature at 14,000rpm for 2min in a microfuge tube to pellet the bacterial cells. The medium was completely removed by pipetting. Cells were re-suspended in 250µl of buffer 1 (resuspension buffer) by vortexing. 250µl of buffer 2 (lysis buffer) was added and the contents of the tube mixed by inversion three times. 350µl of buffer 3 (neutralisation buffer) was added and the tube immediately mixed by inversion three times, followed by centrifugation at 4°C at 14,000rpm for 10min. The cleared lysate was transferred to the DNA binding column tube and centrifuged at room temperature at 14,000rpm for 1min. The flow-through was poured off and the DNA binding filter column reassembled with the collection tube. 700µl of buffer 4 (wash buffer) was added to the column and then centrifuged at room temperature at 14,000rpm for 1min. The flow through was poured off and the column reassembled, before an additional 1.5min centrifugation step to completely dry the filter. The DNA binding filter column was transferred to a new microfuge tube. 75µl of buffer 5 (elution buffer) was added to the filter and incubated at room temperature for 1min before centrifuging to elute the plasmid DNA at room temperature at 14,000rpm for 1min. The column was discarded and the DNA preparation stored at -20°C until required.

2.3.2 Restriction digests

Digestion of DNA was performed with appropriate restriction enzymes (Fermentas and NEB). Prior to gel electrophoresis the volume in each digestion tube was adjusted to 40µl, and digests required for detection were made up to a final

volume of 20µl. 1µl of each enzyme and either 4 or 2µl of the appropriate 10 times concentrated buffer were added to the reaction. Bovine serum albumin (BSA) was added if stipulated in the manufacturer's instructions for a particular enzyme. 5-10µl sample DNA was added to the reaction, and the final volume made up by addition of sterile distilled H_2O. Typically digestions were carried out at 37°C for 2h.

2.3.3 Agarose gel electrophoresis

PCR and restriction digest products were analysed by agarose gel electrophoresis. Gels were made of 1% agarose in TAE buffer (40mM tris-acetate, 1mM EDTA pH 8.0). 1g of agarose was added to 100ml TAE and micro-waved on full power for 1min, before stirring and heating for an additional 30s. The solution was allowed to cool on the work bench, before adding 2µl of ethidium bromide solution (10mg ml^{-1}). After sealing a gel tray the agarose mixture was poured in, and combs inserted, and the gel allowed to set at room temperature. 2µl of loading buffer (top: 0.25% w/v xylene cyanol, 15% w/v ficoll; or bottom: 0.25% w/v bromophenol blue, 15% w/v ficoll) was added to each 10µl of sample. Samples were run simultaneously with a 1kb DNA molecular weight ladder (Fermentas) at 100V/500mA for approximately 45min. DNA was visualised on a UV transilluminator.

2.3.4 Extraction of DNA from an agarose gel

Extraction of DNA from gel slices was performed using the Illustra GFX PCR DNA and gel band purification kit (G.E. Healthcare). All solutions were provided by G. E. Healthcare and the procedure carried out according to the manufacturer's instructions. Required DNA bands were cut from an agarose gel, placed in a

microfuge tube and weighed. 10µl of Capture Buffer was added to the tube for each 10mg of gel slice, or a minimum of 300µl was added. Samples were incubated at 60°C for 15-30min (with inversion every 3min) until the agarose was completely dissolved. The Capture Buffer contains a pH indicator to ensure the solution is at the correct pH for maximum binding of DNA to the silica membrane in the column – if the solution changed from yellow/orange to pink, the pH would need to be brought back down to less than 7.5 by addition of 3M sodium acetate at pH 5.0. The sample was transferred to a column in a collection tube and incubated at room temperature for 1min, before centrifugation at room temperature at 16,000rpm for 30s. The flow through was discarded, 500µl of Wash Buffer added to the column, and centrifuged at room temperature at 16,000rpm for 30s. The flow through was discarded and the column centrifuged again for 90s to fully dry the membrane. DNA was eluted by addition of 15µl of Elution Buffer, followed by incubation at room temperature for 1min and centrifugation at room temperature at 16,000rpm for 1min. The elution step was repeated for each sample and the DNA stored at -20°C until required.

2.2.5 A-tailing blunt-ended PCR products

Velocity DNA polymerase produces blunt-ended products, meaning for ligation into pGEM-T-Easy an 'A' tail needs to be added. The components required for A-tailing (Table 2.22) were mixed in a microfuge tube and incubated at 70ºC for 30min, in advance of ligation with pGEM-T-Easy.

Table 2.22. Components for A-tailing blunt-ended PCR products.

Component	Volume/reaction (µl)
Purified PCR fragment	6
Invitrogen *Taq* $MgCl_2$	1
dATP (2mM)	1
10x Invitrogen *Taq* buffer	1
Invitrogen *Taq* DNA polymerase	1

2.3.5 DNA ligations

Ligations were performed either with the pGEM-T-Easy vector system I kit (for ligations with pGEM-T-Easy vector that utilise the blue/white colony screening to detect for transformants - Promega), with the Quick-stick ligase kit (for 5-15min ligations at room temperature - Bioline), or using the T4 DNA ligase system (Invitrogen) at 4ºC overnight. Firstly the vector and insert samples were run on an agarose gel against a marker to determine the concentration in ng/µl. To determine the amount of insert required for the ligation reaction, the amount of vector (ng) was divided by the multiplication factor (size of the vector divided by the size of the insert,

in kb). This was then multiplied by 3 for a 1:3 vector insert ratio. Usually ligations were performed in a 10µl reaction mixture following the manufacturer's instructions.

2.3.6 DNA transformation

E. coli cells were made competent according to the methods of Cohen (1972). A single colony was used to inoculate 5ml L broth (with appropriate antibiotic supplement) which was subsequently incubated overnight at 37ºC with shaking. The overnight culture was diluted 1:50 with fresh L broth and grown on at 37ºC with shaking until OD_{600} was approximately 0.4-0.6. Cells were pelleted at 5000rpm for 7min at 4ºC. The supernatant was discarded and the pellet resuspended in 2ml of 100mM pre-chilled calcium chloride ($CaCl_2$) per 5ml of culture and vortexed. The cells were incubated on ice for 20min, prior to centrifugation at 5000rpm for 7min at 4ºC. The supernatant was discarded and the pellet of cells re-suspended gently in 0.5ml of 100mM pre-chilled $CaCl_2$ per 5ml culture. Competent cells were stored at 4ºC. 3µl of plasmid DNA was added to 100µl of competent cells and left on ice for 30min, followed by heat shock at 42ºC for 2min. 1ml of L broth was added to the cells and the suspension was incubated at 37ºC for 1-2h, prior to spreading 100µl on L agar plates and incubating at 37ºC overnight.

2.3.7 DNA sequencing

A 5ml overnight culture of the pGEM-T-Easy cloned gene to be sequenced was set up, and plasmid DNA was extracted as described previously. Sequencing was carried out by the functional genomics laboratory at The University of Birmingham using an ABI 3700 analyser. 200-500ng of plasmid DNA and 3-4pmoles

of the appropriate primer were supplied, and made up to a final volume of 10µl. Sequences were analysed using Chromas Lite (http://www.technelysium.com.au/chromas_lite.html).

2.3.8 Sequence analysis

Alignments of DNA and amino acid sequences were carried out using BLAST align (http://blast.ncbi.nlm.nih.gov/Blast.cgi). Multiple amino acid sequence alignments and generating phylogenetic trees was carried out using ClustalW (http://www.ebi.ac.uk/). Structural analysis of proteins was carried out using the PSIPRED protein structure prediction server (http://bioinf.cs.ucl.ac.uk/psipred/). Sequence logos were generated using WebLogo (http://weblogo.berkeley.edu/logo.cgi) (Schneider and Stephens, 1990; Crooks *et al*., 2004).

2.3.9 Conjugation and suicide vector excision

Bi-parental mating was carried out to mobilise the suicide plasmid derivatives and expression vectors from *E. coli* S17-1 to *P. fluorescens* as follows. 1ml each of late-exponential phase cultures of *E. coli* S17-1, containing the relevant plasmid, and *P. fluorescens* were filtered onto a sterile 0.45µM Millipore filter which was subsequently plated onto L agar and incubated at 30ºC overnight to allow conjugation. The mating mixture was re-suspended in 1ml sterile saline solution (0.85%) and serially diluted with saline to give dilutions of 10^{-1}-10^{-4}. 100µl aliquots were plated onto M9 minimal media (200ml salt solution containing: Na_2HPO_4 (6g/l), KH_2PO_4 (3g/l), NH_4Cl (1g/l), $MgSO_4$ (1mM), thiamine HCl (1mM), $CaCl_2$ (0.1mM),

glucose (0.2%) added to 200ml 50% H_2O agar) supplemented with kanamycin at 30ºC for 2-3 days. Single colonies were then re-streaked to kanamycin-containing M9 minimal media and incubated at 30ºC for 3-4 days. Overnight cultures of co-integrant clones were incubated in L broth at 30ºC overnight without any antibiotic selection. The cultures were serially diluted with L broth to give dilutions 10^{-1}-10^{-5} which were plated on L agar supplemented with 5% sucrose at 30ºC for 3-4 days. Single colonies were purified by first streaking to L agar supplemented with ampicillin, followed by simultaneous streaking on L agar plus ampicillin and L agar supplemented with kanamycin incubated at 30ºC for 3-4 days at each stage. Amp^R and Kan^S colonies were selected and subjected to a final round of PCR to check for the mutant genotype.

2.4 Bioassay for mupirocin production

Single-colony-purified mutant and WT strains were used to inoculate L broth containing appropriate antibiotics and the cultures incubated overnight at 30°C. The OD_{600} of each culture was measured and the cultures diluted to the OD_{600} of the least dense culture. 10µl of culture was spotted onto 20ml L agar plates and incubated at room temperature for 24h. Overnight cultures of *B. subtilis* 1064 in L broth, no selection, were grown at 37°C. Agar containing 40µl ml^{-1} *B. subtilis* culture, and 2, 3, 5-triphenyltetrazolium chloride (TTC) (0.25mg ml^{-1}) was used to overlay the 20ml L agar plates and allowed to set, before incubating at 37ºC overnight. TCC is a redox indicator that is reduced to give a red precipitate in the presence of bacteria undergoing respiration. Therefore actively growing *B. subtilis* 1064 turns the agar red, but where there is no growth the agar remains colourless. The size of the clearance

zone, where the antibiotic has prevented growth of *B. subtilis* 1064 cells, relative to the WT zone, was taken as an estimate of the amount of mupirocin production. Assays were completed in triplicate and standard error bars calculated.

2.5 High performance liquid chromatography

Overnight cultures of strains in L broth supplemented with ampicillin were incubated at 25°C, 200rpm, before 1ml was used to inoculate 25ml of fresh SSM broth (25g soya flour, 2.5g spray dried corn liquor, 5.0g $(NH_4)SO_4$, 0.5g $MgSO_4 \bullet 7H_20$, 1.0g Na_2HPO_4, 1.5g KH_2PO_4, 1.09g KCl, 6.25g $CaCo_3$, 50ml glucose, made up to 1l with H_2O) and incubated at 22°C, 200rpm, for 40h. Cultures were centrifuged at 13,000rpm for 7min and the supernatant filtered using 13mm, 0.2µm PTFE syringe filters. HPLC was performed using Unipoint LC system software, reverse phase C18 column (15cm x 4.6mm), with UV detection (Gilson) at 233nm, and mobile phase water/acetonitrile gradient (5-70% acetonitrile trifluoroacetic acid (0.01%)) over 60min at 1ml min^{-1} flow rate.

2.6 Liquid chromatography mass spectrometry (Zhongshu Song)

LCMS was performed by one of our collaborators, Zhongshu Song, at The University of Bristol. L agar plates were inoculated with test strains and incubated at 30°C for 30h. A single colony from each mutant and WT strain was picked from the agar plates and inoculated into L broth with carbenicillin (50µg/ml). The flasks were incubated at 25°C and 200rpm overnight. Three flasks each containing 100ml of fresh mupirocin production medium were inoculated with 5% of seed culture and incubated at 22°C and 220rpm for 48h. After the fermentation finished all the flasks

were examined for pH values, cultural outlook and smell for any sign of contamination. The cultures were combined and cells removed by centrifugation at 16,000rpm for 20min. The supernatant was extracted by ethyl acetate (1:1) once, followed by an extra ethyl acetate extraction after the aqueous solution was acidified to pH 5.0. The two extracts were combined and ethyl acetate was evaporated *in vacuo*. The residue was collected in 3ml MeOH for LCMS analysis. Analytical samples were prepared by tenfold dilution with MeOH and analysed by LCMS using a 2795HT HPLC system. Detection was achieved by UV between 200 and 400nm using a Waters 2998 diode array detector, and by simultaneous electrospray (ES) mass spectrometry using a Waters QM spectrometer detecting between 150 and 600 *m/z* units. Chromatography (flow rate 1 $ml \cdot min^{-1}$) was achieved using Phenomenex LUNA column (5µ, C_{18}, 100Å, 4.6 × 250mm). Solvents were: A, HPLC grade H_2O containing 0.05% formic acid; B, HPLC grade CH_3CN containing 0.045% formic acid. Gradients were as follows: 0min, 5% B; 22min, 60% B; 24min, 95% B; 26min, 95% B; 27min, 5% B; 30min, 5% B. Both positive ion (PI) and negative ion (NI) mode were employed for the characterisation of the target compounds together with UV absorption pattern. The target compounds were measured by selected ion monitoring (SIM). Assigned with purified standard compounds the yield of PA-A was measured at the retention time of 20.4min and a $[M-H]^-$ of *m/z* 499, mupiric acid at retention time of 16.5min and a $[M-H]^-$ of *m/z* 185, and mupirocin H was measured at retention time of 14.7min and a $[M+Na]^+$ of *m/z* 295.

2.7 Protein expression and purification

5ml of L broth (supplemented with appropriate antibiotic) was inoculated with a single colony from a fresh transformation, and incubated at 37ºC with shaking, overnight. The overnight culture was diluted 1:50 (2ml into 98ml) with fresh L broth and grown on at 37ºC with shaking until OD_{600} was approximately 0.4-0.6. Isopropyl-β-D-thiogalactoside (IPTG) was added to the required final concentration to induce expression of the recombinant protein, prior to incubation at either 18ºC or 16ºC with shaking for 16h, 25ºC for 6h, 30ºC for 4h or 37ºC for 2h. The culture was split between two 50ml centrifuge tubes and spun at 11,000rpm for 10min at 4ºC, the supernatant discarded and the cells washed with 20ml of ice cold STE buffer (10mM Tris-Cl pH 8.0, 0.1M NaCl, 1mM EDTA pH 8.0) before centrifugation at 11,000rpm for 10min at 4ºC. The supernatant was discarded and the pellet stored at -20ºC until required.

2.7.1 Cell lysis

Cell pellets were thawed on ice and re-suspended in 5ml BugBuster Master Mix (Novagen) per gram of wet pellet, and incubated at room temperature with rocking for 60min. To separate the cell debris from the soluble fraction the culture was centrifuged at 11,000rpm for 20min at 4ºC. The cleared lysate (supernatant) was transferred to a fresh tube and 20µl saved for analysis. The insoluble pellet was re-suspended in 1% SDS and 20µl also saved for analysis. Select ACPs were lysed by sonication as follows: cell pellets were re-suspended in 5ml per gram of wet pellet in lysis buffer (100mM tris-Cl pH 8.0, 1mM dithiothreitol (DTT), 10% (v/v) glycerol) with10µl/ml Halt™ EDTA-free protease inhibitor cocktail (Thermo Scientific) and

sonicated on ice using 6x10s bursts at 10 microns with a 10s cooling period. Samples were then centrifuged at 11,000rpm for 20-30min to separate the soluble supernatant from the insoluble pellet.

2.7.2 Nickel affinity chromatography

1ml of nickel-agarose (Qiagen) per 4ml of lysate was added and the mixture rotated for 1h at 4ºC before being transferred to a 5ml polypropylene column. The flow-through was collected for analysis prior to washing the column three times with wash buffer A (50mM sodium phosphate buffer pH 6.0, 300mM NaCl, 10% glycerol), or wash buffer B (50mM sodium phosphate buffer pH 8.0, 300mM NaCl, 20mM imidazole). A 1ml sample was collected from the final wash. Proteins were eluted with 6 x 1ml of elution buffer (wash buffer A or B with increasing concentrations of imidazole). Loading buffer was prepared using 2.5ml upper tris (0.5mM Tris-Cl pH 6.8, plus 0.4% SDS), 4ml 10% SDS, 0.4ml 1% bromophenol blue, 2ml glycerol, made up to 10ml with H_2O. Before use 100µl β-mercaptoethanol was added to a 900µl aliquot of loading buffer before adding to the samples on a 1:1 ratio and incubating at 55ºC for 10min. Samples were then loaded onto an SDS-polyacrylamide gel for electrophoresis (SDS-PAGE).

2.7.2.1 Purifying proteins under denaturing conditions

Proteins were denatured according to the Qiagen protocol (2003). Cell pellets were thawed on ice and re-suspended in 8M urea (5ml per gram wet pellet weight) prior to mixing at room temperature for 60min. Cellular debris was pelleted at 10,000rpm for 30min at room temperature. Samples of soluble and insoluble (the

insoluble pellet was resuspended in 1% SDS and 20µl also saved for analysis) fractions were saved for analysis by SDS-PAGE. 1ml of nickel-agarose per 4ml of lysate was added and the mixture rotated for 1h at 4ºC before being transferred to a 5ml polypropylene column. The flow through was collected for analysis prior to washing the column twice with 4ml of buffer C (100mM NaH_2PO_4, 10mM Tris-Cl, 8M urea, pH 6.3). Samples were collected at each stage for downstream analysis. Protein was eluted with 4 x 0.5ml of buffer D (buffer C at pH 5.9) and 7 x 0.5ml of buffer E (buffer C at pH 4.5). All fractions were added to loading buffer on a 1:1 ratio and incubated at 55ºC for 10min prior to SDS-PAGE analysis.

2.7.2.2 Refolding denatured protein

The refolding assay is based on a fractional factorial design and requires empirical research of a number of different variables such as pH, incubation temperature, and amount of protein to add and the concentrations of ingredients to add. The refolding assay used in this study was based on the QuickFold™ protein refolding kit (Athena Enzyme Systems). Before commencing the elutions from buffer E during the purification process were pooled and the pH adjusted to 7.0 by addition of NaOH, in order to start from a neutral protein solution. The protein concentration was adjusted to 1mg/ml with water. 50µl of protein was added to 950µl of each buffer (Table 2.23) in a microfuge tube whist vortexing gently, before incubation for 1h at room temperature. The A_{340} of each sample was measured against a water blank, to give an indication of the amount of refolded protein in the sample (iFOLD Protein Refolding System 2, Novagen). The samples were centrifuged at 14,000rpm for 5min. The refolded soluble protein-containing supernatant was transferred to a fresh

tube, and the insoluble pellet re-suspended in 1% SDS and saved for analysis. 40µl of soluble fraction was mixed with 10µl of SDS-PAGE loading buffer and incubated at 55ºC for 10min prior to SDS-PAGE. Successful refolding was evidenced by the presence of the protein in the soluble fraction. Samples that gave a positive signal in the soluble fraction by SDS-PAGE and had a low A_{340} reading were considered to be successfully refolded and could be optimised and scaled up. Large scale refolding took place by the dialysis method: the denatured soluble protein was dialysed overnight at 4°C, in a volume of refold buffer at least 50 times that of the pooled protein.

Table 2.23. Matrix for refolding denatured protein.

	Buffer component															
Buffer	**MES**	**Tris-Cl**	**pH**	**NaCl**	**KCl**	**$MgCl_2$**	**$CaCl_2$**	**EDTA**	**Suc**	**GuHCl**	**Arg**	**Tri-X***	**PEG***	**DTT**	**GSH**	**GSSH**
1	50	-	6.0	9.6	0.4	2	2	-	-	750	-	0.5	-	1	-	-
2	50	-	6.0	9.6	0.4	2	2	-	-	-	500	-	0.05	-	1	0.1
3	50	-	6.0	9.6	0.4	-	-	1	400	750	-	0.5	0.05	1	-	-
4	50	-	6.0	240	10	2	2	-	-	-	500	0.5	-	-	1	0.1
5	50	-	6.0	240	10	-	-	1	400	750	-	-	-	1	-	-
6	50	-	6.0	240	10	-	-	1	400	-	500	0.5	0.05	-	1	0.1
7	50	-	6.0	240	10	2	2	-	-	750	-	-	0.05	1	-	-
8	-	50	8.5	9.6	0.4	2	2	-	400	-	-	0.5	0.05	-	1	0.1
9	-	50	8.5	9.6	0.4	-	-	1	-	750	500	-	0.05	1	-	-
10	-	50	8.5	9.6	0.4	2	2	-	400	750	500	-	-	-	1	0.1
11	-	50	8.5	9.6	0.4	-	-	1	-	-	-	0.5	-	1	-	-
12	-	50	8.5	240	10	-	-	1	-	-	-	-	0.05	-	1	0.1
13	-	50	8.5	240	10	-	-	1	-	750	500	0.5	-	1	-	-
14	-	50	8.5	240	10	2	2	-	400	750	500	0.5	0.05	-	1	0.1
15	-	50	8.5	240	10	2	2	-	400	-	-	-	-	1	-	-

All values are in mM, except those marked with a * which are %. Mes, 2(N-morphino)ethanesulfonic acid; Suc, sucrose; Arg, arginine; Tri-X, Triton X-100; PEG, polyethylene glycol 3,500; DTT, dithiothreitol; GSH, reduced glutathione; GSSH, oxidised glutathione.

2.7.3 SDS-PAGE

The recipes shown in Table 2.24 were used to make a resolving gel and a stacking gel. Two gel plates were clipped together; the resolving gel was prepared and pipetted in between and the top sealed with isopropanol to create a smooth top. Once the resolving gel was set the isopropanol was removed and the top of the gel washed with two volumes of water. The stacking gel was prepared and pipetted on top of the resolving gel and a comb inserted. When they had set, the gel plates were removed from the clips and the gel tank assembled. Tris-glycine electrophoresis buffer (25mM Tris pH 8.3, 250mM glycine, 0.1% (w/v) SDS) was added to the gel tank, ensuring it filled the gap between the gels. Samples were loaded and the gel was run at 50V, 20mA for approximately 4h. Once complete the gels were removed from the equipment and stained for 15-60min in Instant Blue (Expedeon). The gels were then briefly rinsed in water before being dried.

Table 2.24. Components for SDS-PAGE gels.

Component	15% resolving gel	10% resolving gel	3% stacking gel
H_2O (ml)	2.3	4	3.24
Tris (ml)	2.5*	2.5*	1.25^{+}
1% APS (µl)	120	120	60
30% acrylamide (ml)	5	3.35	0.6
TEMED (µl)	8	8	15

*Lower tris (1.5M tris-Cl pH 8.0, 0.4% SDS); +Upper tris (0.5M tris-Cl pH 6.8, 0.4% SDS); APS, 1% ammonium persulphate.

2.7.4 Determination of protein concentration

Protein concentration was determined by running diluted samples on SDS-PAGE and comparing the gel bands to a marker of known concentration. The concentration of the protein was calculated by multiplying the concentration of the marker by the appropriate dilution factor, depending on which sample matched the marker bands. Where an estimation of protein concentration was required a 1µl sample was loaded onto the NanoDrop ND-100 and the protein concentration estimated using the A_{280} method against a standard blank.

2.8 Acyltransferase assays

Proteins were incubated with 1ml reaction buffer (0.1M sodium phosphate buffer pH 8.0, containing 1mM EDTA) and 50µl of 10mM Ellman's reagent (DTNB – 5,5'-dithiobis-(2-nitrobenzoic acid)) at room temperature for 10min. The spectrophotometer was blanked with the reaction mixture prior to addition of substrate (acyl-CoA derivatives purchased from Sigma-Aldrich). Substrate was added (total reaction volume 1150µl) and the reaction converting DTNB to 2-nitro-5-thiobenzoic acid (TNB) followed at 412nm. The molar extinction coefficient of TNB is 14,150M/cm. Assays were performed in duplicate or triplicate and standard error bars calculated.

2.9 Autoradiography

Proteins were equilibrated in assay buffer (50mM HEPES pH 7.4, 2mM TCEP) at room temperature for 10min before addition of [^{14}C]-malonyl-CoA (Perkin Elmer). The reaction was quenched after 20min by addition of DTT SDS-PAGE loading buffer

with no reducing agent (50mM upper tris, 2% SDS, 0.1% bromophenol blue, and 10% glycerol). The samples were boiled for 3min and analysed by SDS-PAGE. The gels were stained as described before, prior to being dried onto filter paper and placed in a phosphorimager cassette. After 24h the phosphorimager screen was scanned and the images analysed.

2.9.1. Analysis of phosphorimager screen

For each gel that was exposed to a phosphorimager screen a spot test was performed that involved pipetting 0.2µl of [^{14}C]-malonyl-CoA onto the filter paper. Scanned screens were analysed using the Quantity One software (BioRad). Radioactive counts were calculated for each sample, in addition to the spot test. The amount of malonate acquired by the proteins was calculated as a percentage of the spot test and took into account dilution factors. An example is detailed below:

Step 1: The spot test = 181µM [^{14}C]-malonyl-CoA = 26,735 radioactive counts

Step 2: A sample has 693 radioactive counts $\left(\frac{693}{26{,}735}\right)\times 100 = 2.6\,\%$ of 26,735 or 181µM = 4.7µM

Step 3: The sample was diluted with an equal volume of SDS-PAGE loading buffer: $\frac{4.7}{2}$ = 2.35µM

Step 4: Only a quarter of the sample was loaded onto the SDS-PAGE gel: $\frac{2.35}{4}$ = 0.59µM acquired by the protein.

Assays were performed in duplicate or triplicate and standard error bars calculated.

2.10 Circular dichroism

Protein samples eluted from Ni-NTA were dialysed against sodium phosphate buffer at either pH 6.0 or pH 8.0 (depending on which buffer, A or B, was used to elute the proteins) to remove any traces of NaCl, glycerol or imidazole which can all affect the absorbance spectrum of a solution. Dialysis took place at 4ºC overnight, using Spectra/Por dialysis membrane with a 6-8kDa molecular weight cut off (Spectrum Labs). Protein samples were diluted to 1mg/ml and 60µl loaded into a 0.1mm path length quartz cuvette and the absorbance from 190-260nm recorded on a Jasco-J-715 spectropolarimeter. Absorbance spectrums were analysed using Spectra Analysis software (Jasco) and Dichroweb (http://dichroweb.cryst.bbk.ac.uk/html/home.shtml) (Whitmore and Wallace, 2004; 2008). Assays were performed in duplicate or triplicate and standard error bars calculated.

2.11 Protein crosslinking with glutaraldehyde

The protein of interest was incubated at room temperature for 20min with varying concentrations (0.01-0.5%) of glutaraldehyde, in 0.05M bicine-NaOH buffer, pH 8.5, 0.1mM DTT and 0.4M NaOH. The reactions were terminated with ethanolamine-HCl (pH 8.0) added to a final concentration of 0.14M. Samples were then analysed by SDS-PAGE for evidence of crosslinking.

CHAPTER 3

3 EXPRESSION AND PURIFICATION OF MUPIROCIN BIOSYNTHESIS PROTEINS

3.1 Introduction

Proteins are essential constituents of all living organisms and are involved in every aspect of the function of a living cell. Proteins can be characterised at a bioinformatics level, studying the amino acid sequence and predicting structure and function relationships, but additionally at an applied level – performing *in vitro* assays to determine the function(s). Before assays can take place however, protein needs to be expressed in a host and purified.

Escherichia coli has been a model organism in microbiology for many years, due to the ease and inexpense of growing cultures and high expression of foreign proteins (Sambrook and Russell, 2001). As early as the 1940's *E. coli* was used as a model organism and was key in demonstrating that certain bacteria use conjugation as a method of transferring genetic material (Lederberg and Tatum, 1946). In 1973 it was the organism of choice when DNA cloning and recombinant DNA were developed by Stanley Cohen and Herbert Boyer (Russo, 2003). Since then, hundreds of recombinant proteins have been expressed in *E. coli* using a variety of different expression systems. The choice of system depends on the amount of protein required, the size of the protein to be expressed, and whether active protein is required. Vectors can contain IPTG-inducible promoters, bacteriophage T7 promoter or the bacteriophage λ P_L promoter. Proteins can be produced as fusion proteins with β-galactosidase, alkaline phosphatase, glutathione S-transferase (GST), maltose binding protein (MBP), hexa-His, or thioredoxin (Sambrook and Russell, 2001). Special strains are also available to allow expression of genes that

use a range of codons that are not suited to the abundant aa-tRNAs that are usually present in *E. coli*, for example Rosetta (DE3) from Novagen. Previous investigations that have involved expression and purification of polyketide proteins, particularly AT and ACP, have utilised the various plasmids of the pET vector system (Cox *et al*., 2002; Aron *et al*., 2007; Lopanik *et al*., 2008; Arthur *et al*., 2009; Musiol *et al*., 2011). There are 44 pET-derived expression vectors available, and the system has been widely used since development in the 1990's (Sørensen and Mortensen, 2005; Merck, 2005).

Many proteins form insoluble inclusion bodies when over-expressed in *E. coli* leading to incorrectly folded and non-functional protein, which is unproductive for further studies. There are many factors that can lead to proteins having a propensity for insolubility when over-expressed: increased aggregation due to hydrophobic residues; reduced protein translation of ORFs involving rare codons; N- and C-terminal sequences, and inability to interact with proteins participating in folding *in vivo* (Idicula-Thomas and Balaji, 2005). Determining the optimal expression conditions to produce soluble recombinant protein can be difficult and involves empirical research, tweaking various factors such as incubation temperature and time, and concentration of inducer. Insoluble inclusion bodies are thought to arise from improper folding in the *E. coli* host, and if these issues can be rectified then soluble protein may be achievable. Living cells have developed molecular chaperone systems, such as DnaK-DnaJ-GrpE and GroEL-GroES, which bind to proteins to prevent aggregation in the cytoplasm during *in vivo* protein production (Georgiou and Valax, 1996; Baneyx, 1999; Qoronfleh *et al*., 2007). The GroEL-GroES system encodes 2 polypeptides (Figure 3.1): GroEL is a tetradecamer consisting of 14

subunits arranged in 2 heptameric rings while GroES forms a lid on top of the rings trapping the protein inside, where it is unrestricted to begin folding (Horwich *et al*., 2007; Madan *et al*., 2008). After several seconds, GroES is released allowing the protein, folded or not, to be liberated into the cell. These chaperones can be co-expressed with the protein of interest in an attempt to prevent aggregation into inclusion bodies. The search goes on for new ways to improve expression of proteins in soluble form, such as the development of novel fusion tags, developing screening strategies to efficiently search for ideal expression parameters and determining the characteristics that make certain proteins insoluble (Idicula-Thomas and Balaji, 2005; Ohana *et al*., 2009; Vernet *et al.*, 2011).

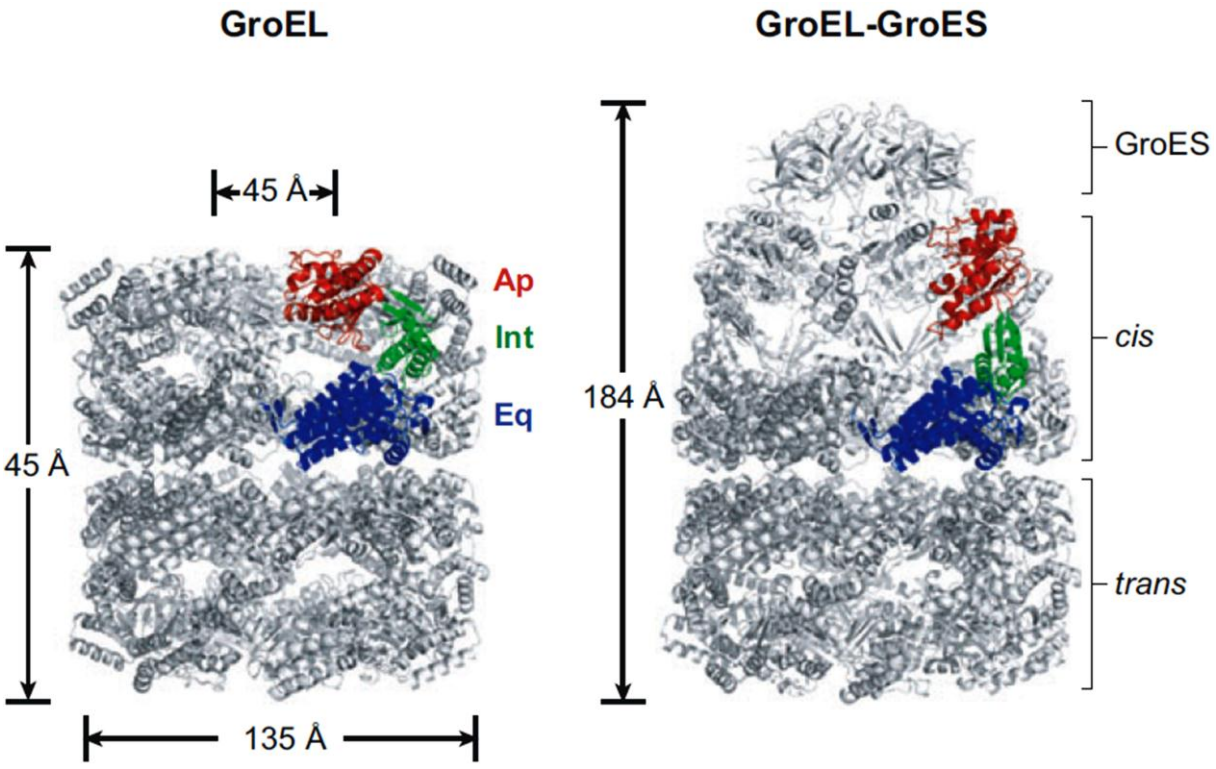

Figure 3.1. Architecture of the *E. coli* GroEL-GroES chaperonin. One subunit has been coloured to reveal the domain structure: Ap, apical domain; Int, intermediate domain; Eq, equatorial domain. GroES binds asymmetrically, encapsulating the *cis* GroEL ring (Horwich *et al*., 2007).

If soluble protein cannot be produced by traditional expression experiments, inclusion bodies can be isolated, purified and the protein refolded *in vitro*, but the process is difficult, may not always work, and if it does may not produce functional protein that can be used in downstream applications. Strong solvents, such as urea or guanidine-HCl, are required for solubilising the aggregates prior to refolding, but this process denatures the proteins (Marston and Hartley, 1990). Denaturation of a protein involves disrupting the secondary and tertiary structure to a point where its standard form and functional activity is lost. The denaturation and renaturation of ribonuclease has been extensively investigated since the 1950's. Complete denaturation took place in the presence of urea and mercaptoethanol, but once these reagents were removed the ribonuclease re-established the native conformation and regained catalytic activity (Anfinsen, 1973). There are many factors that can influence the renaturation of a protein, for example, heat, pH, oxidation state, ionic strength, protein concentration, and the presence of sugars, cofactors, surfactants, detergents and/or chaotrophic agents (Marston and Hartley, 1990; Clark, 1998; Lilie *et al*., 1998). Refolding can occur either by dilution or dialysis methods to remove or at least reduce the concentration of the solubilising agent and replace it with agents required for refolding. Screening systems have been developed in an attempt to facilitate the research involved in determining the ideal conditions for refolding proteins, but the process still requires empirical research with many factors being investigated.

Previous work had already been done on the mupirocin AT and ACP proteins. In her thesis, J. A. Shields details the expression and purification, using the pET-expression vector system, of mupirocin ACP1, 3-7, mAcpA, C and D and one of the

ATs - AT2 (2008). Shields went on to utilise the ACPs for phosphopantetheinylation studies (Shields *et al*., 2010).

The aim of this study was to solubilise difficult proteins, optimise solubility conditions for those already found to be soluble, and purify them. Of particular interest are the ATs that potentially transfer substrates throughout the mupirocin biosynthesis system. As AT2 has previously been purified the focus of this Chapter will mainly be on the AT1 protein. Having both of these proteins pure for biochemical characterisation will help build a complete picture of how mupirocin biosynthesis is initiated and progressed throughout the cluster. It is presumed that one or other of the ATs will transfer substrates to the ACPs throughout the cluster, both type I and type II ACPs, so it is vital to be able to purify a selection of ACPs to utilise in future enzymatic assays.

3.2 Results

The pET28a vector used in previous studies and this study encodes kanamycin selection, contains an f1 origin of replication, is under the control of the T7*lac* promoter, has an N-terminal 6-His tag which can be removed by thrombin cleavage, and an internal T7 tag (Merck, 2005). The vector containing the gene of interest is cloned into an expression host (i.e. *E. coli* BL21 (DE3)) that carries a chromosomal copy of the T7 RNA polymerase gene under the control of the *lacUV5* promoter. Under normal conditions the *lac* repressor binds to the *lac* operator on both the *E. coli* BL21 (DE3) genome and the plasmid, preventing transcription of the T7 RNA polymerase (Figure 3.2). Upon addition of IPTG, the *lac* repressor is released (bound to IPTG), allowing chromosomal transcription of the T7 RNA polymerase, which in turn initiates transcription of the target gene by the T7 promoter on the plasmid (Sørensen and Mortensen, 2005; Merck, 2005).

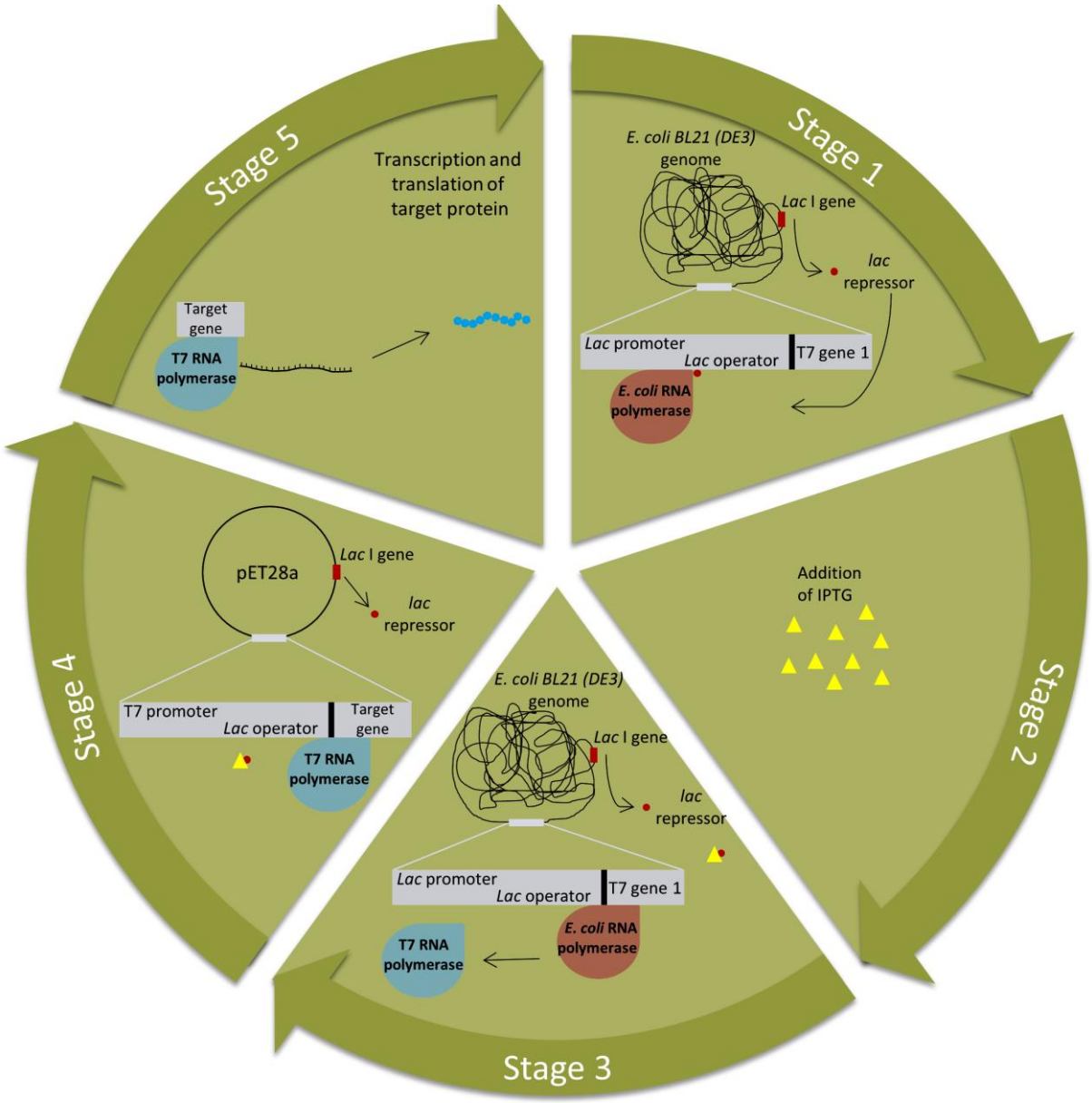

Figure 3.2. Regulating protein expression in pET28a. Stage 1 - The *lac* repressor is bound to the *lac* operator preventing transcription of the T7 RNA polymerase. On addition of IPTG (Stage 2) the *lac* repressor is released, allowing transcription of the T7 RNA polymerase (Stage 3) which switches on transcription of the target gene (Stages 4-5) (Merck, 2005).

3.2.1 Expression and purification of acyltransferase proteins

Acyltransferase 1 and 2 (AT1 and AT2) were previously cloned as *Eco*RI-*Sac*I fragments into pET28a to give vectors pJS559 and pJS560 (Shields, 2008), and transformed into *E. coli* BL21. Induction conditions for over-expression of the proteins were determined by a series of experiments to test the effect of the concentration of IPTG, the post-induction incubation temperature and length of incubation. AT1 was found to be insoluble while AT2 was soluble.

3.2.1.1 Expression and purification of AT1

Preceding work had determined that AT1 was insoluble when expressed in *E. coli* BL21 (DE3) and BL21 star (DE3) at post-induction temperatures ranging from 18°C to 37°C, and varying IPTG concentrations. The use of MagicMedia (Invitrogen) and the MBP fusion tag did not improve the solubility of this protein (Shields, 2008). Therefore in this study AT1 was co-expressed with a 4.5kb plasmid, pSUEH (Lund, 1993) that encodes the *E. coli* chaperonin complex GroEL-GroES. AT1 was insoluble if expressed in *E. coli* without pSUEH, but a small fraction appeared soluble (and there was less insoluble) when the chaperone protein was produced alongside it at 18°C post-induction (Figure 3.3, A).

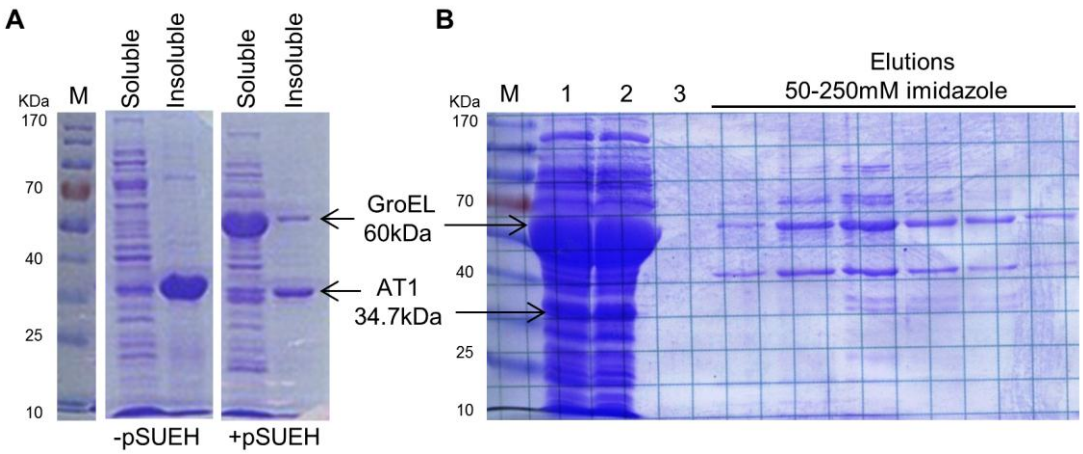

Figure 3.3. Expression and purification of AT1. (A) Expression of AT1 without and with the GroEL-GroES chaperone. **(B)** Purification of AT1 after co-expression with GroEL-GroES. M, molecular weight marker; lane 1, soluble fraction; lane 2, chromatography column flow through; lane 3, final wash through fraction.

Purification of His-tagged AT1 was attempted using nickel-affinity chromatography, but very little of the protein appeared to bind to the column as indicated by AT1 coming out in the flow through in Figure 3.3 (B). This could be due to many reasons: it is possible the protein is being folded in such a way that the His-tag is folded towards the inside, meaning it would not be free to bind to the nickel agarose; the protein remains insoluble; or conditions for binding to nickel agarose and subsequent elution are not optimal.

3.2.1.1.1 Alternative purification strategy for AT1

The plasmid pET28a has an N-terminal His-tag, allowing for purification by nickel-affinity chromatography. If the protein of interest is being folded in such a manner that the tag is not available for binding to the nickel agarose it could hinder the purification process. Therefore, a strategy was designed to incorporate the His-tag at the C-terminus of the protein, and also to extend the His-tag out further from

the protein with the aim of making it more accessible to the nickel agarose on the chromatography column. Therefore, AT1 and a 10 residue Gly-Ala linker were cloned into pET28b using primer pairs AT1BF and AT1BR. After amplifying the region by PCR it was cloned and sequenced in pGEM-T-Easy (pRG300). Following sequencing, linker-AT1 was excised as an *Xho*I-*Nco*I fragment and ligated with pET28b to give plasmid pRG301. The linker was then excised by restriction digest with *Xho*I-*Sal*I overnight, the DNA band purified and ligated to re-linearise the plasmid to produce pRG302. Absence of the linker was double-checked by digest with *Sal*I. To add a 15 residue Gly-Ala linker to pJS559, the plasmid was first digested with *Bam*HI-*Eco*RI, followed by AT1 DNA band purification and ligation with 100pmole of primers LINKAF1 and LINKAR1 (prepared by boiling for 10min) to produce plasmid pRG303. Addition of the linker was checked by restriction digest with *Ahd*I, a restriction site unique to the linker region. Plasmids pRG301, pRG302 and pRG303 were co-expressed with pSUEH in *E. coli* BL21 (DE3), induced with 0.1mM IPTG and incubated at 18°C for 16h to overexpress AT1, prior to purification. It appears that extension of the N-terminal His-tag, use of a C-terminal his-tag with and without an extension linker were unsuccessful in purifying AT1 (Figure 3.4), however, there is no insoluble AT1 when using pRG303 and more in the soluble fraction. This would suggest that the purification conditions do not suit AT1.

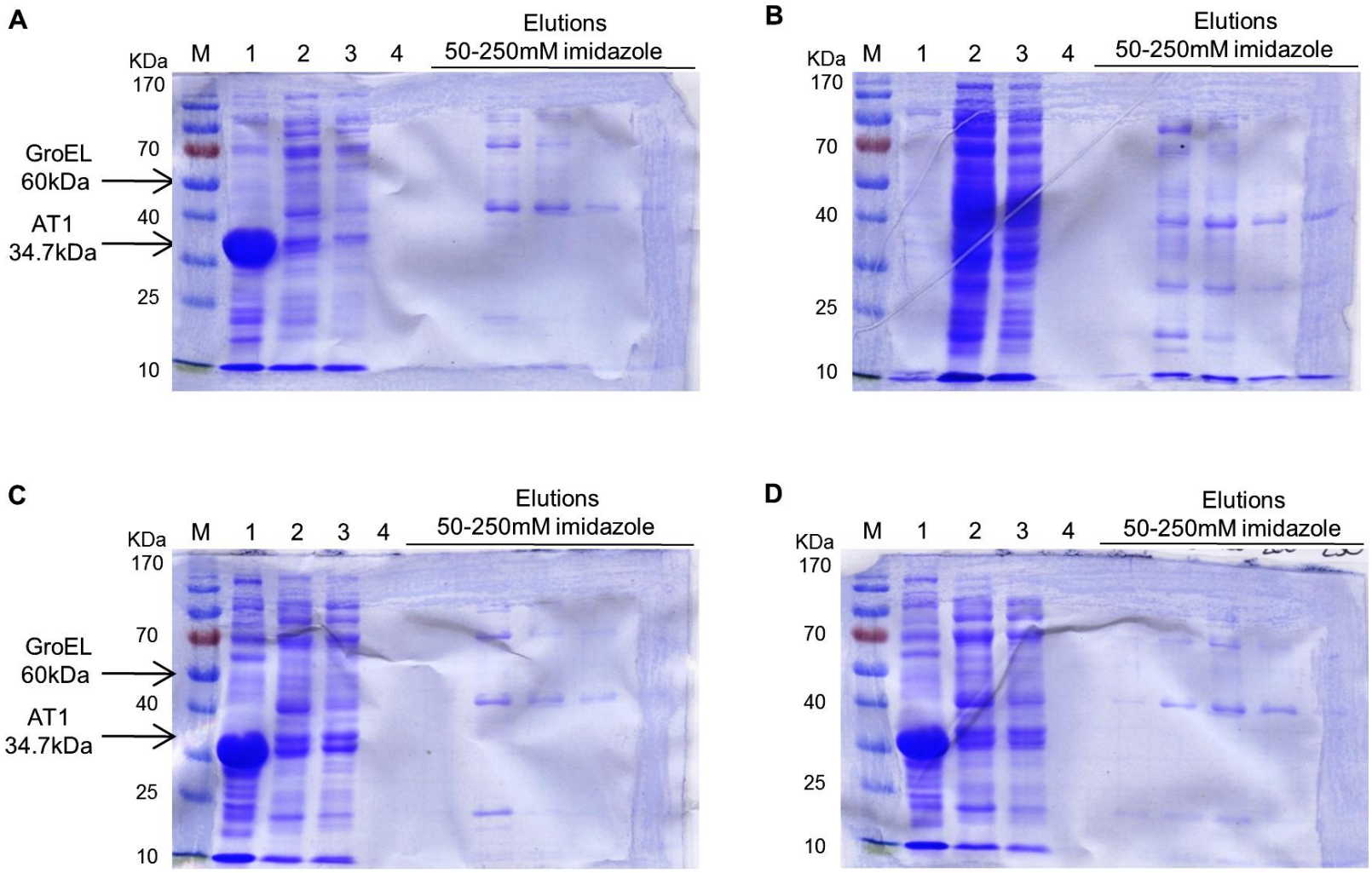

Figure 3.4. Alternative purification of AT1. (A) Coexpression of pJS559 (pET28a-AT1) with pSUEH. **(B)** Coexpression of pRG303 (pET28a-AT1+linker) with pSUEH. **(C)** Coexpression of pRG302 (pET28b-AT1) with pSUEH. **(D)** Coexpression of pRG301 (pET28b-AT1+linker) with pSUEH. M, molecular weight marker; lane 1, insoluble fraction, lane 2, soluble fraction, lane 3, chromatography column flow through; lane 4, final wash through fraction.

3.2.1.1.2 Expression of AT1 in *E. coli* Lemo21(DE3)

E. coli Lemo21 (DE3) cells (NEB) contain the same host features as BL21 (DE3), but allow for tuneable expression of difficult clones, producing more properly folded soluble protein. By varying the level of lysozyme, the natural inhibitor of T7 RNA polymerase, it is possible to fine tune expression of the target protein (Wagner *et al*., 2008). The level of lysozyme is altered by the addition of L-rhamnose to the expression culture. Plasmid pJS559 was transformed into competent *E. coli* Lemo21 (DE3) cells, and small scale expression experiments were conducted at 15°C, 18°C and 30°C to determine: a) the optimum temperature for expression; and b) the optimum L-rhamnose concentration for expression. At each temperature the amount of AT1 in the insoluble fraction is greater at a concentration of 0mM than at 100mM L-rhamnose, and gets successively less as the concentration of L-rhamnose increases (Figure 3.5). At 18°C AT1 remained in the insoluble fraction, at 15°C the amount of insoluble AT1 decreased considerably, and at 30°C, there was no AT1 in the insoluble fraction when the L-rhamnose concentration is 500μM or above. At 15°C there appeared to be a small amount of soluble AT1, so large scale expression and purification was carried out using 100mM L-rhamnose, however AT1 came off in the flow through and did not purify (data not shown).

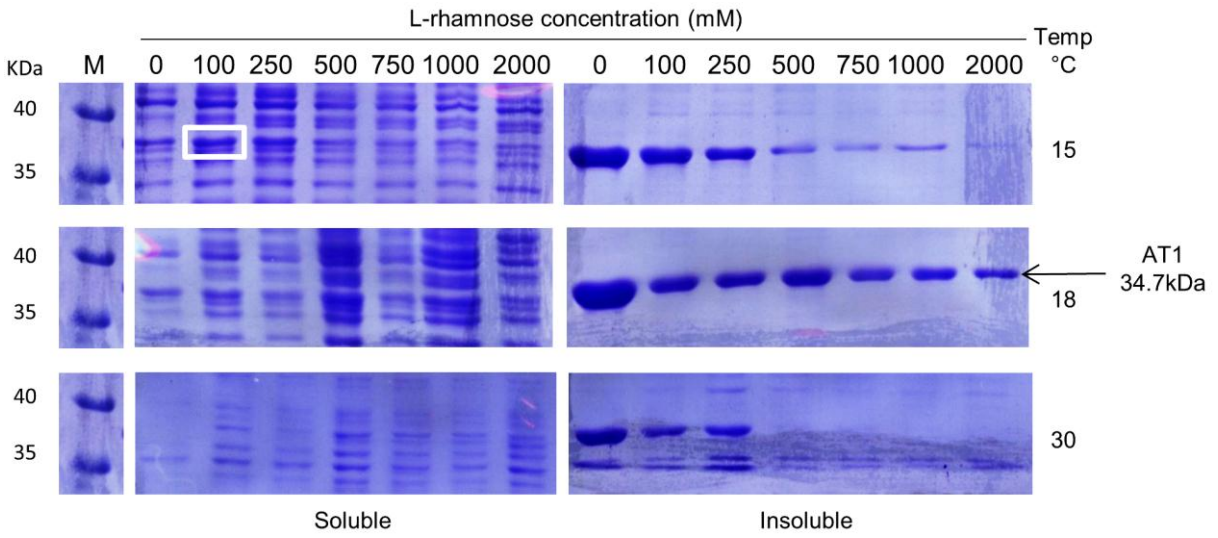

Figure 3.5. Expression of AT1 in *E. coli* Lemo21(DE3). Expression was carried out at a variety of different temperatures (right-hand side) and L-rhamnose concentrations (top), prior to lysis by BugBuster Master Mix and running soluble and insoluble fractions by SDS-PAGE. M, molecular weight marker; the white box indicates soluble AT1.

3.2.1.1.3 Expression of AT1 in Terrific Broth

Terrific Broth was developed in 1987 in order to improve the yield of plasmid DNA in *E. coli* (BD Biosciences, 2011). The broth includes extra peptone, yeast extract, potassium phosphates and glycerol to encourage growth of recombinant strains of *E. coli* to produce a higher cell density, and therefore increase the yield of soluble protein expression. Plasmid pJS559 was expressed in *E. coli* BL21 (DE3) at a range of temperatures and IPTG concentrations to determine if any soluble protein could be detected before scaling up expression to purify AT1. Figure 3.6 shows that at 18°C no soluble protein was detected. At 37°C there appeared to be a small amount of soluble protein, but the most was achieved when incubated at 30°C for 4h post-induction with 0.5mM IPTG, although the amount appears to remain negligible.

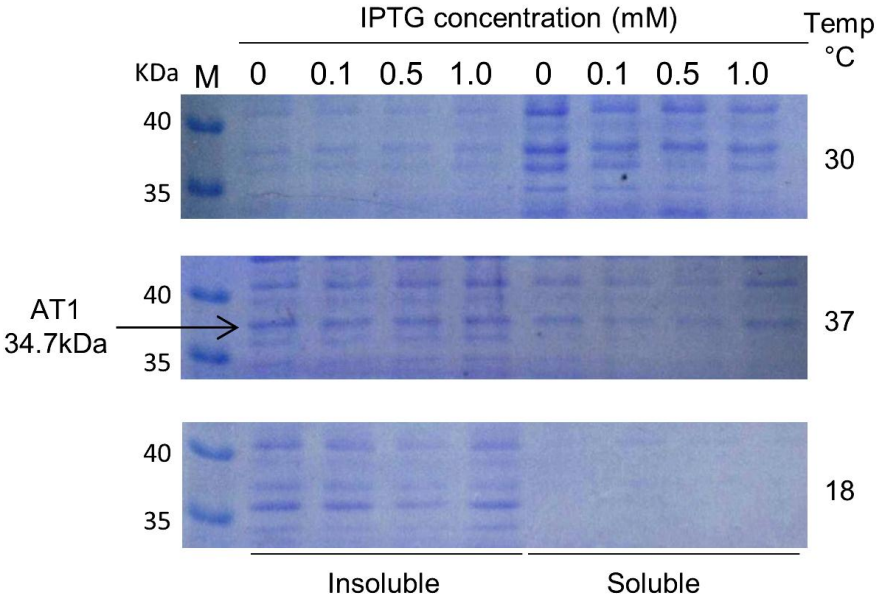

Figure 3.6. Expression of AT1 in Terrific Broth. Expression at different temperatures (right-hand side) and IPTG concentrations (top). The negligible amount of protein visualised by SDS-PAGE ceased further investigation under these conditions. M, molecular weight marker.

3.2.1.1.4 Purification of AT1 with styrene maleic acid

Inclusion bodies are formed when proteins with hydrophobic patches on their surface aggregate. Researchers are developing new technologies to overcome this and increase the solubility, and consequently increase production of proteins. One such product is NVOY (Expedeon), a carbohydrate based polymer which binds to hydrophobic surface patches preventing proteins from aggregating.

Styrene maleic acid (SMA) is a copolymer that forms lipid discs which preserve the integrity of transmembrane proteins, and has been used to increase the solubility of proteins for analysis (Knowles *et al*., 2009). When integrated with a protein SMA forms a lipid particle (SMALP) in the shape of a disc which surrounds the protein (Figure 3.7). The proteins within are protected from denaturation and aggregation.

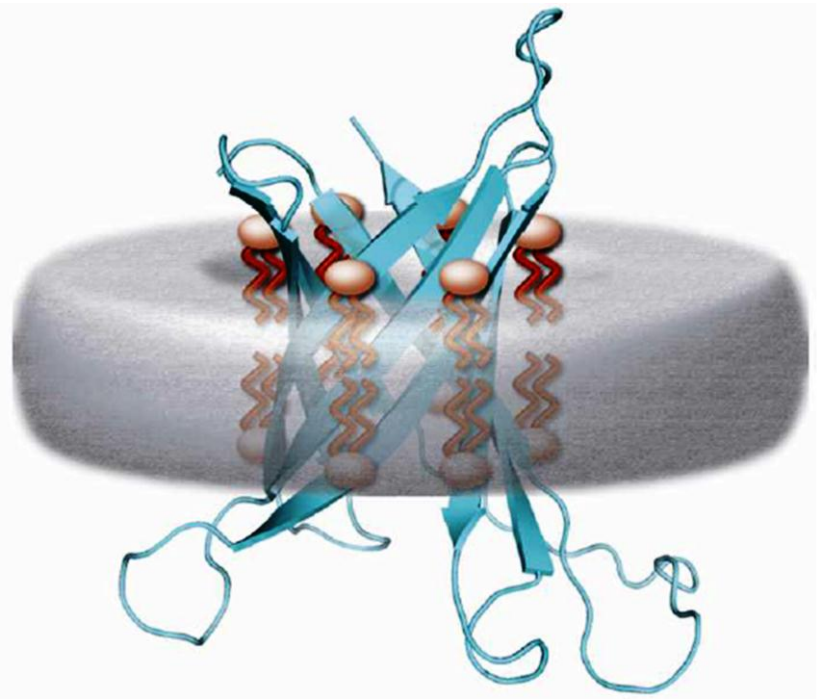

Figure 3.7. The proposed structure of a SMALP. A protein is shown in blue, and phospholipid molecules shown in red (Knowles *et al*., 2009).

Plasmid pJS559 was expressed in *E. coli* BL21 at 18ºC for 16h with and without pSUEH. The cell pellets were re-suspended in Bugbuster Master Mix along with 1mg/ml SMA (Tim Dafforn, 2011). Solubilisation and purification then proceeded as described previously. It appeared that SMA didn't enhance the solubility of AT1, however the soluble fraction was considerably less contaminated than when SMA was not present (Figure 3.8). Purification by nickel-affinity chromatography yielded no pure AT1 – the protein came off in the flow-through fraction as before (data not shown).

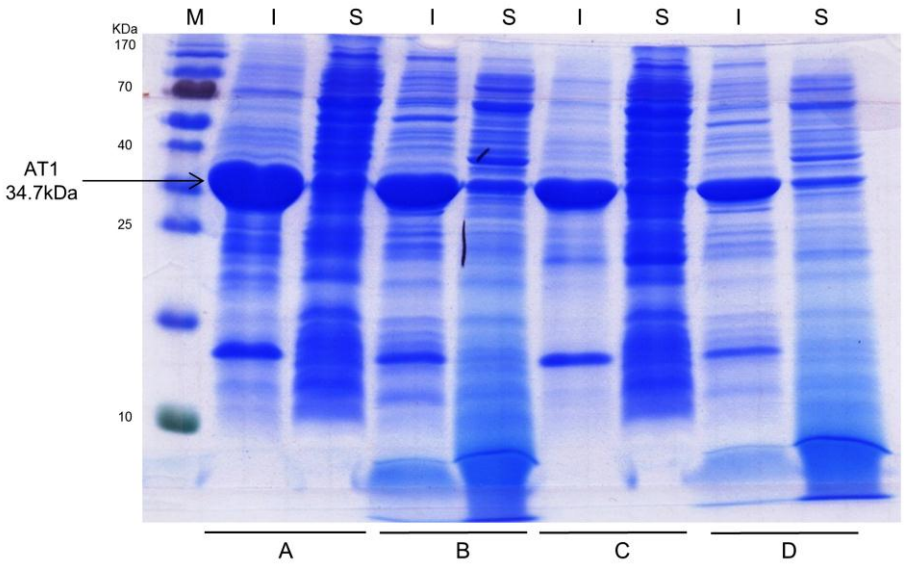

Figure 3.8. Expression of AT1 with and without SMA. M, molecular weight marker; I, insoluble; S, soluble; A, AT1; B, AT1+SMA; C, AT1+pSUEH; D, AT1+pSUEH+SMA.

3.2.1.1.5 Purifying AT1 under denaturing conditions

Due to the continuing problems with expressing and purifying soluble AT1, an alternative strategy was implemented. The denaturation process was optimised by testing different lysis solutions for producing the maximum amount of soluble denatured protein, before purification by nickel-affinity chromatography under denaturing conditions. Figure 3.9 shows that this purification scheme was successful, with a good yield and purity of AT1. The chaperone protein GroEL came out in the flow through, further increasing the purity of the AT1 fraction.

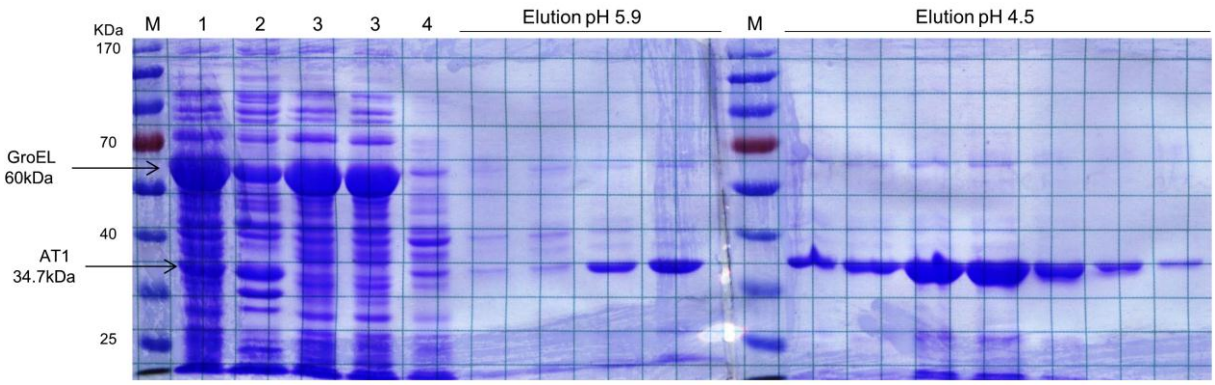

Figure 3.9. Purification of AT1 under denaturing conditions. AT1 was denatured by lysis of host cells with 8M urea prior to purification. M, molecular weight marker; lane 1, soluble lysate; lane 2, insoluble protein; lane 3, chromatography column flow through fraction; lane 4, final wash fraction. AT1 was eluted with 100mM NaH_2PO_4, 10mM Tris-Cl, 8M urea at pH 5.9 (elution buffer D) and pH 4.5 (elution buffer E).

3.2.1.1.6 Refolding purified denatured AT1

In order to test the functions of AT1 it was necessary to renature the protein beforehand. The method adopted in this study was based on a fractional factorial design, first screening for a suitable buffer, and second optimising the buffer conditions for maximum protein refolding (Chen and Gouaux, 1997; Armstrong *et al*., 1999; Qoronfleh *et al*., 2007; Athena Enzyme Systems, 2008). Successful protein refolding was visualised by SDS-PAGE and taking the A_{340}, as described in Chapter 2. The absorption at 340nm is informative because unfolded protein will precipitate, and so less precipitation indicates more properly folded protein. Figure 3.10, (A) shows that AT1 was successfully refolded in the presence of a variety of different factors. Buffer 11 (50mM Tris-Cl pH 8.5, 9.6mM NaCl, 0.4mM KCl, 1mM EDTA, 0.5% triton X-100 and 1mM DTT) was selected for optimisation as it appeared to produce the most soluble protein. Factors optimised were pH and the concentration of DTT in the buffer. Figure 3.10, (B) and (C) shows that all of the optimised buffers produced soluble, refolded protein. Buffer 11.9 was chosen for subsequent refolding on a large scale due to the resultant protein solution having the lowest absorbance reading, and therefore less denatured protein.

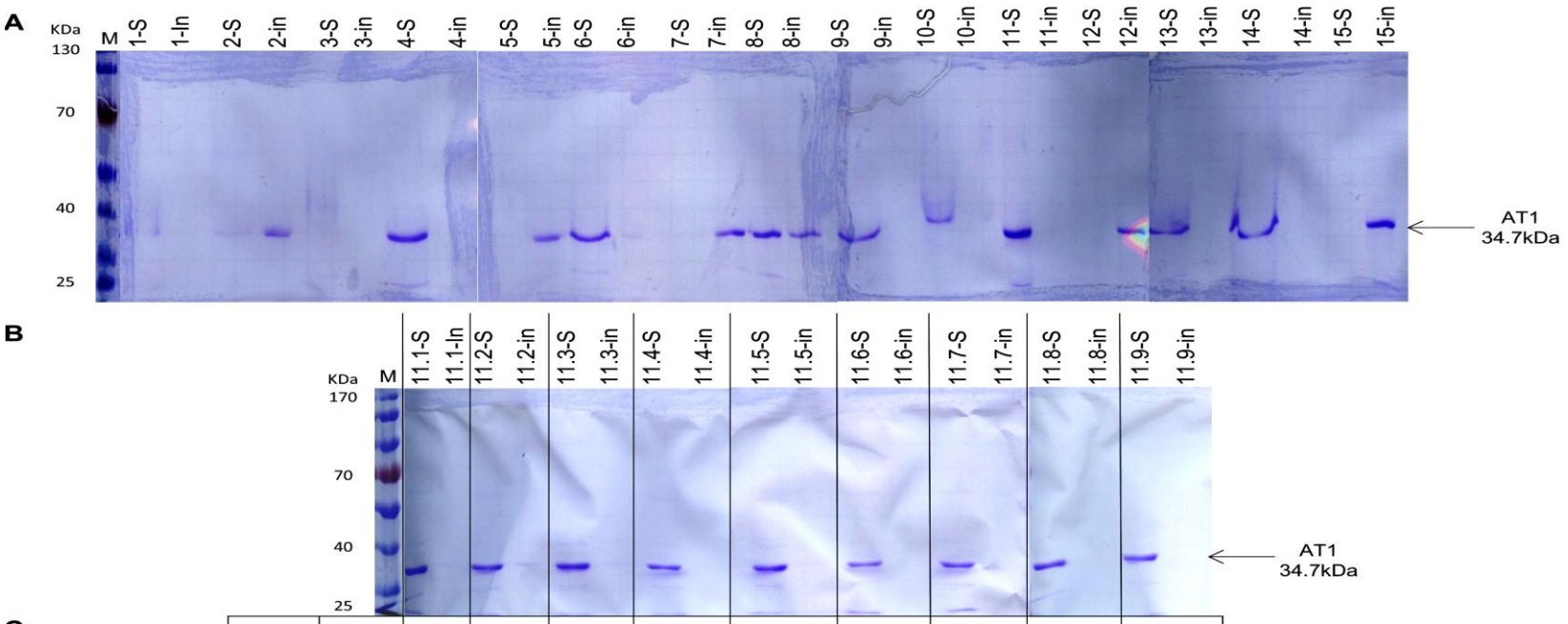

C

DTT	0.5	✓					✓	✓		
	1.0		✓		✓	✓				
	1.5			✓					✓	✓
pH	8.0				✓		✓		✓	
	8.5	✓	✓	✓						
	9.0					✓		✓		✓
Abs[a]		0.034	0.026	0.025	0.0184	0.0185	0.067	0.017	0.049	0.013

Figure 3.10. Refolding of AT1 using a fractional factorial designed assay. A matrix was designed incorporating 19 different elements to be tested (Section 2.7.2.2). **(A)** Buffer 11 produced the strongest refolded band on SDS-PAGE. **(B)** and **(C)** Optimisation of the refolding process for AT1. B, The SDS-PAGE gel shows that each modified buffer produces soluble refolded AT1; C, The table shows the modifications to buffer 11 in each case. [a]Absorbance of the soluble fraction after refolding and lysis shows the degree of refolding for each buffer – a low absorbance meant there was less denatured protein in the sample. M, molecular weight marker.

3.2.1.1.7 Expression of AT1 with the GST tag

A GST fusion protein includes a 26kDa glutathione-S-transferase (GST) fused to the N-terminus of the protein of interest. This strategy was employed as it was thought a larger tag might be more effective at extending from the protein. GST-tagged proteins bind to a reduced glutathione (GSH) affinity column, and can be eluted by displacement of the GST fusion protein by addition of GSH to the column. The GST tag can be removed, if desired, by thrombin cleavage (Smith and Johnson, 1988). AT1 was PCR amplified for cloning into the pGEX-2t vector using the primers AT1pGEXF and AT1pR to produce plasmid pRG304. PCR products were purified and ligated with pGEM-T-Easy for sequencing. Successful cloning of AT1 with pGEX-2t was determined by restriction digest with *Sma*I and *Eco*RI, ahead of transformation into *E. coli* BL21 cells. Small scale experiments showed that most GST-AT1 was expressed at 18°C (Figure 3.11, A). After treatment with BugBuster Master Mix to separate soluble and insoluble fractions it appeared that some GST-AT1 was soluble (Figure 3.11, B).

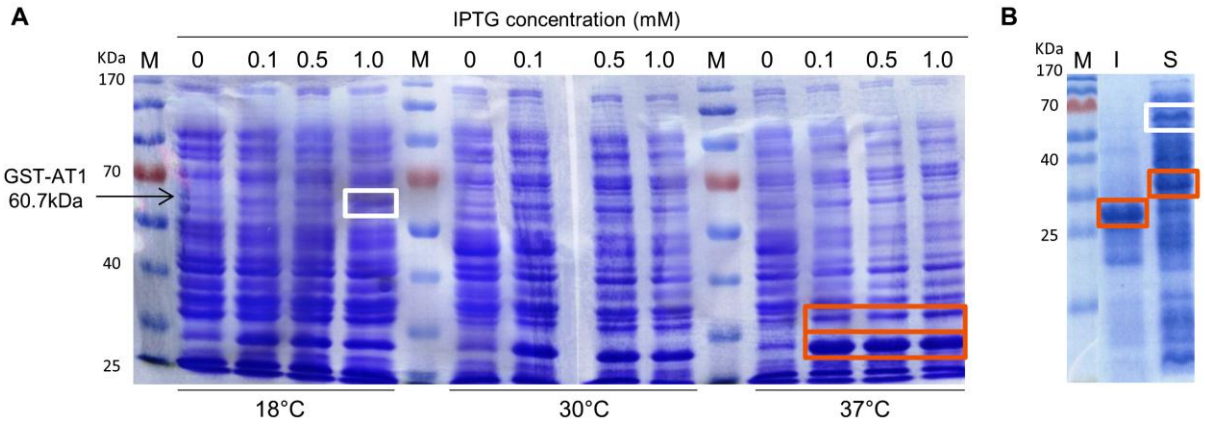

Figure 3.11. Expression of AT1 with the GST tag. (A) Expression experiments at different temperatures (bottom) and IPTG concentrations (top). **(B)** Solubility of AT1 after expression at 18°C and 0.1mM IPTG. M, molecular weight marker; I, insoluble; S, soluble; white box indicates soluble GST-AT1; orange box indicates cleaved GST (bottom) and cleaved AT1 (top).

3.2.1.2 Expression and purification of AT2

Previous work had determined that AT2 was soluble when expressed in *E. coli* BL21 (DE3), and this was confirmed by expression experiments during this study (Figure 3.12, A). It was determined that AT2 was more soluble at the lower temperature of 18°C, as opposed to the previously determined 24°C (Shields, 2008). After induction with 0.1mM IPTG and continued growth at 18°C for 16h, samples were lysed with BugBuster Master Mix and the soluble fraction purified by nickel-affinity chromatography as previously described. Figure 3.12, B shows AT2 purified to a high purity and yield of approximately 7mg/ml.

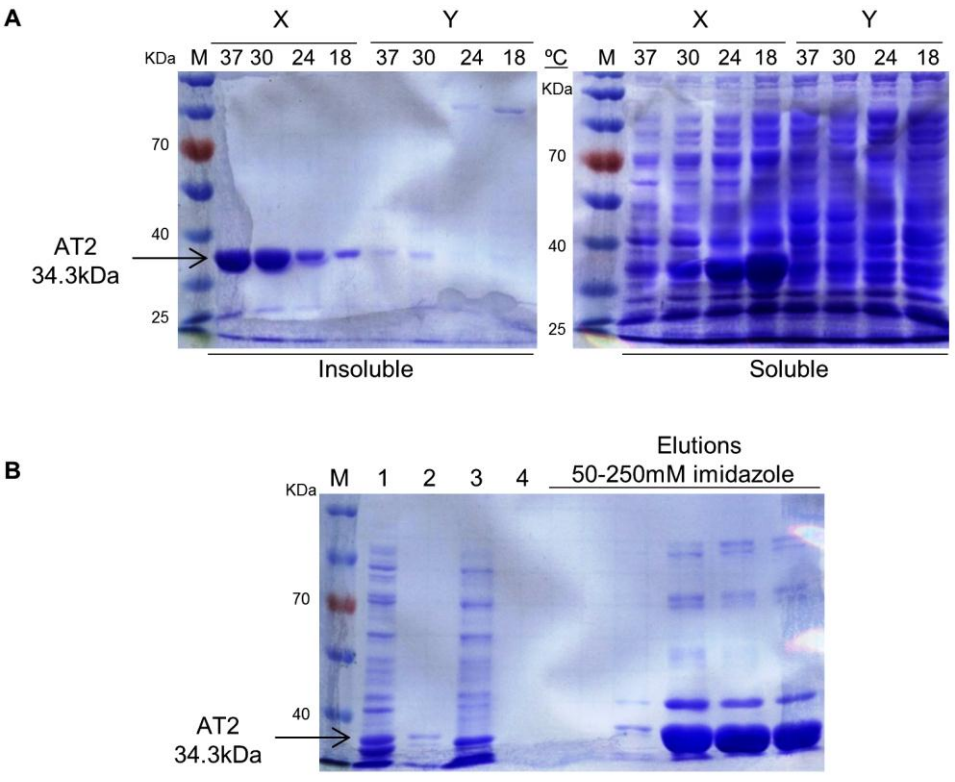

Figure 3.12. Expression and purification of AT2. (A) Solubility of AT2 at a range of temperatures (top in ºC). M, molecular weight marker; lanes X, 0.1mM IPTG; lanes Y no IPTG. **(B)** Purification of AT2. Lane 1, soluble lysate; lane 2, insoluble protein; lane 3, chromatography column flow through fraction; lane 4, final wash fraction.

3.2.1.3 Expression of thiomarinol acyltransferases

As an alternative to using the mupirocin AT1 for assays it was thought it may have been possible to use the AT1 from the related thiomarinol system as the proteins share 43% identity. The thiomarinol ATs were cloned as *Eco*RI-*Sac*I fragments into pET28a to create plasmids pRG305 for AT1 and pRG306 for AT2. Tml-AT1 was found to be soluble at 18ºC (Figure 3.13, A), however attempts at purification were futile (Figure 3.13, B). Tml-AT2 was also found to be soluble at 18ºC, but not to the degree that mup-AT2 was (Figure 3.13, C). Purification was not carried out for this protein as mup-AT2 produced a sufficient yield to work with.

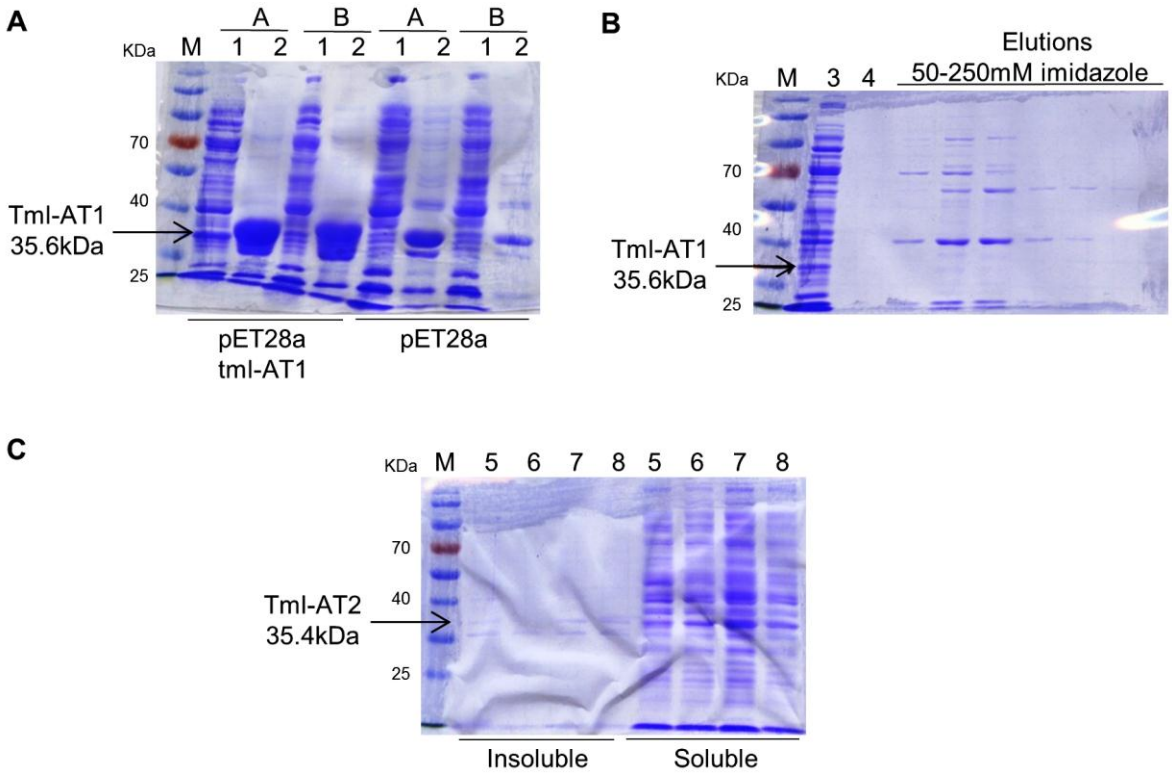

Figure 3.13. Expression of thiomarinol ATs. (A) Solubility of Tml-AT1. M, molecular weight marker; lane 1, soluble fraction; lane 2, insoluble fraction. A, 18ºC; B, 30ºC. **(B)** Purification of Tml-AT1. Lane 3, chromatography column flow through; lane 4, final wash fraction. **(C)** Solubility of Tml-AT2. Lane 5, 0mM IPTG; lane 6, 0.1mM IPTG, lane 7, 0.5mM IPTG; lane 8, 1.0mM IPTG.

3.2.2 Expression and purification of ACPs

Previously the ACPs were cloned into pET28a and the mAcps were cloned into pGBT340, a pET28a derivative lacking the T7 tag (Shields, 2008). For this study, each ACP-containing plasmid was initially transformed into *E. coli* BL21 (DE3) to assess expression conditions compared to the work of Shields (2008). It was confirmed that the ideal expression conditions for ACPs 1, 3-5, 7 and mAcps A, C, and D were as defined previously (Table 3.1). ACP6 was found to be more soluble at 15°C for 16h when induced with 1mM IPTG, than at the previously described 30°C for 4h induced by 0.4mM IPTG. ACP2, 10 and 11 were previously found to be not expressed at all in *E. coli* BL21, so expression conditions were tested using a variety of IPTG concentrations and post-induction incubation temperature and times. By lowering the induction temperatures it was found not only that the proteins were expressed, but that they were in the soluble fraction. Previously ACP8 and 9 were found to be produced, but to be insoluble under all conditions tested. Expression conditions were tested again, but these two ACPs remained in the insoluble fraction. They were cotransformed with pSUEH in the hope that the chaperone plasmid would facilitate protein folding, but this was also unsuccessful. Therefore, plasmids pJS568 and pJS569 were transformed into *E. coli* Lemo21 (DE3), as an alternative expression host and the experiments repeated. Both ACPs were found to require 1mM of L-rhamnose for optimal soluble expression, and induction with 0.4mM IPTG. ACP8 was incubated at 18°C for 16h, ACP9 required 2h at 37°C. The expression conditions of mAcpB were deduced to be as for the previously defined mAcpA, C and D, while mAcpE required a lower post-induction temperature to acquire soluble protein. The ACPs were expressed on a large scale and subjected to purification by

nickel-affinity chromatography as previously described. Figure 3.14 shows that all ACPs, with the exception of 4, 7, 11, B and E purify to a certain degree. While the yield and purity was not optimum, functional ACP was produced for future assays.

Table 3.1. Expression conditions for mupirocin ACPs.

Protein	Solubility phenotype		
	Temperature (°C)[a]	Time (h)[b]	[IPTG] (mM)
‡ACP1	37	2	0.1
ACP2[c]	15	16	0.1
‡ACP3*	30	4	0.4
ACP4	30	4	0.4
‡ACP5*	37	2	0.1
‡ACP6[d]	15	16	1.0
ACP7	37	2	0.1
‡ACP8[e]	18	16	0.4
ACP9[e]	37	2	0.4
ACP10[c]	15	16	1.0
ACP11[c]	18	16	0.25
‡mAcpA	30	4	0.1
mAcpB[e]	30	4	0.1
‡mAcpC*	30	4	0.1
‡mAcpD*	30	4	0.1
‡mAcpE[e]	25	5	0.1

a, post induction temperature; b, post induction incubation time; c, ACPs were previously found not be expressed under a range of conditions; d, previously expressed at 30°C for 4h after induction by 0.4mM IPTG; e, ACPs were previously found to be insoluble under a range of conditions; *, lysis by sonication rather than Bugbuster; ‡, ACPs purified using buffers B (the remainder used buffers A) (Shields, 2008). See Chapter 2.

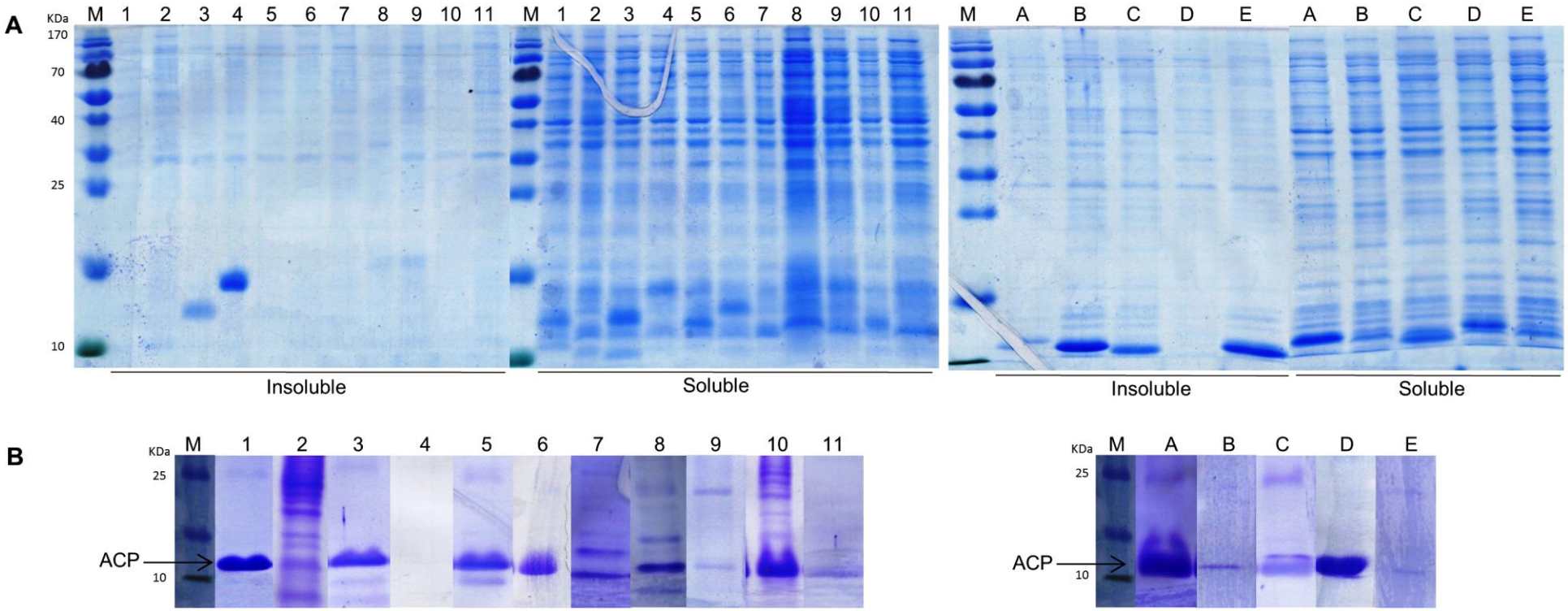

Figure 3.14. Solubility and purification of ACPs. (A) Solubility of ACPs. **(B)** Purification of ACPs by nickel affinity chromatography. M; molecular weight marker; numbers/letters above the gel correspond to ACP.

3.3 Discussion

In order to assay the activity of the mupirocin ATs, soluble functionally active protein needed to be produced. The production of the mupirocin ATs and ACPs is key to the continuation of this work. While AT2 was easily solubilised and purified to a good yield and purity, it was a different story altogether regarding AT1. A number of strategies were deployed in an effort to obtain soluble functionally active protein, but unfortunately none were successful. In the end the rather drastic step of purifying the protein under denaturing conditions and attempting to renature it was taken. While this produced a good yield of protein, it cannot be definitely defined as active until biochemical characterisation. If during the process of characterisation it is not clear if AT1 has regained activity or not, it could be due either to no activity from AT1 or to the fact that the refolding process did not work efficiently. One method to check the refolding of AT1 would be to perform circular dichroism on both AT2 and the refolded AT1 to determine the secondary structure and to compare the two proteins. The structures of AT1 and AT2 should be similar to each other, so the similarity of the refolded AT1 compared to the native AT2 would give an indication of the degree of refolding that has occurred.

Increasing the solubility of AT1 could be crucial in being able to purify active protein in the future. Expressing AT1 with the GST tag appeared to be successful, however time constraints meant this work could not be repeated. The inclusion of protease inhibitors could prevent the cleavage of GST from AT1 and so increase the amount of soluble GST-AT1 that could potentially be purified using glutathione agarose chromatography. There are many other methods than those tested during this work for producing soluble protein. Simply adding glycerol to the buffers could

prevent the aggregation that can lead to insolubility (Gekko and Timasheff, 1981). Various biotechnology companies provide vectors for producing recombinant protein. The SHuffle system (NEB) is marketed as a vector system that can produce soluble protein, particularly proteins that require disulfide bonding for folding. The SHuffle system not only has deletions of reductase genes *gor* and *trxB*, but also expresses DsbC which aids correct protein folding (Chen *et al*., 1999; and de Marco, 2009). Rare codon usage can affect protein translation as the *E. coli* tRNA population can be lacking in particular codons. Both AT1 and AT2 have the rare Pro codon CCC, but additionally AT1 also has rare Arg codons AGG (x1) and CGA (x2). The Rosetta™ host strains have been designed to specifically counteract proteins that use rare codons – they supply rare tRNAs on a Chl^R plasmid (Novagen). As these stains are a variant of *E. coli* BL21 they are compatible with the pET system, and so this may be a viable option to try in the battle of purifying AT1.

While solubility does appear to be a major factor in the problems that have arisen during the work with AT1, it may be that changing the method of purification could produce more protein. Methods such as size-exclusion or ion-exchange chromatography could prove to be more successful than the nickel-affinity chromatography method used in this study. Ammonium sulphate precipitation was tried during this study (data not shown) and appeared to isolate pure AT1, however upon re-suspending the pellet afterwards in a variety of different buffers AT1 remained insoluble. Alternatively there are many other affinity tags that might prove more successful. The PinPoint Xa protein purification system (Promega) produces soluble biotinylated fusion proteins with the benefit that they can be affinity purified under native conditions using the SoftLink™ Soft Release Avidin Resin (Promega).

The HaloTag (Promega) purifies proteins based on ligand specific covalent immobilisation, and is thought to enhance solubility (Ohana *et al*., 2009). An additional tagging system is the cool-tag, a fragment of a penicillin binding protein that binds exclusively to ampicillin sepharose (Expedeon). One option would be to mutate the AT2 active site motifs to match those of AT1 in an attempt to alter the substrate specificity or to match the specificity of AT1. As AT2 is a very soluble protein this could prove successful, so long as those residues in AT1 were not the cause of the insolubility.

Some of the methods discussed to improve the solubility and purification of AT1 can be applied also to the ACPs that proved to be not so soluble (ACP3, 4, B and E) and to those that did not purify by nickel-affinity chromatography (ACP4, 9, 11, B and E). While the biochemical relationship between the ATs and some ACPs can be resolved, for a fuller picture it would be ideal to have access to all of the mupirocin ACPs. It was also hoped that acyl group transfer to the ketosynthase of module 1 would be able to be monitored, but this protein also remained insoluble.

During this chapter the expression and purification of AT1 was achieved and the conditions for AT2 were optimised. All ACPs, with the exception of ACP4, were able to be expressed as soluble protein and purified. These proteins can therefore go on to be utilised in enzymatic assays to assess the functions of the ATs.

CHAPTER 4

4 CHARACTERISATION OF AT1 AND AT2

4.1 Introduction

A transferase is an enzyme which catalyses the transfer of a functional group from one molecule to another, for example, a methyltransferase transfers a methyl group and a glycosyltransferase transfers a monosaccharide. Acyltransferases (ATs) transfer acyl groups and can be found in many biological processes, from production of the neurotransmitter acetylcholine in eukaryotes to fatty acid biosynthesis in prokaryotes (St-Pierre and De Luca, 2000). ATs have particularly important roles in fatty acid and polyketide biosynthesis, transferring the starter and extender units to the enzyme complexes. As mentioned previously, FASs and PKSs are homologous, so important observations about one can frequently correlate to the other.

The mammalian type I FAS is an intertwined polypeptide chain homodimer, with a lower condensing portion and an upper modifying portion (Figure 4.1, A) (Maier *et al*., 2008). The malonyl-acetyl transferase (MAT) is located in the condensing portion and functions to provide both the acetyl-starter and malonyl-extender units. The MAT is connected to neighbouring KS and DH domains by linkers containing α-helices and β-sheets, thought to prevent direct interaction between domains (Maier *et al*., 2008). The fungal type I FAS is an $\alpha_6\beta_6$-heterododecameric complex formed into a central wheel structure with a dome either side; openings provide access to the encompassed reaction chambers (Figure 4.1, B) (Jenni *et al*., 2007). Located in one of the dome segments, an acetyltransferase provides acetyl starter units, while a malonyl/palmitoyl transferase (MPT) provides malonyl extender units to ACPs (Jenni *et al*., 2007).

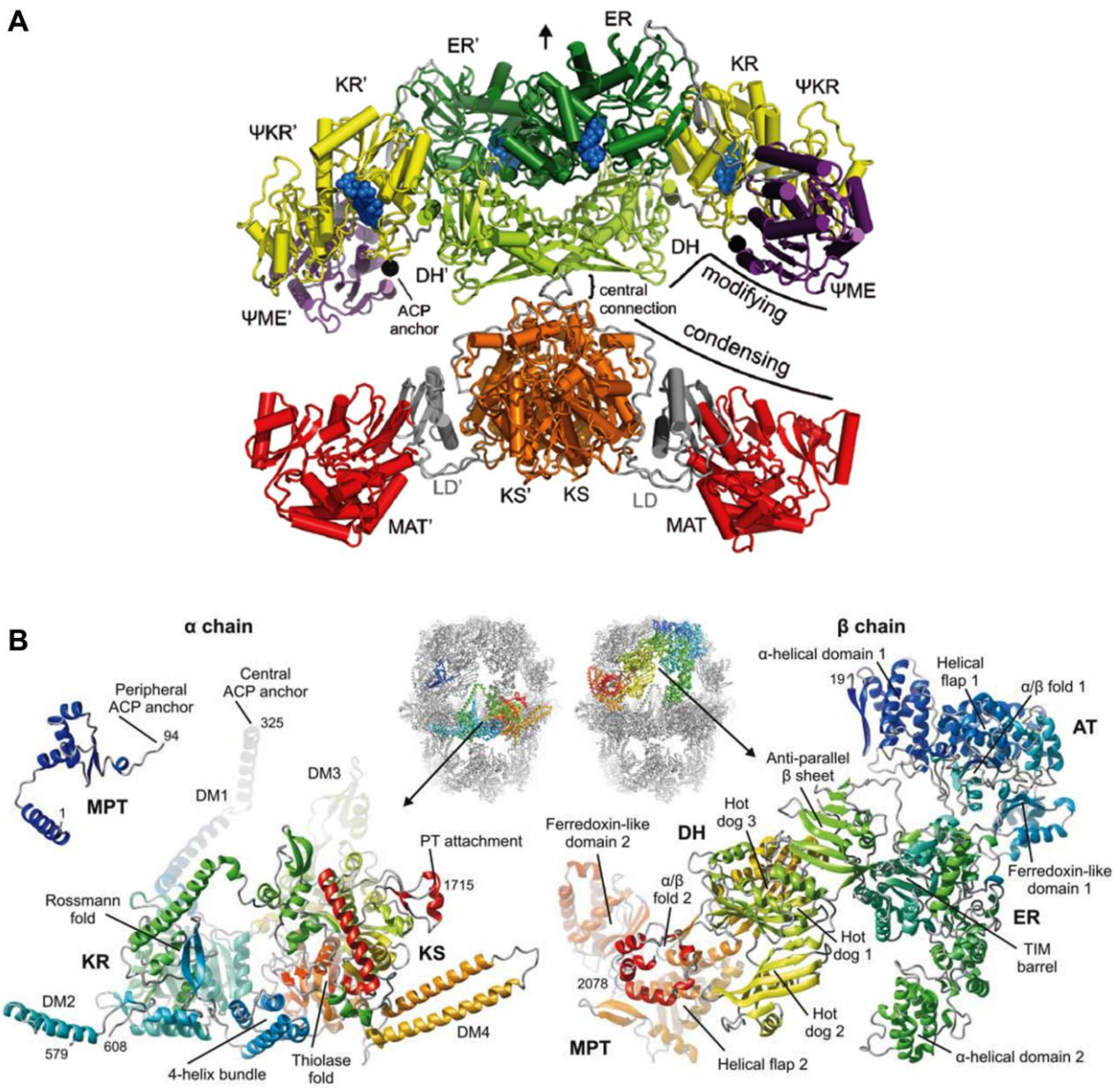

Figure 4.1. Structures of the mammalian and fungal FASs. (A) The structure of a mammalian FAS from pig, comprising of two segments that intertwine to form an X-shape dimer. **(B)** Structure of the α and β subunits that comprise the fungal FAS from *Thermomyces lanuginosus*. A total of 12 subunits form the complex. KR, ketoreductase; ER, enoyl reductase; ME, methyltransferase; DH, dehydratase; MAT, malonyl-acetyl transferase; KS, ketosynthase; ACP, acyl carrier protein; LD, linker domain; MPT, malonyl/palmitoyl transferase, AT, acyltransferase; DM, dimerization module; PT, phosphopantetheinyl transferase; TIM, triose phosphate isomerase. (Jenni *et al*., 2007; Maier *et al*., 2008).

The bacterial type II FAS, in particular that of *E. coli*, has been extensively studied and is comprised of enzymatic functions encoded as discrete proteins that form a large enzymatic complex (Figure 1.6) (Schujman and de Mendoza, 2008). The structures of several of these discrete proteins have been elucidated allowing for important rules to be formed that can be applied to other homologous systems (Huang *et al*., 1998; Price *et al*., 2004). The *E. coli* FAS complex contains two transferases: an acetyl-CoA-ACP transferase (AT) domain for transferring the acetyl-CoA starter unit, and a malonyl-CoA-ACP transferase (MCAT) which transfers an extender malonyl group from malonyl-CoA to the exposed sulfhydryl group of the ACP (Magnuson *et al*., 1993).

The *E. coli* MCAT, encoded by *fabD* is comprised of two domains with the active site located in a cleft between them (Figure 4.2) (Serre *et al*., 1995). Research has indicated that the entire length of the active site cleft is utilised in the binding of substrate during acyl-group transfer (Oefner *et al*., 2006). There are four amino acid residues at the active site that are particularly involved in substrate docking and recognition. Located at a sharp turn between an α-helix and a β-sheet within the major sub domain Ser^{92} attacks the thioester carbonyl of malonate, where it binds, forming a tetrahedral enzyme-substrate complex (Figure 4.2) (Oefner *et al*., 2006). Anchored at the base of the active site cleft is Arg^{117}, which recognises the acidic part of the molecule, and in particular two –NH moieties forming a bidentate salt bridge with malonate (Oefner *et al*., 2006). Gln^{11} further stabilises malonate via hydrogen bonding. His^{201} functions to stabilise the Ser^{92} residue prior to attack of the substrate, and protonates the CoA, releasing it and leaving behind malonyl-FabD (Keatinge-Clay *et al*., 2003). These reactions are the first step of a ping-pong bi-bi mechanism

of substrate acquisition and transfer (Joshi and Wakil, 1971). In the second step, the phosphopantetheine arm of ACP docks in the active site cleft, the substrate is transferred and His^{201} protonates Ser^{92}, releasing malonyl-ACP and leaving the active site of FabD free to acquire more substrate (Keatinge-Clay *et al*., 2003). There are several other residues thought to be involved in substrate specificity and these will be discussed in further detail in Chapter 5.

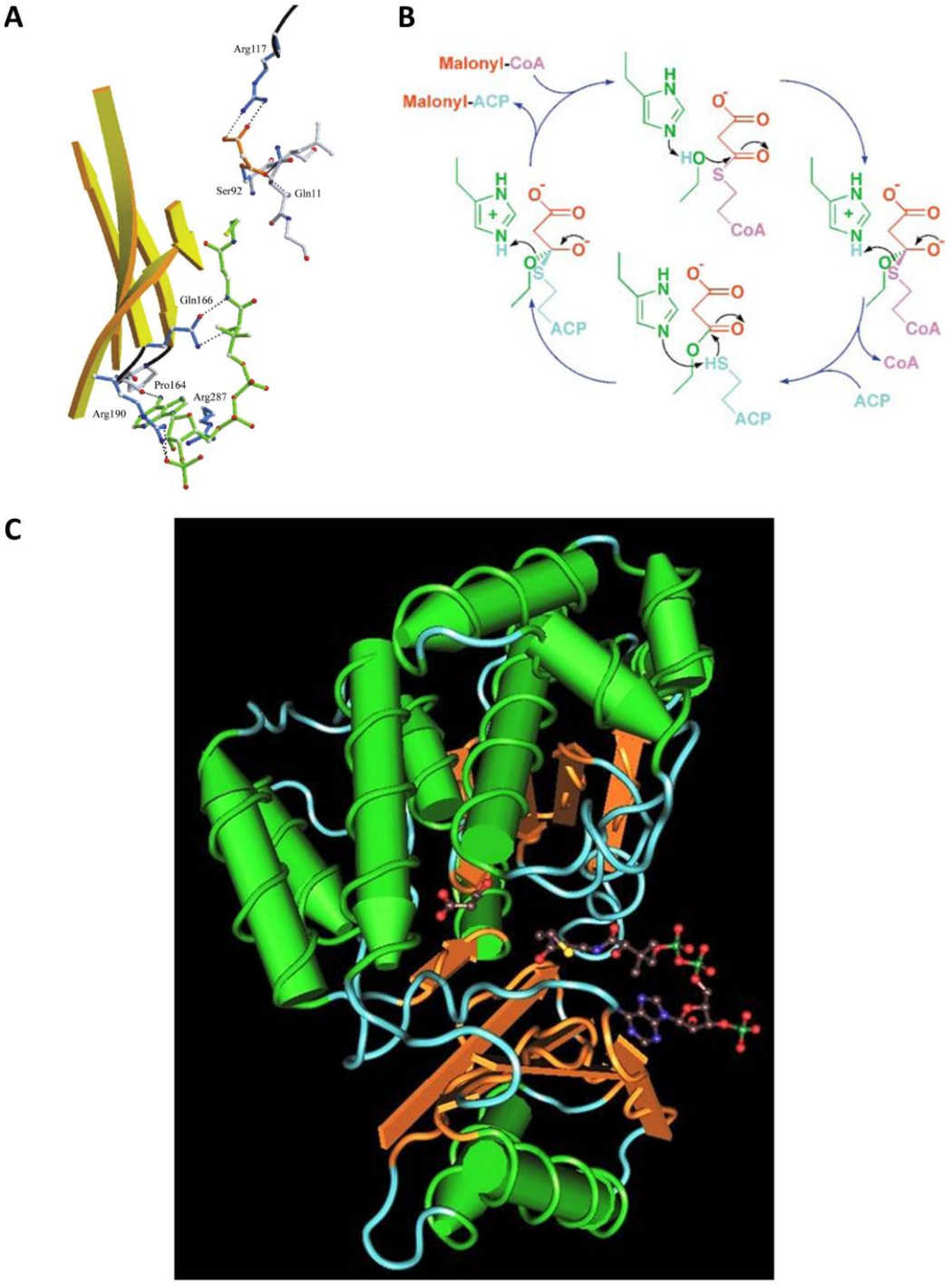

Figure 4.2. Schematic representations of the MCAT active site and the mechanisms taking place in it. (A) Malonyl-CoA binding to MCAT. Malonate is depicted in orange, CoA in green, hydrogen bonds by dotted lines. **(B)** The process of MCAT transferring a malonate group from CoA to ACP. Malonate is depicted in orange, CoA in pink and ACP in light blue. **(C)** The 3D structure of *E. coli* FabD complexed with malonyl-CoA. Helices are shown as green cylinders; strands are shown as brown arrows; random coils are blue; Coenzyme A and malonate are depicted in ball and stick style. PDB ID: 2G2Z. (Keatinge-Clay *et al*., 2003; Oefner *et al*., 2006).

The crystal structures of portions of modules comprising DEBS and FAS have been solved providing valuable structural and mechanistic information that may be applied to other systems. Fragments of modules 3 and 5 of DEBS have been studied in detail after X-ray crystallisation. The fragments from both modules comprise homodimeric proteins that include KS and AT domains along with structurally defined linker sections (Figure 4.3, A). It was shown that the AT domains had an α,β–hydrolase-like core domain and a smaller subdomain, very similar to that of *E. coli* and *S. coelicolor* MCAT (Serre *et al*., 1995; Keatinge-Clay *et al*., 2003; Tang *et al*., 2006; Tang *et al*., 2007). A noticeable difference from the bacterial MCAT structures was that the C-terminal helix of the AT was stacked against one side of the three stranded β-sheet/two α-helix region of the KS-to-AT linker region forming a unique αβα- fold. The post-AT linker region then wraps back over the AT domain and KS-to-AT linker to interact specifically with the KS domain – forming a rigid structure that prevents the AT and KS domains from moving apart. The active site of the AT domain formed a 20Å deep channel between the two subdomains (the invariant Arg^{667} forming a bridge with methylmalonyl-CoA substrate), but the distance between this and the KS active site was too great for the span of a phosphopantetheine arm of ACP to bridge the gap. Thus significant domain reorganisation is required for the ACP/substrate complex to interact first with the AT and then the KS domain (Tang *et al*., 2006; Tang *et al*., 2007).

In contrast to the *cis*-acting ATs from the DEBS system, *trans*-acting ATs do not have the same inter-domain constraints. Until recently little was known about this type of AT, but there are now over 30 PKS systems identified where AT activity is provided in *trans* by one or more discrete proteins.

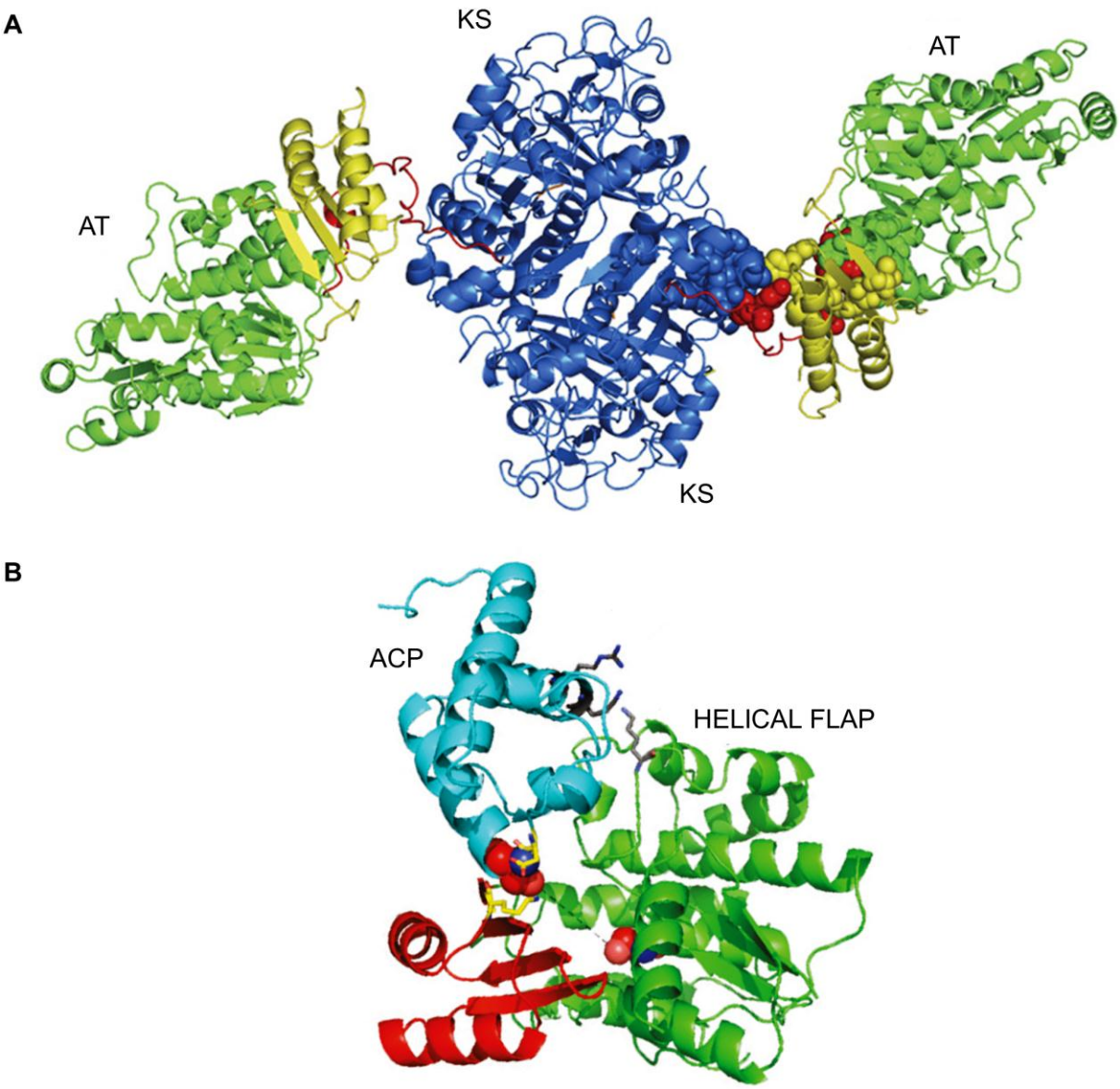

Figure 4.3. Crystal structures of *cis*- and *trans*-acting ATs. (A) Crystal structure of the *cis* KS3/AT3 didomain of DEBS module 3 dimer. The KS3 domain, KS3-AT3 linker, AT3, and post-AT3 linker are shown in blue, yellow, green and red respectively. AT, acyltransferase; KS, ketosynthase (Tang *et al*., 2007). **(B)** Homology model of the *trans*-acting AT DisD docking with disorazol ACP1. ACP is shown in cyan, AT large subdomain in green and AT small subdomain in red. Active site serine residue of the AT and phosphopantetheine attachment site of the ACP are shown as red spheres. ACP, acyl carrier protein (Wong *et al*., 2011).

Out of these *trans*-AT systems the substrate specificity has been determined for only a few ATs and in almost every case the preferred substrate is malonyl-CoA, with the exception of KirCII of the kirromycin system which is specific for ethylmalonyl-CoA (Tang *et al*., 2004b; Aron *et al*., 2007; Lopanik *et al*., 2008; Musiol *et al*., 2011; Wong *et al*., 2011). The first structure of a *trans*-acting AT was published in 2011 providing new insights into the field of *trans*-acting ATs (Figure 4.3, B) (Wong *et al*., 2011). The *trans*-AT was found to be very similar to the *cis*-ATs from modules 3 and 5 of DEBS as well as to FabD from *E. coli*. In keeping with previous predictions DisD was found to be an αβ-hydrolase with a large and a small subdomain. The large subdomain was comprised of 10 α-helices and a short 3-stranded parallel β-sheet, while the small subdomain was comprised of a 4-stranded anti-parallel β-sheet topped with 2 α-helices – this is an α-helix and β-strand less than the *cis*-ATs or FabD. The active site cleft was located in a gorge in between the large and smaller subdomains (Wong *et al*., 2011). This model has also shed light on the second part of the AT reaction – the docking of an ACP. Previous models for *S. coelicolor* MAT indicated that the ACP docked on the larger subdomain of the AT around the helical flap (Keatinge-Clay *et al*., 2003). For *cis*-acting ATs it is also known that the linkers connecting the ATs to the adjacent domains either side are important for ACP recognition and docking (Wong *et al*., 2010). However, *trans*-acting ATs do not have linkers connecting them to the KS domain, and so it is clear that an alternative mechanism must be in operation. The crystal structure of DisD has shown that Asp^{45} of the ACP1 could form a salt bridge with Lys^{197} on the AT surface (Wong *et al*., 2011). This model has also demonstrated that the majority of the ACP-AT interaction appears to involve the smaller AT subdomain, as opposed to the large subdomain. It

is possible that the lack of the C-terminal helix and sheet in this *trans*-AT allows substrates to preferentially dock at the smaller subdomain (Wong *et al*., 2011).

Due to the homology between FASs and PKSs, the conclusions of research undertaken on *E. coli* FabD and *S. coelicolor* MAT can be applied to polyketide ATs, not only those with known substrate specificities, but the information can also be utilised to predict substrate specificity (Yadav *et al*., 2003). Correlating to *E. coli* FabD residues 198-201 (Val, Pro, Ser and the active site His), highly conserved sequence motifs have been found to indicate substrate preferences among polyketide ATs. The sequence motif YASH correlates with methylmalonyl-CoA specificity, while HAFH correlates with malonyl-CoA specificity (Del Vecchio *et al*., 2003). The choice of starter and extender units is determined by the substrate preferences of the ATs. The starter and extender units are simple carboxylic acids that become associated with CoA (for example: acetyl, propionyl, butyryl, isobutyryl, malonyl and methylmalonyl), but the vast pool of substrates available ensures polyketides are a diverse group of metabolites (Ruan *et al*., 1997; McDaniel *et al*., 1999; Staunton and Weissman, 2001). The loading AT (AT_L) of the DEBS system is somewhat promiscuous as it can transfer acetyl, butyryl and isobutyryl groups, in addition to the preferred substrate of propionyl; while the remaining ATs load methylmalonyl derived extender units (Marsden *et al*., 1994; Lau *et al*., 2000). BryP AT1 is a promiscuous *trans*-AT as it can accept both malonate and methylmalonate, although the substrate of preference is malonate (Lopanik *et al*., 2008).

The mupirocin cluster contains two domains classified as ATs – both encoded by *mmpC*, and are proposed to act in *trans* throughout the production of mupirocin (El-Sayed, *et al*., 2003; Wu *et al*., 2008). Sequence alignments have shown that AT1

and AT2 are both homologous to ATs of type I PKS systems, such as DEBS, and AT2 also shows sequence identity to an MCAT involved in fatty acid synthesis (El-Sayed *et al*., 2003). Previous studies on the cluster have shown that in-frame deletion of AT1 only reduced mupirocin production (but did not abolish it), while a similar mutation in AT2 abolished it, leading to the conclusion that AT2 is essential for mupirocin biosynthesis, whereas AT1 is not (El-Sayed *et al*., 2003; Shields, 2008). It is thought that the ATs load the starter acetate unit onto module 1 of MmpD, and then load extender malonate units onto ACP2-11. It is also possible they load 3-hydroxypropionate (3-HP) starter units to mAcpD as a precursor to 9-hydroxynonanoic acid (9-HN) biosynthesis (El-Sayed *et al*., 2003). MmpC is 1110 amino acids (aa) in length, and it is predicted to be split into 3 domains, the 2 ATs and a third domain: AT1 is 286aa and has a molecular weight of 30.9kDa; AT2 is 281aa with a molecular weight of 30.5kDa, and the third domain is 416aa with a molecular weight of 45.9kDa; there are also linkers between the domains.

The third domain has homology to many domains or discrete proteins labelled as FMN-dependant oxidoreductases or PfaD family protein, which are responsible for omega-3 polyunsaturated fatty acid biosynthesis in several bacteria (Metz *et al*., 2001; Bumpus *et al*., 2008). Many of these are encoded by known PKS clusters and are also associated with *trans*-ATs, such CorA (61% identity), DifA (58% identity), PksE (55% identity), ChiA (54% identity), TmpC (62% identity), KirCI (43% identity), BatK (58% identity) and PedB (56% identity). Sequence alignments with ERs from *trans*-AT systems have revealed a remarkable similarity between 15 putative ER domains when aligned with the MmpC third domain - as many as 34 residues are

completely conserved. Inactivation of this putative ER resulted in abolishment of mupirocin production indicating the importance of this domain.

4.2 Results

4.2.1 Phylogenetic analysis

All of the characteristics described that define *trans*-AT PKS systems can be applied to those of the mupirocin cluster: the ATs are encoded by a discrete gene, there are two *cis*-acting methyltransferase (MT) domains (in modules 1 and 3) thought to incorporate the methyl groups of S-adenosyl methionine (SAM) into the growing polyketide chain; and there are no ER domains included in any of the modules - it is thought that the third domain of MmpC could encode an ER domain that would act in *trans* to provide the remaining two enoyl reductions required for 9-HN biosynthesis (MupE performs the C7'-C6' enoyl reduction) (El-Sayed *et al*., 2003). Malonate is the preferred extension substrate for *trans*-acting ATs, and it is highly probable that this is the case in mupirocin biosynthesis.

Phylogenetic analysis of 52 *trans*-acting ATs indicated 2 main evolutionary pathways with the mupirocin ATs falling into separate clades (Figure 4.4). The domain architecture of genes encoding *trans*-acting ATs varies from single ATs, tandem ATs, single AT with a C-terminal ER domain, single AT with a C-terminal TE domain, to tridomain proteins with tandem AT domains and a C-terminal ER domain. While several single ATs group in either AT1- or AT2-like (in relation to the mupirocin ATs) there are also several that appear to be phylogenetically separate, such as FenF, ZmaF, AlbXIII, Orf12 of *S. carzinostaticus*-F41, OzmC and EtnB. Of these, OzmC and EtnB are not the only ATs in their respective clusters – OzmM encodes a tridomain protein and EtnK has bidomain ATs (Menche *et al*., 2008; Zhao *et al*., 2010). There are five tridomain proteins, of which MmpC is one, and in every case the first AT (AT1) clusters in the AT1-like group and the second AT (AT2) clusters in

the AT2-like group, with the exception of BryP – which is reversed (Lopanik *et al*., 2008). There are several proteins that have the tandem AT architecture – of these the first AT is always AT1-like and the second is AT2-like, like the tridomain proteins but lacking the ER domain. When the AT is part of a bidomain protein which encompasses a C-terminal ER or TE domain, the AT is always AT2-like.

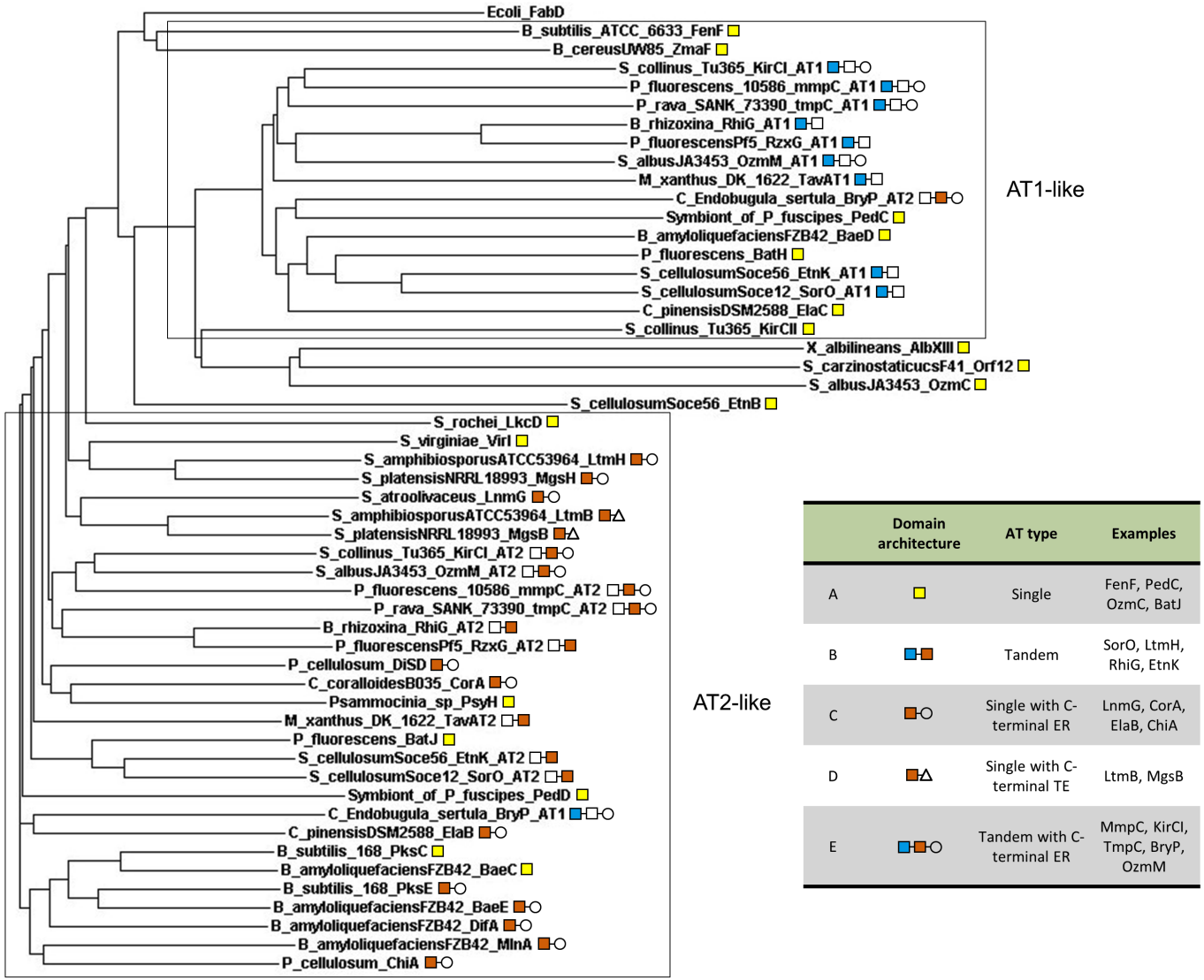

	Domain architecture	AT type	Examples
A		Single	FenF, PedC, OzmC, BatJ
B		Tandem	SorO, LtmH, RhiG, EtnK
C		Single with C-terminal ER	LnmG, CorA, ElaB, ChiA
D		Single with C-terminal TE	LtmB, MgsB
E		Tandem with C-terminal ER	MmpC, KirCI, TmpC, BryP, OzmM

Figure 4.4. Phylogenetic analysis and domain architecture of *trans*-acting ATs. AT1, AT2 and single ATs are coloured blue, orange and yellow respectively. *E. coli* FabD is included as the outgroup for reference. ATs are grouped into 'AT1-like' and 'AT2-like' in reference to grouping with mupirocin AT1 or AT2.

4.2.2 Secondary structure prediction

X-ray crystallography is a method used to determine the spatial arrangement of atoms within a molecule. The electron density information gained can be used to build a 3D model of the molecule. The structure of several bacterial fatty acid MCATs have been solved by X-ray crystallography, thus allowing predictions about the structure of similar enzymes. Predictions of the secondary structures of the mupirocin ATs was carried out using the protein structure prediction server (PSIPRED), and compared to that of FabD and DisD (Jones, 1999; and McGuffin *et al*., 2000). Figure 4.5 shows the predicted results. The prediction confirmed the presence of 14 α-helices in FabD, but predicted the presence of an extra β-strand. The active site GHS motif appears to be located in between a β-strand and an α-helix, which concurs with previous research (Serre *et al*., 1995). PSIPRED predicted DisD to have 13 α-helices and 7 β-strands (8 if you include the small C-terminal one), and this is in agreement with Figure 2 from the research by Wong *et al*., but not with the text – they describe DisD as having 12 α-helices (2011). However based on their figures and the prediction from PSIPRED it seems likely that DisD has one less α-helix than FabD. Again the active site GHS motif is located between a β-strand and an α-helix. MmpC AT2 is predicted to match the structure of DisD – 13 α-helices and 7 β-strands, with the active site GHS located between a β-strand and an α-helix. However, MmpC AT1 appears to have a slightly different structure – there are only 11 predicted α-helices and 5 β-strands. While the position of the active site GSS motif appears to be the same, it is clear there may be structural differences in the active site of AT1. The GSS motif does not appear to be located in a tight turn between a β-strand and an α-helix, but in a space between two sizable α-helices.

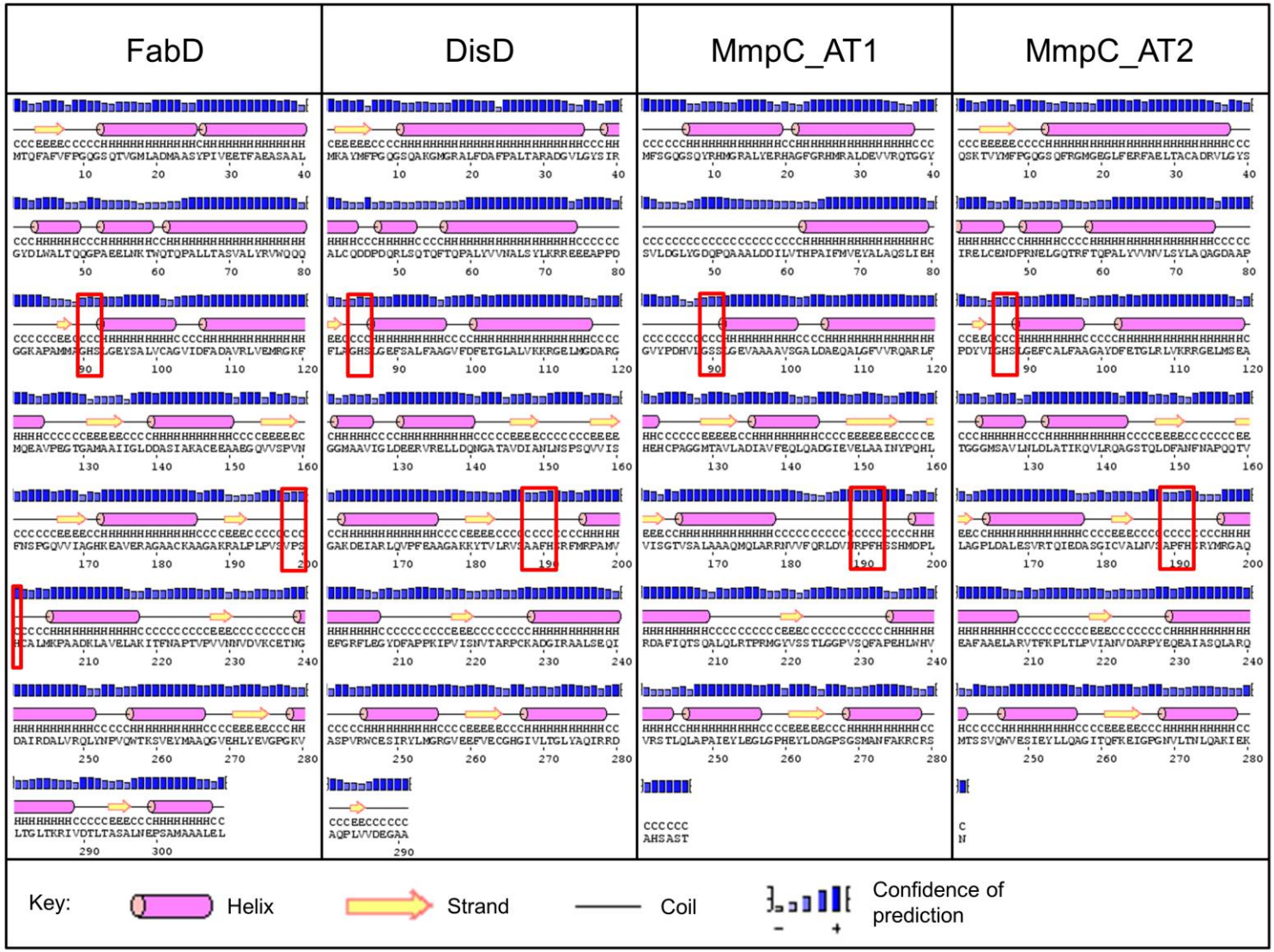

Figure 4.5. Secondary structure prediction of the mupirocin ATs. The ATs are compared to the proteins FabD and DisD, whose structures have been solved by X-ray crystallography. Active site motifs are boxed in red.

4.2.4 Crosslinking of AT2

While the structural models of modules from the DEBS system show that modules 3 and 5 operate as dimeric proteins, it is unknown whether this is the case for *trans*-AT systems (Tang *et al*., 2006; 2007). It is also unknown if the ATs that are absent in these systems function as dimers or monomeric proteins. It may be that dimerization provides a more efficient mechanism for transferring units throughout the cluster. While dimerisation can be assessed by size-exclusion chromatography, in this case glutaraldehyde crosslinking was used to determine whether purified AT2 forms dimers. Glutaraldehyde reacts with amino groups, specifically those on Lys residues, to form stable covalent bonds – Schiff base formation from an amino group from one protein and a carbon-nitrogen bond formation with an amino group from another protein molecule (Wine *et al*., 2007). If two proteins are in close proximity to one another they will both react with the glutaraldehyde to form a dimeric complex which can indicate their ability to dimerise *in vivo*. AT2 at a concentration of 0.1mg/ml was incubated with increasing concentrations of glutaraldehyde as described in Chapter 2 and the reaction terminated after 20min. The data in Figure 4.6 shows that treatment of AT2 with glutaraldehyde does not result in crosslinking to form dimers, which would have resulted in a band corresponding to approximately 68kDa. The presence of a band immediately below AT2 could be explained by the absence of protease inhibitors in the reaction mix, allowing some cleavage of the N-terminal His-tag to take place. The disappearance of this band on addition of glutaraldehyde indicates the crosslinking process is fully functional.

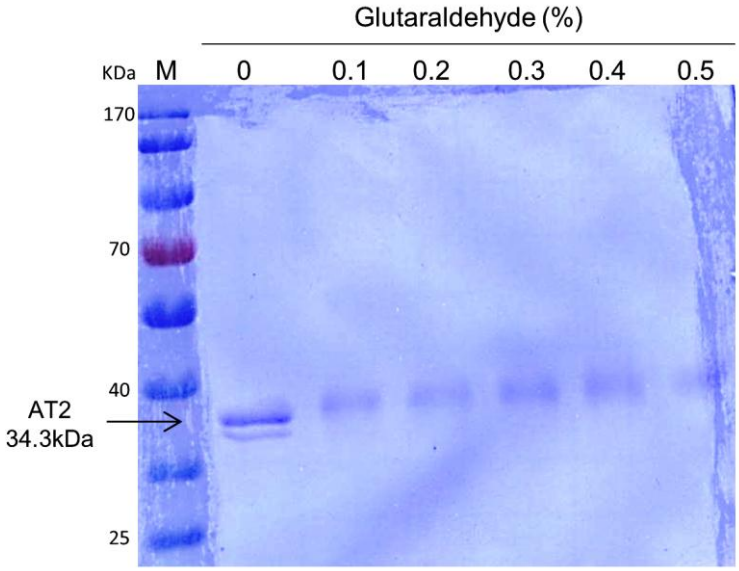

Figure 4.6. Crosslinking AT2 with glutaraldehyde. The absence of a band around 68kDa showed that AT2 does not function as a dimer. The band slightly below the AT2 band can be accounted for by cleavage of the 3.8kDa His-tag.

4.2.5 Substrate specificity assay of AT1 and AT2

The assay to test AT activity *in vitro* involved measurement of free sulfhydryl groups exposed upon transfer of malonate from CoA to AT. Ellman's reagent (5, 5'-dithio-*bis*-(2-nitrobenzoic acid) – DTNB) reacts with free sulfhydryl groups to yield a mixed disulphide and 2-nitro-5-thiobenzoic acid (TNB), which can be measured at 412nm (Ellman, 1959). Preparations of AT1 and AT2, purified as described in Chapter 3, were used to determine specificity for release of CoA from different acyl-CoA substrates. The ATs at 50µM were equilibrated with buffer and Ellman's reagent prior to addition of 100µM acyl-CoA substrate, which was used to start the reaction. The reactions were measured over a 10s period, with measurements being taken every 1s. The ATs were initially tested with acetyl-CoA (the proposed starter unit for mupirocin biosynthesis) and malonyl-CoA (the extender unit). Figure 4.7 shows that neither AT showed significant activity with acetyl-CoA, and only AT2 accepted malonyl-CoA. A possible reason for the negative result with AT1 could be that the refolding process had not reconstituted an active protein and as of the time of writing this Thesis it has not been possible to perform an alternative test of AT1 activity although ideas about this are discussed in Chapter 6.

In addition to the two substrates initially tested, AT2 was also tested with propionyl- and methylmalonyl-CoA, both of which are known to be involved in polyketide biosynthesis (Marsden *et al*., 1994). AT2 did not react with either of these substrates, as was expected from the sequence analysis which had predicted a preference for malonyl-CoA. The reaction between AT2 and its substrate, malonyl-CoA, proceeded very fast – it appeared the majority of the reaction was completed within seconds, the time it took to mix the contents of the cuvette and start recording

the reaction on the spectrophotometer. Assays were completed using less AT2 and at lower temperatures to attempt to slow the reaction down, and while this produced a lower absorbance reading, the reaction still proceeded within the first few seconds. For this reason it was not possible to calculate kinetic parameters from the Ellman's assay.

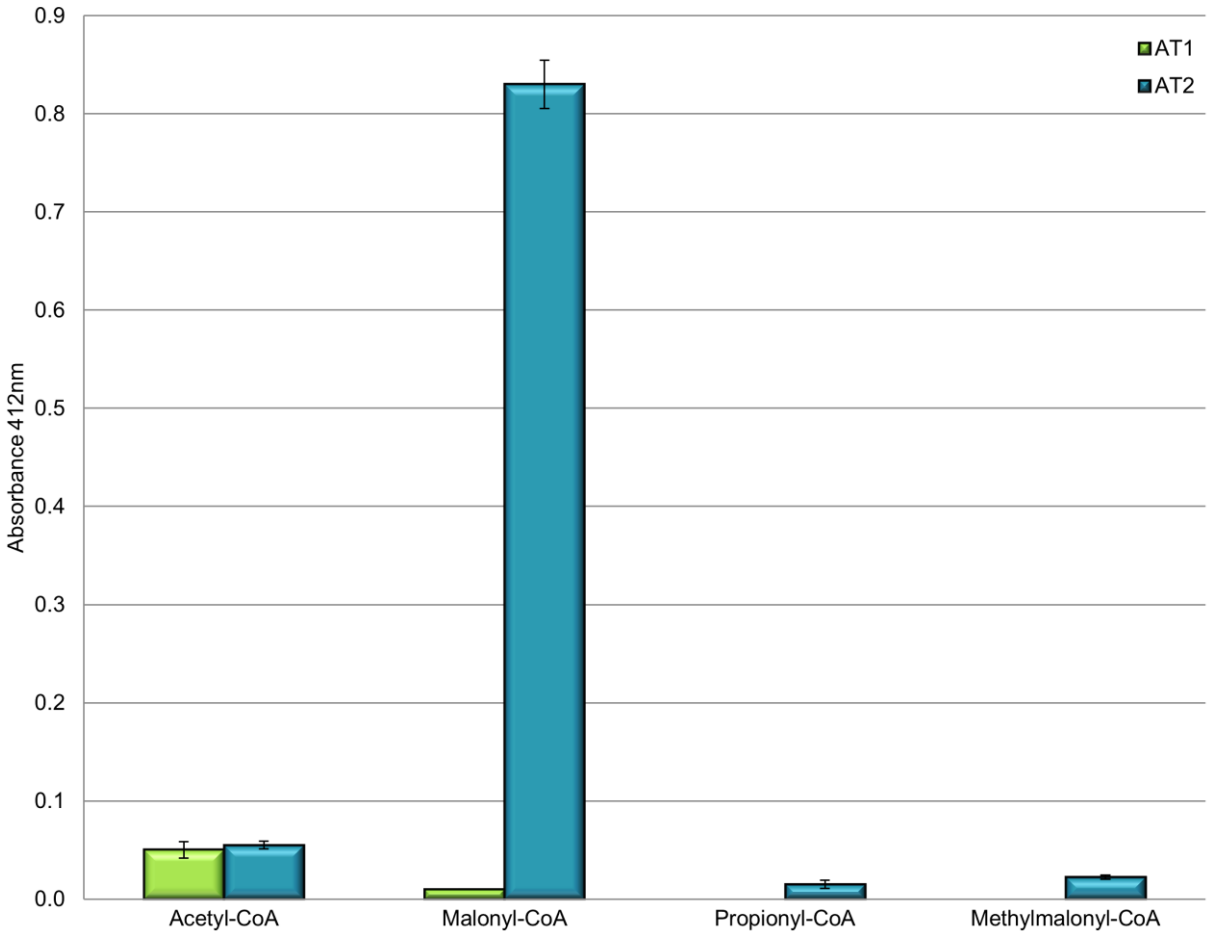

Figure 4.7. Substrate preference of AT2 measured by Ellman's assay. The results indicate AT2 converted 58.6µM of malonyl-CoA to malonate and CoA. [AT2] = 50µM; [substrate] = 100µM; n=2.

4.2.6 Acquisition and transfer of malonate by AT2

Autoradiography was used to confirm the findings from the enzyme assay. Initially AT2 was incubated with [^{14}C]-malonyl-CoA to assess self-loading of malonate. Loading was not detected for either of the negative controls – AT2 with no substrate, and substrate without any AT2. Radioactivity was detected when both [^{14}C]-malonate and AT2 were present (Figure 4.8). As the concentration of unlabelled malonyl-CoA was decreased, the amount of radioactivity on AT2 increased. At maximum concentration of [^{14}C]-malonyl-CoA (20μM), there is approximately 40% incorporation of [^{14}C]-malonyl-CoA – indicating that all 8μM of AT2 has acquired a [^{14}C]-malonyl group. This result confirmed that of the previous section – that AT2 is specific for malonyl-CoA. It also confirmed that this assay could be used to determine the transfer of the malonyl group from AT2 to mupirocin ACPs.

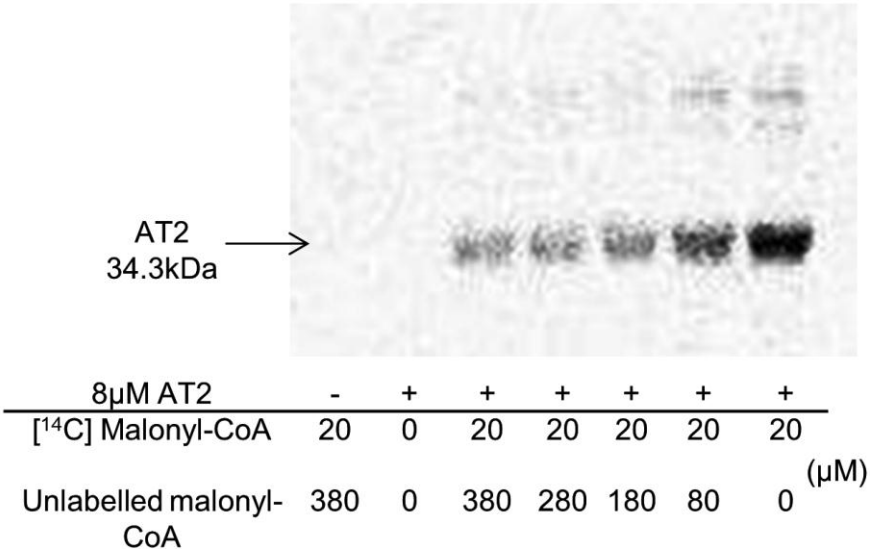

Figure 4.8. Radiolabelling of AT2. AT2 was mixed with unlabelled malonyl-CoA and [^{14}C]-malonyl-CoA at different ratios to assess malonate acquisition.

4.2.6.1 Assessing the appropriate conditions for AT assays

An initial assay to test the ability of AT2 to transfer [^{14}C]-malonate to *holo* ACP3 proved to be negative. On reviewing conditions it was decided to fully assess the conditions required for transfer. Firstly the presence of the reducing agent *tris*(2-carboxyethyl)phosphine (TCEP) was tested. All assays were performed in duplicate with 5µM AT2 and 20µM ACP and [^{14}C]-malonyl-CoA. Figure 4.9 demonstrates that TCEP is required for AT to transfer the [^{14}C]-malonate to the ACP – while AT2 can acquire the malonate without the presence of TCEP, it can then only be transferred to the ACP in the presence of TCEP.

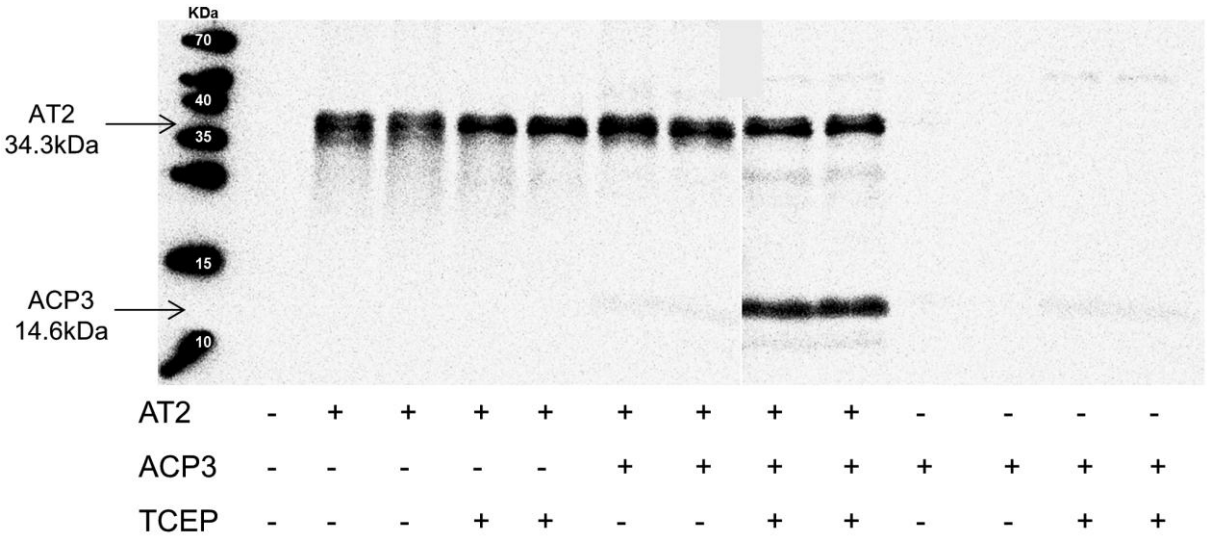

Figure 4.9. Effect of TCEP on the transfer of [^{14}C]-malonate to ACP3. Where present [AT2]=5µM, [ACP]=20µM and [[^{14}C]-malonyl-CoA]=20µM.

To determine the optimal pH to conduct the assay, tests were designed using buffers of varying pH's and the ability of AT2 to transfer malonate to ACP3 was observed. The amount of malonate observed on AT2 and ACP3 was calculated in comparison to a spot test of known concentration, as described in more detail in Chapter 2. An initial assay varying from pH 4.4-10.4 highlighted the area around pH 7.4 as a suitable pH for optimal malonate acquisition by AT2 (Figure 4.10, A), in line with the methods used in the characterisation of BryP (Lopanik *et al*., 2008). Further optimisation of the pH determined pH 8.0 to be optimal for transfer of malonate from AT2 to ACP3 (Figure 4.10, B).

There are many factors in the radiolabelling assay that could affect the transfer of malonate from AT2 to the ACP. Due to the speed at which AT2 acquires malonate the concentration of ACP and [^{14}C]-malonyl-CoA in the assay could be rate limiting. Therefore, tests were conducted to analyse the ideal concentration of AT2 required for maximum transfer of malonate to ACP3. While the concentration of AT2 was lowered from 20µM to 0.1nM, the concentration of both ACP3 and [^{14}C]-malonyl-CoA was fixed at 20µM (Figure 4.11). The highest transfer to ACP3 occurred between AT2 concentrations of 1µM and 10nM. An AT2 concentration higher than 2µM (the AT2/ACP3 cross over point in Figure 4.11 (B)) is likely to result in less malonate being transferred to ACP3. At an AT2 concentration of 50nM the malonylation of ACP3 was at its highest – 3.7µM. At this concentration the malonylation of AT2 was still at a minimal level, so it was decided to use 50nM AT2 in all further assays. This would ensure the concentration of ACP and [^{14}C]-malonyl-CoA in the assay were not rate limiting and so allow the maximum amount of transfer to the ACP to be measured.

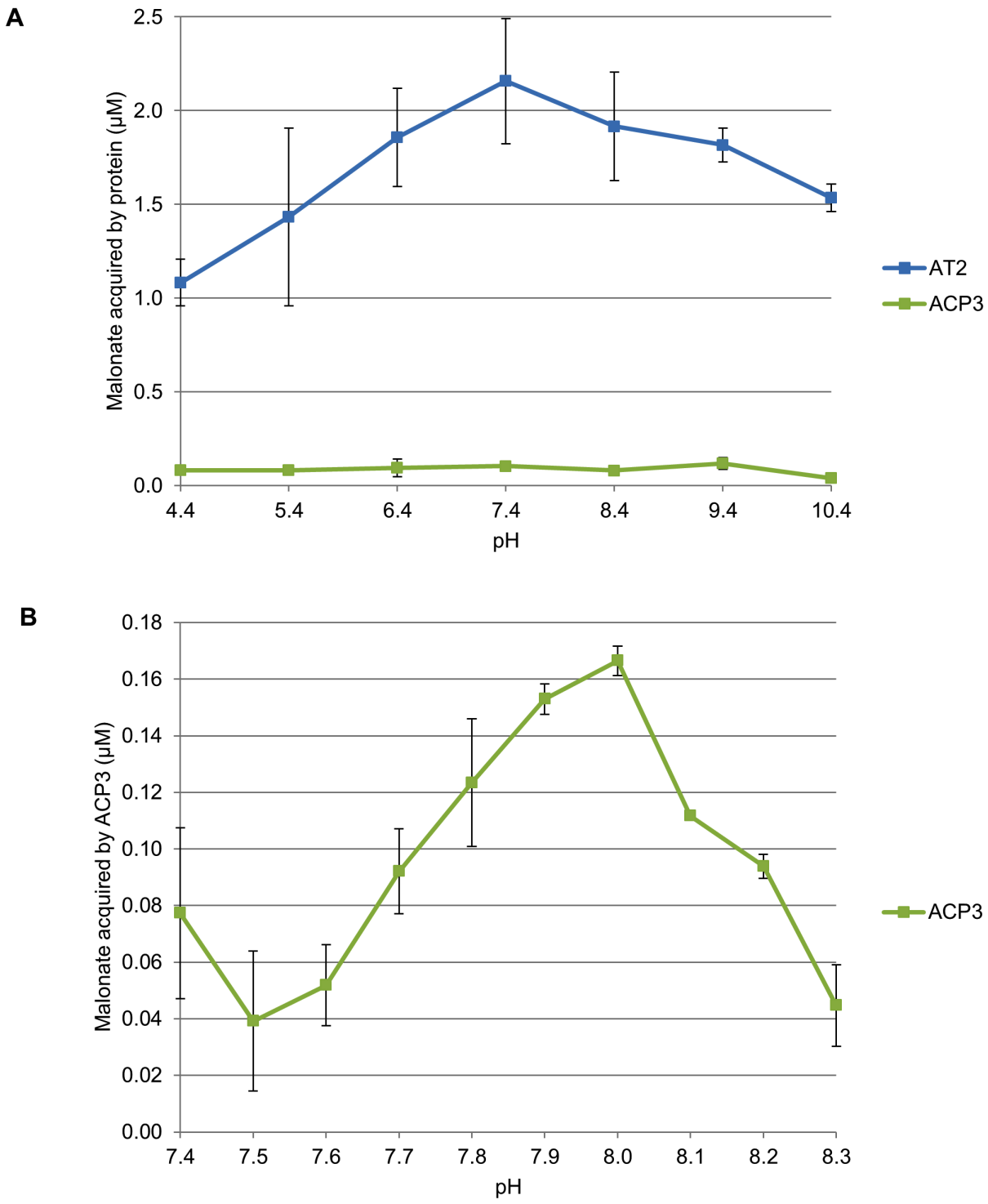

Figure 4.10. Effect of pH on the malonylation of AT2 and ACP3. (A) The malonylation of AT2 and ACP3 were measured between pH 4.4-10.4. n=2. **(B)** The malonylation of ACP3 between pH 7.4 and 8.3. In all cases [AT2]=5µM, [ACP]=20µM and [[^{14}C]-malonyl-CoA]=20µM. n=2.

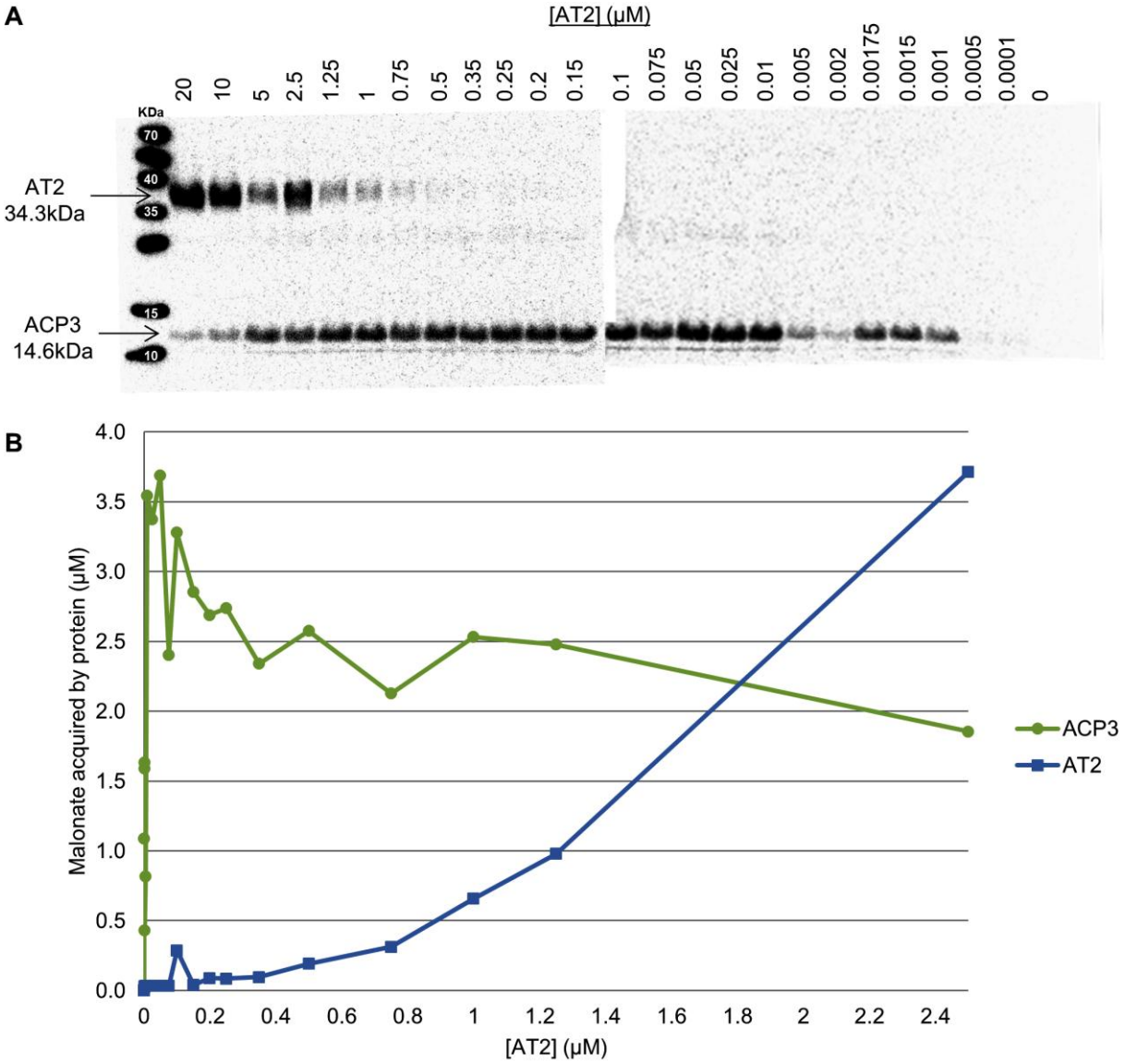

Figure 4.11. Effect of AT2 concentration on the malonylation of ACP3. (A) Autoradiography showing the effect of decreasing AT2 concentration on malonate transfer to ACP3. **(B)** Line graph showing the amount of malonate acquired by AT2 and ACP3 as the concentration of AT2 was lowered (data is only shown for [AT2]<2.5μM). In all cases [ACP]=20μM and [[^{14}C]-malonyl-CoA]=20μM. n=1.

4.2.6.2 AT2 malonylation of type I and type II ACPs

Individual ACPs were incorporated into the assay at the same stage as AT2 and allowed to equilibrate before addition of [^{14}C]-malonyl-CoA. In the first instance soluble fraction ACP was added to the assay to get an idea of the ACPs that could accept malonate as not all ACPs in the cluster could be purified (data not shown). The empty pET28a vector and *apo* ACPs were used as negative controls. All type I ACPs appeared to self-malonate to a certain degree and to malonate in the presence of AT2, although as this was using soluble fraction it is possible the self-malonylation could have been due to a separate protein. mAcpA, C, D and E all appeared to self-malonylate and accept malonate in the presence of AT2. This preliminary experiment confirmed previous findings that *E. coli* phosphopantetheinyl transferase (PT), Sfp, can phosphopantetheinylate *apo* mAcpA and convert it to the active *holo* form (Shields, 2008). These results also found that this was likely for mAcpB, C and E, although further investigation would be required to confirm this. Interestingly, although converted from *apo* to *holo* from by Sfp, where it was able to accept malonate (perhaps as a by-product from the reaction, rather than self-acquisition), *holo* mAcpB was not malonylated in the presence of AT2.

Using the conditions determined in the previous section the ability of AT2 to transfer malonate to pure ACPs was investigated. The assay was performed in pH 8.0 buffer containing 1mM TCEP, with an AT2 concentration of 0.05µM, an ACP concentration of 20µM, and a [^{14}C]-malonyl-CoA concentration of 20µM. Autoradiography showed that AT2 transferred malonate to ACP3, 5, 8 and mAcpC and D, but not to ACP 1 (Figure 4.12, A). Controls consisting of just AT2, or AT2 plus extract from bacteria with the empty pET28a expression vector showed no

radioactive signal in the ACP region of the gel. Further experiments to quantify the amount of malonate transferred were only performed using ACP1, 3, 5 and C, due to poor yields when purifying ACP8 and D. Alongside extracts from bacteria with the empty vector, the *apo* ACPs were analysed as additional negative controls (data not shown). ACP1, ACP3 and ACP5 were chosen to be assayed for malonylation by AT2 as they are present during different steps in mupirocin biosynthesis. mAcpC was chosen to represent the type II ACPs in the cluster. ACPs were purified by nickel-affinity chromatography and the protein concentration calculated by Coomassie staining. No radioactivity in the region of ACP1 was detected with or without AT2. The remaining ACPs all appeared to self-malonylate, however, the addition of AT2 did increase the amount of radioactivity detected (Figure 4.12, B). AT2 increased the malonylation of ACP3 by 247%, ACP5 by 513% (sixfold increase) and mAcpC by 938% (tenfold increase).

It should be noted that despite best efforts the proteins did not represent 100% purity due to undergoing one round of metal affinity chromatography and no further rounds of purification, therefore the results presented here are semi-quantitative when concerning malonyl transfer and protein structure.

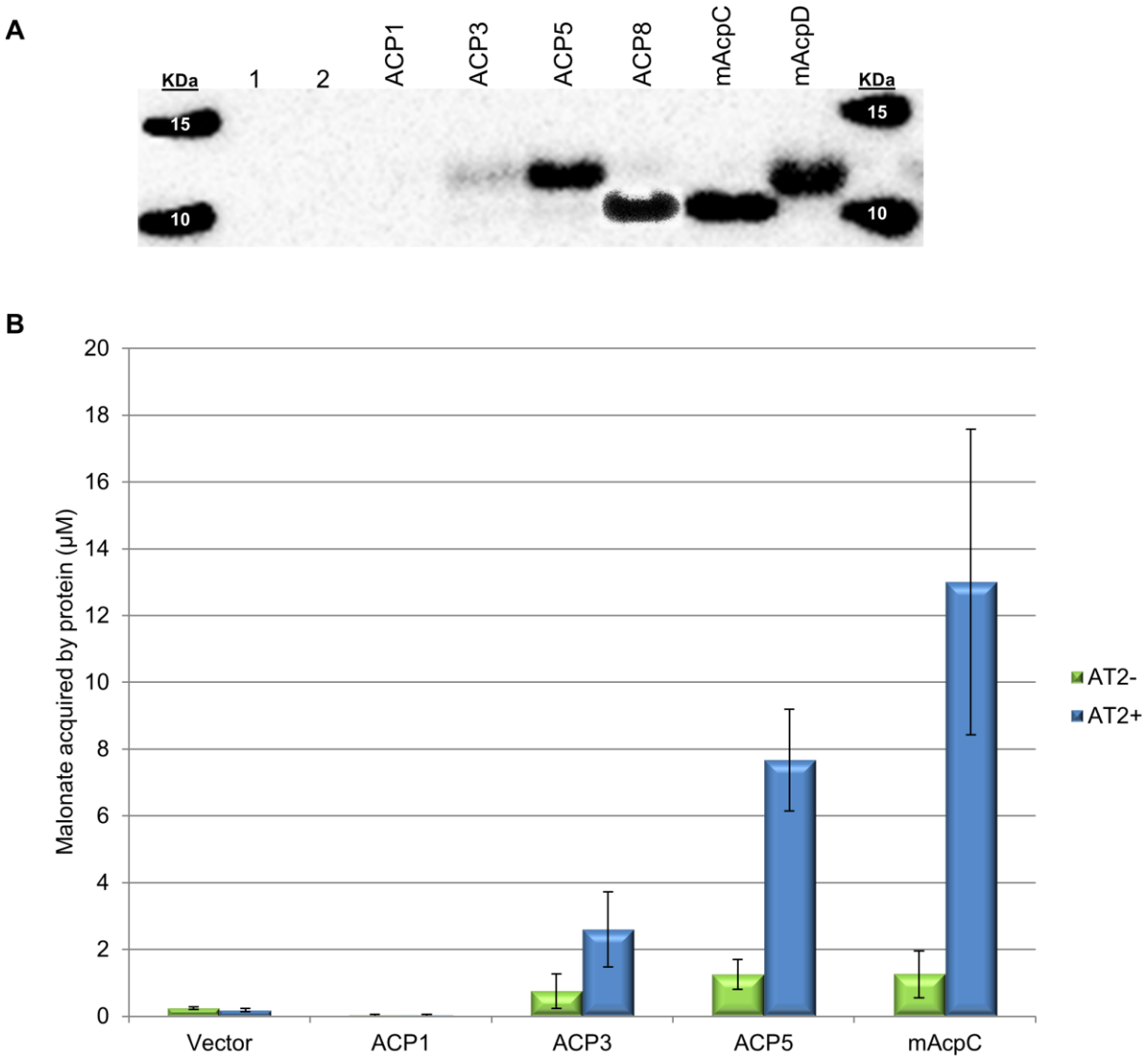

Figure 4.12. Malonate transfer from AT2 to mupirocin ACPs. (A) Autoradiography showing transfer of [^{14}C]-malonate to select ACPs from the mupirocin cluster. Lane 1, AT2 no ACPs; Lane 2, AT2 + empty expression vector. **(B)** Chart showing the malonylation of ACPs with and without AT2. Empty expression vector was used as the negative control. In all cases [AT2]=0.05µM, [ACP]=20µM and [[^{14}C]-malonyl-CoA]=20µM; n=2.

4.3 Discussion

Previously, feeding studies have shown that mupirocin is made from acetate-derived units (Feline *et al*., 1977) (presumably largely via formation of malonate by acetyl-CoA carboxylase) and sequence alignments in this study have shown the ATs cluster with others showing malonyl-CoA substrate specificity. Due to the phenotypes of the individual AT mutants (ΔAT2=no mupirocin production, ΔAT1=reduced mupirocin production) it had been hypothesised that AT2 could perform all essential acyl transfer reactions at some level of efficiency but that AT1 may be needed for a step that is only inefficiently performed by AT2, for example loading of the acetyl-CoA starter unit. However, this study has shown that AT2 exclusively prefers malonyl-CoA as a substrate over any of the other substrates tested, and that it transfers the malonate group to ACPs throughout the cluster. This would indicate that it is responsible for transferring extender units to the ACPs throughout the cluster. If this is the case, AT1 could be responsible for loading the starter unit, however in the absence of AT1 it is possible that AT2 or another uncharacterised protein could inefficiently take over, accounting for the reduction in mupirocin.

To consider the process of chain initiation further a closer inspection of other *trans*-AT systems indicates a wide diversity of functional loading modules thought to be involved in transferring and/or accepting the starter molecule. The lack of an obvious loading module within the mupirocin cluster is unusual, but not unique, the macrolactin and disorazol biosynthetic systems being the best studied examples. Many PKS systems, of both *cis*- and *trans*-AT architecture, have loading modules specifically designed to accept the starter unit for initiation of metabolite production (Hertweck, 2009). The model DEBS system contains a loading module consisting of

an AT and an ACP, thought to provide the propionyl-CoA starter unit to module 1 (Hill and Staunton, 2010). The loading modules of *trans* AT PKSs vary in the domains that are present, from the NRPS of leinamycin, to the minimal ACP of chivosazol and virginiamycin, and to the more intricate loading module of bryostatin which contains four domains – DH- and KR-like domains, an FkbH phosphatase-like domain and an ACP (Cheng *et al*., 2003; Perlova *et al*., 2006; Pulsawat *et al*., 2007; Sudek *et al*., 2007). Rhizoxin, myxovirescin and pederin have a GCN5-related N-acetyltransferase (GNAT) domain, thought to catalyse incorporation of the starter unit for system initiation (Partida-Martinez and Hertweck, 2007; Simunovic *et al*., 2006; Piel *et al*., 2004). Until recently it was thought these domains merely directed the transfer of acetyl groups to the loading-ACP. However, work on curacin A led to a new mechanism of chain initiation being recognised: it was demonstrated that the GNAT domain catalysed the decarboxylation of malonyl-CoA to form acetyl-CoA, followed by transfer to the adjacent ACP (Gu *et al*., 2007; Jones *et al*., 2009). The mupirocin ATs both have a portion of the identified GNAT acetyl-specific motif ((R/Q)xxGx(G/A)(T/S)) – AT1 reads RHMGRAL, while AT2 reads RGMGEGL, however the conserved T/S residue is replaced by Leu, reducing the acetyl-specificity – demonstrated by AT2 accepting malonyl-CoA as a substrate. A possible loading mechanism of a malonyl-CoA-specific AT (such as AT2) catalysing the loading of a malonate residue followed by decarboxylation to provide the first acetate molecule to the first KS domain has been proposed for several PKS clusters, with both *trans*- and *cis*-acting ATs: macrolactin, disorazol, picromycin and niddamycin (Kakavas *et al*., 1997; Xue *et al*., 1998; Bisang *et al*., 1999; Kopp *et al*., 2005; Schneider *et al*., 2007). This mechanism could also apply to systems where the loading mechanism is

unclear, such as virginiamycin and kirromycin (Pulsawat *et al*., 2007; Weber *et al*., 2008). The macrolactin and disorazol systems appear to lack an obvious loading domain and the *trans*-ATs are specific for malonyl-CoA extension units. In these systems it has been proposed that a malonate residue is loaded to the first KS domain and then decarboxylated to provide the required starter acetate unit (Kopp *et al*., 2005; Schneider *et al*., 2007). Such a mechanism might occur in the mupirocin system, with an as yet unidentified protein providing the decarboxylative function to generate the first acetate for module 1 of MmpD. Alternatively KS5 may decarboxylate malonate to acetate before the first condensation. It is also possible that one of the uncharacterised type II mAcps accepts malonate and catalyses the decarboxylation before transfer to KS5. It may well be that the AT2-like enzymes (orange squares, Figure 4.4) represent the 'main' ATs within clusters, while the AT1-like enzymes provide increased turnover, or more specialized functions.

Despite proposing an AT role for AT1 above, several results from this study indicate an alternative role for AT1. There are a group of AT1-like proteins that cluster together in sequence similarity, and there are several more single ATs in or closer to this group than to the AT2-like group. If AT1 is partially redundant in a system it may be that the systems are evolving and consequently making some ATs redundant – thus explaining why only five systems have the tridomain, but many systems have an AT2-ER bidomain. The structural differences also point to an alternative role for AT1 – the active site is predicted to have a different morphology indicating alternative substrate specificity. This structural difference could also account for the inability to solubilise and purify AT1. Although it is inconclusive it may be that AT1 transfers an acetate starter unit, alongside an alternative role, and that in

the absence of AT1, AT2 can take over, albeit inefficiently. Solving the solubility and purification problems of AT1 will be key in determining a definitive role for this AT, and for this group of ATs.

In summary, this work has shown AT2 to be an AT specific for malonyl-CoA – transferring malonate to ACPs throughout the mupirocin cluster, and has proposed the option that AT1 may have an alternative role to that of a typical transferase.

CHAPTER 5

5 SITE DIRECTED MUTATIONAL ANALYSIS OF AT2

5.1 Introduction

Chapter 4 describes work that leads to a clear conclusion about the biochemical activity of the AT2 component of the mupirocin biosynthetic cluster as a malonyl-CoA-specific acyltransferase (AT). Unfortunately due to solubility problems it was not possible to provide the same sort of evidence for the function of AT1. As an alternative approach it was therefore decided to combine bioinformatic and mutational analysis as a way to gain an insight into the function of AT1.

A key aspect of any investigation of protein function is bioinformatic analysis of the sequence or sequences of the genes and proteins of interest. The DNA or protein sequence of a gene can tell us a great deal about that gene and its protein product, for example, structural predictions and evolutionary relationships, as demonstrated in Chapter 4. The study of sequence alignments can lead to predictions of specificity and function, and by searching for similar sequences one can identify specific genes as having specific roles based on prior biochemical characterisation of proteins produced by related genes. These techniques have led to a greater understanding of genes such as *fabD*, the gene that encodes the *E. coli* malonyl-Coenzyme A-acyl carrier protein transacylase (MCAT) utilised in fatty acid biosynthesis, and consequently a variety of polyketide ATs. *E. coli fabD* and the model polyketide system of DEBS have been extensively studied and consequently many conclusions have been drawn that can be applied to other polyketide systems. The most common method for determining domain importance and function is inactivation or mutation. A widely utilised method to discover or synthesise novel metabolites is to swap

domains, for example to replace the domain of interest with one that displays a different specificity. Much of the research focuses on ATs due to their role in substrate delivery throughout polyketide synthesis. Swapping the methylmalonyl-CoA specific ATs from modules in DEBS for malonyl-CoA specific ATs from the rapamycin, picromycin, avermectin and niddamycin systems resulted in the production of several (and in one case over 50) novel metabolites (Oliynyk *et al*., 1996; Liu *et al*., 1997; Ruan *et al*., 1997; Marsden *et al*., 1998; Stassi *et al*., 1998; McDaniel *et al*., 1999). However, when the AT domain from module 4 in DEBS was exchanged with malonyl-CoA specific ATs from the rapamycin, FK520 or epothilone systems no product was produced leading the researchers to speculate about the structural importance of that domain in the overall protein. Their alternative method for altering the specificity of module 4 eventually came from site-directed mutagenesis rather than exchanging the whole domain. Three motifs were identified as possibly being important for substrate specificity and subsequent mutagenesis which changed the motifs from methylmalonyl-CoA to malonyl-CoA specificity resulted in mutants producing the expected novel products (Reeves *et al*., 2001). The motifs were identified by aligning several ATs of predicted specificity to the sequence of FabD from *E. coli* and are shown in Table 5.1 (Serre *et al*., 1995).

Table 5.1. AT specificity motifs.

AT specificity	Motif
Malonyl-CoA	$QTxYTQ^{63}$ GHS^{92}[IVL]GE $HAFH^{201}$
Methylmalonyl-CoA	$RVDVVQ^{63}$ GHS^{92}QGE $YASH^{201}$

Superscript number relates to the corresponding FabD residue. (Haydock *et al*., 1995; Ikeda *et al*., 1999)

The crystal structure of FabD highlighted the importance of several residues and also gave an indication of the interactions between active site residues: Ser^{92} is hydrogen bonded with His^{201} and Arg^{117}; His^{201} is also hydrogen bonded with Gln^{250}; Gln^{11} provides hydrogen bonds for water molecules, and the stereochemistry of the active site demonstrates the importance of other residues such as Val^{255}, Asn^{231}, His^{91}, Leu^{93}, and Ser^{200} (Figure 5.1) (Serre *et al*., 1995). A study investigating the prediction of substrate specificity of *cis*-acting ATs highlighted that all malonyl-CoA ATs clustered together and methylmalonyl-CoA specific ATs clustered together separately (Yadav *et al*., 2003). ATs that were specific for unusual substrates tended to cluster with the methylmalonyl-CoA group. Out of the 13 active site residues analysed in the study, 9 in the malonyl-CoA group, 10 of the methylmalonyl-CoA group and 4 of the unusual substrate group, were completely conserved.

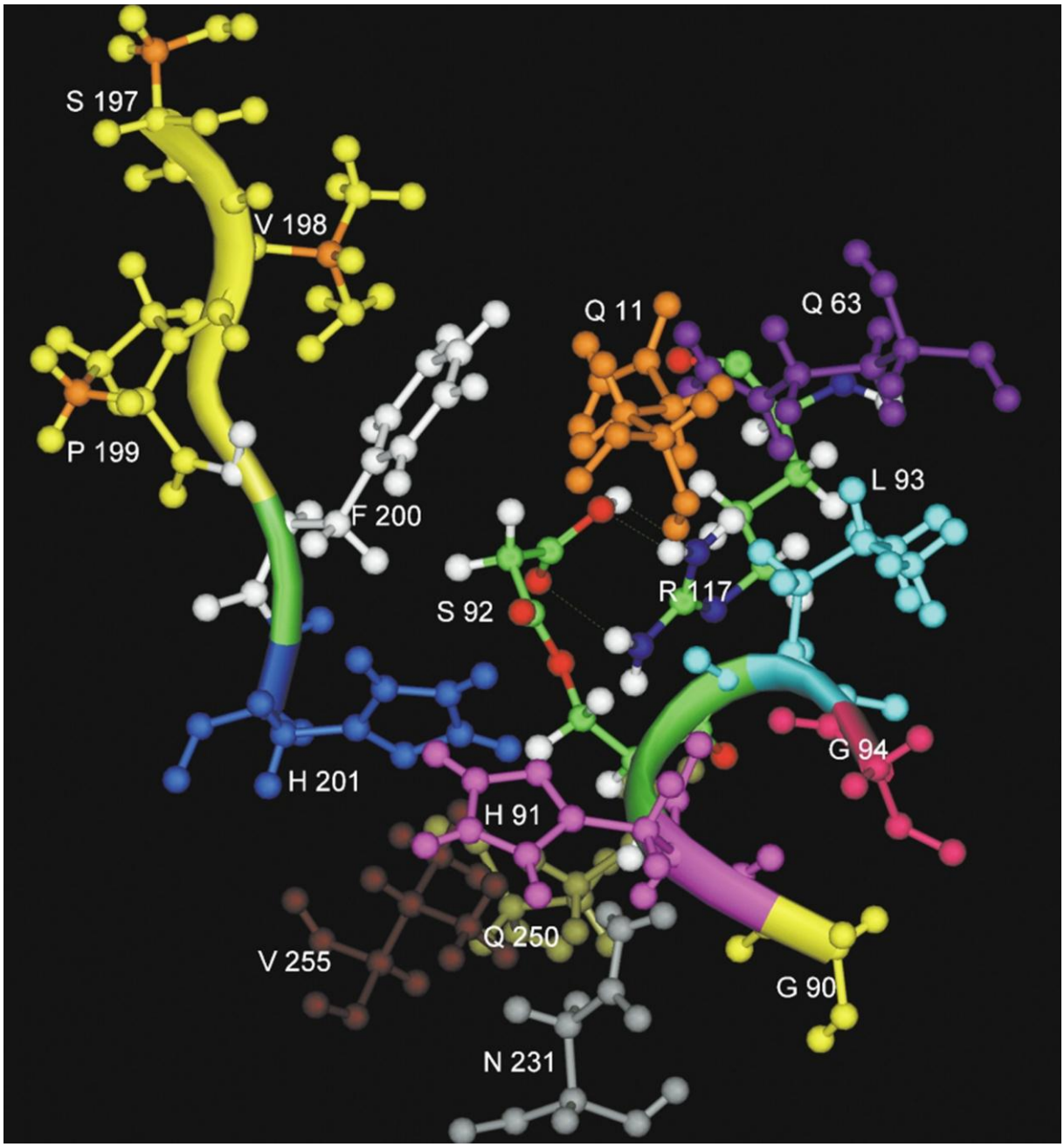

Figure 5.1. Structural model of a malonate group in the active site of a typical malonyl-CoA specific AT domain. The 13 active site residues and 3 of the additionally conserved residues (197-199) are shown (Yadav *et al*., 2003).

Arg^{117} was conserved in all malonate- and methylmalonate-specific ATs, while some ATs in the unusual group had variations at this position. Arg^{117} is thought to play a role in differentiating between mono- and dicarboxylic acids – the basic guanidinium group forms bidentate salt bridges with a dicarboxylic acid substrate (Keatinge-Clay *et al*., 2003). The stigmatellin loading AT has Leu in this position and is specific for acetyl-CoA which lacks the second carboxylate component (Gaitatzis *et al*., 2002). A study of an animal MAT mutating the residue corresponding to Arg^{117} to either Ala or Lys successfully altered the substrate preference from malonyl-CoA to acetyl-CoA, confirming the role of Arg^{117} in dicarboxylic acid interactions (Rangan and Smith, 1997). In addition to the 13 active site residues there were an additional 11 residues in conserved positions further away from the catalytic Ser but nonetheless important. Residues 198-201 comprise the YASH/HAFH motif that is so important for distinguishing malonate and methylmalonate specificity, and while residue 197 is also important, the critical residue in this motif is Ser or Phe^{200}. In ATs specific for malonyl-CoA this position is almost completely conserved as Phe and in methylmalonyl-CoA specific ATs it is completely conserved as Ser (Yadav *et al*., 2003). Phe^{200} is in direct contact with the methylene group of the malonate, explaining why it is a crucial residue in the substrate specificity of ATs. An AT with Phe^{200} is unable to accept methylmalonate due to steric clashing between the methyl carbon and carbon atoms of the Phe ring, while a Ser in this position allows methylmalonate to bind (Yadav *et al*., 2003).

The aims of this study were to mutate active site residues of AT2 to match those of AT1 and characterise the mutants by Ellman's assay, circular dichroism and autoradiography. In addition to determining the importance of the active site residues

it was hoped this would also provide a potential function for AT1 that could be investigated further in a later chapter.

5.2 Results

5.2.1 Sequence analysis

The phylogenetic analysis in Chapter 4 clearly displays two separate clades of *trans*-acting ATs. This relationship was examined with further sequence analysis of the active site residues based on the methods by Yadav *et al*. (2003). Tables 5.2 and 5.3 show the active site residues and some of the additional conserved residues of the AT1-like and AT2-like ATs shown in Figure 4.4 compared to the out-group *E. coli* FabD. Despite not being consigned an evolutionary group in the previous chapter, EtnB was included in the AT1-like group for the more detailed sequence analysis due to the unusual active site motif, GYS. AlbXIII, Orf12, and OzmC were excluded from further analysis due to the inability of the sequences to align with either group. Out of the 14 residues analysed there was complete conservation of 3 in the AT1-like group and 10 in the AT2-like group (Figure 5.2).

[QV]**G**[HYAST]**S**[RQ]MLVF][SLNTKPR][VAGFRQYHIV][PAG][SF]**H**[NGSCT][QHVTSAN][VFLIQR]

QGHSRM[SRG][GA][PA]**FH**[NTS]**QV**

Figure 5.2. AT active site motifs. Top, motif of the AT1-like group of ATs. Bottom, motif of the AT2-like group of ATs, which is more ordered than that of the AT1-like group. Emboldened residues highlight complete conservation within that group.

The AT2-like group all display the archetypal AT active site motif of GHS, followed by the crucial Arg^{117} for dicarboxylic acid specificity. Met^{121}, Phe^{200} and His^{201} all indicate malonyl-CoA specificity. The three residues where there are variations in the conservation are 198 which is Gly or Ala, 199 which is either Ala or Phe, and 231 which is Asn in all but two cases.

The AT1-like group has far more active site diversity than the AT2-like group. The GHS motif is present in three ATs from this group, replaced in many cases by GAS, and in some by GSS, GTS, or GYS. Arg^{117} is present in four cases within this group, but the incorporation of these proteins in this group could be questioned as they are outliers, so it is likely they are more AT2-like: FenF is already known to be malonyl-CoA-specific and the residues match the AT2-like motif with the exception of His^{250} instead of Gln; ZmaF has many similarities to FenF, yet it has a motif of GYS at the active site and lacks the malonyl-CoA-specific Met at position 121 (Lopanik *et al*., 2008); KirCII is already known to be specific for the unusual ethylmalonyl-CoA despite having GHS at the active site, but there are variations from the malonyl-CoA specificity that tie in with this unusual specificity, particularly Leu^{121} and Ser^{200}; EtnB has GYS at the active site and unusually Trp at position 200. Most of the remainder of the AT1-like group have Gln at position 117, except EtnK AT1 and SorO AT1 which both have His. In the research by Yadav *et al*. the only group to have residues other than Arg at position 117 was the unusual substrates group – one protein with Gln^{117} was specific for 2-methyl-butyrate, another with His^{117} was specific for 3-methyl-butyrate, while those with Trp^{117} were specific for propionate or 2-methyl-butyrate (2003). Similarly the only deviations from Phe or Ser^{200} (malonate or methylmalonate specificity respectively) were in the unusual substrate group.

Position 200 is Phe in all cases across AT1- and AT2-like ATs, with the exception of KirCII (which we know to be ethylmalonyl-CoA specific) and EtnB which have Ser^{200}. Residue 200 varied from Ala, Thr, Gly, Val, and Pro in the unusual substrate group (Yadav *et al*., 2003). Other notable differences between the two groups of ATs include position 231, which is predominantly Asn in the AT2-like group, but Cys or Ser in the AT1-like group; position 250 and 255 are Gln and Val respectively in the AT2-like group, but Val, Ala, Gln, Thr, Ser, Asn, His, and predominantly Ile for 255 in the AT1-like group.

The active site GHS…R motif, where Ser is the catalytically active Ser, and His and Arg are both in contact with the substrate, is conserved in AT2, whilst for AT1 the His residue is replaced with an additional Ser and the Arg replaced with Gln. Both mupirocin ATs contain partial HAFH motifs, particularly the crucial FH residues, indicating malonyl-CoA specificity (Del Vecchio *et al*., 2003): AT1 reads RPFH, and AT2 reads APFH. This analysis has highlighted several residues that differ significantly between the two groups of ATs (these are highlighted bold in the MmpC AT1 and AT2 motifs shown below), and that were selected for investigation by mutagenesis to determine whether they could help to decipher a potential role for the AT1-like ATs.

The MmpC AT1 motif:	QG**S**S**QFNR**PFH**SVL**
The MmpC AT2 motif:	QG**H**S**RMSA**PFH**NQV**

Table 5.2. Active site amino acid alignment of AT1-like ATs from *trans*-AT PKS clusters compared to *E. coli* FabD.

Domain name	*E. coli* residue reference number													
	11*	90*	91*	92*	117*	121+	197+	198+	199+	200*	201*	231*	250*	255*
FabD	Q	G	H	S	R	M	S	V	P	S	H	N	Q	V
FenF	Q	G	H	S	R	M	S	A	P	F	H	N	H	V
ZmaF	V	G	Y	S	R	L	S	G	P	F	H	N	Q	V
KirCI_AT1	Q	G	A	S	Q	F	L	F	P	F	H	G	V	F
MmpC_AT1	Q	G	S	S	Q	F	N	R	P	F	H	S	V	L
TmpC_AT1	Q	G	S	S	Q	F	T	Q	A	F	H	S	V	I
RhiG_AT1	Q	G	T	S	Q	F	K	Q	A	F	H	C	T	I
RzxG_AT1	Q	G	A	S	Q	F	N	Q	A	F	H	C	S	I
OzmM_AT1	Q	G	A	S	Q	V	P	Y	A	F	H	C	A	I
TaV_AT1	Q	G	A	S	Q	F	R	Y	P	F	H	C	V	Q
BryP_AT2	Q	G	H	S	Q	L	S	H	G	F	H	C	V	I
PedC	Q	G	A	S	Q	F	S	I	A	F	H	C	V	I
BaeD	Q	G	A	S	Q	V	S	Y	G	F	H	S	V	R
BatH	Q	G	A	S	Q	F	S	Y	A	F	H	C	A	I
EtnK_AT1	Q	G	A	S	H	L	S	F	A	F	H	C	V	I
SorO_AT1	Q	G	A	S	H	L	S	F	A	F	H	C	A	I
ElaC	Q	G	S	S	Q	V	K	Y	A	F	H	S	V	I
KirCII	Q	G	H	S	R	L	T	V	A	S	H	T	N	V
EtnB	Q	G	Y	S	R	M	T	V	A	S	H	N	H	V

* indicates putative active site residues; + indicates additional conserved residues.

Table 5.3. Active site amino acid alignment of AT2-like ATs from *trans*-AT PKS clusters compared to *E. coli* FabD.

Domain name	*E. coli* residue reference number													
	11*	90*	**91***	92*	**117***	**121+**	**197+**	**198+**	199+	200*	201*	**231***	**250***	**255***
FabD	Q	G	H	S	R	M	S	V	P	S	H	N	Q	V
LkcD	Q	G	H	S	R	M	S	G	A	F	H	T	Q	V
VirI	Q	G	H	S	R	M	S	G	P	F	H	N	Q	V
LtmH	Q	G	H	S	R	M	S	G	A	F	H	N	Q	V
MgsH	Q	G	H	S	R	M	S	G	A	F	H	N	Q	V
LnmG	Q	G	H	S	R	M	S	A	A	F	H	S	Q	V
LtmB	Q	G	H	S	R	M	S	A	A	F	H	N	Q	V
MgsB	Q	G	H	S	R	M	S	A	A	F	H	N	Q	V
KirCI_AT2	Q	G	H	S	R	M	S	A	P	F	H	N	Q	V
OzmM_AT2	Q	G	H	S	R	M	S	A	P	F	H	N	Q	V
MmpC_AT2	Q	G	**H**	S	**R**	**M**	**S**	**A**	P	F	H	**N**	**Q**	**V**
TmpC_AT2	Q	G	H	S	R	M	S	A	P	F	H	N	Q	V
RhiG_AT2	Q	G	H	S	R	M	S	A	P	F	H	N	Q	V
RzxG_AT2	Q	G	H	S	R	M	S	A	P	F	H	N	Q	V
DisD	Q	G	H	S	R	M	S	A	A	F	H	N	Q	V
CorA	-	G	H	S	R	M	S	A	A	F	H	N	Q	V
PsyH	Q	G	H	S	R	M	S	G	A	F	H	N	Q	V
TaV_AT2	Q	G	H	S	R	M	R	A	P	F	H	N	Q	V
BatJ	Q	G	H	S	R	M	S	A	A	F	H	N	Q	V
EtnK_AT2	Q	G	H	S	R	M	S	A	A	F	H	N	Q	V
SorO_AT2	-	G	H	S	R	M	G	A	A	F	H	N	Q	V
PedD	-	G	H	S	R	M	S	G	A	F	H	N	Q	V
BryP_AT1	Q	G	H	S	R	M	S	A	A	F	H	N	Q	V
ElaB	Q	G	H	S	R	M	S	G	A	F	H	N	Q	V
PksC	Q	G	H	S	R	M	S	G	A	F	H	N	Q	V
BaeC	Q	G	H	S	R	M	S	G	A	F	H	N	Q	V
PksE	Q	G	H	S	R	M	S	G	A	F	H	N	Q	V
DifA	Q	G	H	S	R	M	S	G	A	F	H	N	Q	V
MlnA	Q	G	H	S	R	M	G	G	A	F	H	N	Q	V
ChiA	Q	G	H	S	R	M	S	G	A	F	H	N	Q	V

* indicates putative active site residues; + indicates additional conserved residues; residues in bold were mutated during this study.

5.2.2 Construction of AT2 point mutants

The solubility and purification problems of AT1 combined with the bioinformatics study identifying key active site differences between the two groups of ATs, suggested that a way to investigate possible AT1 function would be to mutate key AT2 residues to match those in the same position of AT1 – in effect, attempting to make AT2 more AT1-like. Rather than mutating the chromosome, plasmid pJS560 was the template for mutation by QuikChange® site-directed PCR mutagenesis (Chapter 2), which enabled comparisons to be made between *in vitro* assays of the mutant strains when compared to the WT (pJS560). Briefly, primers (Table 2.10) were designed to introduce point mutations in the PCR products, the PCR reaction products were then subjected to restriction digest by *Dpn*I (which recognises GATC, when the A is methylated), thus digesting the template WT DNA leaving the mutated product intact (Figure 5.3). Table 5.4 details mutants constructed during this study, while Table 5.5 provides a summary of the results. Once mutations were confirmed by sequencing, plasmids were transformed into *E. coli* BL21 (DE3) for expression and purification.

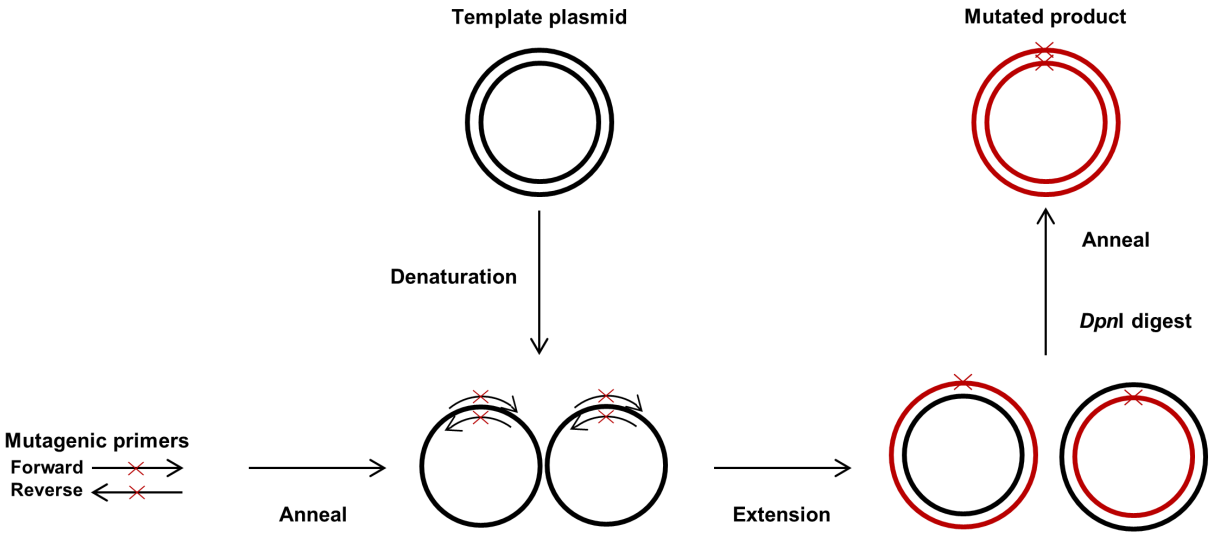

Figure 5.3. Principle of QuikChange® PCR. (Adapted from Loening, 2005).

Table 5.4. Mutants constructed during this study.

Mutant	Mutation	Plasmid
WT	-	pJS560
1	H89S	pRG501
2	R115Q	pRG502
3	M119F	pRG503
4	S190N	pRG504
5	A191R	pRG505
6	N224S	pRG506
7	Q242V	pRG507
8	S190V A191R	pRG509
9	R115Q Q242V	pRG510
10	R115Q Q242V S190N A191R	pRG511
11	V247L	pRG508
12	H89S Q242V	pRG512
13	H89S R115Q	pRG516
14	H89S Q242V R115Q	pRG513
15	H89S Q242V R115Q V247L	pRG514
16	S190N A191R M119F	pRG515

17	R115Q Q242V S190N A191R V247L	pRG517
18	R115Q Q242V S190N A191R V247L M119F	pRG518

5.2.3 Expression and purification of AT2 point mutants

Pure protein was required before the mutant proteins could be assayed for malonyl-CoA acquisition via the Ellman's assay, transfer to an ACP by autoradiography and for structural changes by circular dichroism. Mutant strains 1 and 11-18 were all found to be insoluble and so no further analysis could be made. Interestingly strains 12-15 all include the mutation made in mutant 1 (H89S), implying this residue, although buried within the protein, could be important for solubility. However, mutating the corresponding residue in pJS559 which encodes AT1 from Ser to His (S95H – plasmid pRG519) did not result in the protein changing from insoluble to soluble. Strains 11, 17 and 18 had the mutation V247L in common, suggesting that Val^{247} residue could also be important for solubility. For those strains that were found to produce soluble mutant AT proteins, all could be purified by nickel-affinity chromatography to a certain degree (Figure 5.4) and could be assayed for activity.

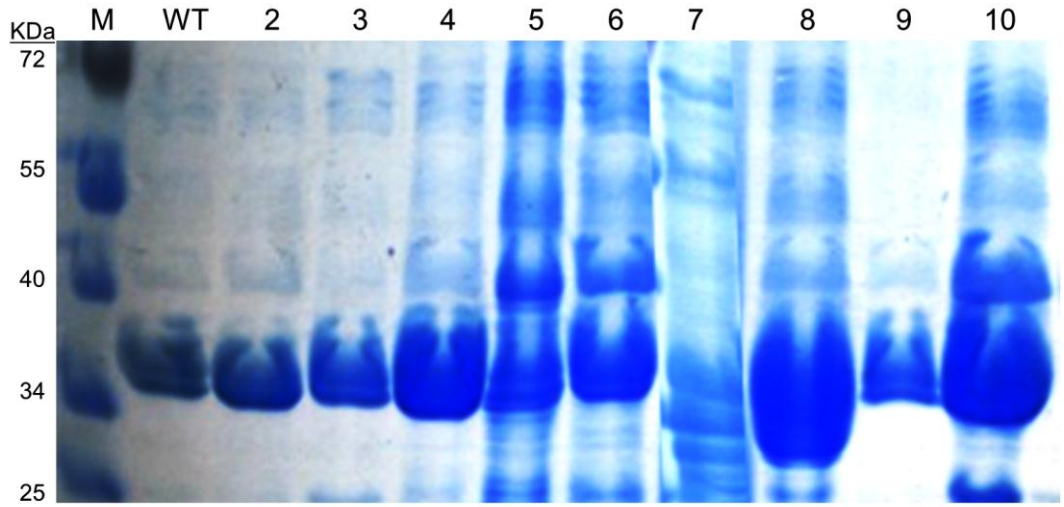

Figure 5.4. SDS-PAGE of mutant AT2 proteins. M, molecular weight marker; WT, wild type; 2-10, mutants (34.3kDa).

5.2.4 Substrate specificity of mutant AT2 proteins

Two stages of Ellman's assays were performed to test the mutant proteins: firstly, the assays were performed as described previously, but with 20µM protein and 20µM malonyl-CoA and monitored for 30min; secondly, the assay was started in the same way but a further 20µM malonyl-CoA was added half way through the assay (15min). The proteins were only tested with malonyl-CoA, as this was the determined substrate of choice for AT2 in Chapter 4. A negative control consisting of the protein, but no malonyl-CoA was included to measure the background absorbance as AT2 has four Cys residues and if the thiol groups were exposed they would react with the Ellman's reagent. All of the mutant strains were able to acquire malonate to a level at least equal to the WT, with the exception of strains 2 and 9. The yield of mutant 3 protein was too low for the Ellman's assay (Figure 5.5). All of the mutants displayed a background absorbance that was less than when malonyl-CoA was added. For mutant 10 this absorbance was considerably higher than for the other mutants, and on addition of malonyl-CoA the absorbance only increased by 0.16. Mutants 2 and 9 also released less CoA than WT on addition of malonyl-CoA – both of these mutants incorporate the R115Q mutation. Mutant 10 also incorporates this mutation, so it is possible that R115Q is responsible for the reduced acceptance of malonate from malonyl-CoA and subsequent release of CoA. Mutants 4, 5, 7 and 10 all released over twice as much CoA from malonyl-CoA as the WT. Mutant 5 released as much as four times more than the WT. Mutant 10 is a quadruple mutant incorporating mutants 2, 4, 5 and 7 but the mutations did not have a cumulative effect on malonate acquisition. Mutants 6 and 8 released 1.2 and 1.4 times more CoA from malonyl-CoA than the WT.

Stage two of the Ellman's assay was to add a further 20μM malonyl-CoA to the assay half way through the period of the experiment. For the WT this had the effect of increasing the absorbance by 1.5 times, and so increasing the amount of malonyl-CoA converted. Mutants 4, 6, and 8 all converted more malonyl-CoA in this stage of the assay than the WT, with mutant 4 converting 2.2 times more than when malonyl-CoA was only added to start the reaction, and mutant 6 converting 1.9 times more. For some mutants the availability of more substrate had little or no effect – mutants 5 and 9 appeared to have a similar increase to the WT, while mutants 2, 7 and 10 had little effect.

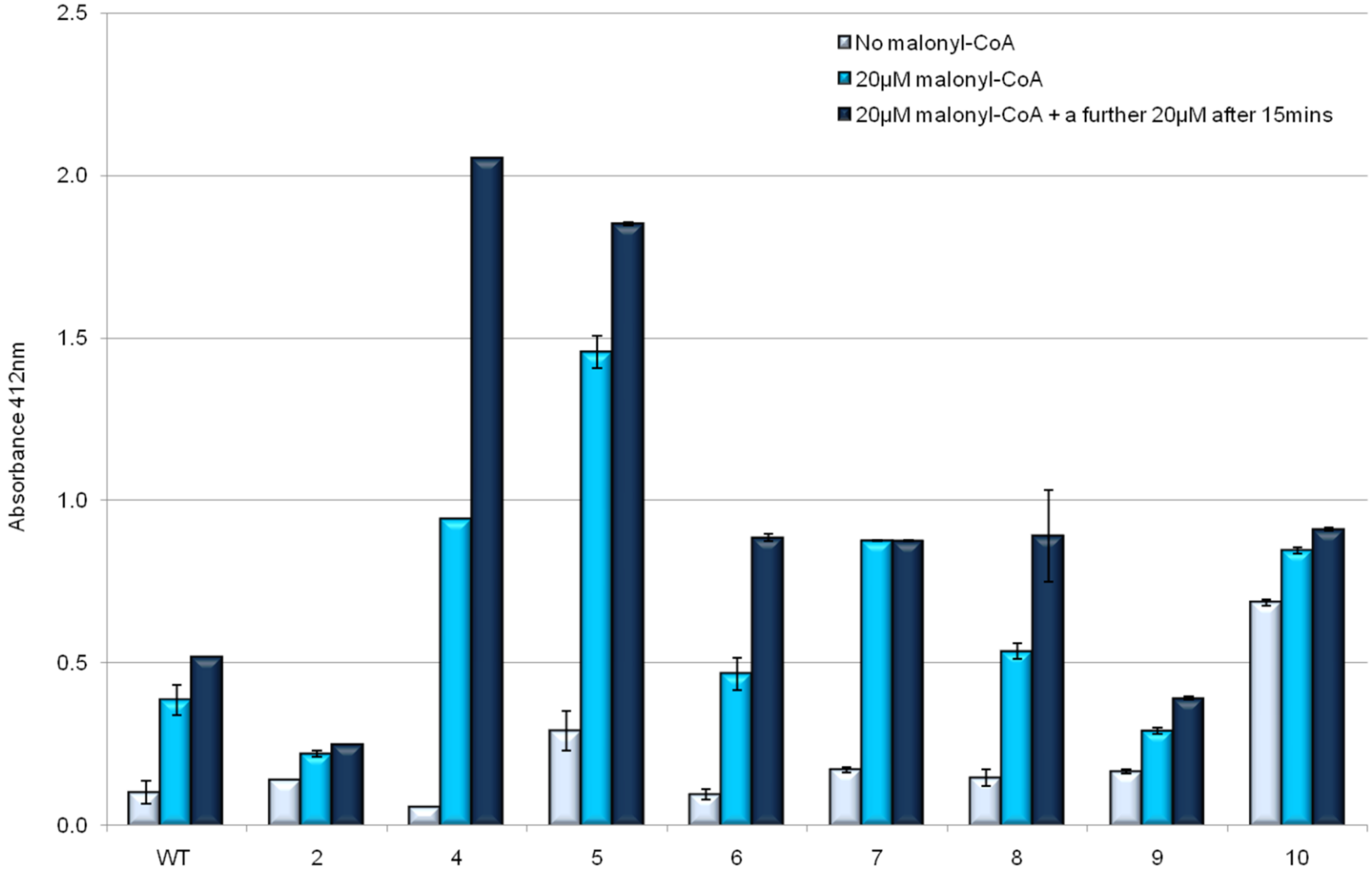

Figure 5.5. Characterisation of AT2 mutants by CoA release from malony-CoA. CoA release was measured by Ellman's reagent; [protein]=20μM; n = 2.

5.2.5 Circular dichroism of mutant AT2 proteins

Circular dichroism (CD) was performed firstly to see if any of the mutant strains had any structural changes when compared to the WT, and secondly to observe the degree of structural change when malonyl-CoA was added. Once the data was collected it was analysed by Dichroweb software (Whitmore and Wallace, 2004; 2008) for the percentage of different types of secondary structures present (Table 5.5). The WT AT2 protein has a typical CD spectrum of an α-helical protein, with negative peaks at 208 and 222nm (red line in Figure 5.6). All mutants, with the exception of mutant 7, have the same helical spectrum, with varying magnitudes of the CD signal indicating variations in helical structure and length. Mutant 4 is the least altered from the WT, with mutant 8 the most altered, in agreement with the calculated helical content from Dichroweb. The remainder of mutants have different degree of changes in predicted helical content. Mutant 7 is the most altered from the WT structure, in that rather than remaining helical it appears to be comprised of random coils as demonstrated by the negative peak at 200nm. This is consistent with the Dichroweb data which predicts only 17% helices compared to the 36% helical WT.

When the WT has accepted malonate from malonyl-CoA the CD spectrum does not appear to alter significantly, indicating little structural change in the protein when it has bound its substrate (Figure 5.7). However, Dichroweb analysis of the data indicates that the WT protein loses 4% of its helical structure when malonate is bound. All of the mutants, with the exception of 5 and 8, experienced helical loses upon binding of malonate. Mutants 2, 4, 8 and 10 showed the least degree of structural change on binding of malonate (loss of 1% for 2 and 4, and gain of 1% for

8). Mutant 6 showed a 39% loss of helical content when malonate was bound, while mutant 5 became more helical on binding of malonate, as demonstrated by the CD spectra and Dichroweb data. The randomly coiled mutant 7 lost a further 10% of its helical structure and remained mainly randomly coiled.

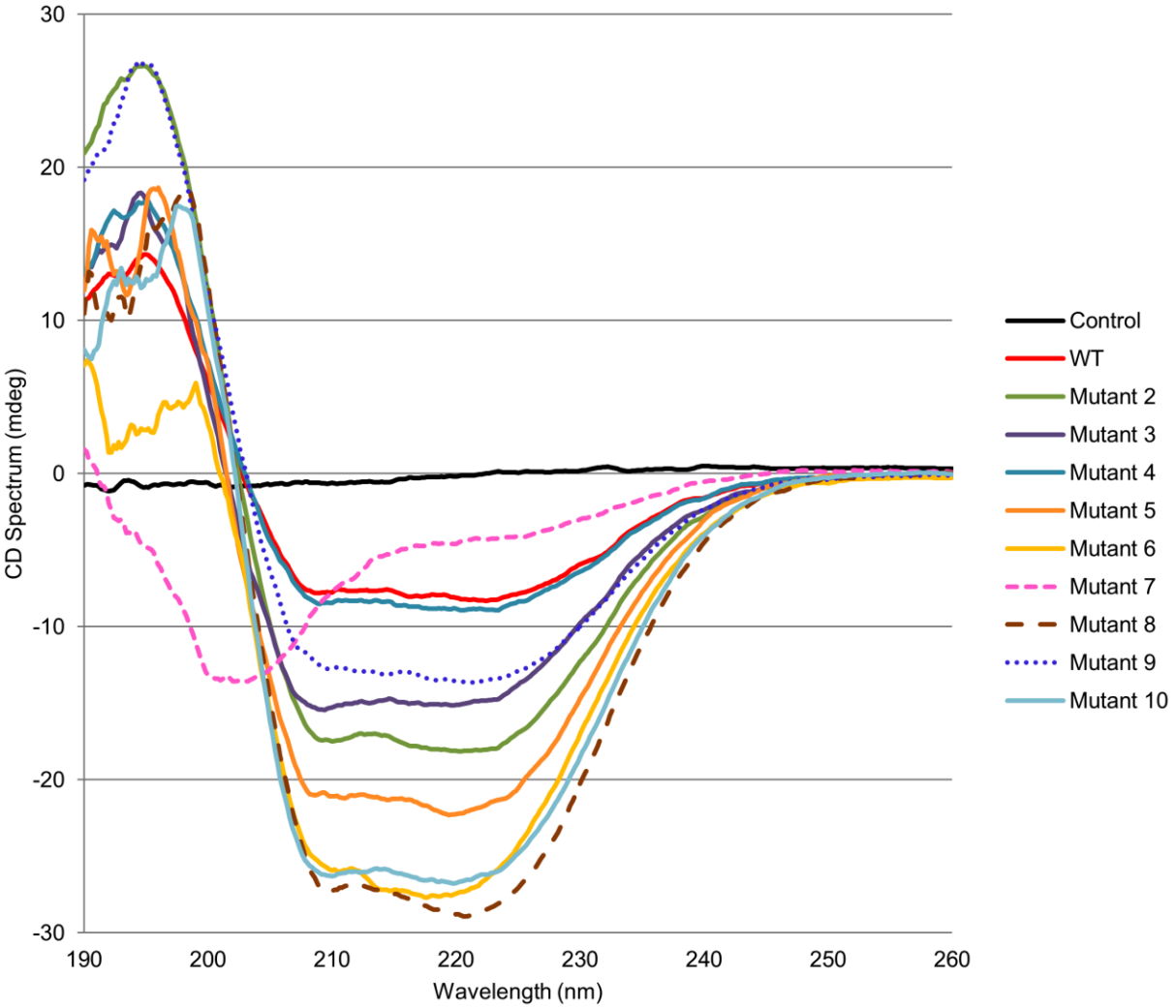

Figure 5.6. Circular dichroism spectra of AT2 mutant proteins. Mutants were analysed against a negative control of assay buffer and a positive control of the WT protein (red line).

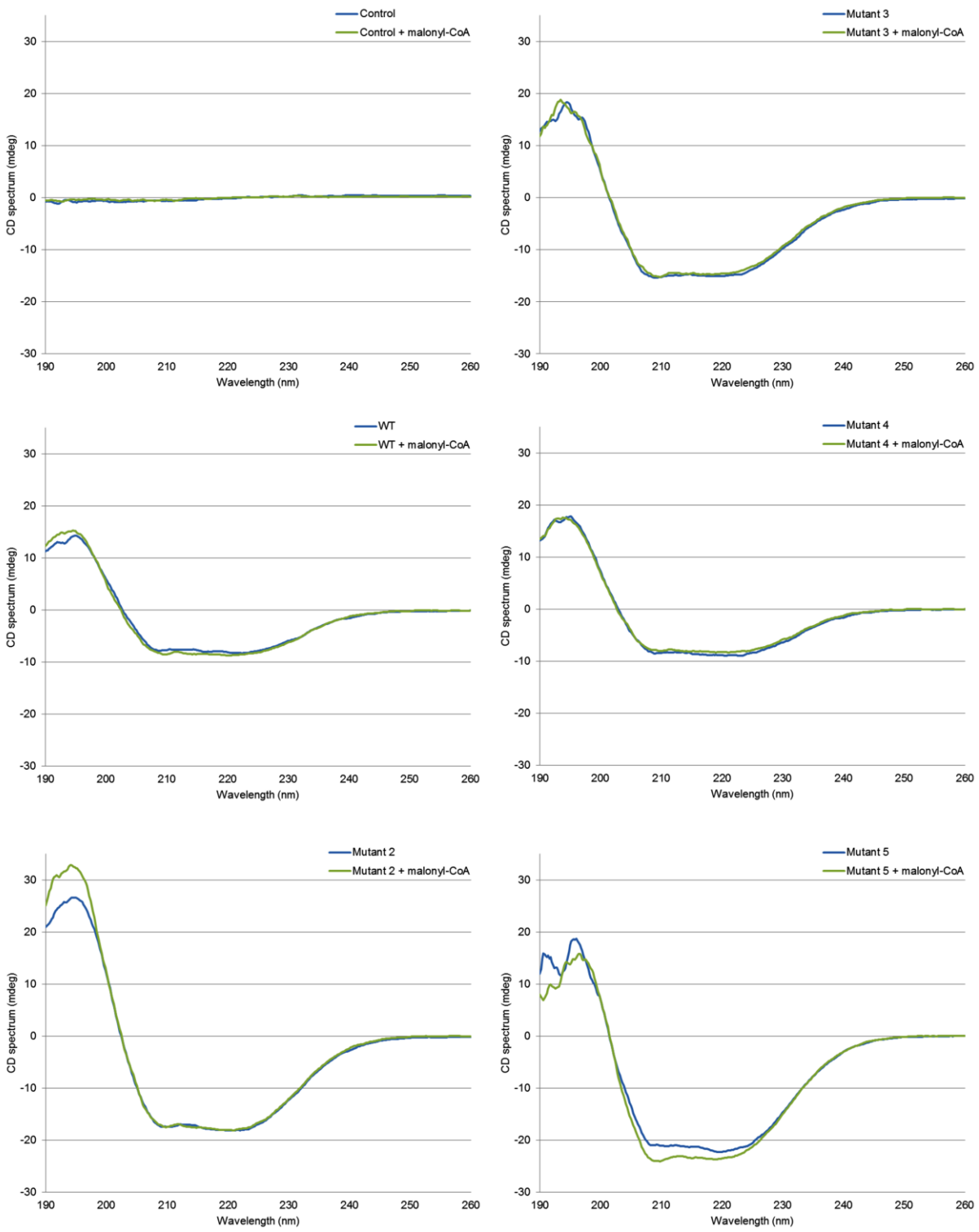

Figure 5.7, A. Circular dichroism spectra of mutant AT2 proteins compared to when bound to malonate.

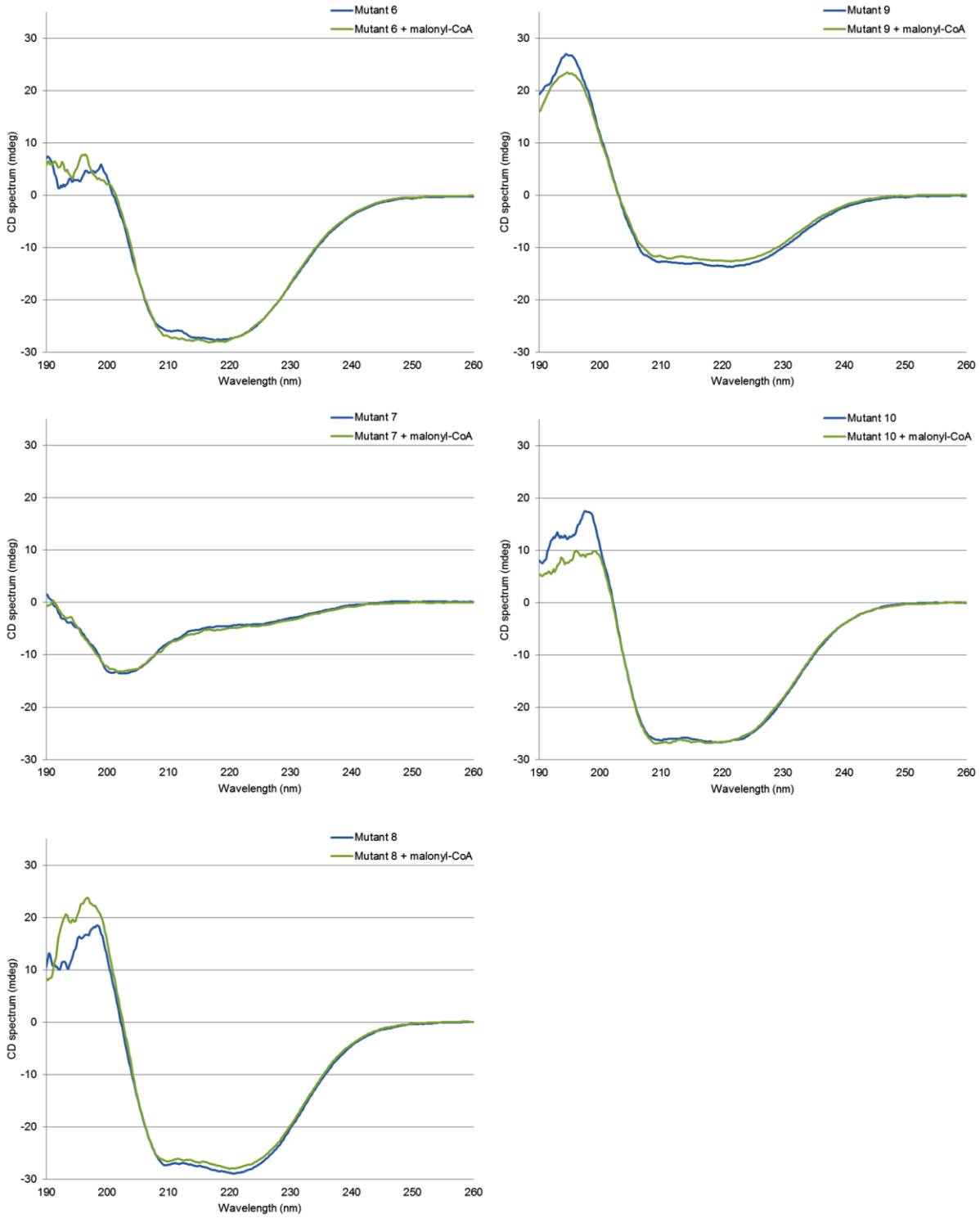

Figure 5.7, B. Circular dichroism spectra of mutant AT2 proteins compared to when bound to malonate.

5.2.6 Acquisition and transfer of malonate by mutant AT2 proteins

An initial radiolabelling assay was done to assess each mutants ability to acquire [^{14}C]-malonate. Assays were performed as described in Chapter 2, with 20µM AT and [^{14}C]-malonyl-CoA with the concentration of unlabelled malonyl-CoA decreasing from 380-0µM. The chart in Figure 5.8 (A) shows the results for when the 20µM [^{14}C]-malonyl-CoA did not have a competing substrate (blue box in (B)). The results show that all mutants, with the exception of mutants 5 and 8, acquired less malonate than the WT.

The second stage of radiolabelling was used to demonstrate the ability of the mutant proteins to malonate mAcpC from the mupirocin cluster, as shown in Figure 5.9. In this assay the concentration of AT was 0.05µM, and mAcpC and [^{14}C]-malonyl-CoA were 20µM. Assay conditions were as previously assessed for maximum transfer from AT to ACP (Section 4.2.6.1). As a negative control, the ability of mAcpC to self-malonate was tested – this demonstrated a background level of radioactivity corresponding to acquisition of less than 0.6µM of malonate. Similar levels were also detected in mutants 7 and 10. None of the mutants malonylated mAcpC as efficiently as the WT (15.2µM transferred), however mutants 4 and 6 were most like the WT with 11.7µM and 14.2µM transferred respectively. As mutants 4 and 6 were most like the WT it seems they have retained the most archetypal AT2 activity. Mutant 5 has lost over half of its activity and mutants 2 and 8, at least one fifth.

Large margins of error displayed in Figures 5.8 and 5.9 could be explained by inaccurate protein concentration determination. More accurate protein concentration readings could be acquired by the Bradford or Lowry protein assays.

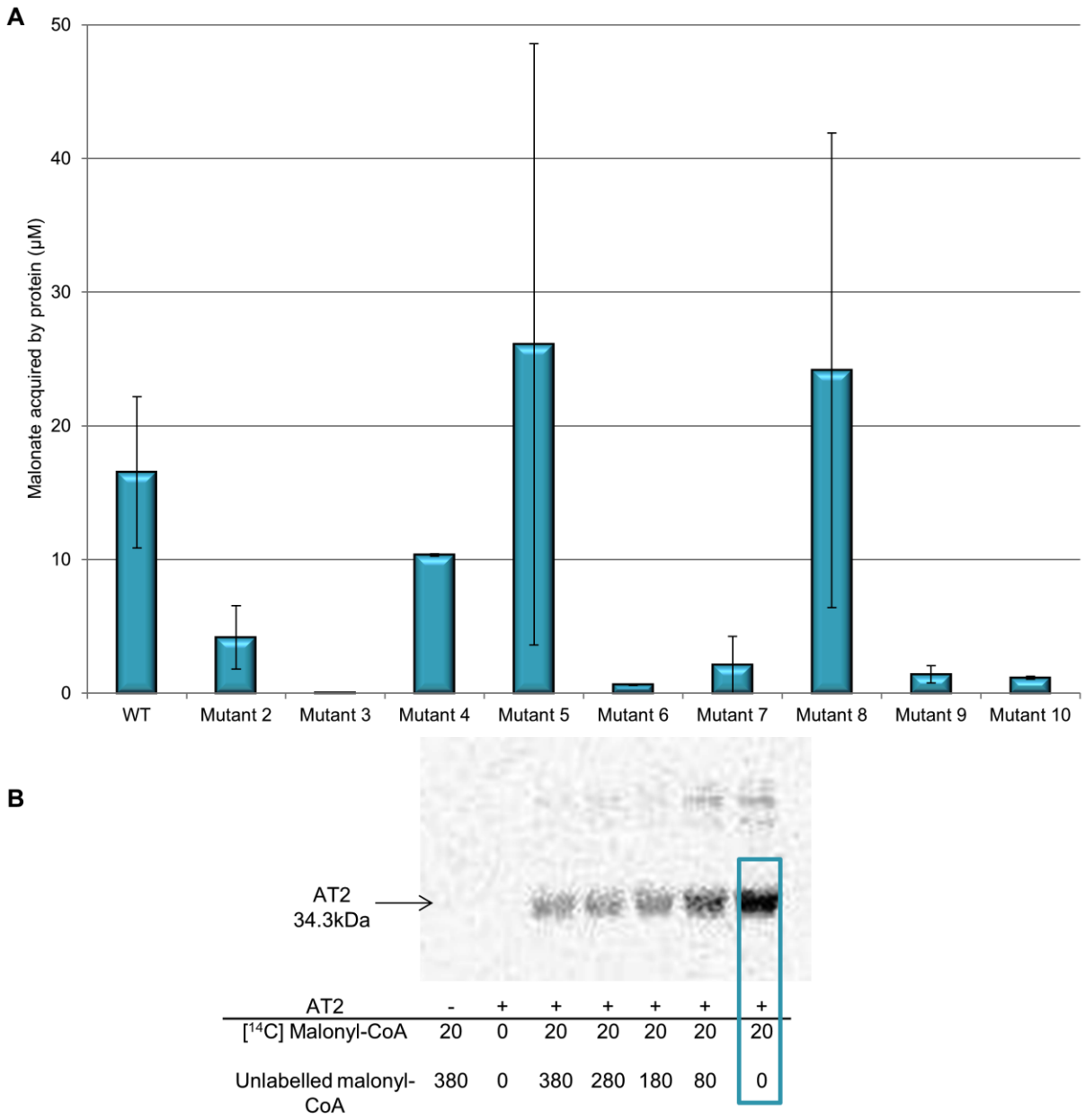

Figure 5.8. Acquisition of malonate by mutant AT2 proteins. (A) Chart showing acquisition of malonate by mutant AT2 proteins. [AT]=20µM; WT, wild type; mutants 2-10, AT2 mutant proteins; for WT, mutants 6, 9 and 10, n = 3; for mutants 2-5 and 7-8, n = 2. **(B)** Example of autoradiography gel showing radioactivity acquisition by WT AT2. Blue box shows lane with 20µM [^{14}C]-malonyl-CoA.

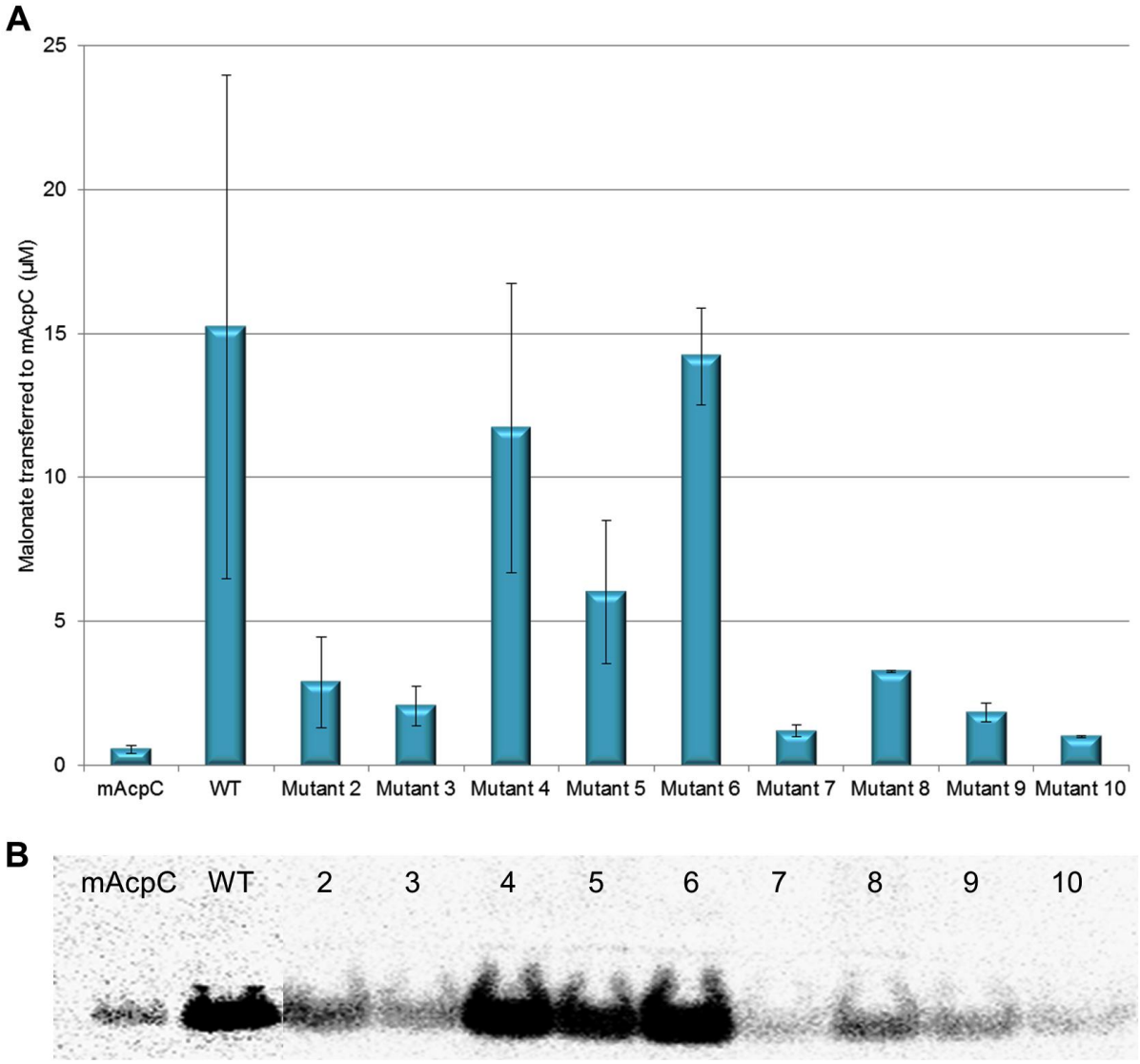

Figure 5.9. Ability of mutant AT2 proteins to transfer malonate to mAcpC. [AT]=0.05μM; [[^{14}C]-malonyl-CoA]=20μM; [mAcpC]=20μM. **(A)** Chart showing the transfer of malonate to mAcpC. **(B)** Autoradiography of [^{14}C]-malonate-mAcpC (12.4kDa). mAcpC, negative control with no AT present; WT, wild type; 2-10, AT2 mutants; n = 2.

5.3 Discussion

To date there have been over 30 *trans*-AT systems identified and the importance of this group of PKSs is becoming increasingly obvious with each investigation published. It is thought they have evolved completely independently from *cis*-AT PKS systems, patched together based on substrate specificity from multiple gene segments, but that the PKS modules contain catalytically inactive remnant AT residues in the form of docking domains (Nguyen *et al*., 2008; Cheng *et al*., 2009; Piel, 2010). Several studies have highlighted the fact that these *trans*-acting ATs fall into two distinct groups – those that are AT1-like and those that are AT2-like (Gurney and Thomas, 2011; Jensen *et al*., 2012; Musiol and Weber, 2012). The AT2-like ATs appear to be the more demonstrably functional out of the two groups, with many research groups predicting they transfer the extender unit, while the function of the AT1-like ATs has remained enigmatic until recently – with bioinformatics not revealing any specific roles.

A role has been determined for AT2 (Chapter 4), however, the solubility issues of AT1 have led to problems investigating this protein. Bioinformatics tells us that AT1 clusters with a group of ATs where the role is not as apparent as the AT2 malonate-transfer group. The differences in active site amino acid residues led to the investigation of trying to make AT2 more 'AT1-like' by mutating select residues, with the aim of determining a role for AT1.

Of particular importance appears to be residue 117 – Arg in the AT2-clade, and mostly Gln in the AT1-clade. Interestingly, two of the ATs with confirmed specificity, FenF and KirCII, in the AT1-clade both retain the Arg^{117}. As Arg^{117} appears to act as a substrate anchor for dicarboxylic acids within the active site cleft,

it stands to reason that a different residue in this position could indicate different substrate specificity, such as monocarboxylic acids (Rangan and Smith, 1997). As such this was demonstrated in mutant 2 which resulted in half as much conversion of malonyl-CoA to malonate and CoA in the Ellman's assay, sixfold less acquisition of malonate in radiolabelling assays and fivefold less transfer of [^{14}C]-malonate to mAcpC in the transfer assays. Mutants 9 and 10 (both incorporating the R115Q mutation) were also less efficient at malonate acquisition and transfer when compared to the WT. This is consistent with the proposed role of this residue in the docking of the dicarboxylic malonate, and thus it is likely that a protein which has Gln at this position instead of Arg cannot accept dicarboxylic acids. This is also demonstrated in the myxalamid PKS where the loading AT has Gln at this position and loads 2-methyl-butyrate to initiate metabolite synthesis (Silakowski *et al*., 2001). Obscurely, the BryP ATs can both load malonate and methylmalonate, and in both cases malonate is the preferred choice, however BryP AT2 has Gln in position 117 (Lopanik *et al*., 2008).

Residue 242 is also incorporated into mutants 9 and 10 – mutating Q242V in AT2. However, the single Q242V mutant (mutant 7) was still able to release CoA from malonyl-CoA in the Ellman's assay, but was not able to transfer [^{14}C]-malonate to mAcpC efficiently in the transfer assays. Structurally mutant 7 was the most altered from the WT, which displayed an α-helical profile. In this mutant, the profile shifted to that of random coiling, and could well explain the inefficiency of this mutant at transferring malonate to mAcpC. AT2 has four Cys residues which presumably contribute to the structural integrity of the protein in the form of disulphide bridges. If a point mutation introduced prevents the Cys residues from interacting it may be that

consequently the protein loses significant secondary structure. While it is tempting to state that the reasons mutant 7 is less efficient is due to a structural change that prevents docking with or transfer of malonate to mAcpC, it may well be that the protein is simply too unordered to function in its usual manner. While mutant 10 was also dramatically altered from the WT and had no more activity that mutant 7, it still retained an α-helical structure, perhaps as a result of the incorporation of mutants 4 and 5 which were at least as efficient as the WT protein.

Mutants 4, 5 and 8 were all more efficient at releasing CoA from malonyl-CoA in the Ellman's assay than the WT. Mutants 5 and 8 were more efficient at acquiring malonate in the initial radiolabelling assays, whereas mutant 4 was less efficient than the WT. However, when it came to transferring the [^{14}C]-malonate to mAcpC mutant 4 was the most efficient but not as efficient as the WT. This data combined would indicate that mutant 4 retained more AT2-like functionality while mutants 5 and 8 did not – they were able to acquire the malonate but were then not efficient at transferring it onto the ACP indicating a role for residue 191 in ACP docking, or in the transfer of malonate to ACP. This residue is the first in the HAFH/YASH motif thought to be so important for distinguishing between malonyl-CoA or methylmalonyl-CoA specificity. In FabD the corresponding residue is Val yet it is still specific for methylmalonyl-CoA, and in the malonyl-CoA-specific AT2 it is Ala. Replacing Ala with Arg in mutants 5 and 8 (to match the Arg in the corresponding position in AT1) would have resulted in quite a dramatic change as the guanidinium side-chain of Arg is more bulky than the methyl-group of Ala. It could be postulated that this prevented the phosphopantetheine arm from extending into the active site cleft towards the malonyl-CoA.

Mutant 6 appeared to be the single amino acid substitution mutant that was most like the WT: It had slightly higher CoA release than the WT in the Ellman's reagent assay, although it did not appear to accept malonate as efficiently as the WT, while transfer to mAcpC was similar to the WT. It may be that this mutant is efficient at converting malonyl-CoA to malonate and CoA, but in the absence of an ACP simply releases the malonate rather than holding onto it. Mutant 3 was not as efficient at accepting or transferring [^{14}C]-malonate as the WT indicating that this is also an important residue.

Analysis of the mutants by CD highlighted the fact that the active site residues are vital to maintain the secondary structure of the AT. Indeed, this was also shown by the fact that some mutations caused AT2 to become insoluble so no further experiments could be completed - H89S is one such mutation. The single H89S mutant (mutant 1) and all multiple mutants incorporating this mutation (mutants 12-15) rendered the mutant protein insoluble, indicating this residue has a vital role in structural stability and most likely transfer ability and must be investigated further. The remainder of the mutants varied in the magnitude of helical structuring and length from the WT profile, with 4, 9 and 3 being the least altered and 10, 6 and 8 the most. It is likely that the structural alterations caused by the mutations have had a knock-on effect on the function of the protein, as would be expected.

CD demonstrated that every mutant had a change in secondary structure when compared to the WT AT2, and some had major changes when malonate was bound. In most cases however, the consequences of those changes resulted in the AT acquiring more substrate. The Ellman's assays demonstrated that the WT AT2 does has a continual turnover of malonate, however 4 of the mutants (4-6 and 8)

appeared to increase the conversion of malonyl-CoA to malonate and CoA more than the WT, suggesting that these proteins may have more of a propensity for quick turnover. However, this could be due to exposure of thiol groups from Cys residues, particularly in the case of mutants 5 and 10, where the background level was higher than the background level for the WT.

It should be noted that despite best efforts the proteins did not represent 100% purity due to undergoing one round of metal affinity chromatography and no further rounds of purification, therefore the results presented here are semi-quantitative when concerning malonyl transfer and protein structure.

This study involved identifying residue differences between AT1-like and AT2-like *trans*-acting ATs and determining the reason for those differences. Mutation of residues in AT2 to match those in AT1 demonstrated not only the importance of those residues for AT2 activity, but also a potential alternative role for AT1 as a hydrolase. Three particular residue mutations point to this conclusion: mutants 5 and 8 were more efficient at acquiring malonate, but not at passing it to an ACP, most likely due to the bulkier Arg residue replacing Ala; Mutants incorporating Q242V (responsible for forming a hydrogen bond with His^{201} and stabilising the active site complex) appeared to acquire more malonate but not release it, which could be due to active site destabilisation caused by this mutation; finally, the inefficiency of mutant 2 to acquire malonate leads to the conclusion that Arg is required in this position in order to acquire dicarboxylic acid substrates, and the presence of only one amine group is not sufficient to bind to malonyl-CoA. This data combined points to a role for AT1 as a hydrolase, removing short-chain intermediates from a stunted pathway and will be examined further in the following chapter (Jensen *et al*., 2012).

Table 5.5 Summary of AT2 active site mutagenesis results.

Mutant number	Mutation	Plasmid	Solubility	% Helical[+]	% Helical[+] when complexed with malonyl-CoA	Ellman's assay 1* (abs)	Ellman's assay 2**(abs)	Malonate acquisition (μM)[a]	Malonate transfer to mAcpC (μM)[a]
WT	-	pJS560	Soluble	36	32	0.38	0.52	16.5	15.2
1	H89S	pRG501	Insoluble	-	-	-	-	-	-
2	R115Q	pRG502	Soluble	62	61	0.22	0.25	4.2	2.9
3	M119F	pRG503	Soluble	53	50	-	-	0.01	2.1
4	S190N	pRG504	Soluble	34	33	0.94	2.1	10.4	11.7
5	A191R	pRG505	Soluble	55	73	1.46	1.9	26.1	6.0
6	N224S	pRG506	Soluble	63	24	0.47	0.89	0.63	14.2
7	Q242V	pRG507	Soluble	17	7	0.88	0.88	2.1	1.2
8	S190V A191R	pRG509	Soluble	68	69	0.54	0.89	24.2	3.3
9	R115Q Q242V	pRG510	Soluble	59	55	0.29	0.39	1.4	1.8
10	R115Q Q242V S190N A191R	pRG511	Soluble	68	68	0.85	0.91	1.2	1.0

+, as a percentage of total secondary structural content for the protein as determined by Dichroweb; *, 20μM protein, 20μM malonyl-CoA, monitored for 30min; **, 20μM protein, 20μM malonyl-CoA, an additional 20μM malonyl-CoA added after 15min; a, calculated from radioactivity counts as described in Chapter 2.

CHAPTER 6

6 ACYLTRANSFERASE ACTIVE SITE MUTAGENESIS

6.1 Introduction

The *E. coli* FabD active site has been extensively studied along with the active site of ATs from the DEBS PKS. However, there is a lack of information about the *trans*-acting AT active site. Predictions can be made based on knowledge from FAS and *cis*-acting ATs from PKSs, but more experimental evidence is required. At the centre of the AT active site is the GHSxG motif, corresponding to FabD residue numbers 90-94 (Yadav *et al*., 2003). Gly^{90} and Gly^{94} are residues that are conserved amongst all ATs, whether *cis*- or *trans*-acting (Yadav *et al*., 2003; Chapter 5, pages 184-185). Ser^{92} is also completely conserved, as expected from the vital role it plays in attacking and bonding to the substrate. However, His^{91} and residue 93 are not fully conserved. Residue 93 is further away from the substrate than the His or Ser residues, however it is clear it may play an important role in the substrate specificity of the AT: malonate specific ATs have a branched amino acid in this position, while methylmalonate specific ATs have either Gln or Met; ATs with unusual substrates are more varied at this position with either Ile, Gln, Leu, Tyr, Val or Ala (Yadav *et al*., 2003). All of the *trans*-acting ATs included in this study have a branched chain amino acid at this position, with the exception of KirCII and TaV AT1, which both have Met. As we already know KirCII to be specific for the unusual ethylmalonate, it seems highly likely that TaV AT1 also has an unusual specificity based purely on this residue (Musiol *et al*., 2011). Residue 91 is in direct contact with the substrate, be it malonate, methylmalonate or a more unusual substrate such as 3-methyl-butyrate (Figure 6.1).

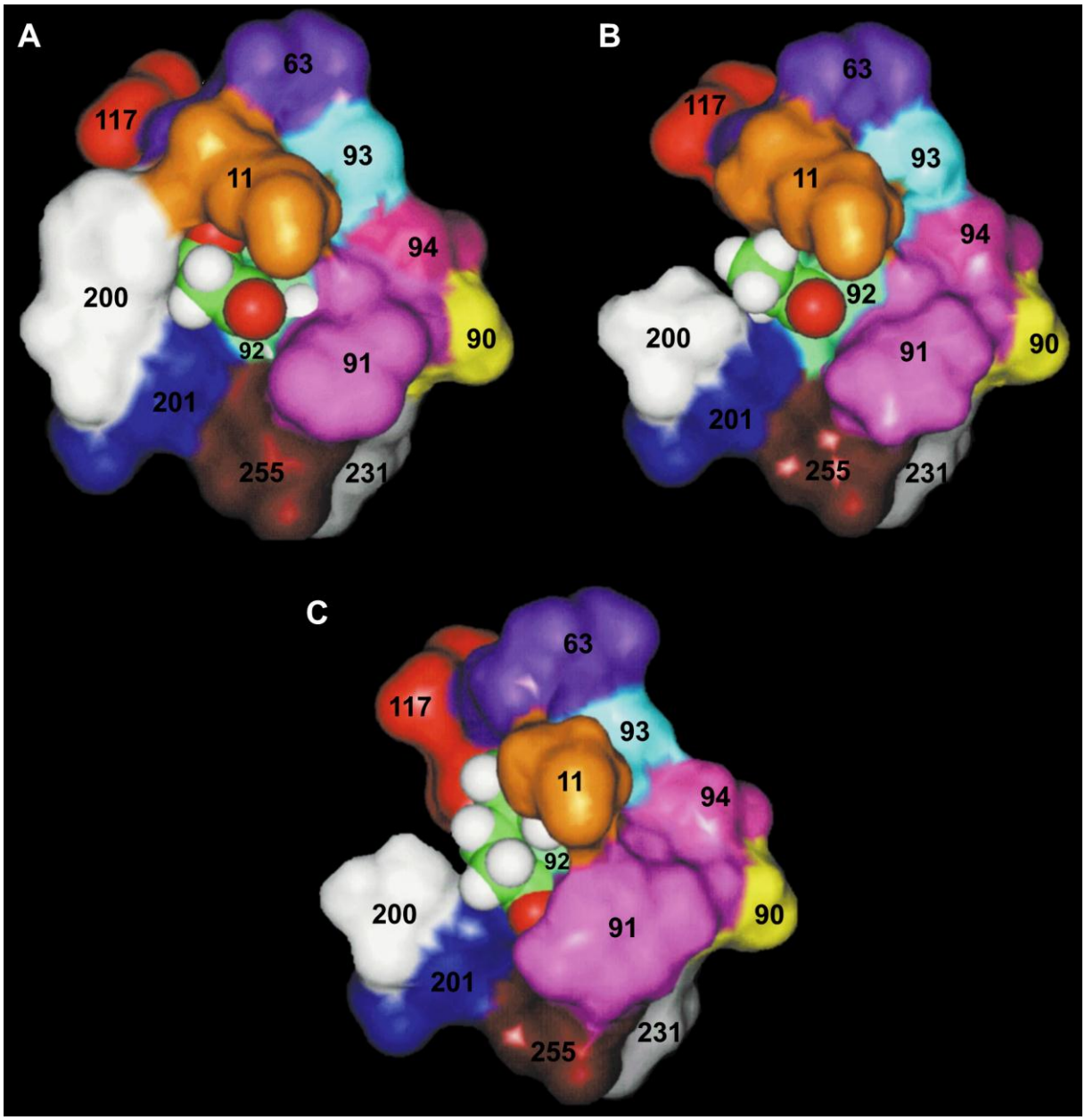

Figure 6.1. Surface rendering of the active site pockets in three typical AT domains. All substrates are covalently attached to Ser^{92}. Residues are numbered according to *E. coli* FabD. (A) The active site of a typical malonate specific AT, with residues Q^{11}, Q^{63}, G^{90}, H^{91}, S^{92}, L^{93}, G^{94}, R^{117}, F^{200}, H^{201}, N^{231}, Q^{250}, V^{255}. Methylene group of malonate is in direct contact with F^{200}. (B) The active site of a typical methylmalonate specific AT, with residues Q^{11}, Q^{63}, G^{90}, H^{91}, S^{92}, L^{93}, G^{94}, R^{117}, S^{200}, H^{201}, N^{231}, Q^{250}, V^{255}. Additional space is created for the methyl group by F200S. (C) The active site of an AT specific for 3-methyl-butyrate, with residues A^{11}, L^{63}, G^{90}, Y^{91}, S^{92}, V^{93}, G^{94}, H^{117}, A^{200}, H^{201}, T^{231}, N^{250}, V^{255}. (Adapted from Yadav *et al*., 2003).

Due to this contact is seems unusual then that several ATs in the AT1-like group have a different residue replacing His at position 91 (Chapter 5, page 184). Out of the 18 AT1-like ATs, 9 have Ala at this position, 3 have His, 3 have Ser and 2 have Tyr. Of the three that have His at this position, FenF has demonstrated malonate specificity, BryP AT2 has demonstrated malonate and methylmalonate specificity, and KirCII has demonstrated ethylmalonate specificity (Aron *et al*., 2007; Lopanik *et al*., 2008; Musiol *et al*., 2011). No specificity has been determined for the remainder of the AT1-like ATs, however, a potential role as a thioester hydrolase has been put forward for PedC, which has Ala at position 91 (Jensen *et al*., 2012). Within the phylogeny of the AT1-group there appears to be two separate clades: one grouping KirCI AT1, MmpC AT1, TmpC AT1, RhiG AT1, RzxG AT1, OzmM AT1 and TaV AT1 together; with the other grouping BryP AT2, PedC, BaeD, BatH, EtnK AT1, SorO AT1 and ElaC (Figure 4.4). The group including the hydrolase PedC have several residues in common – all have Ser^{197} (except ElaC which has Lys) and five out of the seven have Ala^{91}. The group including MmpC AT1 has more residue diversity at these positions, indicating there could be more than one function amongst the AT1-like group of ATs.

Work described in the previous Chapter demonstrated that MmpC AT1 is likely to have a role different to that of AT2, most likely as a protein that accepts simple substrates and does not dock with an ACP. It also demonstrated the mutation H89S *in vitro* caused AT2 to become insoluble. The work in this Chapter further investigates the role of His/Ser^{91} in the mupirocin ATs with the aim of providing potential answers as to the function of AT1.

6.2 Results

6.2.1 Construction of point mutations in MmpC AT domains (Harry Thorpe)

To investigate the possibility of the different roles of AT1 and AT2 we focussed on the catalytic centre motif which is GHS in the known acyltransferase AT2 but is GSS in AT1 whose biochemical function is unknown. While it is well documented that the Ser is vital for substrate docking, the role of the adjacent His is unknown. We hypothesised that the unusual motif displayed by AT1 may prevent it from transacylating certain ACPs or from selecting certain substrates, hence why the chromosomal point mutant of AT2 did not produce mupirocin, and thus providing further evidence of the variant roles of the two groups of ATs. Point mutations were introduced to mutate S95H in AT1 (GSS to GHS) and H89S in AT2 (GHS to GSS). Thus, the AT1 active site would become more AT2-like and the AT2 active site more AT1-like.

To construct point mutations two set of primers were designed, each having an end primer and an internal mutagenic primer (primer pairs AT1F1/R1, AT1F2/R2, AT2F1/R1 and AT2F2/R2). The initial round of PCR created two 500bp fragments which overlapped at the mutation site. The second round of PCR joined the fragments to create a 1kb fragment containing the mutation. These were cloned into pGEM-T-Easy, to create plasmids pHT601 (for AT1 S95H) and pHT602 (for AT2 H89S) for sequencing. Ligation with pAKE604 formed plasmids pHT603 for AT1 and pHT604 for AT2. The plasmids were transformed into *E. coli* S17-1 and introduced into *P. fluorescens* NCIMB 10586 by conjugation, followed by selection of cointegrants and plasmid excision.

Not only were these mutations introduced into *P. fluorescens* WT chromosome (strain $AT1^{WT}AT2^{WT}$) but also to *P. fluorescens* AT2 S90A point mutant (strain $AT1^{WT}AT2^{GHA}$) and *P. fluorescens* AT1 S95A, S96A point mutant (strain $AT1^{GAA}AT2^{WT}$). Figure 6.2 demonstrates the strain architecture and nomenclature. The mutated strains were then analysed by bioassay, HPLC and LCMS for phenotyping.

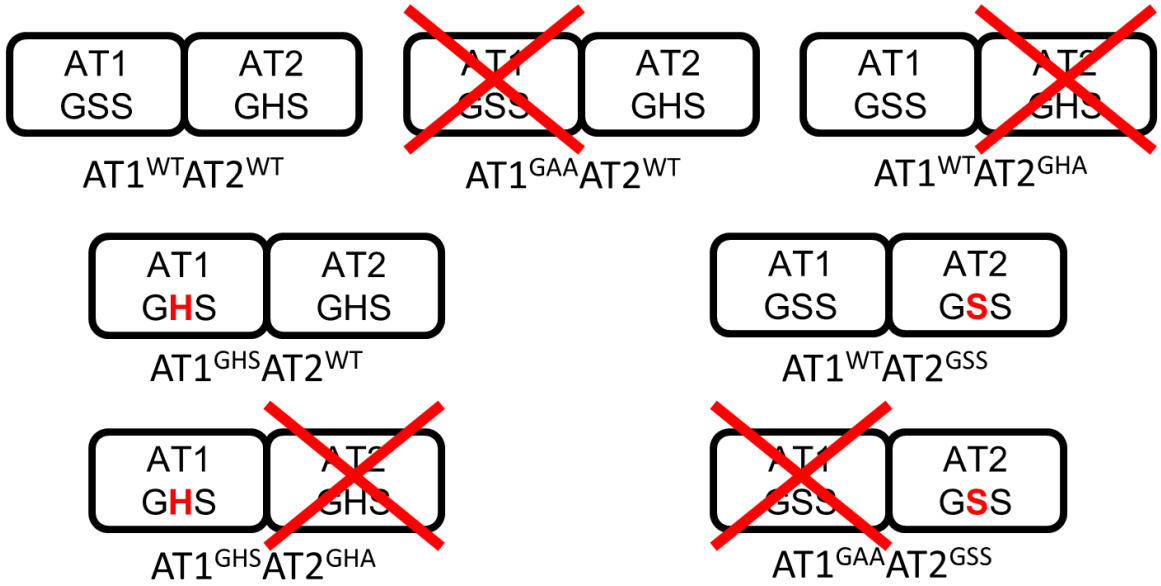

Figure 6.2. Strain architecture of the AT active site mutants. Top row shows the original strains which the mutations were introduced to. Bottom two rows show the strains produced by the intended mutations. Mutated residues are coloured red, inactivated AT domains are indicated by a red cross, and strain identifiers are written below the models.

6.2.2 Plate bioassay of antibiotic activity in MmpC point mutants (Harry Thorpe)

Plate bioassay showed the antibiotic activity of the mutants against the indicator strain *B. subtilis* 1064. The zones of inhibition were measured and the mean calculated from the replicates. The bioassay showed that the $AT1^{WT}AT2^{GHA}$ strain, where AT2 activity was knocked-out, produced a reduced amount of antibiotic activity, 34% of $AT1^{WT}AT2^{WT}$, and the $AT1^{GAA}AT2^{WT}$ strain, where AT1 activity was knocked-out, produced approximately 86% of activity compared to $AT1^{WT}AT2^{WT}$ (Figure 6.3 and Table 6.1). This confirmed the previous results that a mutation of AT2 has more of an effect on mupirocin production than a mutation of AT1 (Shields, 2008). Mutants $AT1^{GHS}AT2^{WT}$ and $AT1^{WT}AT2^{GSS}$ displayed the most antibiotic activity – both 103% of $AT1^{WT}AT2^{WT}$. Mutant $AT1^{GHS}AT2^{GHA}$ displayed a slightly higher background activity than $AT1^{WT}AT2^{GHA}$ displaying 39% compared to $AT1^{WT}AT2^{WT}$, while mutant $AT1^{GAA}AT2^{GSS}$ displayed 87% of activity, a level similar to that of $AT1^{GAA}AT2^{WT}$.

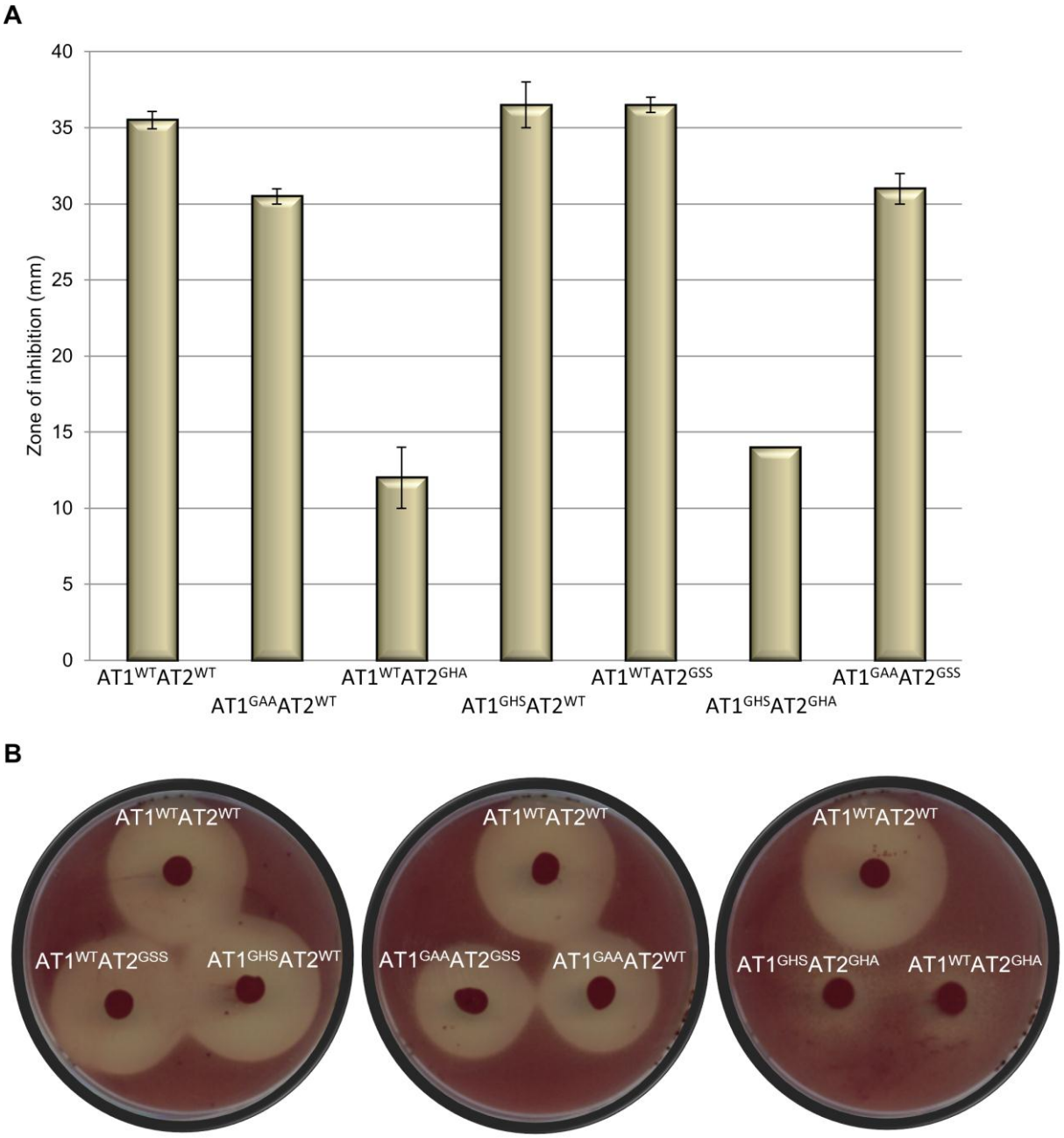

Figure 6.3. Antibiotic assay of AT active site mutants. (A) Chart comparing zones of inhibition. **(B)** Bioassay plates showing zones of inhibition. n=3.

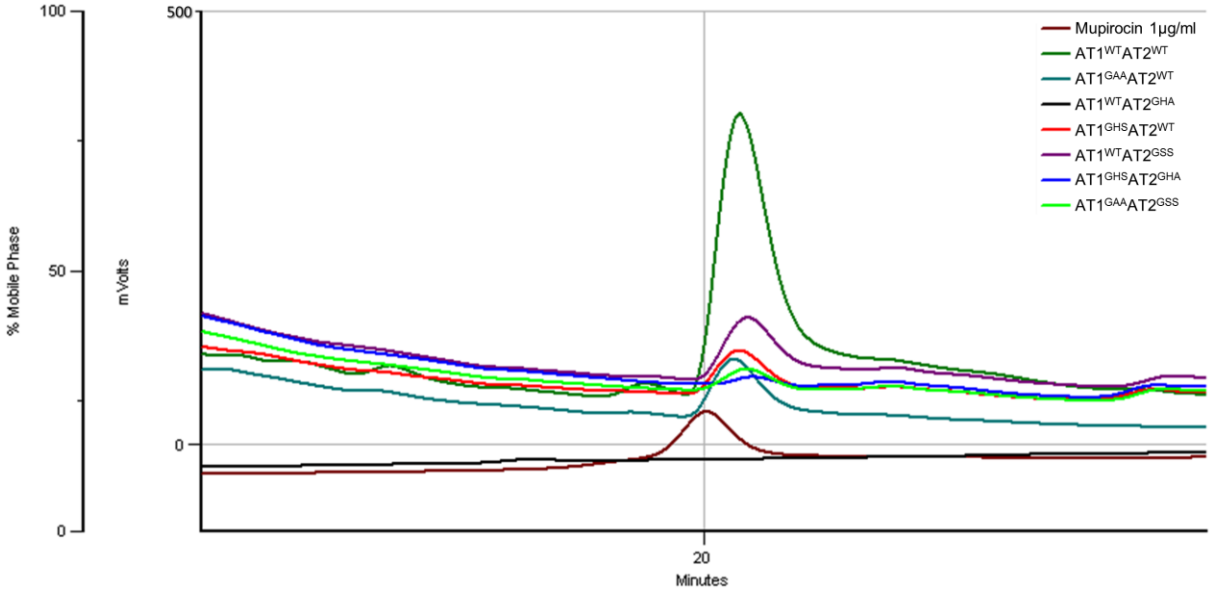

Figure 6.4. HPLC analysis of AT active site mutants. PA-A retention time, 21min.

Table 6.1. Summary of metabolite production AT point mutants.

	$AT1^{WT}$ $AT2^{WT}$	**$AT1^{GAA}$ $AT2^{WT}$**	**$AT1^{WT}$ $AT2^{GHA}$**	**$AT1^{GHS}$ $AT2^{WT}$**	**$AT1^{WT}$ $AT2^{GSS}$**	**$AT1^{GHS}$ $AT2^{GHA}$**	**$AT1^{GAA}$ $AT2^{GSS}$**
Bioassay $\%^{+}$*	100	86	34	103	103	39	87
HPLC (mupirocin) %*	100	17.5	2	19	21	3	8
LCMS (PA-A) %*	100	67	2.7	63.2	72.1	0	71.4
LCMS (mupiric acid) %*	100	90.5	0	42.3	34.5	0	32.7
LCMS (mupirocin H) %*	100	23.8	0	3.3	44.2	0	2.3

+, zone of clearing in mm; *, values have been normalised to WT.

6.2.3 HPLC analysis of mupirocin production in MmpC point mutants (Harry Thorpe)

Analysis of mupirocin by HPLC demonstrated a loss of antibiotic production in all mutants tested (Figure 6.4 and Table 6.1). However, as with the plate bioassay, mutants $AT1^{GHS}AT2^{WT}$ and $AT1^{WT}AT2^{GSS}$ produced the most mupirocin when compared to $AT1^{WT}AT2^{WT}$, but this was considerably lower than the $AT1^{WT}AT2^{WT}$ value. Mutant $AT1^{GAA}AT2^{GSS}$ produced approximately half the amount as the $AT1^{GAA}AT2^{WT}$ strain, and mutant $AT1^{GHS}AT2^{GHA}$ produced only 1% more than the $AT1^{WT}AT2^{GHA}$ strain.

6.2.4 LCMS analysis of compounds produced by MmpC point mutants (Zhongshu Song, University of Bristol)

Previous LCMS analysis not only detected PA-A production, but also the early release intermediates mupiric acid and mupirocin H (Wu, *et al*., 2007; 2008). In line with previous findings the $AT1^{WT}AT2^{GHA}$ mutant produced background levels of PA-A, no mupiric acid and no mupirocin H (Table 6.1). As AT2 is predicted to transfer the malonyl-CoA extender units throughout the entire mupirocin pathway, the lack of production makes sense. Mutant $AT1^{GHS}AT2^{GHA}$ produced similar results, however in this case no PA-A was produced (indicating AT1 cannot complement the loss of AT2). As expected, the $AT1^{GAA}AT2^{WT}$ strain produced a reduced amount of PA-A, indicating production can still continue when this protein is inactivated. The level of mupiric acid in this strain was only 10% less than the $AT1^{WT}AT2^{WT}$ strain, however the level of mupirocin H was reduced to only 24%, indicating the mutation has an

effect on the release of mupirocin H from the pathway. This could also account for the reduced amount of PA-A produced if mupirocin H is blocking the pathway.

Mutant $AT1^{WT}AT2^{GSS}$ appeared to be the most effective PA-A producer, even more so than the $AT1^{GAA}AT2^{WT}$ strain, indicating that AT2 activity has not been lost. This mutant is the only one where the amount of mupirocin H released is more than the amount of mupiric acid released (44.2% and 34.5% respectively). This could be an indication that the GHS to GSS mutation in AT2 has increased the AT1-functionality within the pathway, however, the loss of the active site His residue has caused a reduced production of PA-A (lose the Ser – only 2.7% compared to WT, lose the His, 72.1% compared to WT).

Mutant $AT1^{GHS}AT2^{WT}$ demonstrated a reduction in PA-A production slightly more than the $AT1^{GAA}AT2^{WT}$ strain. It is likely in this strain that AT2 functionality is normal, as expected, but that AT1 functionality has been affected more by the GSS to GHS mutation than the GSS to GAA mutation – indicated by the reduction in amounts of mupiric acid and mupirocin H released from the pathway. It may be that the bulky His residue prevents AT1 from interacting with mupirocin H, whereas Ser and Ala both have relatively small side-chains. The $AT1^{GAA}AT2^{GSS}$ mutant produced similar results to $AT1^{GHS}AT2^{WT}$ – reduced PA-A compared to $AT1^{WT}AT2^{WT}$ and reduced mupiric acid and mupirocin H compared to the $AT1^{GAA}AT2^{WT}$ strain. This contradicts the hypothesis that the His in strain $AT1^{GHS}AT2^{WT}$ prevents AT1 from interacting with mupirocin H, indicating instead that the GSS motif is vital for AT1 function. It would appear that this strain is 8% more efficient at producing PA-A than strain $AT1^{GHS}AT2^{WT}$, as was strain $AT1^{WT}AT2^{GSS}$, which would indicate the GHS to GSS active site mutation of AT2 has improved the activity.

6.3 Discussion

The characterisation of AT2 in Chapter 4 concluded that this was the only AT required for transferring the extender malonate onto the ACPs. This begged the question as to the role of the other AT - AT1. As described in Chapter 5 there are several *trans*-AT PKSs that have a similar architecture to the mupirocin system – in that two ATs are encoded by a separate gene. The work carried out in Chapter 5 identified the fact that AT1 may have an alternative role to the typical AT. This study carried on the investigation into AT1 function by mutating specific residues of the active site in the chromosome of *P. fluorescens* NCIMB 10586. Mutants were analysed by plate bioassay for antibiotic activity, by HPLC for mupirocin production, and by LCMS for PA-A, mupiric acid and mupirocin H production.

The bioassay results demonstrating mutants $AT1^{GHS}AT2^{WT}$ and $AT1^{WT}AT2^{GSS}$ did not lose any antibiotic activity indicates that the two mutated residues (S95H in AT1 and H89S in AT2) are not essential for antibiotic production. Similarly the $AT1^{GAA}AT2^{WT}$ and $AT1^{GAA}AT2^{GSS}$ strains retained about 86% of antibiotic activity when compared to $AT1^{WT}AT2^{WT}$ demonstrating a loss of activity similar to that of losing AT1 activity rather than AT2 activity. The same could be said for mutant $AT1^{GHS}AT2^{GHA}$, which produced an amount of activity similar to the $AT1^{WT}AT2^{GHA}$ strain indicating a loss of AT2 activity. This is also the case for the HPLC results, where similar results were achieved for mutant pairs $AT1^{GAA}AT2^{WT}$/$AT1^{GAA}AT2^{GSS}$ and $AT1^{GHS}AT2^{GHA}$/$AT1^{WT}AT2^{GHA}$. However, the mutants $AT1^{GHS}AT2^{WT}$ and $AT1^{WT}AT2^{GSS}$ did not produce an amount of mupirocin that corresponded to the high bioassay activity, indicating there may be another compound responsible for the increased antibiotic activity in these mutants.

Previous studies have shown that certain deletions cause intermediates to be released early from the mupirocin pathway – for example, when you delete MupH you no longer get production of PA-A, but get the truncated hexaketide mupirocin H instead (Figure 6.5) (Wu *et al*., 2007). Likewise, inactivation of the KR in module 4 results in accumulation of the tetraketide mupiric acid (Wu *et al*., 2008). Accumulation of these products in certain mutants can indicate whereabouts in the pathway certain proteins are functioning. For example, accumulation of mupirocin H by a mutant would indicate that the mutated protein functioned somewhere in the pathway after the MupH cassette, and so works later in the pathway. Accumulation of mupiric acid indicates that the mutated protein works at some point after MmpD. If none of these products are detected it would indicate that the mutated protein works early on in the pathway.

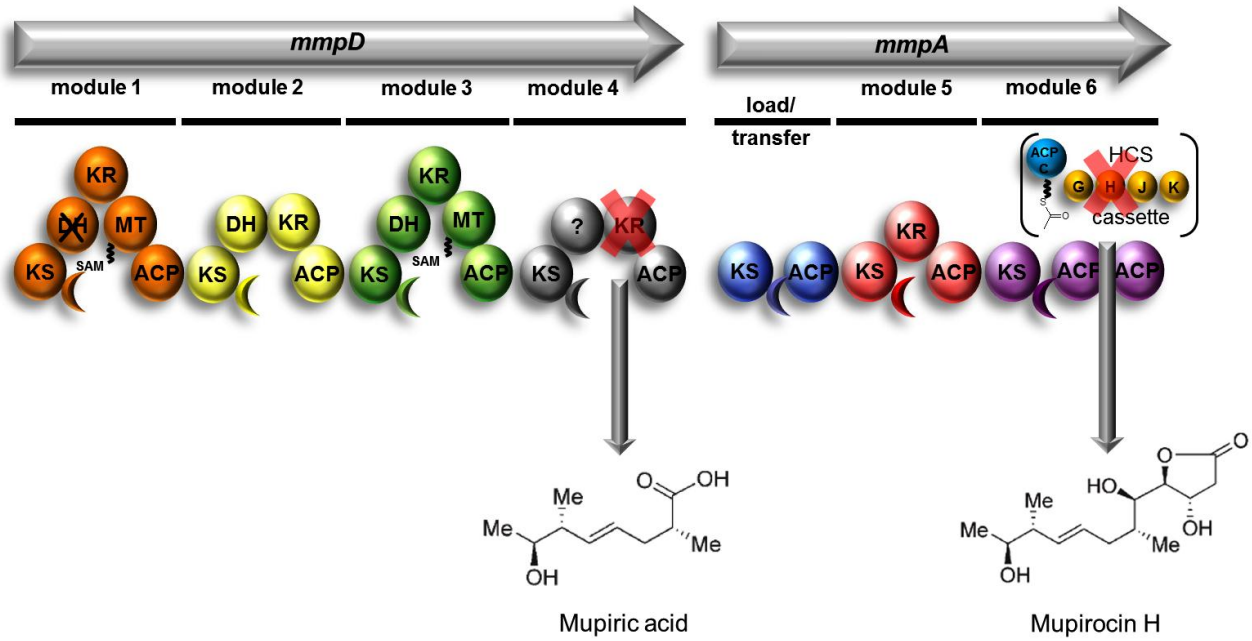

Figure 6.5. Release of mupiric acid and mupirocin H from the mupirocin pathway. Inactivation of KR results in release of mupiric acid from the pathway, while inactivation of mupH releases mupirocin H.

As AT2 transfers malonate to ACPs throughout the cluster it is vital for the entire pathway, therefore the LCMS results for the $AT1^{WT}AT2^{GHA}$ strain were expected: no mupiric acid or mupirocin H was released from the pathway indicating AT2 functions right from module 1. The small percentage of PA-A detected in this strain is in agreement with previous results demonstrating 3% productivity in relation to a WT (Shields, 2008). It is possible that AT1 may be able to take over the transacylation properties of AT2 in its absence, but obviously quite inefficiently. The two strains where the AT2 GHS motif was mutated to GSS ($AT1^{WT}AT2^{GSS}$ and $AT1^{GAA}AT2^{GSS}$) both affected the metabolites produced. In $AT1^{WT}AT2^{GSS}$ it would appear the mutation in AT2 is affecting its activity as there is less mupiric acid being produced (a characteristic of non-functional AT2 due to the nature of it working throughout the entire pathway), and this would also affect the amount of mupirocin H being released as AT2 would be required to transfer malonate in the pathway preceding mupirocin H production. In the $AT1^{GAA}AT2^{GSS}$ mutant however, the amount of mupirocin H being produced has reduced to almost zero, indicating AT1 activity is affected, and cannot be complemented by the GHS to GSS mutation in AT2. Similarly the $AT1^{GHS}AT2^{WT}$ strain does not increase AT2 activity, or if it does, the loss of AT1 function counteracts it. The $AT1^{GHS}AT2^{GHA}$ mutant produced nothing, indicating the GHS motif introduced into AT1 does not complement the inactivation of AT2.

The LCMS results for the AT1 inactivation strain, $AT1^{GAA}AT2^{WT}$, demonstrate a reduced PA-A production, which was also described previously (Shields, 2008). While this mutation did not appear to affect mupiric acid production but did affect the amount of mupirocin H detected it can be postulated that AT1 functions between

MmpD and the end of MmpA, potentially facilitating release of mupirocin H from the pathway. The results for strains $AT1^{GHS}AT2^{WT}$ and $AT1^{GAA}AT2^{GSS}$ also demonstrate this potential function. It is tempting to postulate that the presence of the His residue in place of the Ser in AT1 prevents interaction with potential substrates, but as the same dip in mupirocin H production occurs when Ser is replaced with Ala this is unlikely. Therefore it can be concluded that the Ser at position 95 in AT1 is vital for its functionality and replacing it with the non-reactive Ala results in either a loss of structural integrity or loss of catalytic activity.

In terms of active site residues of the AT1-like ATs, there is variation within the GxS motif, as shown in Table 6.2. The three ATs with the GHS motif have been demonstrated to transfer a malonate-based substrate to ACPs in their respective clusters (Aron *et al*., 2007; Lopanik *et al*., 2008; Musiol *et al*., 2011). As they have the same motif as the classic AT, such as AT2 or *E. coli* FabD their transfer of these substrates is logical. But what happens when the motif is altered to exclude the central His residue that comes into contact with the substrate? It stands to reason that a different residue in this position enables a different type of substrate to interact with the protein, especially when one considers the general role of His as an acid/base catalyst. An example of this is PedC from the pederin biosynthesis pathway which has the motif GAS replacing the classic GHS. PedC has been revealed to display hydrolase activity, interacting with ACPs to cleave acyl chains, yet unable to hydrolyse the malonyl group from the ACPs in question (Jensen *et al*., 2012). It therefore seems prudent that the other ATs within the AT1-like group that contain the motif GAS perform a similar function. Thioesterase domains contain the active site motif GxSxG, which is very similar to the canonical AT motif GHSxG

(Pazirandeh *et al*., 1991). An alignment of TE domains with *trans*-acting ATs revealed the active sites are most similar to the AT2-like ATs, many displaying the characteristic GHS motif (Figure 6.6). However, both the bryostatin and one of the leinamycin TEs do not contain the His residue.

Table 6.2. Active site motif of AT1-like ATs.

Domain	Active site motif		
FenF	G	H	S
ZmaF	G	Y	S
KirCI_AT1	G	A	S
MmpC_AT1	G	S	S
TmpC_AT1	G	S	S
RhiG_AT1	G	T	S
RzxG_AT1	G	A	S
OzmM_AT1	G	A	S
TaV_AT1	G	A	S
BryP_AT2	G	H	S
PedC	G	A	S
BaeD	G	A	S
BatH	G	A	S
EtnK_AT1	G	A	S
SorO_AT1	G	A	S
ElaC	G	S	S
KirCII	G	H	S
EtnB	G	Y	S

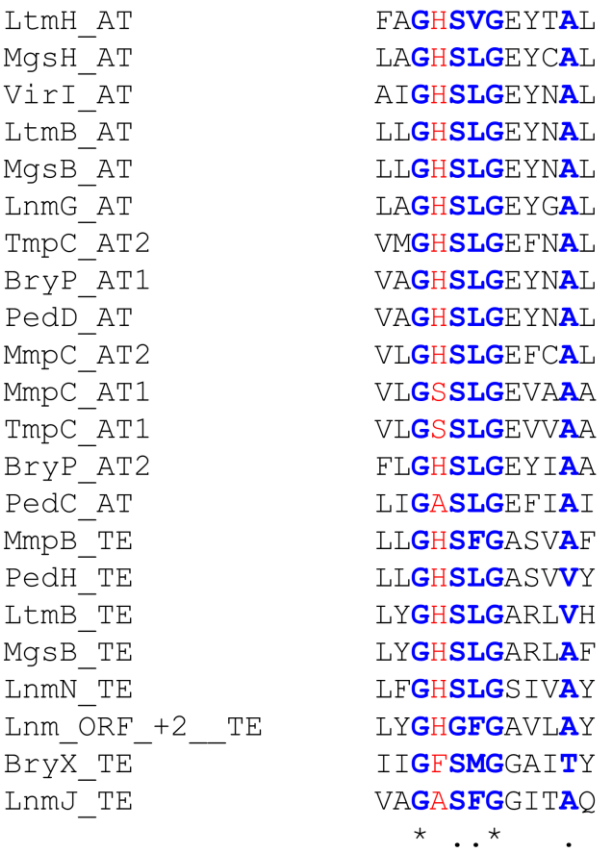

Figure 6.6. A comparison of acyltransferase and thioesterase active sites. Residues highlighted in blue are conserved; those in red are the active site His or equivalent; AT, acyltransferase; TE, thioesterase; *, complete conservation, **.**, partial conservation.

Mupirocin AT1 is one of three ATs (along with TmpC AT1 and ElaC) in this group to have GSS at the active site, rather than GHS or GAS. As its already been demonstrated that AT1 is not required for malonylation of mupirocin ACPs, and results in the previous chapter indicated an alternative function from that of a normal AT, we hypothesised that AT1 may function as a hydrolase, in a similar manner to PedC. It is likely that the different residues in the middle of the GxS motif allow the protein to interact with different types of substrates. Data produced in this Chapter has demonstrated that AT1 most likely functions to remove intermediate compounds

from the pathway, thereby keeping the pathway clear for mupirocin production. The $AT1^{GAA}AT2^{WT}$, $AT1^{GHS}AT2^{WT}$, and $AT1^{GAA}AT2^{GSS}$ strains corroborated this and demonstrated that AT1 likely removes mupirocin H from the pathway.

This can be backed up by recent work within our group. It demonstrated that ACP3/4 can be successfully replaced with thiomarinol (tml) ACPs-A3abc, which are involved in β-methylation in tml production (Dong *et al*., 2012; Fukuda *et al*., 2011). When ACP3/4 are replaced with the tml non-β-branching ACPs-D3ab, no mupirocin is produced. One striking conclusion from this investigation was that the strain with tml ACPs-D3ab produced smaller colonies, compared to the WT or either the ΔACP3/4 strain or when ACP3/4 are replaced by tml ACPs-A3abc (Haines, 2012). It was hypothesised that in this case a toxic product was being released from the pathway. A simple experiment was set up to test this: *mmpC* has two start codons, one prior to the gene and the other prior to AT2 (Hothersall, 2012). A mutant inactivating the initial start codon still produces mupirocin, albeit at a lower rate, so presumably the WT is producing a mixture of MmpC1 (AT1-AT2-ER) and MmpC2 (AT2-ER), while the mutant is only producing MmpC2, which is lacking AT1. ACP3/4 were replaced with tml ACPs-D3ab in this start codon mutant and the result was no mupirocin production as before, but bacterial colonies were of a normal size compared to the previous investigation, indicating that no toxic by-product was being released to affect population cell growth (Haines, 2012).

These data clearly demonstrate an alternative role for AT1-like enzymes as hydrolases removing stunted and toxic products from the PKS pathways to allow metabolite production to continue in the normal manner.

CHAPTER 7

7 GENETIC ANALYSIS OF DOCKING DOMAINS

7.1 Introduction

The *trans*-acyltransferase (*trans*-AT) group of polyketide synthases (PKSs) is no longer unusual. The group has grown dramatically since the initial few were documented almost decade ago (Piel 2002; El-Sayed *et al*., 2003; Tang *et al.*, 2004b). There are now over 30 documented *trans*-AT PKS systems that produce antibacterial, anti-fungal, anti-cancer, anti-tumour, cytotoxic, and plant antibiotic compounds (see Appendix). Among the other characteristics detailed in the Appendix that these systems share is the presence of so-called “docking domains”.

Docking domains (DD) were initially observed in 2002 while analysing the pederin pathway. Piel identified the YTLQxGR and YPF motifs downstream of KS domains that form the boundaries of DDs, and noted that the AT active site GHSxS motif was absent (2002). In 2004 it was proposed they were named AT-docking domains (DD) as homage to a proposed function in the docking of AT domains to multifunctional proteins (Tang *et al*., 2004b). They appear to be remnants of once-functional *cis*-acting AT domains, lacking the crucial active site and substrate specificity motifs (Figure 7.1) (Tang *et al*., 2004b). Several *trans*-AT PKSs have been annotated with DDs, but there is a distinct lack of functional evidence (Piel, 2002; Tang *et al*., 2004; Kopp *et al*., 2005; Calderone *et al*., 2006; Straight *et al*., 2007; Aron *et al*., 2007; Pulsawat *et al*., 2007; Lopanik *et al*., 2008; Lim *et al*., 2009; Fukuda *et al*., 2011). Studies on the mycosubtilin PKS have shown that the AT, FenF, carried out malonyl transfer 100 times faster to the KS-DD-ACP construct than to the DD-ACP construct, but this was approximately half as slow as the lone ACP construct.

The lone ACP construct displayed over 1,000 times more affinity for malonyl-CoA than the DD-ACP construct, and 7 times more affinity than the KS-DD-ACP construct. The authors concluded that DD didn't affect AT specificity, but may play a role in the timing of malonyl transfer – preventing the reaction between AT and KS from proceeding too fast, or indeed to slow, by conformational interactions between the DD, the KS and AT domains (Aron *et al*., 2007).

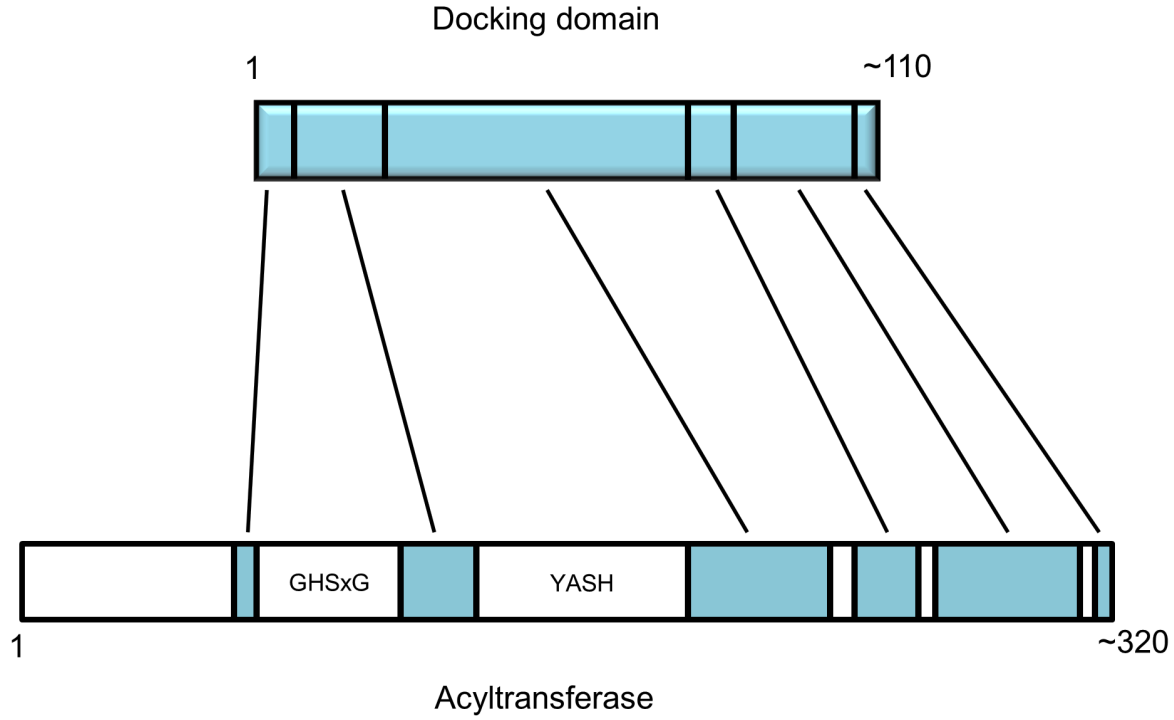

Figure 7.1. Homologous regions between the AT docking domain and a functional methylmalonate-specific AT domain. The active site GHSxG motif and methylmalonate substrate specific motif YASH are absent from the docking domain (Tang *et al*., 2004b).

Previously it was proposed that all the *trans*-AT PKS systems contained DDs (Tang *et al*, 2004b). DDs have been identified in the mupirocin system, but several questions remain to be answered: Are DDs present in every *trans*-AT PKS system? Do DDs have any secondary structure? If DDs are deleted from the producing organism's chromosome, is the secondary metabolite still produced?

7.2 Results

7.2.1 Sequence analysis

A mupirocin DD was used to identify DDs in other *trans*-AT systems – this demonstrated that all *trans*-AT PKSs contain DDs (see Appendix). A BLAST search using the DD from MmpB also identified several uncharacterised *trans*-AT PKS systems revealing an untapped resource of putative polyketide products (Table 7.1).

The mupirocin DDs were aligned with 275 docking domains from the other 29 *trans*-AT PKS systems included in this bioinformatic study. While this alignment showed conserved regions, it was necessary to generate a sequence logo to be able to demonstrate the conservation that occurs, particularly at the N- and C-termini. Figure 7.2 shows that they consist of a maximum of 132 amino acids containing conserved motifs at each end, with a less conserved region in between. There are several completely conserved residues, including an Arg at position 18, Leu^{33}, Pro^{122} and Trp^{132}. There are several other highly conserved residues including a Leu at the beginning, Thr^{7} and Leu^{8}, Gly^{11} and Arg^{12}, Gly^{100} and Tyr^{124}, Pro^{125} and Phe^{126}.

Table 7.1. BLAST results showing *trans*-AT PKS proteins containing docking domains, responsible for uncharacterised polyketide products.

Accession	Producing organism	Identity[a]
YP_777798.1	*Burkholderia ambifaria* AMMD	47%
YP_004084148.1	*Micromonospora* sp. L5	43%
YP_003124922.1	*Chitinophaga pinensis* DSM 2588	43%
YP_002987049.1	*Dickeya dadantii* Ech703	42%
EHK80195.1	*Saccharomonospora azurea* SZMC 14600[b]	42%
ZP_09832368.1	*Saccharomonospora azurea* NA-128[b]	42%
YP_001231835.1	*Geobacter uraniireducens* Rf4	41%
YP_003871372.1	*Paenibacillus polymxa* E681	41%
YP_003947589.1	*Paenibacillus polymxa* SC2	40%
ZP_04622165.1	*Yersinia kristensensii* ATCC 33638	40%
YP_004207774.1	*Bacillus subtilis* BSn5[b]	39%
YP_005556846.1	*Bacillus subtilis* subsp. *subtilis* RO-NN-1[b]	39%
ZP_08194894.1	*Clostridium papyrosolvens* DSM 2782[b]	39%
EHA29456.1	*Bacillus subtilis* subsp. *subtilis* str. SC-8[b]	39%
ZP_02406696.1	*Burkholderia pseudomallei* DM98	39%
ZP_02493571.1	*Burkholderia pseudomallei* NCTC 13177	39%
ZP_02509683.1	*Burkholderia pseudomallei* BCC215	39%
ZP_02501787.1	*Burkholderia pseudomallei* 112	39%
YP_111014.1	*Burkholderia pseudomallei* K96243	39%
ZP_03790871.1	*Burkholderia pseudomallei* Pakistan 9	39%
ZP_03450044.1	*Burkholderia pseudomallei* 576	39%
ZP_04812633.1	*Burkholderia pseudomallei* 1106b	39%
YP_001075429.1	*Burkholderia pseudomallei* 1106a	39%

ZP_04899204.1	*Burkholderia pseudomallei* S13	39%
YP_003973164.1	*Bacillus atrophaeus* 1942	39%
YP_005312202.1	*Paenibacillus mucilaginosus* 3016[b]	39%
AFH61261.1	*Paenibacillus mucilaginosus* K02[b]	39%
YP_004640305.1	*Paenibacillus mucilaginosus* KNP414	38%
YP_001062476.1	*Burkholderia pseudomallei* 668	38%
YP_004877340.1	*Bacillus subtilis* subsp. *spizizenii* TU-B-10[b]	38%
YP_002773468.1	*Brevibacillus brevis* NBRC 100599[b]	38%
AFI28406.1	*Bacillus* sp. JS	38%
ZP_06873410.1	*Bacillus subtilis* subsp. *spizizenii* ATCC 6633	36%
YP_002505216.1	*Clostridium cellulolyticum* H10	36%

a, with MmpB DD; b, contains more than one *trans*-AT PKS.

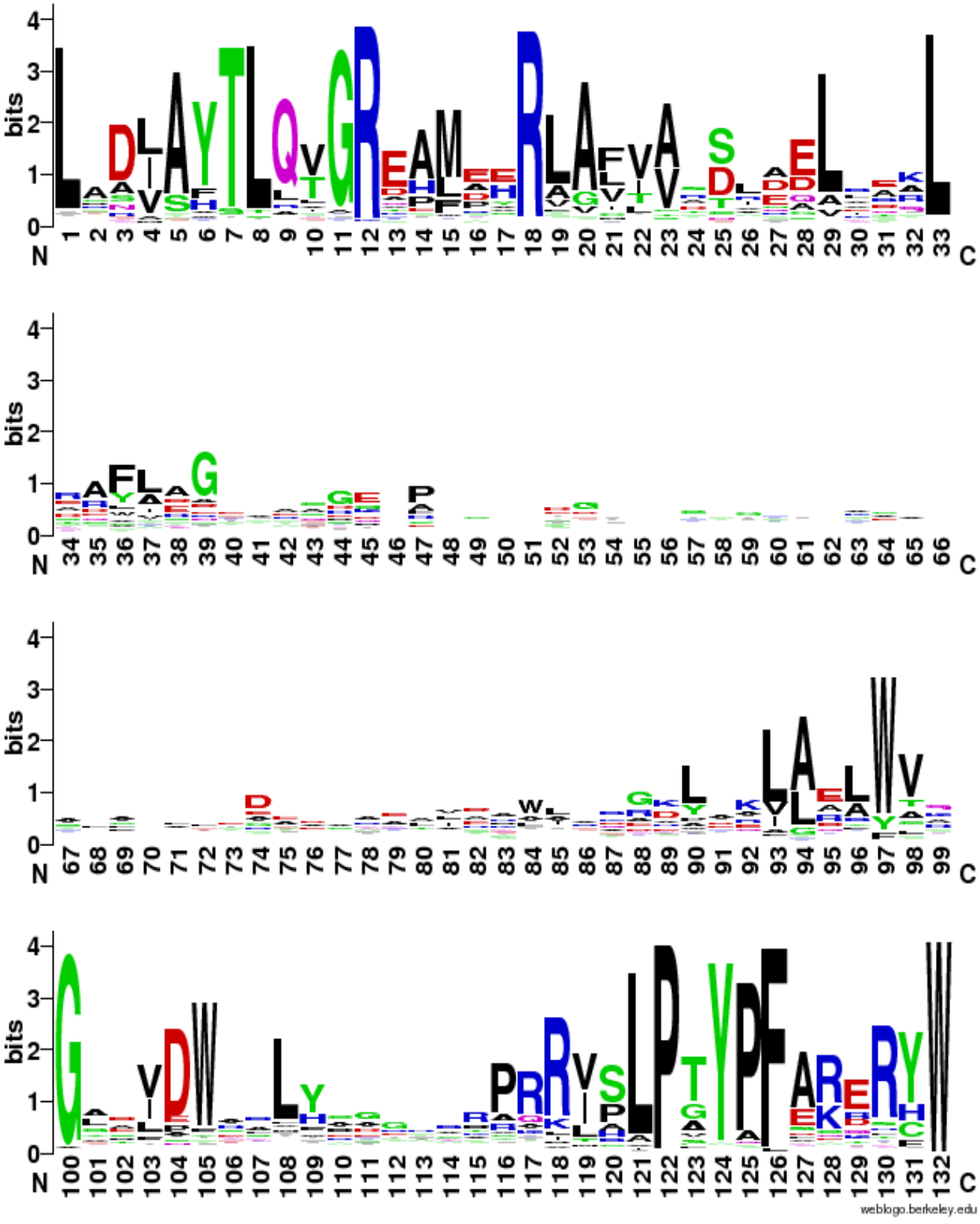

Figure 7.2. Sequence logo showing conservation among docking domain sequences. 285 docking domain sequences from 30 *trans*-AT PKS systems were used to generate the sequence logo. Colour coding: blue, basic; red, acidic; black, non-polar; green, polar; purple, nonessential (Schneider and Stevens, 1990; Crooks *et al*., 2004).

This has enabled the DD boundaries to be characterised, with LxDLAYTLQxGRxxMxxRLAxxAxxxxxLxxxL representing the N-terminus consensus sequence, and WVxGxxxDWxxLxxxxxxxPRRxxLPTYPFARERYW representing the C-terminus sequence. The LPTY motif shown in the C-terminus sequence can be found downstream of *cis*-acting ATs, and represents the invisible boundary between AT and ACP (Tang *et al*., 2006). The GHSxG motif characteristic of the AT active site was not evident in any sequence analysed. The docking domains analysed in this study varied in length from 90 to 132 amino acids, with the disordered central segment accounting for between 17 and 60 residues.

A mupirocin DD was mapped to a portion of module 5 from DEBS including the C-terminus of the KS domain, the KS-AT linker, the AT and the post-AT linker (Tang *et al*., 2006). Figures 7.3 and 7.4 highlight two particular regions of the DEBS module that aligned with the N and C-terminal consensus sequences of the DDs – approximately half of the KS-AT linker aligned with the N-terminus (termed region 1), while post AT-linker aligned to the C-terminus (region 2). This identified two structural regions to be deleted from the chromosome alongside deletion of a whole docking domain.

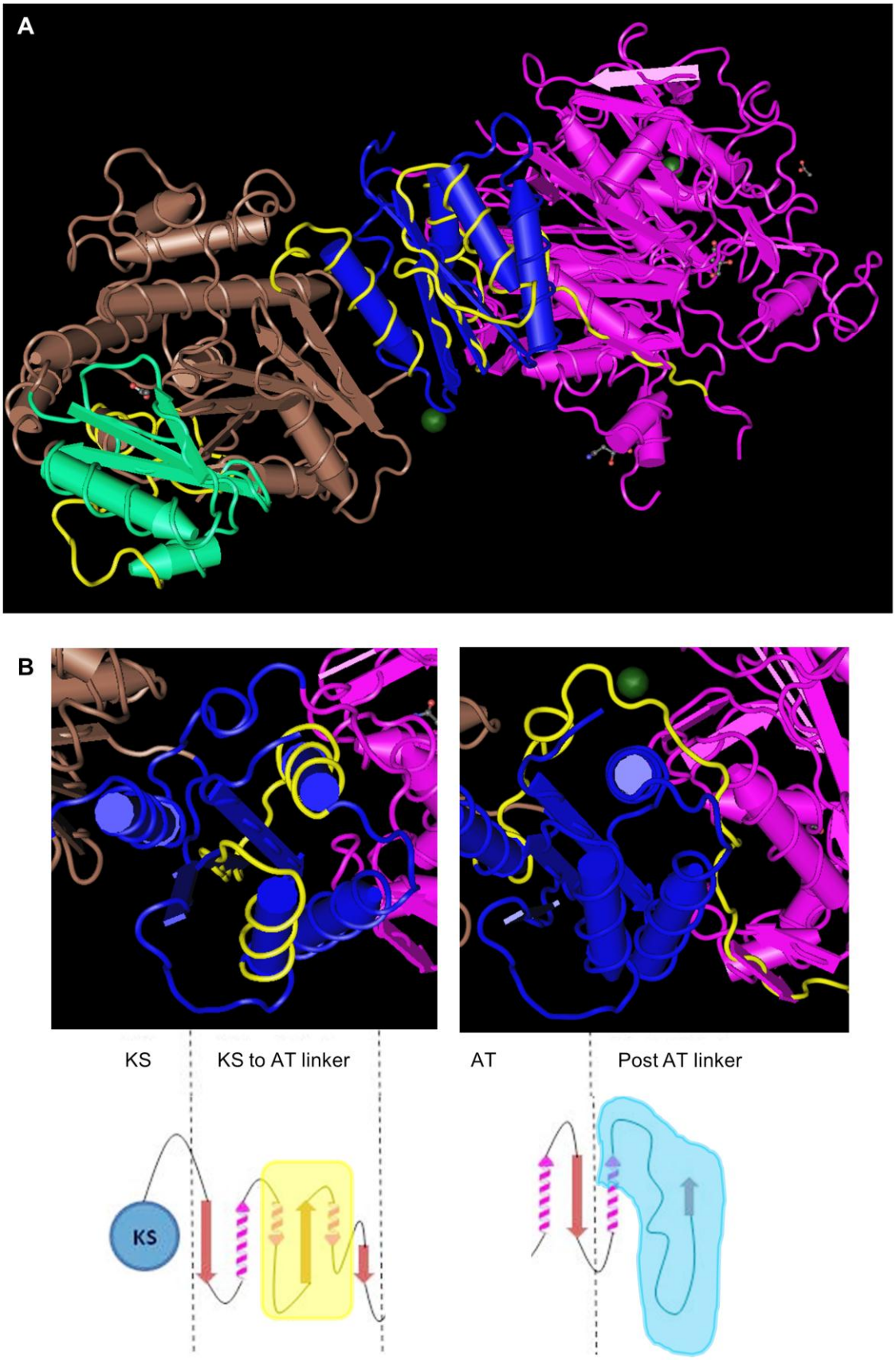

Figure 7.3. Mapping of a docking domain to DEBS module 5. (A) A portion of DEBS module 5 showing ketosynthase (pink), acyltransferase subdomains (brown and green) and KS-AT and post-AT linkers (blue) with a docking domain mapped in yellow. **(B)** Left, region 1 to be deleted is highlighted yellow in cartoon; right, region 2 to be deleted is highlighted blue in cartoon.

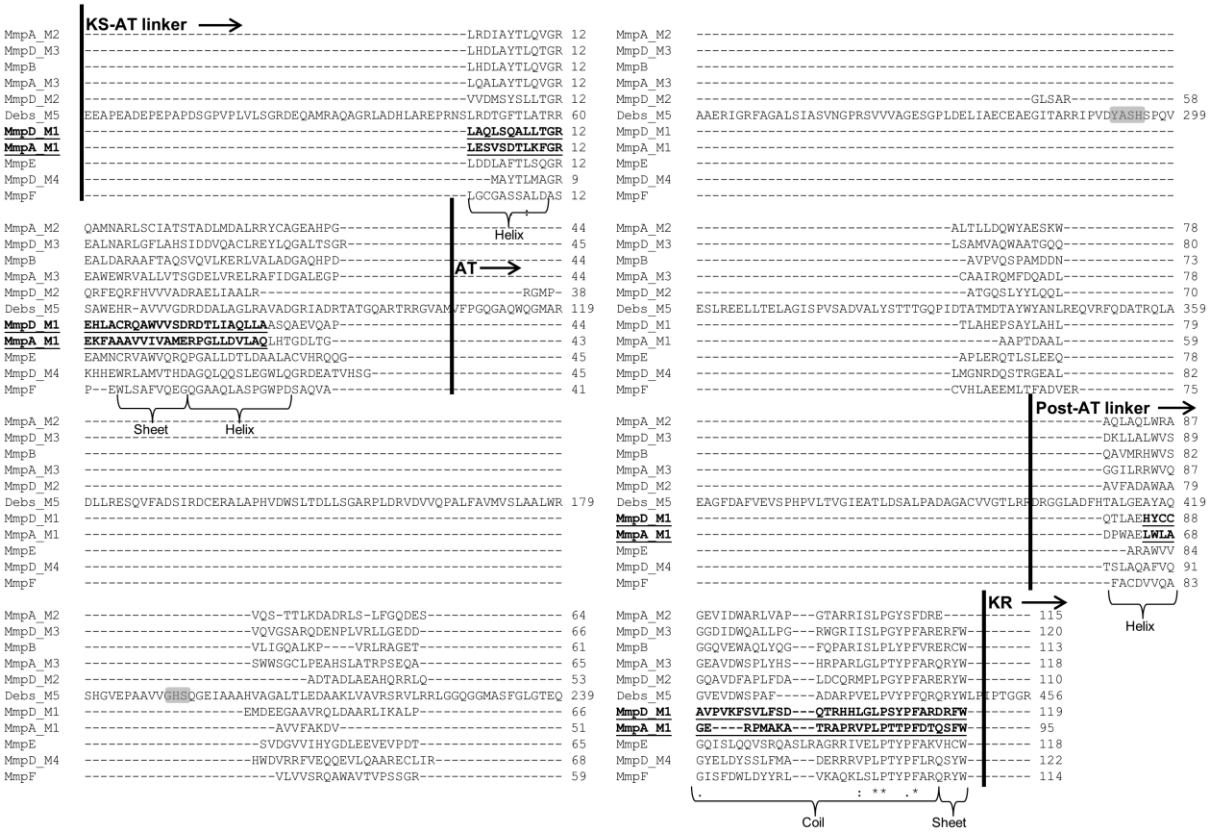

Figure 7.4. Sequence alignments of mupirocin docking domains with a portion of DEBS module 5. Secondary structures are annotated on the alignment to show areas of the mupirocin DDs that potentially have structure. KS, ketosynthase; AT, Acyltransferase; KR, ketoreductase.

7.2.2 Construction of *P. fluorescens* NCIMB 10586 deletion mutants

MmpD and MmpA were targeted for deletion of an entire docking domain (ΔD3 and ΔA3), alongside separate deletions of regions 1 (ΔD1 and ΔA1) and 2 (ΔD2 and ΔA2) (Figure 7.5). The first docking domain on MmpD was targeted as being the first docking domain in the mupirocin pathway, while the first docking domain on MmpA was targeted as being part of a non-elongating module. Primers were designed to amplify two 500bp fragments that flanked either side of the region to be deleted with external restriction sites for cloning into plasmids (Table 2.12). PCR was carried out using Velocity DNA polymerase (Bioline). The PCR products were gel purified, A-tailed and ligated with pGEM-T-Easy to produce plasmids pRG701-pRG708. Following successful sequencing, fragments were excised from pGEM-T-Easy with the appropriate restriction enzymes for ligation into the suicide vector pAKE604. Ligations were performed in triple, that is, the pAKE604 vector, and two 500bp arms were ligated simultaneously, and then transformed into *E. coli* DH5α. Plasmid DNA extraction and restriction digests using the sites at either end of the fragments confirmed the presence of 1kb fragment with the selected area deleted. Plasmids pRG710-pRG715 were then transformed into *E. coli* S17-1 ahead of conjugation with *P. fluorescens* NCIMB 10586 where integration into the chromosome occurred by homologous recombination. Integrants were isolated by checking for sucrose resistance and kanamycin sensitivity, as the integrated plasmid carries *sacB*, which encodes the enzyme levansucrase, and Kan^R. The mutant genotype was checked by PCR.

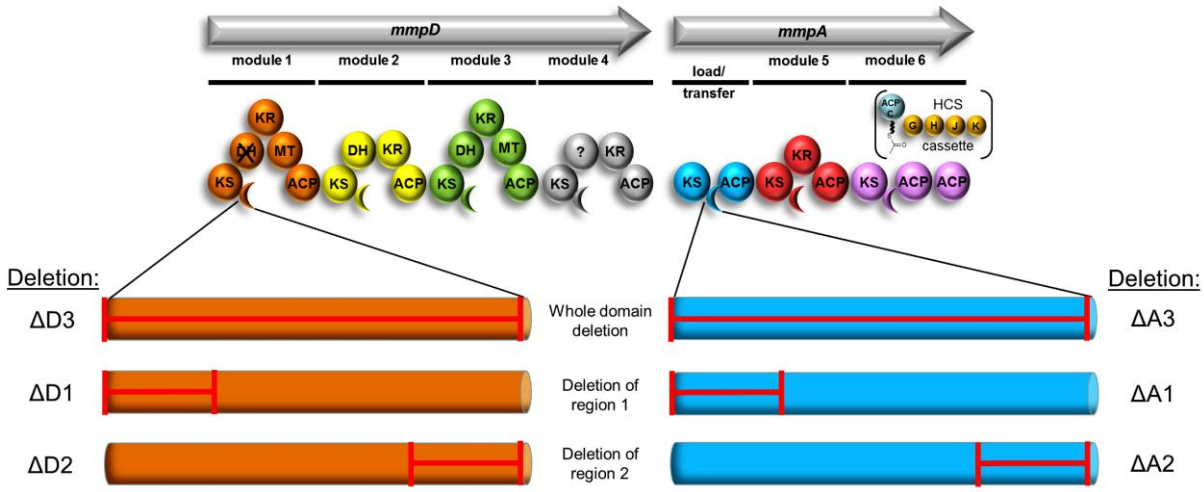

Figure 7.5. Location of docking domain deletions. Δ, deletion; D, MmpD; A, MmpA; crescents, docking domains.

7.2.5 Bioassay and HPLC analysis of docking domain mutants

Plate bioassays and HPLC were employed to determine the phenotype of the six DD deletion mutants (Sections 2.4 and 2.5). Each mutant resulted in a complete loss of mupirocin production when compared to WT and the negative control, Δ*mmp*A which is known to knock-out mupirocin production (Figure 7.6, A and B). Mutants ΔA3 and ΔD2 had zones of inhibition that were 23% of the WT (3% more than Δ*mmp*A), and appeared more diffuse than the remaining zones. Mutants ΔA1, ΔA2, ΔD1 and ΔD3 all had zones that were less than those for Δ*mmp*A. HPLC analysis was carried out to confirm the results from the plate bioassay. Figure 7.6 (C) shows that compared to the WT, a mupirocin standard and Δ*mmp*A, none of the mutants produced PA-A.

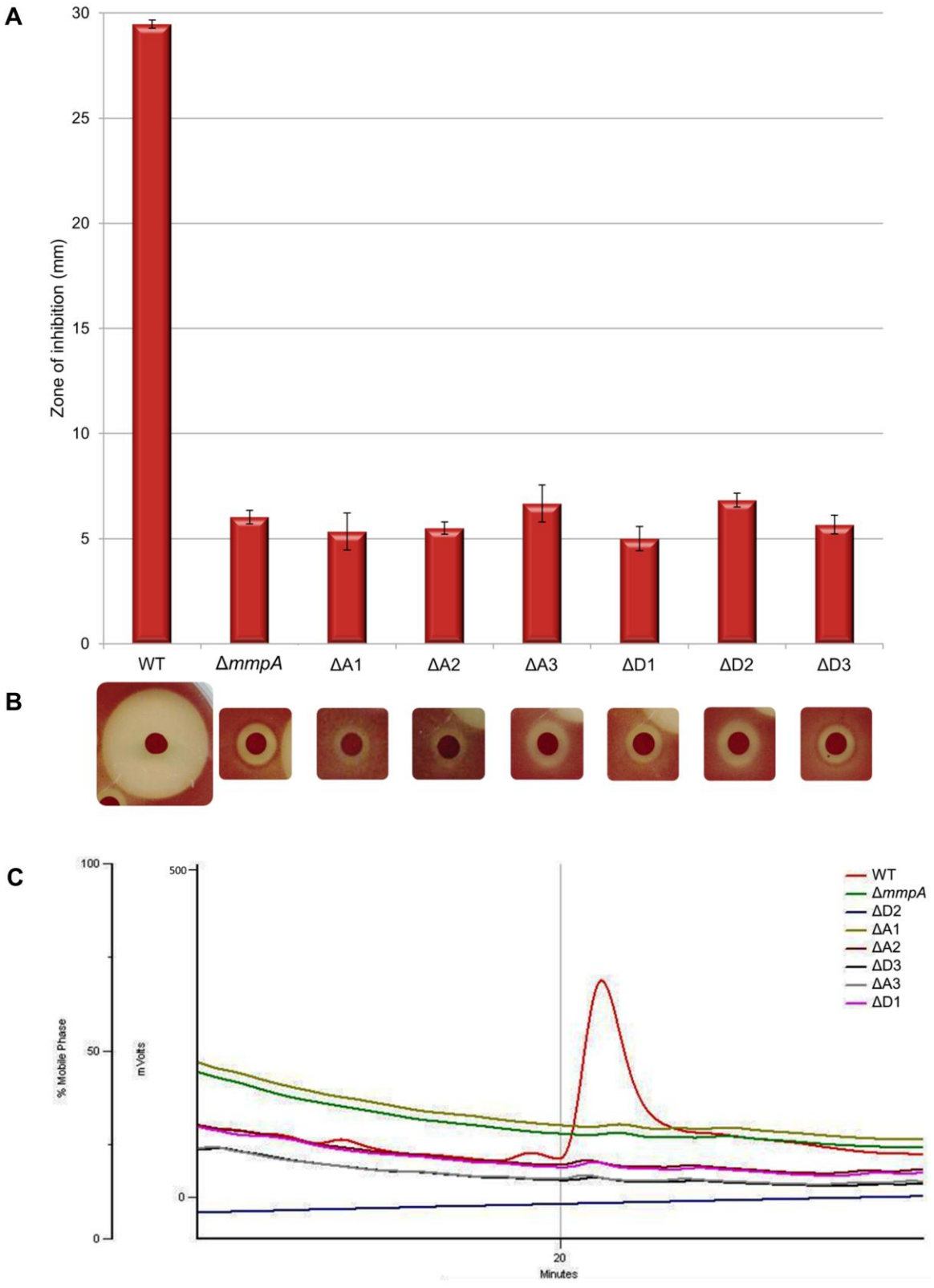

Figure 7.6. Analysis of docking domain deletion mutants. (A) Chart of inhibition zones, (n=3). **(B)** Bioassay plates. **(C)** HPLC analysis. WT, wild type; ΔA1-A3 and ΔD1-D3, deletion of *mmpA* regions, 1, 2 and entire docking domain (3), and deletion of mmpD regions 1, 2 and entire docking domain (3).

7.2.6 LCMS of docking domain mutants

It was predicted that the deletions on *mmp*A may produce mupiric acid – as this is the last intermediate to be released before the assembly line reaches *mmp*A. Alongside the negative control Δ*mmp*A, none of the mutants produced either mupiric acid or the other early intermediate, mupirocin H (Figure 7.7).

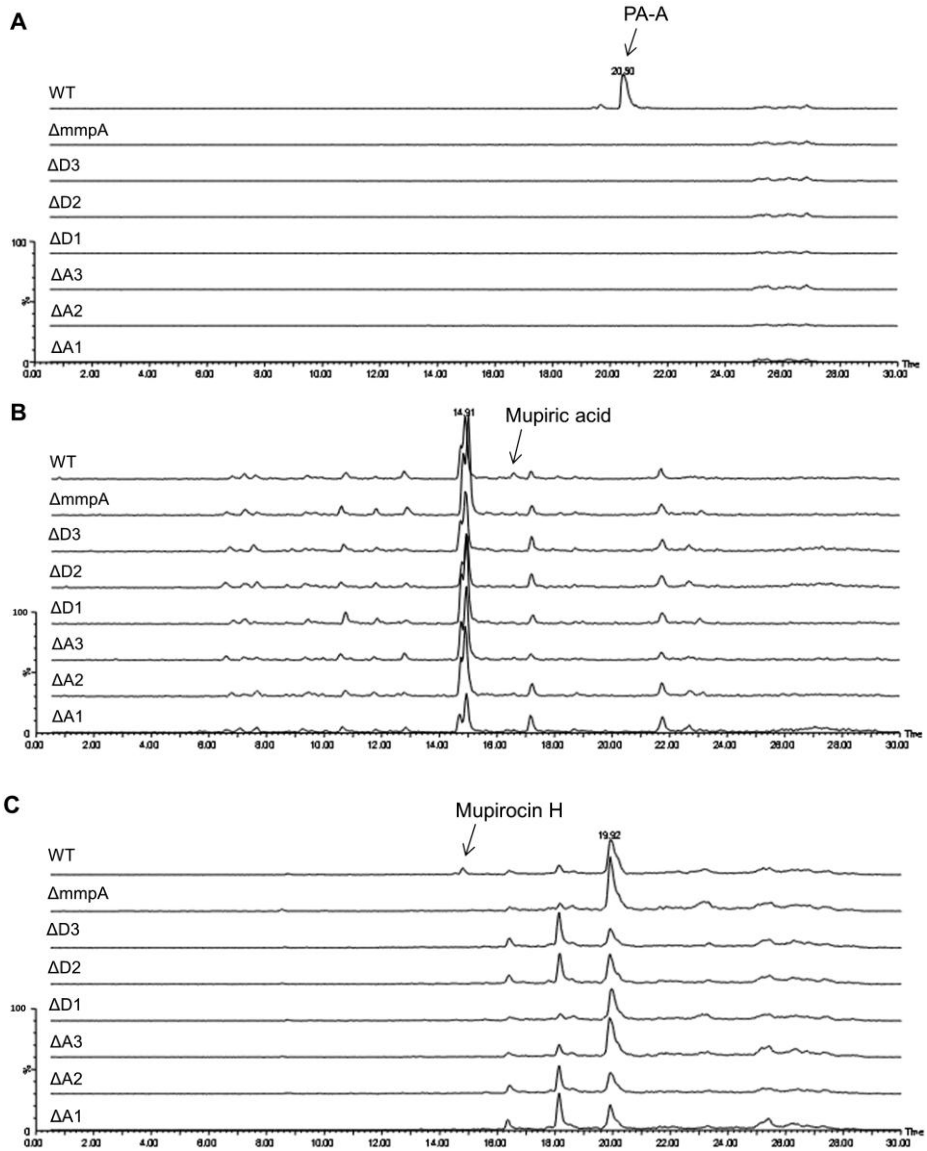

Figure 7.7. LCMS analysis of docking domain deletion mutants. (A) Detection of PA-A. **(B)** Detection of mupiric acid. **(C)** Detection of mupirocin H. WT, wild type; ΔA1-A3 and ΔD1-D3, deletion of mmpA regions, 1, 2 and entire docking domain (3), and deletion of mmpD regions 1, 2 and entire docking domain (3).

7.3 Discussion

Until fairly recently the linking regions between domains on *trans*-AT multifunctional PKSs were thought to be just that, regions that linked catalytically active domains to one another. Several investigations have revealed striking similarities between some of these so called linkers (specifically the KS to the next downstream domain linker) and *cis*-AT PKSs. Despite *cis*- and *trans*-AT PKS systems evolving separately, it has been postulated that these linkers immediately downstream of the KS domain were the remnants of ATs that once would have functioned in *cis* in the same way as the modern day *cis*-AT PKS systems, such as DEBS (Tang *et al*., 2004b). Previous studies showed it was portions of AT-like fragments remaining after multiple deletion events that formed these DDs (Figure 7.1).

This study has demonstrated the evolutionary deletion extends further than previously thought - DDs are comprised of two segments that are similar to portions of an AT, with an N-terminal similar to part of a KS-AT linker, and a C-terminal similar to a post-AT linker. Figure 7.1 can now be remodelled to this effect, as shown in Figure 7.8. Of the 285 DDs analysed during this study, the GHSxG motif characteristic of the AT active site was absent, indicating these are not functioning as partial ATs.

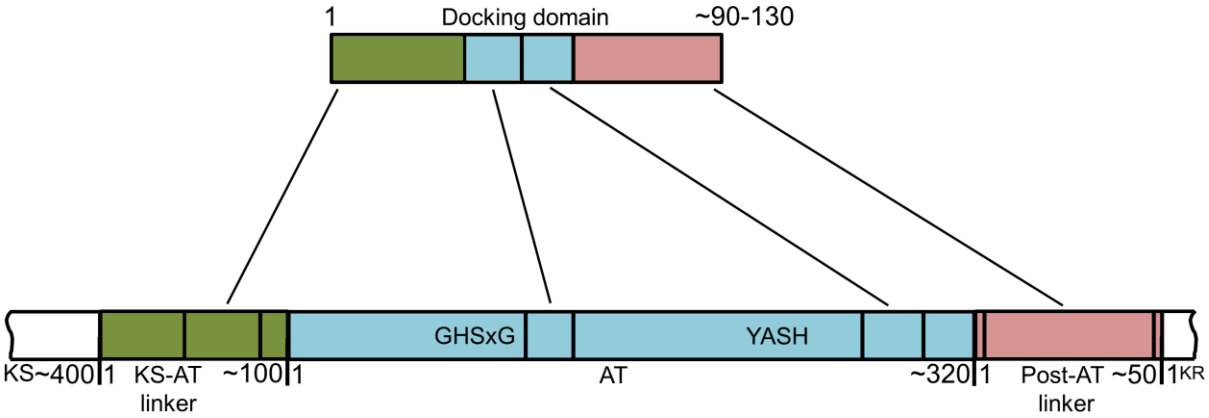

Figure 7.8. Homologous regions between the AT docking domain and a portion of DEBS module 5. KS-AT linker is shown in green, AT is shown in blue and the post-AT linker is shown in pink. Lines connecting the two models indicate homologous regions. KS, ketosynthase; AT, acyltransferase; KR, ketoreductase.

Sequence alignments have demonstrated conservation of the docking domain with both the KS-AT linker and post-AT linker from module 5 of DEBS. The crystal structure of DEBS module 5 has been solved, and by aligning this module with the mupirocin DDs one can predict that a docking domain has at least some secondary structure (Tang *et al*., 2006). This alignment has shown that the KS-AT linker could be comprised of three α-helices and three β-sheets, while the post-AT linker mainly of random coils.

In *cis*-AT PKSs the positioning of the domains requires certain movement or reorganisation for the transfer of substrate from AT to ACP and to KS for condensation. It is thought the AT domain interacts with the KS-AT linker to form interdomain contact. At the KS to KS-AT linker and KS-AT linker to AT interfaces there are hinge regions – regions of flexibility designed to bring domains in closer proximity to one another (Anand and Mohanty, 2012). However it would seem that the hinge regions do not provide adequate flexibility for the ACP to dock at one site

and have access to the active sites of both the AT and KS domains. A key residue has been identified in the KS-AT linker region of *cis*-AT PKS systems that is thought to be involved in KS-ACP interaction, specifically to guide the biosynthesis of the polyketide in a unidirectional manner. The ratchet mechanism is based on the acidity/basicity of specific amino acid residues. The premise is that if a module has an acidic residue in a specific position (for example Arg^{551} of the KS-AT linker of DEBS module 5) an ACP from the same module will have an acidic residue at position 23 meaning the ACP cannot pass the growing chain back to the KS, but will instead pass it forward to the next module which would have a basic residue in the corresponding position (Kapur *et al*., 2012). The same study also identified residues 44 and 45 of ACPs as being important for docking in the KS/KS-AT linker/AT cleft during the elongation process. It is tempting to hypothesis that the same residues could be of importance in *trans*-AT PKS systems however, Arg^{551} of DEBS module 5 is not in a region that aligns with the mupirocin docking domains, suggesting that another residue holds this responsibility within *trans*-AT PKSs.

Due to the disordered state of the post-AT linker, compared to the rigid secondary structure of the KS-AT linker, it was predicted to have a role in facilitating movement of the ACP between catalytic sites during biosynthesis (Anand and Mohanty, 2012). This is consistent with the crystal structure of part of DEBS module 3 which indicates that the post-AT linker forms interactions with the KS and AT domains which ultimately enable the synthase to form a deep ACP-docking groove (Tang *et al*., 2007). Further studies have demonstrated that the post-AT linker is not required for AT acquiring substrate, passing it to ACP or for the KS acquiring

substrate, but is required for KS-catalysed β-ketoacyl-ACP synthase activity (Chen *et al*., 2007; Wong *et al*., 2010).

The number of domains varies between systems, but a *trans*-AT PKS cluster contains a DD for every KS-containing module that lacks a cognate AT domain. If these domains are the result of an evolutionary recombination event designed to eliminate AT domains, there are two notable clusters containing *trans*-AT PKSs that could be further behind in the evolutionary process. The zwittermicin and FK228 clusters both contain a mixture of *cis*- and *trans*-acting ATs, which is not entirely unusual as so does the kirromycin cluster - KirAVI contains a *cis*-acting AT while the remaining PKS modules do not and are instead supplied by KirCI and KirCII, and the neocarzillin cluster – modules 1 and 3 have *cis*-acting ATs, while modules 2 and 4 do not (Otsuka *et al*., 2004; Cheng *et al*., 2007; Weber *et al*., 2008; Kevany *et al*., 2009; Musiol *et al*., 2011). What is unusual however, is the length of the proposed docking domains – they are between 200-250 amino acids in length, and one was annotated on DepB as a non-functional AT domain (Cheng *et al*., 2007). An alignment of these three DDs with DDs from other systems showed the same areas of homology, with the exception of there being more residues of the segment between the N and C-termini sequences.

An alternative hypothesis for the role of DDs comes in the form of interdomain (ID) regions identified on a tetrameric iterative PKS that produces 6-methylsalicyclic acid (6-MSA) (Moriguchi *et al*., 2006). Based on previous studies it is highly likely that the mupirocin multifunctional proteins take on the form of dimers during mupirocin production (Tang *et al*., 2006). Therefore IDs may be required to form the functional dimers.

It would seem prudent to hypothesise that the reason these DDs have remained in place throughout the evolutionary process is due to their functional nature, rather than by serendipity. The results shown in this study indicate DDs play a vital role in mupirocin biosynthesis – when even part of them is deleted it completely disrupts antibiotic production. As they have retained most of the post-AT linker, it seems highly likely that they play an as yet unidentified role in acyl-group transfer and/or condensation catalysation, even if it is a structural role. As yet, there are no crystal structures of complete polyketide synthases and until such a time we can only hypothesise about the complete conformation that a synthase may take. It is highly likely that in a *trans*-AT system the interactions between the AT domain and the post-AT region (now located within the DD) still occur, indeed they may be even more important in guiding the *trans*-acting AT to the correct position for acyl transfer or for facilitating the ACP into the correct position.

CHAPTER 8

8 MUTAGENESIS OF β-BRANCHING ACP3

8.1 Introduction

Acyl carrier proteins (ACPs) are an integral part of both fatty acid synthesis and polyketide synthesis. ACPs are modified from *apo* to *holo* form by the addition of a 4'-phosphopantethiene group to a conserved Ser residue located in a loop close to helix two (Lambalot *et al*., 1996; Mercer and Burkart, 2007). This phosphopantetheine arm serves to anchor acyl groups prior to Claisen condensation with the growing molecule. While ACPs have the same role, the nature of polypeptide organisation in different systems means the interactions of these small proteins are varied (Mercer and Burkart, 2007). In the assembly line set up of type I PKS systems the ACP is located within a multidomain polypeptide and is required to interact with neighbouring domains, including those located on a separate polypeptide. For type I FAS systems the ACP acts iteratively throughout the entire process of molecule synthesis and can interact with as many as 12 different domains (Rawlings and Cronan, 1992). In type II FAS and PKS systems each catalytic domain is located on a separate protein, including the ACP, which is required to repeatedly interact selectively with the correct enzymes in the correct sequence (Mercer and Burkart, 2007).

There are 11 type I and 5 type II ACPs involved in mupirocin biosynthesis (El-Sayed *et al*., 2003). Studies have shown these are phosphopantetheinylated by the phosphopantetheinyl transferase (PT) MupN and acquire malonate from MmpC (Shields *et al*., 2010; Chapter 4 of this Thesis). As in many *trans*-AT PKSs systems, the mupirocin cluster has two cases of tandem ACPs – ACP3 and 4 in MmpA, and

ACP5, 6 and 7 in MmpB – thought to function independently and increase the pathway rate – a deletion of any one of these would be rate limiting (Rahman *et al*., 2005).

Methyl groups can be added to the growing molecule by one of three methods – *cis*-AT systems such as DEBS may employ methylmalonate specific ATs which incorporate methyl groups into the molecule (Ruan *et al*., 1997); *trans*-AT systems such as mupirocin, leinamycin and pederin have methyltransferase (MT) domains within catalytic modules incorporating α-methyl groups from S-adenosyl methionine (SAM) (Piel, 2002; Cheng *et al*., 2003; El-Sayed *et al*., 2003); the final method is the incorporation of β-methyl groups by the actions of a hydroxymethylglutaryl-CoA synthase (HCS) cassette (Calderone *et al*., 2006). The presence of an HCS cassette is not limited to either *cis*- or *trans*-acting AT PKS pathways as demonstrated by their presence in the *cis*-AT PKSs of curacin A and jamaicamide, and in many of the *trans*-AT PKSs as demonstrated in the Appendix (Chang *et al*., 2004; Edwards *et al*., 2004). The mupirocin cluster has an HCS cassette thought to associate with module 6 on MmpA to add the C_{15}-methyl group to monic acid. This module also happens to be the location for one of the tandem pairs of ACPs – ACP3 and 4. HCS cassettes generally involve a set of five proteins incorporating a decarboxylating KS (MupG), an HMG-CoA synthase (MupH), two enoyl-CoA hydratases (ECHs) (MupJ, MupK) and an ACP (mAcpC). It is proposed that AT2 would transfer a malonate group from malonyl-CoA to mAcpC, prior to decarboxylation by MupG. MupH then catalyses a condensation to join the acetyl-mAcpC with the β-ketothiolester moiety, presumably anchored on ACP3, before dehydration and a further decarboxylation by MupJ and MupK (Wu *et al*., 2007).

ACPs holding an intermediate which has a β-methyl group introduced by the activity of a HCS cassette are referred to as branching ACPs. Recent investigations have identified a sequence motif unique to branching ACPs, DSxxxxxW where S is the active site Ser, that once identified was utilised to identify branching ACPs from 17 PKS clusters (Dong *et al*., 2012). In addition to this specific motif there were a number of differences identified between branching and non-branching ACP sequences, highlighting the potential for the different roles of these ACPs. The nuclear magnetic resonance (NMR) structure of the ACP3/4 didomain as determined by Matt Crump and co-workers indicated that both ACPs were very similar consisting of four α-helices and a loop, and they were joined by an unstructured linker (Figure 8.1) (Dong *et al*., 2012). The active site Ser was located at the N-terminus of helix II, while the conserved Trp residue of each ACP was buried in the core of the protein located between helices I and II – replacing smaller residues at this position in non-branching ACPs.

Site directed mutations (W>L) in ACP3 or 4 or both ACP3 and 4 of the didomain resulted in a reduction of pseudomonic acid (PA-A) with the double mutant having the least production, indicating the importance of this residue for a fully functioning branching ACP (Dong *et al*., 2012).

The aim of this project was to determine the phenotype of the W>L mutation in ACP3.

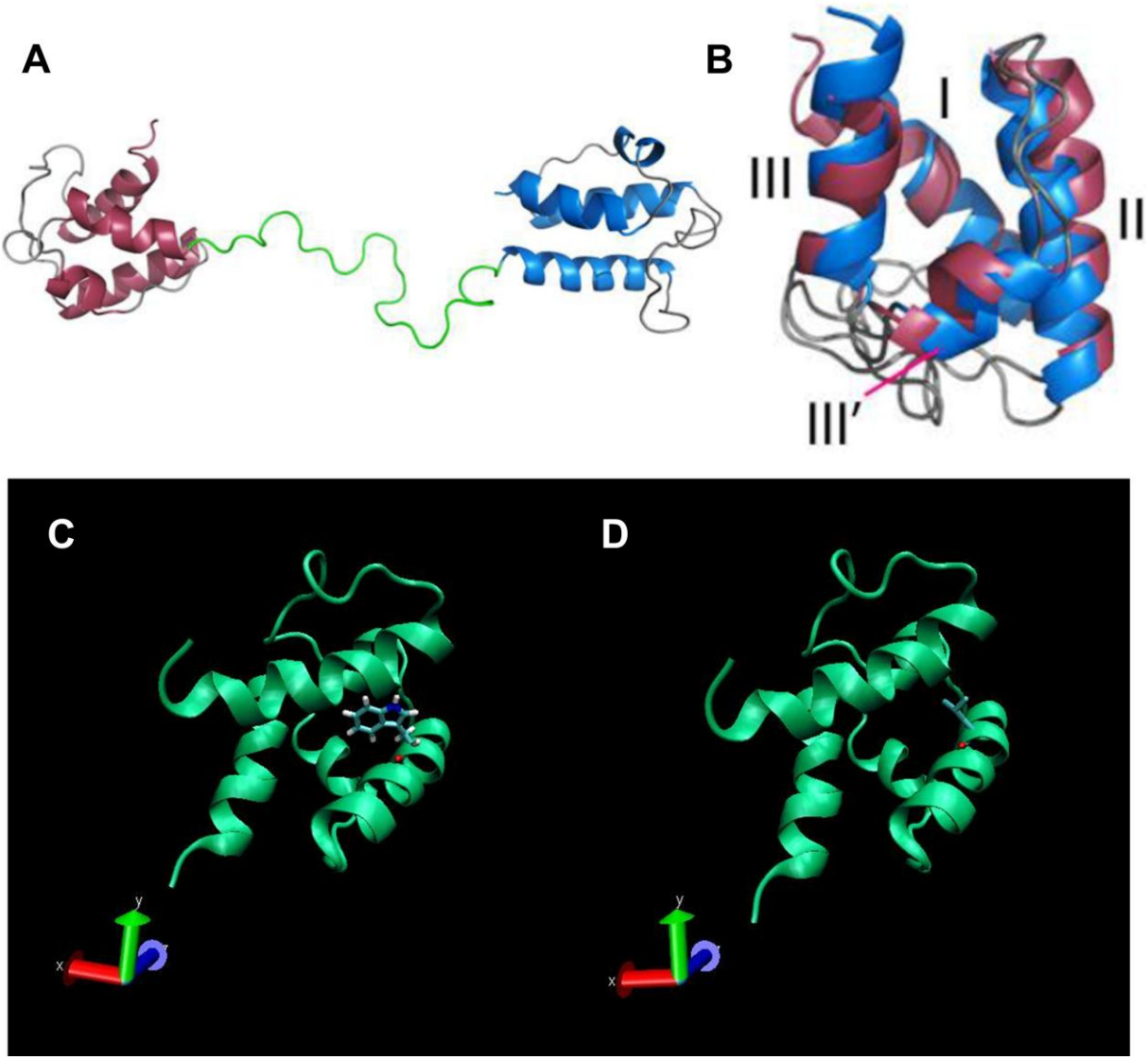

Figure 8.1. Structures of ACP3 and ACP4. (A) Solution NMR structures of ACP3/4 didomain. Maroon, ACP3; blue, ACP4; green, domain-domain linker. **(B)** The superimposed structures of ACP3 (maroon) and ACP4 (blue). Helices are numbered. ACP3 wildtype **(C)** and mutant **(D)** structures visualised on visual molecular dynamics (VMD) from NMR coordinates. Wildtype ACP3 with Trp^{55} shown in blue and mutant ACP3 where Trp^{55} has been replaced with Leu (shown in blue). (Y. Takebayashi, 2011; Dong *et al*., 2012).

8.2 Results

8.2.1 Construction of ACP3 W55L point mutant (Erika Yamanda)

Using pAH800 as the template, mutant ACP3 was amplified using primer pairs ACP3FP/ACP3RP and BIO-X-ACT long DNA polymerase. The reaction involved denaturation for 2min at 94°C, followed by 10 cycles of denaturation for 15s at 94°C, annealing for 30s at 60°C, and elongation for 1min at 70°C, followed by 20 cycles of the same with 5s increment at the elongation stage in each cycle, and a final elongation of 7min at 70°C. After purification of DNA from the corresponding bands on an agarose gel and cloning into pGEM-T-Easy, the product was sequenced to check for PCR errors. Sequencing revealed the insertion of eight residues prior to the N-terminus of the mutant protein (Figure 8.2).

```
WT >EF--------MPLAAKAAPVVPVADDECAQFLRQSLAAMLYCEPGQIRDGSRFLELGLDSV
Mut>EFDCELTIEFMPLAAKAAPVVPVADDECAQFLRQSLAAMLYCEPGQIRDGSRFLELGLDSV
    **        **************************************************

WT >IAAQWIREINKHYQLKIPADGIYTYPVFKAFTQWVGTQLQ
Mut>IAAQLIREINKHYQLKIPADGIYTYPVFKAFTQWVGTQLQ
    **** **********************************
```

Figure 8.2. Sequencing comparison of ACP WT and mutant clones. WT, wildtype ACP3; mut, mutant ACP3; residues shown in grey remain from pGEM-T-Easy; residues underlined show the additional residues in the mutant; residues in red highlight the W>L mutation.

Digestion with *Eco*RI and subsequent re-ligation successfully removed these extra residues. After re-sequencing to confirm the sequence was now correct with a W55L mutation the DNA fragment was cloned into pET28a to create plasmid pEY802 for expression of mutant ACP3.

8.2.2 ACP3 mutant protein expression and purification

Due to the insolubility and purification issues of ACP4 (Figure 3.14) studies continued using ACP3 only. Plasmids pEY802 and pJS563 were introduced into *E. coli* BL21 for expression. Where *holo* protein was required for assays the plasmids were co-expressed with pJHN11. The WT ACP3 was solubilised and purified as described previously (Table 3.1). The mutant protein required the same induction conditions as the WT (0.4mM IPTG, 30ºC for 4h) but only half the protein was soluble (Figure 8.3). Purification of the mutant took place using the same methods as for the WT; however the protein only eluted at 250mM imidazole, whereas the WT protein began eluting at 200mM, indicating the WT has more affinity for Ni-NTA than the mutant.

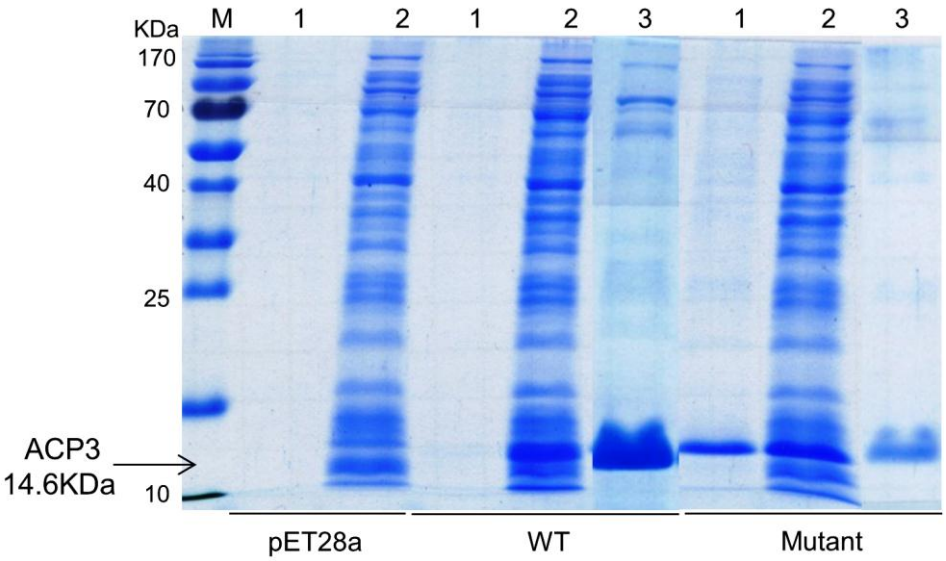

Figure 8.3. Expression of WT and mutant ACP3. pET28a, negative control; WT, wildtype; M, molecular weight marker; 1, insoluble fraction; 2, soluble fraction; 3, pure fraction.

8.2.3 Circular dichroism of ACP3 WT and mutant proteins

Circular dichroism (CD) was employed to determine structural differences brought on by the W55L mutation. The spectra demonstrate the difference in structure between the inactive *apo* and active *holo* forms of the WT ACP3 protein (Figure 8.4, A). WT ACP3 displays an α-helical spectrum with negative peaks at 208 and 222nm and a positive peak at 190nm - in this case the peak at 208nm is stronger than that at 222nm. The *apo* and *holo* forms of the mutant both vary in spectra from the WT - as for the WT, the mutant displays a more negative peak at 208nm than 222nm, but it is the *holo* form of the mutant where this characteristic is particularly noticeable. This would indicate the mutant has a higher helical content than the mutant, more coil-coil interactions of the helices, or is dimerising more than the WT.

8.2.4 Malonylation assay of ACP3 WT and mutant proteins

Autoradiography was used to determine the amount of malonate acquired by the WT and mutant ACP3 proteins. As determined in Chapter 4, the concentration of AT was 0.05μM, and ACP and [^{14}C]-malonyl-CoA were 20μM. Autoradiography demonstrated that whilst both *holo* ACP3 proteins appear to self-malonate to a certain degree, the addition of AT2 in the assay increases the malonylation of the WT by 207% and the mutant by 67% (Figure 8.4, B and C). If the WT malonylation is considered as 100%, then in comparison the mutant is only 2.8% malonylated.

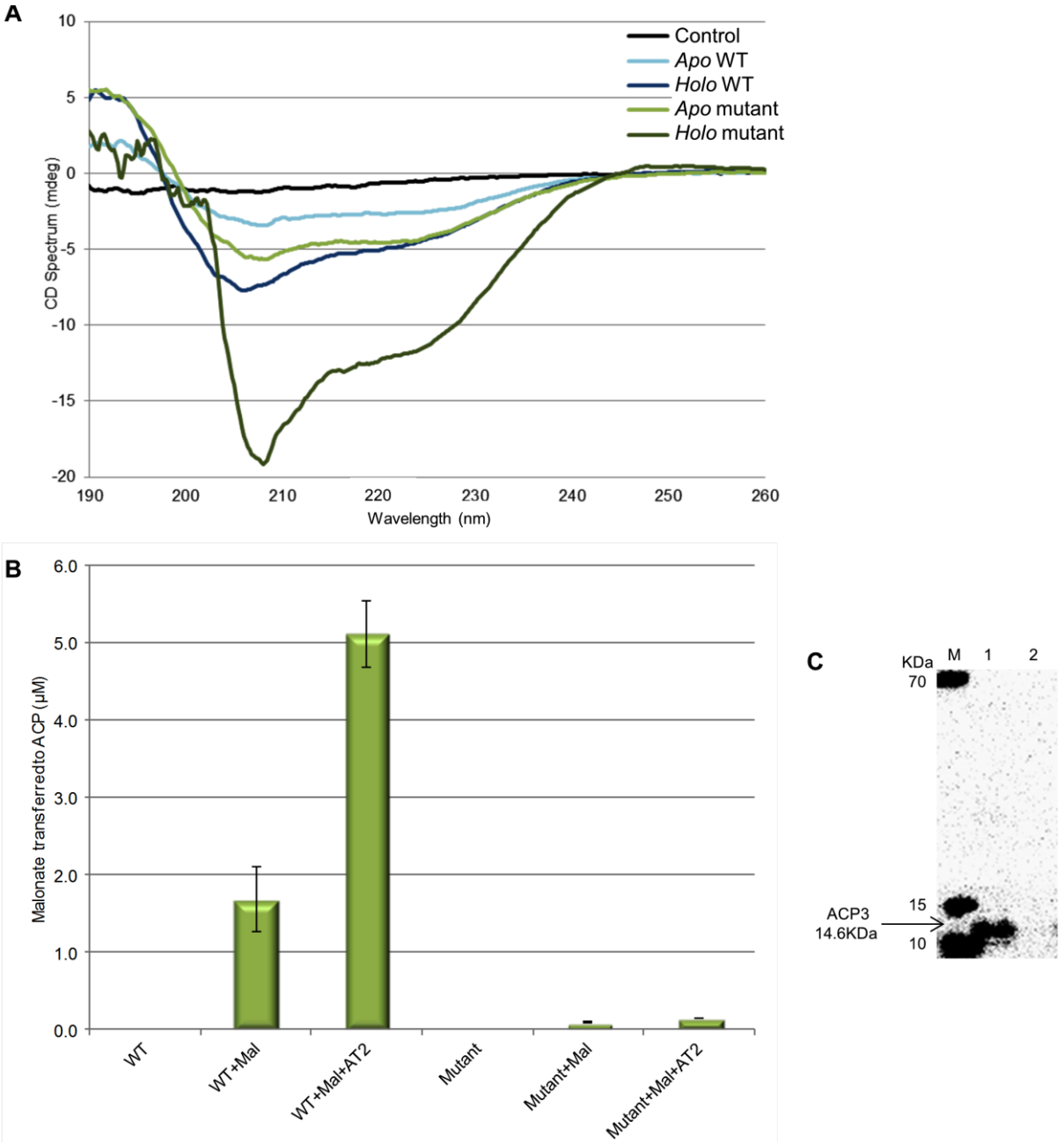

Figure 8.4. Determining the phenotype of mutant ACP3. (A) Circular dichroism spectra of WT and mutant ACP3 proteins. Mutant ACP3 was assayed against a negative assay buffer control and against the WT as a positive control. **(B)** Chart showing the acquisition of malonate by the *holo* WT and mutant ACP3 proteins. **(C)** Autoradiography of [^{14}C]-malonate-*holo*-ACP3. M, molecular weight marker; 1, *holo* WT ACP3; 2, *holo* mutant ACP3.

8.3 Discussion

β-branching ACPs are present in a wide variety of PKS clusters, both with *cis*- and *trans*-acting ATs. Recently several residues were identified that were thought to be significant in distinguishing branching ACPs from non-branching ACPs (Dong *et al*., 2012). In terms of ACP3 these residues were Leu^{21}, Leu^{25} and Leu^{29}. Phe^{42} and Trp^{55} and were found to cluster within the core of the ACP. Computer modelling was used to visualise the interactions between the mupirocin ACP3/4 and MupH HMG-CoA synthase of the HCS cassette. This technique demonstrated that Tyr^{73}, Asp^{70} and Thr^{74} of helix III were at the interface between ACP3 and MupH; however these residues are not unique to branching ACPs. This led to the conclusion that recognition between ACP and MupH was most likely due to the position of helix III rather than the amino acid composition (Dong *et al*., 2012). However it was still clear that there were several residues that were exclusive to branching ACPs – corresponding to ACP3 residues Leu^{25} Leu^{29}, Phe^{42}, Asp^{48}, and Trp^{55}. The Trp^{55} residue stood out as in this position whereas on non-branching ACPs the residue was much smaller – either Leu, Phe, Val, Ile, or Met. Therefore it was decided to mutate this residue to Leu to see what the effect would be on the production of mupirocin. As demonstrated in Figure 8.1 (C+D) Leu is a much smaller amino acid than Trp and so significantly changes the packing of side chains between helices I and II. Introducing these mutations into the chromosomal genes also demonstrated that the W>L mutation in both ACP3 and 4 reduced the amount of mupirocin produced (Dong *et al*., 2012).

During this study the structure of the mutant protein and the ability to acquire malonate were assessed. The studies utilising CD to assess the changes in protein

secondary structure demonstrated significant structural changes in the mutant protein compared to the WT protein – it appeared the mutant was more helical and had more helical coil-coil interactions than the WT. This fits in with the model of the WT and mutant in Figure 8.1 – the mutant protein has a cleft due to the absence of the bulky Trp residue, allowing interactions between helices I and II to occur. The ability of the mutant protein to acquire malonate was tested and it was clear the ability was severely impaired, with the mutant protein acquiring a mere 2.8% of the amount of malonate as the WT protein did. The protein was also more difficult to work with *in vitro* in terms of solubility and purification, contributing to the conclusion that significant changes in structure had occurred.

Dong *et al*. also experimented with domain swapping – replacing the mupirocin branching ACPs for both branching and non-branching ACPs from the very similar thiomarinol PKS cluster (2012). As detailed in Section 1.4.1, the thiomarinol PKS cluster is very similar to the mupirocin PKS system. The first experiment involved replacing the mupirocin ACP3/4 branching ACPs with the thiomarinol ACPs-A3abc triplet, and showed they were successful in complementing the mupirocin ACP3/4. Interestingly the extra ACP appeared to have little effect on PA-A production when analysed by LCMS. The second experiment involved swapping ACP3/4 for thiomarinol ACPs-D3ab, which are non-branching. The data indicated that, although colony morphology was altered (see Chapter 6, page 223 for probable cause), no mupirocin was produced, conclusively agreeing that the HCS cassette cannot work with non-branching ACPs, but can work with branching ACPs from different clusters (Dong *et al*., 2012).

The experimental data produced during this study combined with the results from recent research clearly display differences between β-branching and non-branching ACPs (Dong *et al*., 2012). It would be interesting therefore to investigate the protein-protein interactions between the WT and mutant ACP3 proteins and MupH.

CHAPTER 9

9 GENERAL DISCUSSION AND FUTURE WORK

Antibiotic resistance is worryingly becoming an increasingly common phenomenon. Brought on by decades of antibiotic misuse, be it by over prescribing, misprescribing, not finishing courses of antibiotics and misuse in the agricultural world, antibiotic resistance is a very real disaster waiting to happen. The World Health Organisation is at the forefront of the war against antibiotic/antimicrobial resistance and has several initiatives in place in order to: track antibiotic use and resistance, encourage better use of antibiotics, reduce the use of antibiotics in agriculture, prevent infection in the community and health care organisations, encourage innovation and research into combating antimicrobial resistance (Grayson *et al*., 2012). Recently a group of scientists from academia and industry came together to discuss issues relating to antibiotic resistance and to brainstorm how the issues could be addressed (Bush *et al*., 2011). Research required into controlling and tackling resistance included intercepting the development of resistance and preventing it altogether, educating the public, developing new antibiotics, reinvestigating the potential of previously discarded antibiotics, developing alternatives to antibiotics and perhaps most importantly, collaboration between members of academia, industry, and government agencies (Bush *et al*., 2011).

It has already been discussed in Chapter 1 that mupirocin is an effective agent in the treatment of MRSA and that resistance to mupirocin is developing throughout the world, however continued research on this antibiotic is providing more answers about the pathway, and is generating novel antimicrobial compounds (Fukuda *et al*., 2011; Hothersall *et al*., 2011; Murphy *et al*., 2011). Therefore, it is vitally important

this research continues. The conclusions of this current study have contributed to the field of antibiotics, and more specifically to the field of PKS produced antibiotics, and *trans*-AT PKS produced antibiotics.

The mupirocin biosynthetic cluster is homologous to that of the modular type I PKSs and type II – comprising of multifunctional polypeptides and discrete proteins. Although much information has already been deduced about the biosynthesis of mupirocin, there are many aspects of the pathway still to be fully investigated and putative gene functions to be confirmed. The two discretely encoded ATs of the cluster play a crucial role in the biosynthesis of mupirocin – transferring substrates to commence biosynthesis and for continual extension of the polyketide. It has previously been shown that deletion of AT2 results in a complete loss of mupirocin production and deletion of AT1 results in reduced production, demonstrating the importance of these proteins within the cluster (El-Sayed *et al*., 2003; Shields, 2008). The work described here is part of an on-going investigation into the specific functions of the ATs. Biochemical characterisation of the ATs and domains they are predicted to interact with will result in a better understanding of the processes they undertake and will contribute to the overall knowledge of the cluster, and to that of similar clusters.

9.1 Mupirocin proteins can be difficult to work with

Solving the solubility and purification issues of AT1 will be significant in defining the roles of the individual ATs. A recent study has shown that a protein similar to MmpC is responsible for the loading of malonyl-CoA to an ACP within the kirromycin cluster (Musiol *et al*., 2011). However, this study was completed using the whole of KirCI, which is an AT-AT-ER tridomain, rather than a breakdown of the individual domains. Therefore it is impossible to say which AT domain performed the transfer to the ACP. Based on the results in this study it is highly likely to be the second AT of KirCI that performed the transfer, which makes it all the more intriguing as to what function the first ones have.

Work focussing on solving the solubility and purification issues of AT1 is definitely high priority in terms of concluding the AT work undertaken in this study. While several suggestions for future work were suggested in Chapter 3, including following on the work using the GST-tag, another option could be to utilise the facilities at the Oxford Protein Production Facility (OPPF). The OPPF has the facilities and resources to screen for solubility of the gene/protein of interest in a variety of plasmids and host cells (2011). Creating a double His-tagged protein by combing pET28a and pET28b to AT1 could provide the platform required for purification by nickel-affinity chromatography. Alternatively purification by other means, such as ion exchange or liquid chromatography may prove to be more successful. AT1 is not the only protein from the mupirocin system to be somewhat difficult to work with, several of the ACPs were difficult to solubilise and subsequently purify, and insoluble mupirocin proteins have been causing difficulties for many members of the Thomas group (Personal communications).

Expression of mupirocin proteins from a *Pseudomonas* host as opposed to an *E. coli* host could prove to be more successful. While *E. coli* is the standard host for use in protein expression, differences in codon usage and promoter structure can cause difficulties expressing proteins from Pseudomonads (Watson *et al*., 1996). There are however, several expression vectors that have been developed for use in *Pseudomonas* spp. and there is an increasing amount of research in this area. The vectors pUCPKS and pUCPSK have been demonstrated to produce recombinant proteins in *P. aeruginosa* (Watson *et al*., 1996). A c-type cytochrome subunit (PchC) from *Pseudomonas putida* could not be produced as recombinant protein when using the pET expression system in *E. coli*, but when expressed from the pUCP-Nde vector in *P. aeruginosa* recombinant protein was produced (Cronin and McIntire, 2000). More recently the stable shuttle vector pGNS-BAC and the broad host range shuttle vector pEBP have been shown to be effective for production of recombinant proteins in *Pseudomonas* spp. (Kakirde *et al*., 2010; Troeschel *et al*., 2012). A method has even been developed for transporting DNA into *Pseudomonas* strains that involves nanofibres absorbing DNA and releasing it into the bacterial cytoplasm upon cellular entry via cell wall penetration (Rodrígues-Beltrán *et al*., 2012).

9.2 AT2 exclusively prefers malonyl-CoA as a substrate and transfers it to mupirocin type I and type II ACPs

It was originally hypothesised that because AT2 was essential for mupirocin biosynthesis it loaded the acetyl-CoA starter unit to ACP1. However, substrate assays in this study have shown that AT2 exclusively prefers malonyl-CoA as a substrate over acetyl-CoA and doesn't transfer to ACP1, indicating it does not load

the starter unit or interact with this ACP. This therefore, has set forth the questions of how biosynthesis of mupirocin is initiated and how the starter acetate unit comes to be at the KS of module 1? Currently insoluble, AT1 could be responsible for loading the starter units. If AT1 did load the starter units, it could be that in the absence of AT1, AT2 could take over – albeit inefficiently. However, evidence in this study indicates an alternative role for AT1, so there could be another mode of initiation such as a decarboxylative mAcp or uncharacterised protein within the cluster.

While the biochemical characterisation of AT2 was successful in determining substrate specificity and transfer of substrate to ACPs within the cluster, it was not possible to determine kinetic parameters due to the speed that the reaction took place. Determining the kinetic parameters for the affinity of AT2:malonyl-CoA and AT2:ACP would allow comparisons to be made between AT2 and other ATs. The reaction between AT and substrates is termed as a ping-pong bi-bi mechanism (Joshi and Wakil, 1971). By generating double reciprocal plots, varying the substrate concentrations, it can be determined if a tertiary complex is formed during the reaction, i.e. if both substrates are complexed with AT2 at the same time. If the lines of the plot intersect it indicates a tertiary product is formed, but if the lines are parallel it indicates a ping-pong bi-bi mechanism, as in the case of MCAT (Joshi and Wakil, 1971; Szafranska *et al*., 2002; Nelson and Cox, 2005). Important kinetic parameters to determine are V_{max} and K_m. V_{max} describes the limit of the initial rate with regards to enzyme saturation, and K_m (determined from ½ V_{max}) is the Michaelis constant – it describes the affinity of an enzyme for its substrate. If the K_m is large this generally means it has a low affinity for its substrate (a high substrate concentration is required to reach V_{max}), whereas if the K_m is smaller it indicates a higher affinity for substrate

(V_{max} is reached at low substrate concentration) (Reed *et al*., 2003). Determining the K_m value not only provides substrate affinity information, but can also give an indication of the substrate concentration required to give maximum reaction velocity (Reed *et al*., 2003). K_{cat} is the specificity constant which relates to the number of enzymatic reactions catalysed per second (Moran *et al*., 1994). The ratio with K_{cat}/K_m can give an indication of substrate specificity and is a measure of the efficiency of the reaction of converting substrate into product (Moran *et al*., 1994). There are other assays that could be used to determine these parameters rather than the Ellman's assay. When studying *Streptomyces coelicolor* MCAT one group utilised radiolabelling to measure kinetic parameters by varying times and concentrations of the components involved (Szafranska *et al*., 2002). The same group utilised the reductive functions of α-ketoglutarate dehydrogenase (KDH) to measure the CoA being released (KDH utilises the free CoA in the production of succinyl-CoA and thus the concomitant reduction of NAD^+ to NADH is measured) by the transfer of substrate to *S. coelicolor* MCAT during the study of the actinorhodin minimal PKS (Beltran-Alvarez *et al*., 2007). Either of these methods could prove fruitful in producing kinetic parameters for AT2 malonate acquisition and transfer, but as the reaction proceeds very fast between AT2 and malonyl-CoA the use of a continuous assay would be beneficial. If a reaction proceeds too fast for mixing by hand stopped- or quenched-flow methods provide a platform for rapid mixing of reaction components, and microfluidics provide an alternative method that can measure millisecond kinetics utilising nanoliter amounts of solutions (Han *et al*., 2009).

The structure of several FAS MCATs and two ATs from the DEBS cluster have been solved and have aided our understanding of ATs as a whole. However, to date

only one *trans*-acting AT has been crystallised (Wong *et al*., 2011). Therefore, it would contribute greatly to both the mupirocin and the *trans*-AT PKS knowledge base to solve the structures of the mupirocin ATs, particularly AT1 as it is predicated to have an altered structure and alternative role.

9.3 AT1 demonstrates potential hydrolase activity

Previous research hinted that AT1 may have a different role to play in mupirocin biosynthesis compared to AT2 (Lopanik *et al*., 2008). This difference has been noticed in other systems and has now been confirmed during this study. Phylogenetic analysis has demonstrated the AT1-like proteins cluster separately from the AT2-like proteins, and a comparison of secondary structure predictions has shown that AT1 displays a slightly altered structure compared to AT2, *E. coli* FabD and DisD, leading to the conclusion that AT1 had an alternative role to play. This was confirmed by creating active site mutants of AT2 in order to assess the effect on malonate acquisition and transfer. This work also highlighted the importance active site residues play in the structure of the AT protein and in the recognition of ACPs by the AT. Two specific point mutations (R115Q and Q242V) highlighted the fact that AT1 is unlikely to accept dicarboxylic acids as substrates and would be unable to interact with mupirocin ACPs. Further mutations involving *in vivo* work in Chapter 6 also led to the conclusion that AT1 is likely to function as a hydrolase releasing stalled intermediates from the mupirocin pathway. This was demonstrated again when work based on the β-branching ACP3 and 4 highlighted the fact that AT1 appeared to be releasing a toxic substance from the pathway causing alteration of colony morphology - when AT1 was inactivated normal morphology was resumed (A.

Haines, 2012). Removing stalled intermediates from the mupirocin biosynthesis pathway will ultimately improve pathway throughput to produce the full polyketide antibiotic mupirocin.

There are many ways this research could be taken forward to substantiate the claims that AT1 is a hydrolase. One example of such work demonstrated recently involved studying the hydrolysis of short chain intermediates derived from N-acetylcysteamine (SNAC) by PedC (Jensen *et al*., 2012). Performing similar experiments with AT1 would enable us to determine if this is a role that can be assigned to this protein, and other AT1-like proteins, or if it is exclusive to PedC. The phylogenetic clustering and sequence similarity between PedC and AT1 certainly suggests a comparable role for these two proteins. Another method of analysis for the role of AT1 would be to investigate protein-protein interactions between AT1 and ACPs from the mupirocin cluster. Presumably for AT1 to release stalled intermediates it would be required to interact with mupirocin ACPs. Intermediate-bound ACPs could be utilised as substrates (potentially radiolabelled) for future experiments to demonstrate AT1-ACP interactions and to investigate the function of AT1. Using AT2 as a control (which based on the transfer assays presumably interacts with all type I ACPs, except ACP1, and several type II ACPs the interaction for AT1 for ACP1 and several other ACPs throughout the cluster could be measured. This would at least indicate where in the pathway AT1 would be likely to function.

AT1 is not the only AT to have consecutive Ser residues at the active site – the MCAT involved in lovastatin biosynthesis in *Aspergillus terreus* also has consecutive Ser residues, but instead of reading GSS like AT1, reads GHSS (Ma and Tang, 2007). During that study it was discovered that Ser1 was important for loading

ability and Ser2 may have a structural role. The same could be said for AT1 as it certainly indicates the mutation of Ser^{95} affects the functionality of the protein. The amount of PA-A and mupiric acid being produced dropped compared to the WT, but not as much as the amount of mupirocin H, which was reduced almost to zero, indicating this mutation is affecting mupirocin function around the HCS cassette.

9.4 Docking domains are essential for mupirocin biosynthesis

Very little experimental evidence is available for the analysis of docking domains (DDs) and so it was important to assess the importance of these domains for mupirocin biosynthesis, irrelevant of their proposed role. Sequence analysis of over 280 DDs allowed specific conserved boundaries to be highlighted that can be used in future investigations to highlight a) DDs and b) *trans*-acting AT PKS clusters. As shown in this study a simple BLAST search of a mupirocin DD revealed many uncharacterised putative PKS clusters. While the role of DDs may not have been defined during this study, plate bioassay, HLPC and LCMS all demonstrated that even deletion of part of the region caused a halt in mupirocin biosynthesis. Whether their role is in docking of *trans*-acting ATs, interaction of multifunctional protein dimers, maintenance of structural integrity or facilitating AT and ACP interaction, the system cannot produce antibiotic without them.

Protein-protein interactions would also be useful in investigating the roles of the DDs. It is obvious from this study that they play an important role in metabolite biosynthesis but it is unknown exactly how. In *cis*-AT PKSs it is thought the corresponding areas (KS-AT domain linker and post-AT linker) facilitate the transfer of substrate from AT to ACP and KS by positioning the domains in the correct

positions (Tang *et al*., 2006; 2007; Wong *et al*., 2010). There is no reason why these regions cannot have the same function in *trans*-AT PKSs. Crystallisation of one of these domains would be useful in confirming the structure predicted in Chapter 7 (Figure 7.4), and modelling this structure with AT domains and mupirocin multifunctional proteins may provide answers as to the specific roles.

9.5 The role of Trp55 is essential for malonylation of ACP3

This study was part of an on-going investigation into the differences between β-branching and non-branching ACPs (Dong *et al*., 2012). The importance of this residue for mupirocin production had already been demonstrated, although whether this was due to inactivity of the ACP or interfering with the interaction of ACP3 with MupH was unknown. This study demonstrated the importance of this residue in malonylation of ACP3, and most likely of malonylation of other β-branching ACPs. The inability of the mutant protein to accept malonate, combined with the structural changes inferred the lack of mupirocin production in the *in vivo* mutants was most likely due to the altered phenotype of this protein rather than inability to interact with MupH, although that interaction could still be a factor.

9.6 Future work on the third domain of MmpC

Determining the role of the third domain of MmpC is important for the completion of this study. This domain aligns with enoyl reductase proteins often found in *trans*-AT PKSs and polyunsaturated fatty acid producing bacteria and has been shown to be essential for mupirocin biosynthesis (Gurney *et al.*, 2012). As there are only three enoyl reductions (ERs) required for mupirocin biosynthesis and they

are for 9-hydroxynonanoic acid biosynthesis, protein-protein interaction studies could demonstrate which domains of MmpB this potential ER could interact with. Purification of this domain would also allow enzymatic assays to be performed to assay for ER activity, such as described by Ames *et al.* (2012). In this instance the activity of the *trans*-acting ER, LovC, was assayed with several potential substrates by following the oxidation of the LovC cofactor, NADPH, by fluorescent spectrometry (Ames *et al*., 2012). The *trans*-ER activity of PksE from the bacillaene biosynthesis system was analysed by mass spectrometry (to monitor the 2Da increase associated with enoyl reduction), by phosphopantetheinyl ejection assay (to measure the mass of the substrate attached to the ejected phosphopantetheine arm) and autoradiography to assess interactions of PksE with substrate-PksJ (Bumpus *et al*., 2008).

9.10 Model for MmpC function

MmpC is a multifunctional protein that operates in *trans* throughout the process of mupirocin biosynthesis. The work presented in this Thesis demonstrates a clear model for the combined function of MmpC as a trifunctional Edit, Reload, Reduce (ERR) protein (Figure 9.1). This combines the hydrolysis functionality of AT1 with the malonylation properties of AT2, and the potential ER role of the third domain. Thus this *trans*-acting tridomain protein has developed a multifunctional nature that is vitally important for mupirocin biosynthesis. Determining the structure of this complete protein would provide information as to how this protein performs three functions during mupirocin biosynthesis.

While the current aims of this project related mainly to the acyltransferases of the mupirocin cluster, there are many different pathways the work could take in the future.

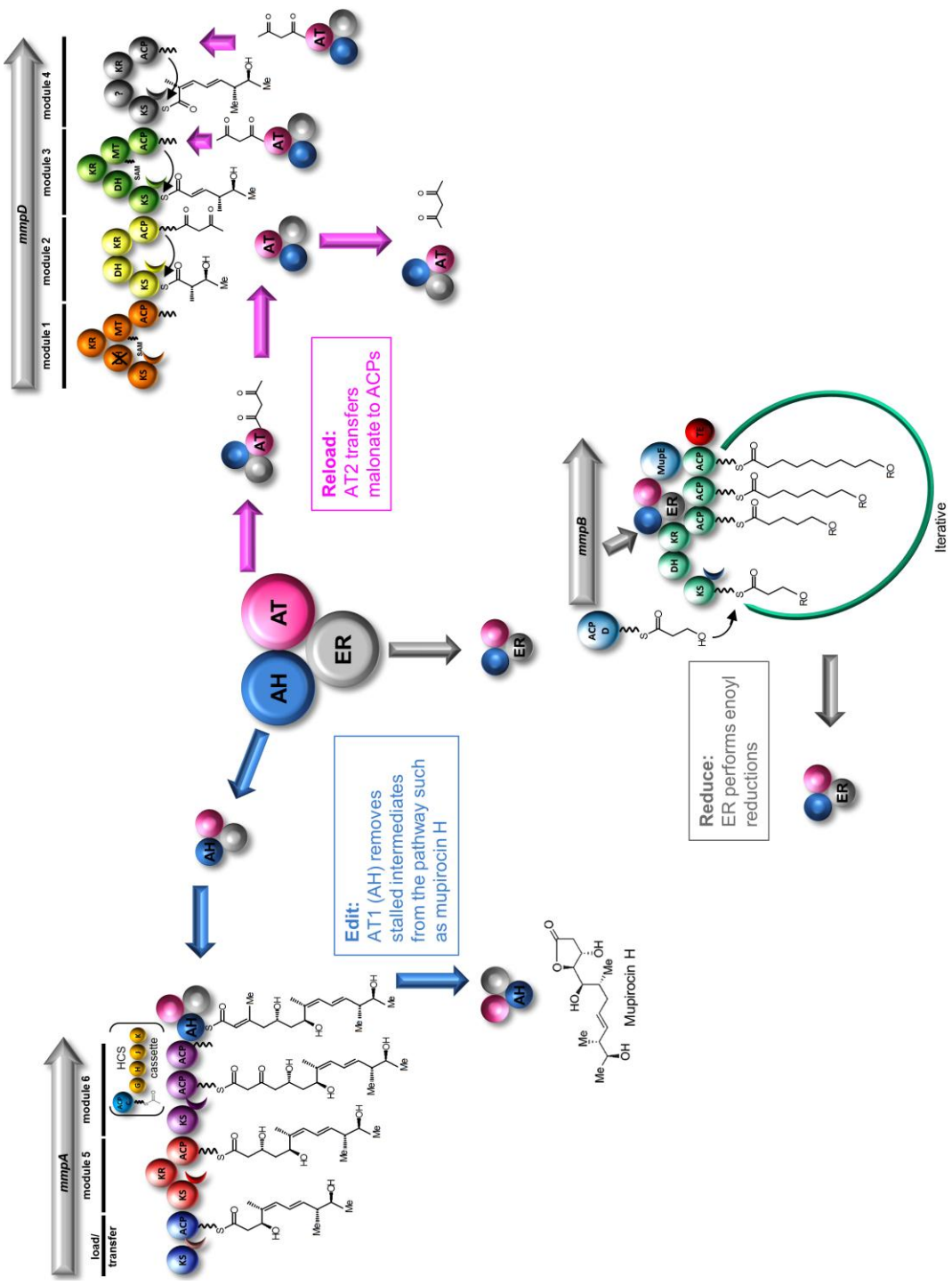

Figure 9.1. Edit, reload, reduce model for MmpC. In this model AT1 (AH) would remove stalled intermediates from the mupirocin pathway; AT2 (AT) would supply malonyl-CoA to the ACPs; ER would perform enoyl reductions during the process of 9-hydroxynonanoic acid synthesis; AH, acyl hydrolase; AT, acyltransferase; ER, enoyl reductase. (Gurney *et al.*, 2012)

APPENDIX

APPENDIX CHARACTERISTICS OF *TRANS*-AT PKS SYSTEMS

Compound	Use	Producing organism	PKS/NRPS	PKS proteins	Docking domains	HCS Cassette	MT domains	*Trans* ER/OR	Duplicate ACPs	Split modules	Reference
Albicidin	Antibiotic	*Xanthomonas albilineans*	PKS/NRPS	AlbI	2	-	+	-	+	-	Royer *et al.*, 2004
Bacillaene	Antibiotic	*Bacillus amyloliquefaciens* FZB-42; *Bacillus subtilis* 168	NRPS/PKS	BaeJ, L, M, N, R	11	+	+	+	+	+	Chen *et al.*, 2006
Bryostatin	Anti-cancer agent	*Candidatus* Endobugula sertula	PKS	BryA-D	13	+	+	+	-	-	Sudek *et al.*, 2007
Chivosazol	Antibiotic	*Sorangium cellulosum* Soce56	PKS/NRPS	ChiB-F	15	+	+	+	+	+	Perlova *et al.*, 2006
Corallopyronin A	Antibiotic	*Corallococcus coralloides* B035	PKS	CorI-L	13	+	+	+	+[a]	+	Erol *et al.*, 2010
Difficidin	Antibiotic	*Bacillus amyloliquefaciens* FZB-42	PKS	DfnF-L	12	+	+	+	+	+	Chen *et al.*, 2006
Disorazol	Cytotoxic	*Sorangium cellulosum* Soce56	PKS/NRPS	DisA-C	10	+	+	+	+[a]	+	Kopp *et al.*, 2005
Elansolid	Antibiotic Cytotoxix	*Chitinophaga pinensis* DSM2588	PKS	ElaJ-K, ElaO-R	13	+	+	+	+	+	Dehn *et al.*, 2011
Etnangien	Antibiotic	*Sorangium cellulosum* Soce750; Soce1045	PKS	EtnF-I	19	+	+	-	+	+	Menche *et al.*, 2008
FK228 (depsipep-tide)	Anti-cancer agent	*Chromobacterium violaceum* No 968	NRPS/PKS	DepB-C	2		-	+	-	-	Cheng *et al.*, 2007
Kalimanticin/Batumin	Antibiotic	*Pseudomonas fluorescems* BCCM_ID9359	PKS/NRPS	Bat1-3	10	+	+	+	+	+	Mattheus *et al.*, 2010
Kirromycin	Antibiotic	*Streptomyces collinus* Tü365	PKS/NRPS[b]	KirAI-AVI	12	-	+	+	-	+	Weber *et al.*, 2008
Lactimidom-mycin	Anti-cancer agent	*Streptomyces amphibiosporus* ATCC53964	PKS	ORF4-6	9			+			Farnet *et al.*, 2002
Lankacidin	Antibiotic	*Streptomyces rochei* 7434AN4	NRPS/PKS	LkcA, C, F, G	5	-	+	-	+	+	Arakawa *et al.*, 2005

Leinamycin	Antitumor Antibiotic	*Streptomyces atroolivaceus* S-140	NRPS/PKS	LnmJ, I	6	+	+	+	-	+	Tang *et al.*, 2004
Macrolactin	Antibacterial, antiviral Anti-cancer	*Bacillus amyloliquefaciens* FZB-42	PKS	MlnB-G	9	+	-	+	+	+	Schneider *et al.*, 2007
Migrastatin	Anti-metas--tatic agent	*Streptomyces platensis* NRRL18993	PKS	MgsE-G	10	+	+	+	+[a]		Lim *et al.*, 2009
Mupirocin	Antibiotic	*Pseudomonas fluorescens* NCIMB10586	PKS	MmpA-F	10	+	+	+	+	-	El-Sayed *et al.*, 2003
Mycosubtil--lin	Anti-fungal	*Bacillus subtilis* ATCC6633	PKS/NRPS	MycA	1	-	-	-	-	-	Duitman *et al.*, 1999
Myxovires--cin (TA)	Antibiotic	*Myxococcus xanthus* DK1622	PKS/NRPS	Ta1, O, P, I, L	13	+	+	+	-	+	Simunovic *et al.*, 2006
Neocarzil--lin	Antitumor agent	*Streptomyces carzinostaticus* var. F-41	PKS	ORF5-6	2		-		-	-	Otsuka *et al.*, 2004
Onamide A	Antitumor agent	Symbiont of *Theonella swinhoei*	PKS/NRPS	OnmB, I	6	+	+	+	+	-	Piel *et al.* 2004
Oxalomyc--in A	Antibiotic	*Streptomyces albus* JA3453	PKS/NRPS	OzmH, J, K, N, Q	11	-	+	+	+	+	Zhao *et al.*, 2010
Pederin	Antitumor agent	*Pseudomonas* symbionts of *Paederus fuscipes*	NRPS/PKS	PedH, F	9	+	+	+	+	+	Piel 2002
Rhizoxin	Anti-mitotic	*Burkholderia rhizoxinica* B1	NRPS/PKS	RhiA-F	15	-	+	-	+	+	Partida-Martinez and Hertweck 2007
Rhizoxin S2 and analogues	Anti-mitotic Anti-fungal	*Pseudomonas fluorescens* Pf-5	NRPS/PKS	RzxB-F	16	+	+		-	+	Brendel *et al.*, 2007
Sorangicin	Antibiotic	*Sorangium cellulosum* Soce12	PKS	SorA-D, G-I	22		+	+	+	+	Irschik *et al.*, 2010
Thiomarin--ol	Antibiotic	*Pseudoalteromonas* sp. SANK 73390	PKS/NRPS	TmlA-F	10	+	+	+	+	-	Fukuda *et al.*, 2011
Virginiamy--cin M	Antibiotic	*Streptomyces virginiae*	PKS/NRPS	VirA, F-H	7	+	+		+	+	Pulsawat *et al.*, 2009
Zwittermic--in	Antibiotic	*Bacillus cereus* UW85	PKS/NRPS[b]	ZmaA	1	-	-	-	-	-	Chan and Thomas, 2010

a, duplicated ACP domains were found to be degraded; b, mixture of *cis* and *trans*-ATs; Boxes left blank are due to an incomplete characterisation of the biosynthetic cluster and so some details are unknown.

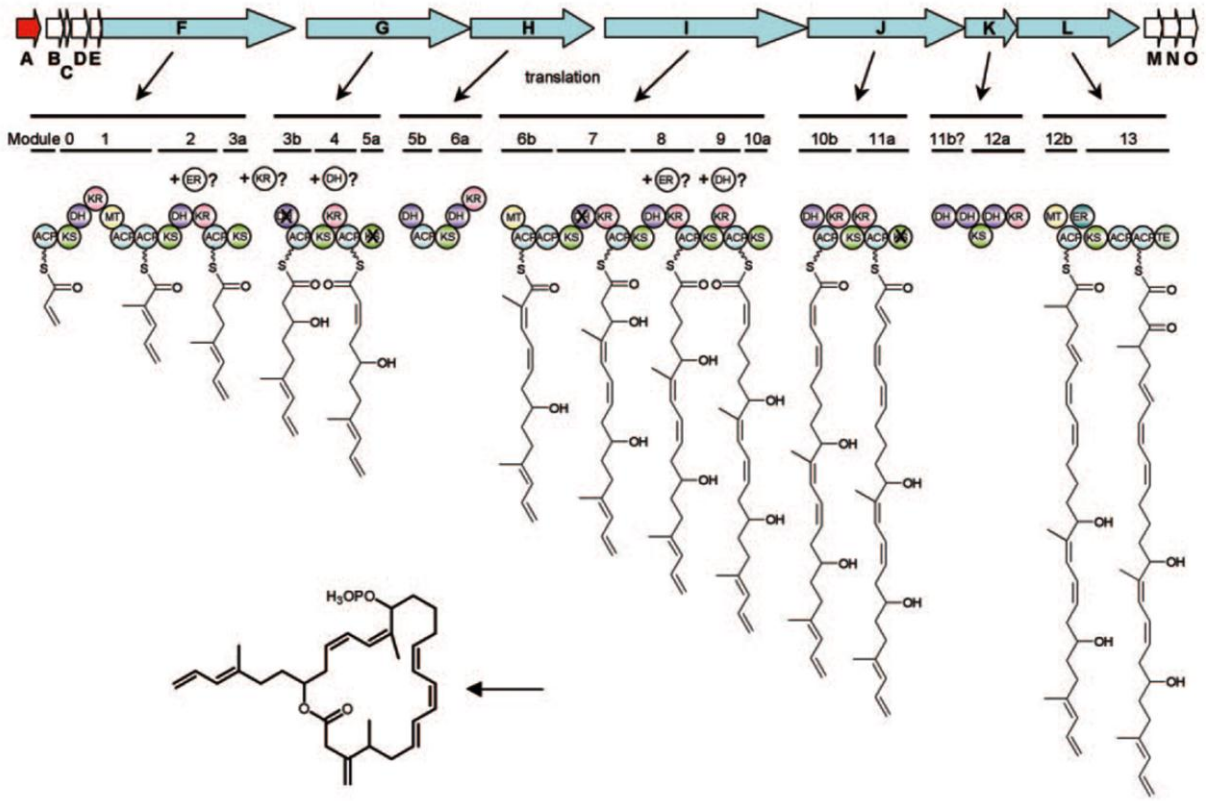

Figure A.1. Model for difficidin biosynthesis. Some activities are predicted to be provided in *trans* by unknown enzymes, which are shown above some of the modules. ACP, acyl carrier protein; KS, ketosynthase; DH, dehydratase; KR, ketoreductase; MT, methyltransferase; ER, enoyl reductase; TE, thioesterase; X, inactive domain (Che *et al*., 2006).

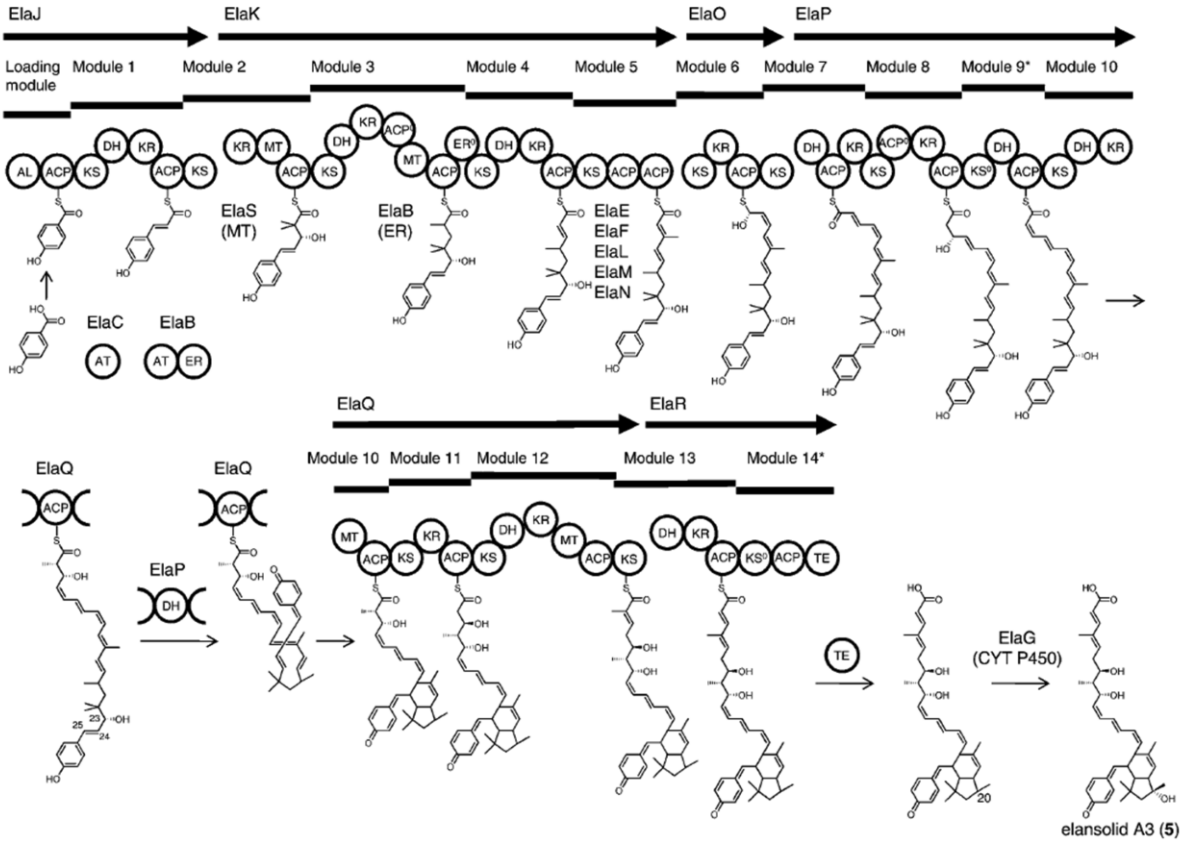

Figure A.2. Model for elansolid A3 biosynthesis. Modules 9 and 14 do not insert extender units and are marked with an asterisk. AL, AMP ligase; ACP, acyl carrier protein; KS, ketosynthase; DH, dehydratase; KR, ketoreductase; MT, methyltransferase; AT, acyltransferase; ER, enoyl reductase; TE, thioesterase; º, inactive domains (Dehn *et al*., 2011).

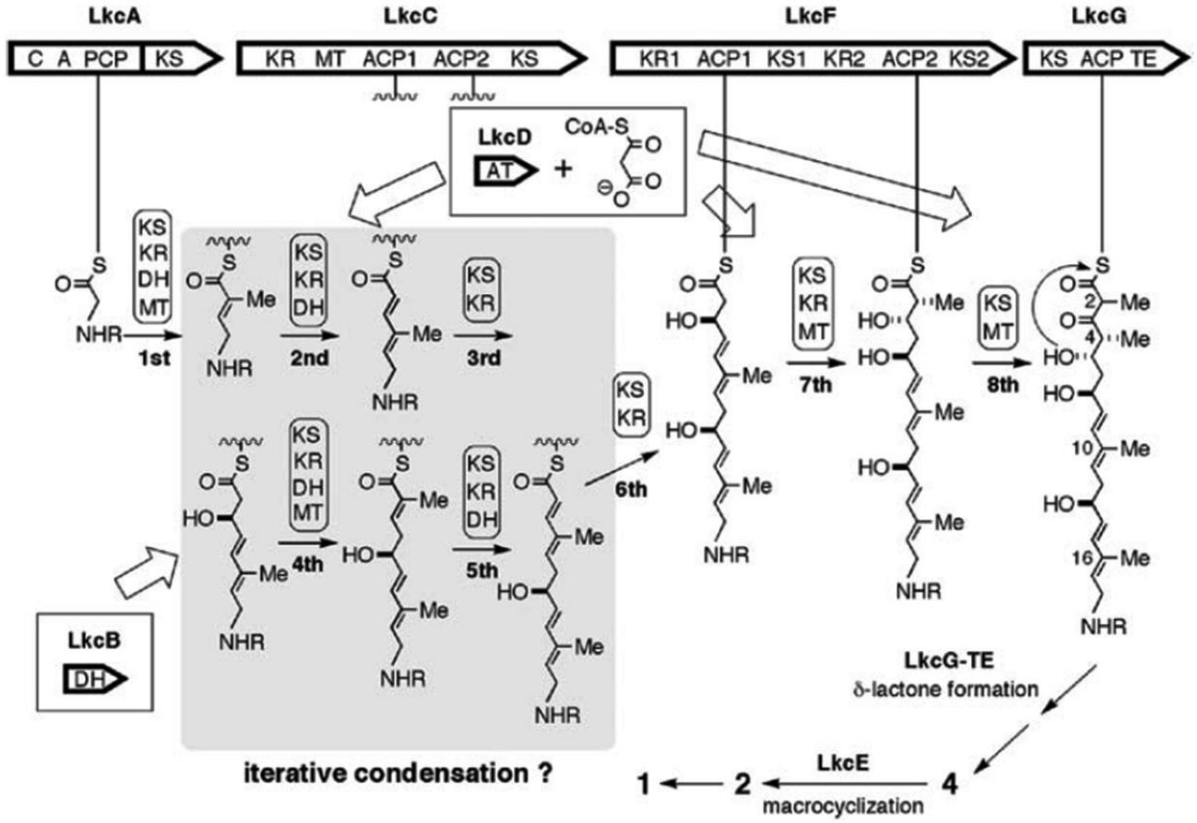

Figure A.3. Model for lankacidin biosynthesis. R, CH3-C(=O)C(=O)- or CH3-CH(OH)C(=O)-; KS, ketosynthase; ACP, acyl carrier protein; TE, thioesterase; KR, ketoreductase; AT, acyltransferase; MT, methyltransferase; DH, dehydratase; C, condensation domain; A, adenylation domain; PCP, peptidyl carrier protein (Arakawa *et al*., 2005).

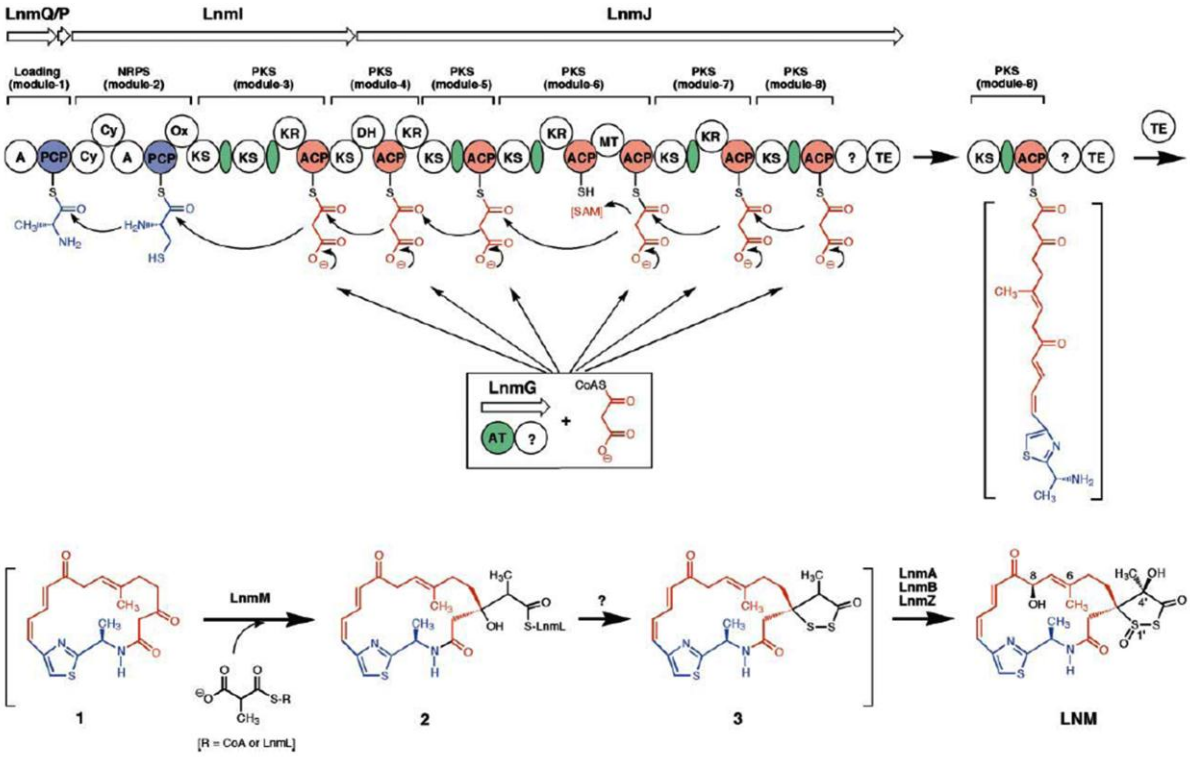

Figure A.4. Model for leinamycin biosynthesis. The structures in brackets are hypothetical. Color coding indicates the moiety of LNM that is of peptide (blue), polyketide (red), and other (black) origin. A, adenylation; PCP (blue); peptidyl carrier protein; ACP (red), acyl carrier protein; AT (green), acyltransferase; green ovals, docking domains; Cy, condensation/cyclization; DH, dehydratase; KR, ketoreductase; KS, ketosynthase; MT, methyltransferase; Ox, oxidation; TE, thioesterase.

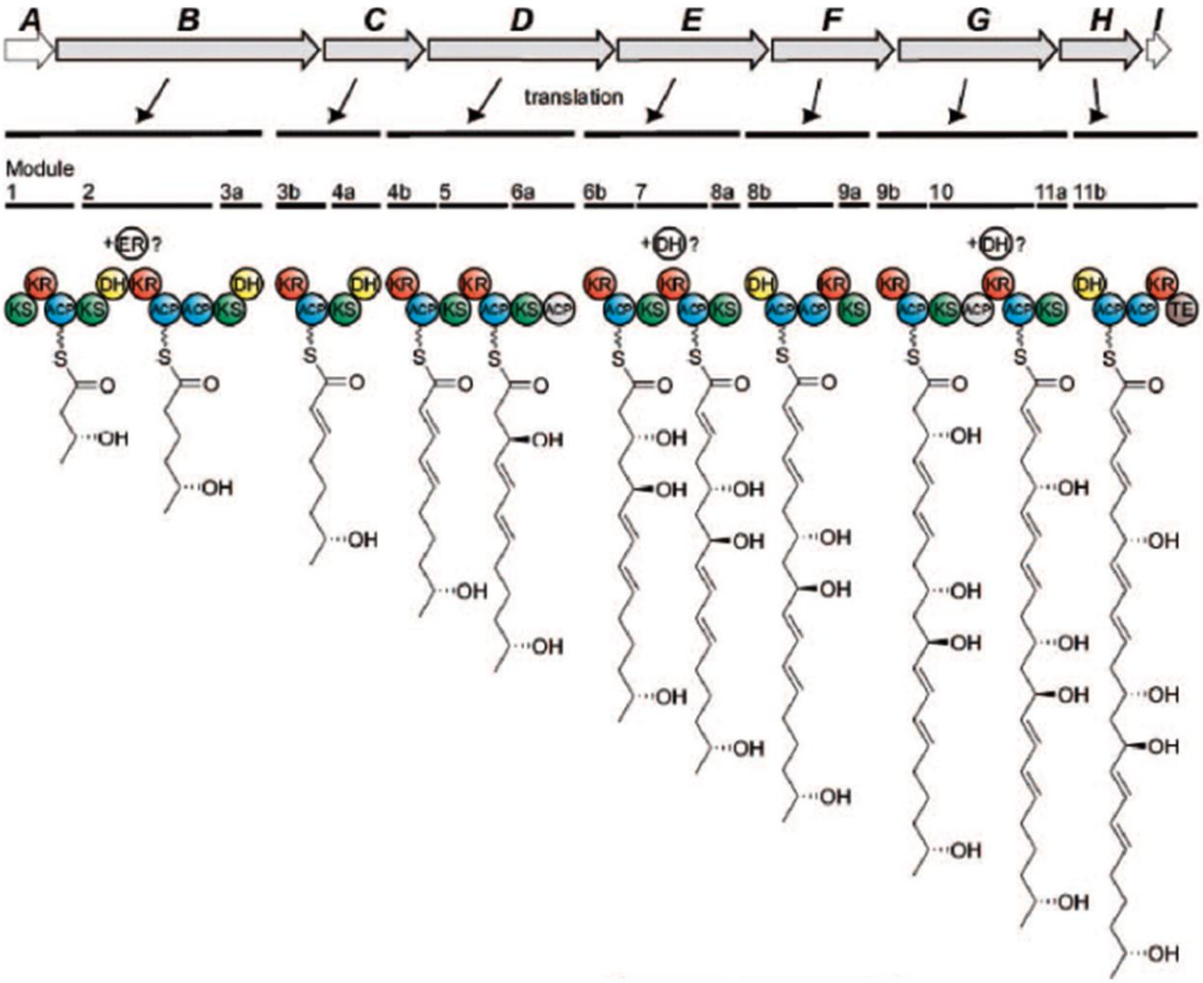

Figure A.5. Model for macrolactin biosynthesis. Functions thought to be provided in *trans* are shown above some of the modules. ACP, acyl carrier protein; KS, ketosynthase; DH, dehydratase; KR, ketoreductase; MT, methyltransferase; ER, enoyl reductase; TE, thioesterase (Schneider *et al*., 2007).

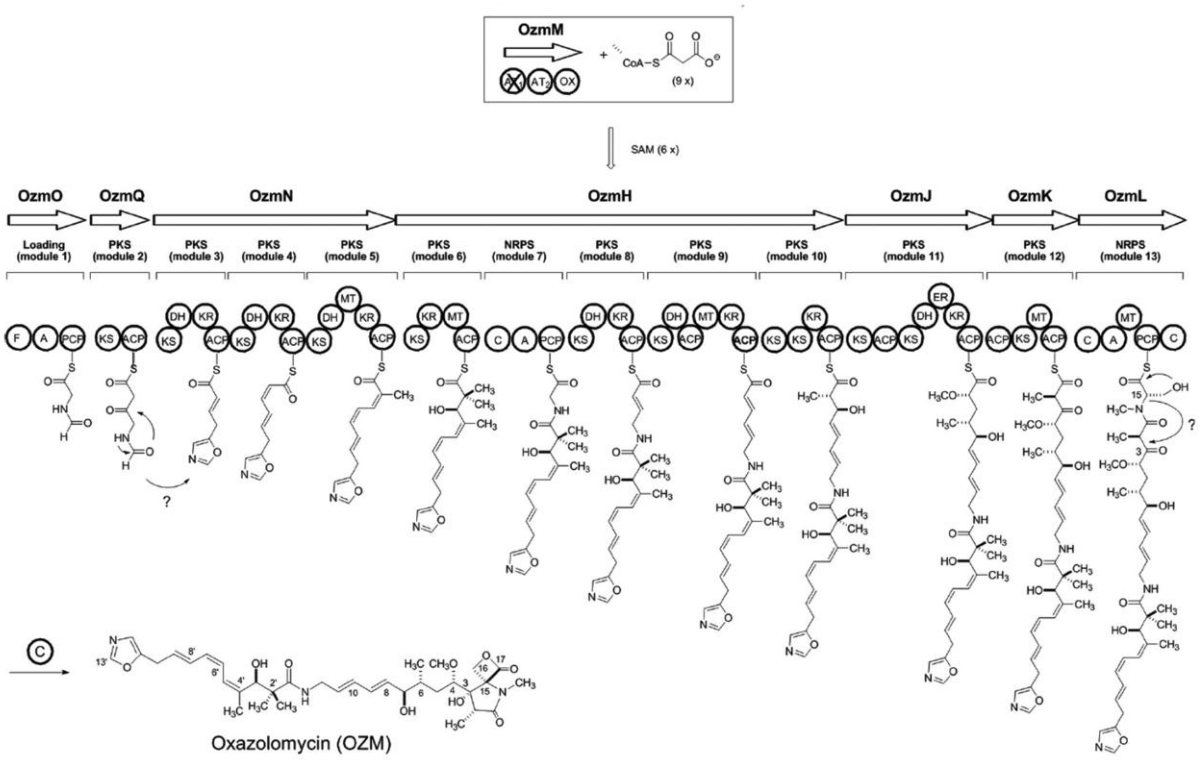

Figure A.6. Model for oxalomycin A biosynthesis. F, formylation domain; KS, ketosynthase; ACP, acyl carrier protein; TE, thioesterase; KR, ketoreductase; AT, acyltransferase; OX, oxidoreductase; ER, enoylreductase; MT, methyltransferase; DH, dehydratase; C, condensation domain; A, adenylation domain; PCP, peptidyl carrier protein, SAM, *S*-adenosylmethionine; X, domain thought to be inactive (Zhao *et al*., 2010).

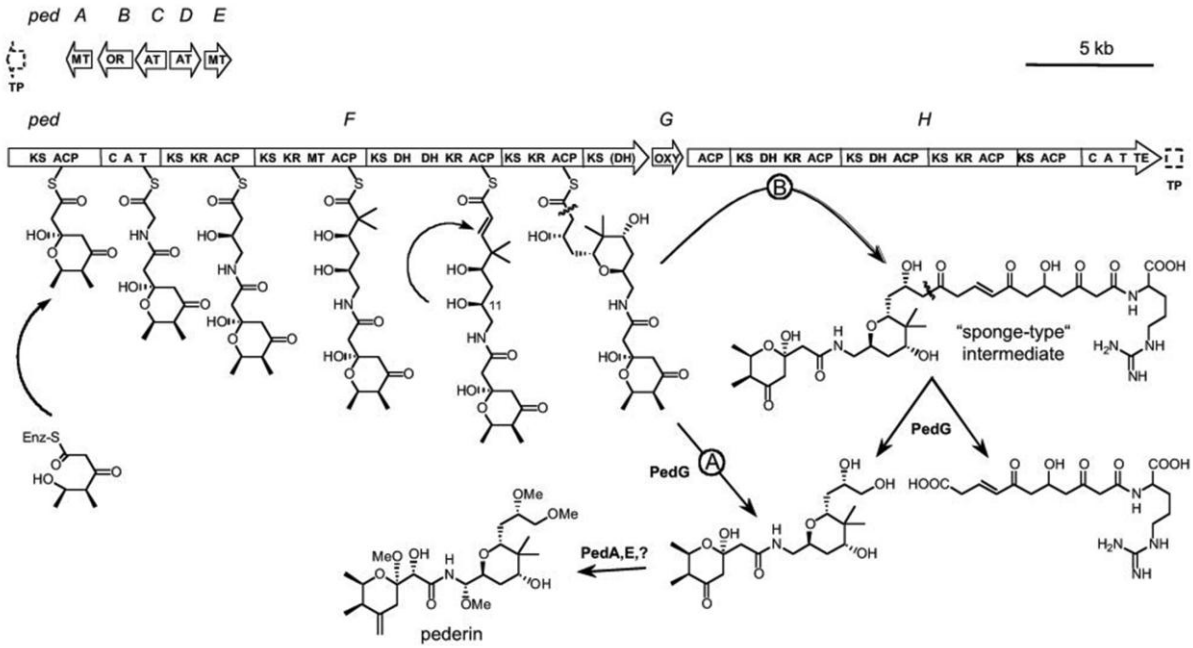

Figure A.7. Model for pederin biosynthesis. The product of PedF could be directly cleaved off the enzyme (route A) or elongated further by PedH to yield an onamide-type intermediate and subsequently cleaved (route B). TP, transposase pseudogene; MT, methyltransferase; OR, oxidoreductase; OXY, oxygenase; C, condensation domain; A, adenylation domain; T, thiolation domain; DH, putative nonfunctional dehydratase domain; ACP, acyl carrier protein; KS, ketosynthase; KR, ketoreductase; MT, methyltransferase; TE, thioesterase (Piel, 2002).

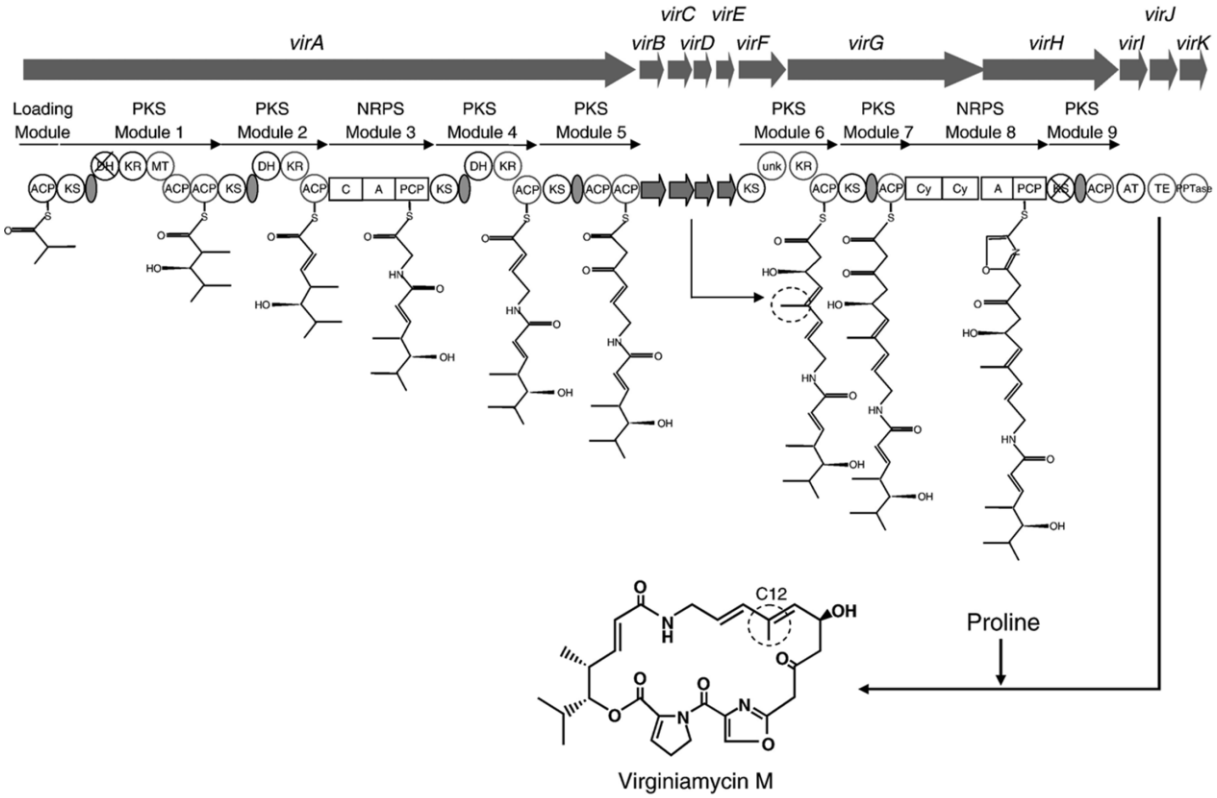

Figure A.8. Model for virginiamycin M biosynthesis. The circles and squares represent enzymatic domains in the PKS and NRPS polypeptide, respectively. The gray ovals symbolize the AT-docking sites and unk of PKS module 6 denotes a region of unknown function. The broken circle indicates the methyl group incorporated at C12 in the VM framework. ACP, acyl carrier protein; KS, ketosynthase; DH, dehydratase; KR, ketoreductase; MT, methyltransferase; ER, enoyl reductase; AT, acyltransferase; Cy, condensation domain; A, adenylation domain; PCP, peptidyl carrier protein; TE, thioesterase (Pulsawat *et al*., 2009).

REFERENCES

REFERENCES

Abe, I., Utsumi, Y., Oguro, S. and Noguchi, H. (2004) 'The first plant type III polyketide synthase that catalyzes+ formation of aromatic heptaketide.' *FEBS Letters*, 562, 171-176.

Abraham, E. P. and Chain, E. (1940) 'An Enzyme from Bacteria Able to Destroy Penicillin.' *Nature*, 146, 837.

Alcorn, T. (2012) 'Antibiotic use in livestock production in the USA.' *The Lancet*, 12, 273-274.

Alexander, R. G., Clayton, J. P., Luk, K., Rogers, N. H. and King, T. J. (1978) 'The Chemistry of Pseudomonic Acid. Part 1. The Absolute Configuration of Pseudomonic Acid A.' *Journal of the Chemical Society Perkin Transactions I*, 561-565.

Allen, N. E., J. N. Hobbs, J. and W. E. Alborn, J. (1987) 'Inhibition of Peptidoglycan Biosynthesis in Gram-Positive Bacteria by LY146032.' *Antimicrobial Agents and Chemotherapy*, 31, (7): 1093-1099.

Ames, B. D., Nguyen, C., Bruegger, J., Smith, P., Xu, W., Ma, S., Wong, E., Wong, S., Xie, X., Li, J. W. H., Vederas, J. C., Tang, Y. and Tsai, S.-C. (2012) 'Crystal structure and biochemical studies of the trans-acting polyketide enoyl reductase LovC from lovastatin biosynthesis.' *PNAS*, 109, (28): 11144-11149.

Anand, S. and Mohanty, D. (2012) 'Inter-domain movements in polyketide synthases: a molecular dynamics study.' *Molecular Biosystems*, 8, (4): 1157-1171.

Anderl, J. N., Frankin, M. J. and Stewart, P. S. (2000) 'Role of Antibiotic Penetration Limitation in *Klebsiella pneumoniae* Biofilm Resistance to Ampicillin and Ciprofloxacin.' *Antimicrobial Agents and Chemotherapy*, 44, (7): 1818-1824.

Anfinsen, C. B. (1973) 'Principles that Govern the Folding of Protein Chains ' *Science*, 181, (4096): 223-230.

Anon (2012a) 'Promoting Anti-Infective Development and Antimicrobial Stewardship through the U.S. Food and Drug Administration Prescription Drug User Fee Act (PDUFA) Reauthorization.' Infectious Diseases Society of America.

Anon (2012b) 'A history of antibiotic use in farm animals ' The Seattle Times. 20th April 2012.

Antibiotic-Action (2011) 'Antibiotic Action The Arms Race.' http://antibiotic-action.com/. Accessed: 22nd August 2012.

Antonio, M., McFerran, N. and Pallen, M. J. (2002) 'Mutations Affecting the Rossman Fold of Isoleucyl-tRNA Synthetase Are Correlated with Low-Level Mupirocin Resistance in *Staphylococcus aureus*.' *Antimicrobial Agents and Chemotherapy*, 46, (2): 438-422.

Aparicio, J. F., Molnár, I., Schwecke, T., König, A., Haydock, S. F., Khaw, L. E., Staunton, J. and Leadlay, P. F. (1996) 'Organization of the biosynthetic gene cluster for rapamycin in *Streptomyces hygroscopicus*: analysis of the enzymatic domains in the modular polyketide synthase.' *Gene*, 169, 9-16.

Arakawa, K., Sugino, F., Kodama, K., Ishii, T. and Kinashi, H. (2005) 'Cyclization Mechanism for the Synthesis of Macrocyclic Antibiotic Lankacidin in *Streptomyces rochei*.' *Chemistry and Biology*, 12, 249-256.

Arias, C. A. and Murray, B. E. (2012) 'The rise of the *Enterococcus*: beyond vancomycin resistance.' *Nature Reviews Microbiology*, 10, 266-278.

Armstrong, N., Lencastre, A. D. and Gouaux, E. (1999) 'A new protein folding screen: Application to the ligand binding domains of a glutamate and kainate receptor and to lysozyme and carbonic anhydrase.' *Protein Science*, 8, 1475–1483.

Aron, Z. D., Fortin, P. D., Calderone, C. T. and Walsh, C. T. (2007) 'FenF: Servicing the Mycosubtilin Synthetase Assembly Line in *trans*.' *Chembiochem*, 8, 613-616.

Arthur, C. J., Williams, C., Pottage, K., Płoskoń, E., Findlow, S. C., Burston, S. G., Simpson, T. J., Crump, M. P. and Crosby, J. (2009) 'Structure and Malonyl CoA-ACP Transacylase Binding of *Streptomyces coelicolor* Fatty Acid Synthase Acyl Carrier Protein.' *ACS Chemical Biology*, 4, (8): 625-636.

Athena Enzyme Systems (2008) 'QuickFold™ Protein Refolding Kit.' http://www.athenaes.com/QuickFoldProteinRefoldingKit.php. Accessed: 3rd August 2008.

Austin, M. B., Bowman, M. E., Ferrer, J.-L., Schröder, J. and Noel, J. P. (2004) 'An Aldol Switch Discovered in Stilbene Synthases Mediates Cyclization Specificity of Type III Polyketide Synthases.' *Chemistry and Biology*, 11, (9): 1179-1194.

Austin, M. B. and Noel, J. P. (2003) 'The chalcone synthase superfamily of type III polyketide synthases.' *Natural Product Report*, 20, 79-110.

Baneyx, F. (1999) 'Recombinant Protein Expression in *E. coli*.' *Current Opinion in Biotechnology*, 10, 411-421.

Bangera, M. G. and Thomashow, L. S. (1999) 'Identification and Characterization of a Gene Cluster for Synthesis of the Polyketide Antibiotic 2,4-Diacetylphloroglucinol from *Pseudomonas fluorescens* Q2-87.' *Journal of Bacteriology*, 181, (10): 3155-3163.

Basker, M. J., Comber, K. R., Clayton, P. J., Hannan, P. T., Mizen, L. W., Rogers, N. H., Slocombe, B. and Sutherland, R. (1980) 'Ethylmonate A: a semisynthetic antibiotic derived from pseudomonic acid A.' In: J. D. Nelson and C. Grassi (Ed.) 'Current Chemotherapy and Infectious Disesease.' Washington, American Society for Microbiology.

Bathoorn, E., Hetem, D. J., Alphenaar, J., Kusters, J. G. and Bonten, M. J. M. (2012) 'Emergence of High-Level Mupirocin Resistance in Coagulase-Negative *Staphylococci* Associated with Increased Short-Term Mupirocin Use.' *Journal of Clinical Microbiology*, 50, (9): 2947-2950.

B.D. Biosciences (2011) http://www.bdbiosciences.com/eu/index.jsp. Accessed: 5th May 2011.

Bellamy, W. D. and Klimek, J. W. (1948) 'Some properties of Penicillin-resistant *Staphylococci*.' *Journal of Bacteriology*, 55, (2): 153-160.

Beltran-Alvarez, P., Cox, R. J., Crosby, J. and Simpson, T. J. (2007) 'Dissecting the Component Reactions Catalyzed by the Actinorhodin Minimal Polyketide Synthase.' *Biochemistry*, 46, (50): 14672-14681.

Bhullar, K., Waglechner, N., Pawlowski, A., Koteva, K., Banks, E. D., Johnston, M. D., Barton, H. A. and Wright, G. D. (2012) 'Antibiotic Resistance Is Prevalent in an Isolated Cave Microbiome.' *PLoS ONE*, 7, (4): e34953.

Birkenstock, T., Liebeke, M., Winstel, V., Krismer, B., Gekeler, C., Niemiec, M. J., Bisswanger, H., Lalk, M. and Peschel, A. (2012) 'Exometabolome Analysis Identifies Pyruvate Dehydrogenase as a Target for the Antibiotic Triphenylbismuthdichloride in Multiresistant Bacterial Pathogens.' *The Journal of Biological Chemistry*, 287, (4): 2887-2895.

Birnboim, H. C. and Doly, J. (1979) 'A Rapid Alkaline Extraction Proceedure for Screening Recombinant Plasmid DNA.' *Nucleic Acids Research*, 7, 1513-1523.

Bisang, C., Long, P. F., Cortés, J., Westcott, J., Crosby, J., Matharu, A.-L., Cox, R. J., Simpson, T. J., Staunton, J. and Leadlay, P. F. (1999) 'A chain initiation factor common to both modular and aromatic polyketide synthases.' *Nature* 401, 502-505.

Blunt, J. W., Copp, B. R., Munro, M. H. G., Northcote, P. T. and Prinsep, M. R. (2011) 'Marine natural products.' *Natural Product Reports*, 28, (2): 196-268.

Bosch, F. and Rosich, L. (2008) 'The Contributions of Paul Ehrlich to Pharmacology: A Tribute on the Occasion of the Centenary of His Nobel Prize.' *Pharmacology*, 82, 171-179.

Brendel, N., Partida-Martinez, L. P., Scherlacha, K. and Hertweck, C. (2007) 'A cryptic PKS–NRPS gene locus in the plant commensal *Pseudomonas fluorescens* Pf-5 codes for the biosynthesis of an antimitotic rhizoxin complex.' *Organic and Biomolecular Chemistry*, 5, 2211–2213.

Brown, M. G. and Balkwill, D. L. (2009) 'Antibiotic Resistance in Bacteria Isolated from the Deep Terrestrial Subsurface.' *Microbial Ecology*, 57, 484-493.

Brunel, J. (1951) 'Antibiosis from Pasteur to Fleming.' *Journal of the History of Medicine*, Summer 1951, 287-301.

Bumpus, S. B., Magarvey, N. A., Kelleher, N. L., Walsh, C. T. and Calderone, C. T. (2008) 'Polyunsaturated Fatty-Acid-Like Trans-Enoyl Reductases Utilized in Polyketide Biosynthesis.' *Journal of the Americal Chemical Society*
130, 11614–11616.

Bush, K., Courvalin, P., Dantas, G., Davies, J., Eisenstein, B., Huovinen, P., Jacoby, G. A., Kishony, R., Kreiswirth, B. N., Kutter, E., Lerner, S. A., Levy, S., Lewis, K., Lomovskaya, O., Miller, J. H., Mobashery, S., Piddock, L. J. V., Projan, S., Thomas, C. M., Tomasz, A., Tulkens, P. M., Walsh, T. R., Watson, J. D., Witkowski, J., Witte, W., Wright, G., Yeh, P. and Zgurskaya, H. I. (2011) 'Tackling antibiotic resistance.' *Nature Reviews Microbiology*, 9, 894-896.

Butcher, R. A., Schroeder, F. C., Fischbach, M. A., Straight, P. D., Kolter, R., Walsh, C. T. and Clardy, J. (2007) 'The identification of bacillaene, the product of the PksX megacomplex in *Bacillus subtilis*.' *Proceedings of the National Academy of Sciences of the United States of America*, 104, (5): 1506-1509.

Caffrey, A. R., Quilliam, B. J. and LaPlante, K. L. (2010) 'Risk factors associated with mupirocin resistance in meticillin-resistant *Staphylococcus aureus*.' *Journal of Hospital Infection*, 76, 206-210.

Caffrey, P., Bevitt, D. J., Staunton, J. and Leadlay, P. F. (1992) 'Identification of DEBS 1, DEBS 2 and DEBS 3, the multienzyme polypeptides of the erythromyein-producing polyketide synthase from *Saccharopolyspora erythraea*.' *FEBS Letters*, 304, (2,3): 225-228.

Calderone, C. T., Kowtoniuk, W. E., Kelleher, N. L., Walsh, C. T. and Dorrestein, P. C. (2006) 'Convergence of isoprene and polyketide biosynthetic machinery: Isoprenyl-S-carrier proteins in the pksX pathway of *Bacillus subtilis*.' *PNAS*, 103, (24): 8977–8982.

Cane, D. E. (2010) 'Programming of Erythromycin Biosynthesis by a Modular Polyketide Synthase.' *Journal of Biological Chemistry*, 285, (36): 27515-27523.

Cars, O., Mölstad, S. and Melander, A. (2001) 'Variation in antibiotic use in the European Union.' *The Lancet*, 357, 1851-1853.

CDC (2011) 'Antibiotic/Antimicrobial Resistance. Public Health Action Plan.' http://www.cdc.gov/drugresistance/actionplan/actionPlan.html. Accessed: 22nd August 2012.

Chain, E., Florey, H. W., Gardener, A. D., Heatley, N. G., Jennings, M. A., Orr-Ewing, J. and Sanders, A. G. (1940) 'Penicillin as a Chemotherapeutic Agent.' *The Lancet*, 236, (6104): 226-228.

Chain, E. B. and Mellows, G. (1974) 'Structure of Pseudomonic Acid, an Antibiotic from *Pseudomonas fluorescens*.' *Journal of the Chemical Society, Chemical Communications*, 847-848.

Chain, E. B. and Mellows, G. (1977a) 'Pseudomonic Acid. Part 1. The Structure of Pseudomonic Acid A, a Novel Antibiotic produced by *Pseudomonas fluorescens*.' *Journal of the Chemical Society Perkin Transactions I* 294-309.

Chain, E. B. and Mellows, G. (1977b) 'Pseudomonic Acid. Part 3. Structure of Pseudomonic Acid B.' *Journal of the Chemical Society Perkin Transactions I*, 318-322.

Chan, Y. A. and Thomas, M. G. (2010) 'Recognition of (2S)-Aminomalonyl-Acyl Carrier Protein (ACP) and (2R)-Hydroxymalonyl-ACP by Acyltransferases in Zwittermicin A Biosynthesis.' *Biochemistry*, 49, 3667-3677.

Chang, Z., Sitachitta, N., Rossi, J. V., Roberts, M. A., Flatt, P. M., Jia, J., Sherman, D. H. and Gerwick, W. H. (2004) 'Biosynthetic Pathway and Gene Cluster Analysis of Curacin A, an Antitubulin Natural Product from the Tropical Marine Cyanobacterium *Lyngbya majuscula*.' *Journal of Natural Products*, 67, 1356-1367.

Chen, G.-Q. and Gouaux, E. (1997) 'Overexpression of a glutamate receptor (GluR2) ligand binding domain in *Escherichia coli*: Application of a novel protein folding screen.' *Proceedings of the National Academy of Sciences of the United States of America*, 94, 13431–13436.

Chen, J., Song, J.-l., Zhang, S., Wang, Y., Cui, D.-f. and Wang, C.-c. (1999) 'Chaperone Activity of DsbC.' *The Journal of Biological Chemistry*, 274, (28): 19601–19605.

Chen, X.-H., Vater, J., Piel, J., Franke, P., Scholz, R., Schneider, K., Koumoutsi, A., Hitzeroth, G., Grammel, N., Strittmatter, A. W., Gottschalk, G., Süssmuth, R. D. and Borriss, R. (2006) 'Structural and Functional Characterization of Three Polyketide Synthase Gene Clusters in *Bacillus amyloliquefaciens* FZB 42.' *Journal of Bacteriology*, 188, (11): 4024–4036.

Chen, X. H., Koumoutsi, A., Scholz, R., Eisenreich, A., Schneider, K., Heinemeyer, I., Morgenstern, B., Voss, B., Hess, W. R., Reva, O., Junge, H., Voigt, B., Jungblut, P. R., Vater, J., Süssmuth, R., Liesegang, H., Strittmatter, A., Gottschalk, G. and Borriss, R. (2007) 'Comparative analysis of the complete genome sequence of the plant growth–promoting bacterium *Bacillus amyloliquefaciens* FZB42.' *Nature Biotechnology*, 25, (9): 1007-1014.

Cheng, Y.-Q., Coughlin, J. M., Lim, S.-K. and Shen, B. (2009) 'Type I Polyketide Synthases That Require Discrete Acyltransferases.' In: D. A. Hopwood (Ed.) 'Complex Enzymes in Microbial Natural Product Biosynthesis, Part B: Polyketides, Aminocoumarins and Carbohydrates.' London, Academic Press.

Cheng, Y.-Q., Tang, G.-L. and Shen, B. (2003) 'Type I polyketide synthase requiring a discrete acyltransferase for polyketide biosynthesis.' *Proceedings of the National Academy of Sciences of the United States of America*, 100, (6): 3149-3154.

Cheng, Y.-Q., Yang, M. and Matter, A. M. (2007) 'Characterization of a Gene Cluster Responsible for the Biosynthesis of Anticancer Agent FK228 in *Chromobacterium violaceum* No. 968.' *Applied and Environmental Microbiology*, 73, (11): 3460-3469.

Chopra, T., Banerjee, S., Gupta, S., Yadav, G., Anand, S., Surolia, A., Roy, R. P., Mohanty, D. and Gokhale, R. S. (2008) 'Novel Intermolecular Iterative Mechanism for Biosynthesis of Mycoketide Catalyzed by a Bimodular Polyketide Synthase.' *PLoS Biology*, 6, (7): 1584-1598.

Clark, E. D. B. (1998) 'Refolding of Recombinant Proteins.' *Current Opinion in Biotechnology*, 9, 157-163.

Clatworthy, A. E., Pierson, E. and Hung, D. T. (2007) 'Targeting virulence: a new paradigm for antimicrobial therapy.' *Nature Chemical Biology*, 3, (9): 541-548.

Clayton, J. P., O'Hanlon, P. J. and Rogers, N. H. (1980) 'The Structure and Configuration of Pseudomonic Acid C.' *Tetrahedron Letters*, 21, 881-884.

Clayton, J. P., O'Hanlon, P. J., Rogers, N. H. and King, T. J. (1982) 'The Chemistry of Pseudomonic Acid. Part 5.' Structure and Chemistry of Pseudomonic Acid C. X-Ray Crystal Structure of Ethyl Monate C.' *Journal of the Chemical Society Perkin Transactions I*, 2827-2833.

Cohen, S. N., Chang, A. C. Y. and Hsu, L. (1972) 'Nonchromosomal Antibiotic Resistance in Bacteria: Genetic Transformation of *Escherichia coli* by R-Factor DNA.' *Proceedings of the National Academy of Sciences of the United States of America*, 69, (8): 2110-2114.

Colson, A. (2008) 'Policy responses to the growing threat of antibiotic resistance.' Extending the Cure.

Cookson, B. D., Lacey, R. W., Noble, W. C., Reeves, D. S., Wise, R. and Redhead, R. J. (1990) 'Mupirocin-resistant *Staphylococcus aureus*.' *The Lancet*, 335, 1095-1096.

Cooper, S. M., Cox, R. J., Crosby, J., Crump, M. P., Hothersall, J., Laosripaiboon, W., Simpson, T. J. and Thomas, C. M. (2005a) 'Mupirocin W, a novel pseudomonic acid produced by targeted mutation of the mupirocin biosynthetic gene cluster.' *The Royal Society of Chemistry Chemical Communications*, 1179–1181.

Cooper, S. M., Laosripaiboon, W., Rahman, A. S., Hothersall, J., El-Sayed, A. K., Winfield, C., Crosby, J., Cox, R. J., Simpson, T. J. and Thomas, C. M. (2005b) 'Shift to Pseudomonic Acid B Production in *P. fluorescens* NCIMB10586 by Mutation of Mupirocin Tailoring Genes *mupO, mupU, mupV,* and *macpE.*' *Chemistry and Biology*, 12, 825-833.

Cortés, J., Wiesmann, K. E. H., Roberts, G. A., Brown, M. J. B., Staunton, J. and Leadlay, P. F. (1995) 'Repositioning of a Domain in a Modular Polyketide Synthase to Promote Specific Chain Cleavage.' *Science*, 268, 1487-1489.

Cox, R. J., Crosby, J., Daltrop, O., Glod, F., Jarzabek, M. E., Nicholson, T. P., Reed, M., Simpson, T. J., Smith, L. H., Soulas, F., Szafranska, A. E. and Westcott, J. (2002) '*Streptomyces coelicolor* phosphopantetheinyl transferase: a promiscuous activator of polyketide and fatty acid synthase acyl carrier proteins.' *Journal of the Chemical Society Perkin Transactions*, 1, 1644-1649.

Critchley, I. A. and Ochsner, U. A. (2008) 'Recent Advances in the Preclinical Evaluation of the Topical Antibacterial Agent REP8839.' *Current Opinion in Chemical Biology*, 12, 409-417.

Cronin, C. N. and McIntire, W. S. (2000) 'Heterologous Expression in *Pseudomonas aeruginosa* and Purification of the 9.2-kDa c-Type Cytochrome Subunit of p-Cresol Methylhydroxylase.' *Protein Expression and Purification*, 19, (1): 74-83.

Crooks, G. E., Hon, G., Chandonia, J. M. and Brenner, S. E. (2004) 'WebLogo: A sequence logo generator.' *Genome Research*, 14, 1188-1190.

Crosby, J., Sherman, D. H., Bibb, M. J., Revill, W. P., Hopwood, D. A. and Simpson, T. J. (1995) 'Polyketide Synthase Acyl Carrier Proteins from *Streptomyces*: Expression in *Escherichia coli*, Purification and Partial Characterisation. .' *Biochimica et Biophysica Acta*, 1251, 32-42.

Crump, M. P., Crosby, J., Dempsey, C. E., Murray, M., Hopwood, D. A. and Simpson, T. J. (1996) 'Conserved secondary structure in the actinorhodin polyketide synthase acyl carrier protein from *Streptomyces coelicolor* A3(2) and the fatty acid synthase acyl carrier protein from *Escherichia coli*.' *FEBS Letters*, 391, 302-306.

D'Costa, V. M., King, C. E., Kalan, L., Morar, M., Sung, W. W. L., Schwarz, C., Froese, D., Zazula, G., Calmels, F., Debruyne, R., Golding, G. B., Poinar, H. N. and Wright, G. D. (2011) 'Antibiotic Resistance in Ancient.' *Nature*, 477, 457-461.

Dacre, J. E., Emmerson, A. M. and Jenner, E. A. (1983) 'Nasal Carriage of Gentamicin and Methicillin Resistant *Staphylococcus Aureus* Treated With Topical Pseudomonic Acid.' *The Lancet*, 1036.

Dafforn, T. (2011) 'Personal communication.' The University of Birmingham.

Dehn, R., Katsuyama, Y., Weber, A., Gerth, K., Jansen, R., Heinrich Steinmetz, Höfle, G., Müller, R. and Kirschning, A. (2011) 'Molecular Basis of Elansolid Biosynthesis: Evidence for an Unprecedented Quinone Methide Initiated Intramolecular Diels–Alder Cycloaddition/Macrolactonization.' *Angew. Chem. Int. Ed.*, 50, 3882-3887.

Del Vecchio, F., Petkovic, H., Kendrew, S. G., Low, L., Wilkinson, B., Lill, R., Cortés, J., Rudd, B. A. M., Staunton, J. and Leadlay, P. F. (2003) 'Active-site residue, domain and module swaps in modular polyketide synthases.' *J Ind Microbiol Biotechnol*, 30, 489–494.

Department of Health (2012) 'Funding for new research into antibiotic-resistance bacteria announced.' http://www.dh.gov.uk/health/2012/02/research-esbl-producing-bacteria/. Accessed: 22nd August 2012.

Deurenberg, R. H., Vink, C., Kalenic, S., Friedrich, A. W., Bruggeman, C. A. and Stobberingh, E. E. (2007) 'The molecular evolution of methicillin-resistant *Staphylococcus aureus*.' *Clinical Microbiology and Infection*, 13, (3): 222-235.

de Marco, A. (2009) 'Strategies for successful recombinant expression of disulfide bond-dependent proteins in *Escherichia coli*.' *Microbial Cell Factories*, 8, 26.

Donadio, S., McAlpine, J. B., Sheldon, P. J., Jackson, M. and Katz, L. (1993) 'An erythromycin analog produced by reprogramming of polyketide synthesis.' *Proceedings of the National Academy of Science USA*, 90, 7119-7123.

Dong, X., Haines, A. S., Song, Z., Farmer, R., Williams, C., Hothersall, J., Płoskoń, E., Wattana-amorn, P., Stephens, E. R., Yamada, E., Gurney, R., Takabayashi, Y., Masschelein, J., Cox, R. J., Lavigne, R., Crosby, J., Simpson, T. J., Winn, P. J., Thomas, C. M. and Crump, M. P. (2012) 'A conserved structural motif in Acyl Carrier Proteins involved in β-branch insertion during type I polyketide synthesis.' *Manuscript in preparation*.

Dreier, J., Shah, A. N. and Khosla, C. (1999) 'Kinetic Analysis of the Actinorhodin Aromatic Polyketide Synthase.' *The Journal of Biological Chemistry*, 274, (35): 25108–25112.

Du, L., Sánchez, C., Chen, M., Edwards, D. J. and Shen, B. (2000) 'The biosynthetic gene cluster for the antitumor drug bleomycin from *Streptomyces verticillus* ATCC15003 supporting functional interactions between nonribosomal peptide synthetases and a polyketide synthase.' *Chemistry and Biology*, 7, 623-642.

Duitman, E. H., Hamoen, L. W., Rembold, M., Venema, G., Seitz, H., Saenger, W., Bernhard, F., Reinhardt, R., Schmidt, M., Ullrich, C., Stein, T., Leenders, F. and Vater, J. (1999) 'The mycosubtilin synthetase of *Bacillus subtilis* ATCC6633: A multifunctional hybrid between a peptide synthetase, an amino transferase, and a fatty acid synthase.' *PNAS*, 96, (23): 13294-13299.

Dyke, K. G. H., Curnock, S. P., Golding, M. and Noble, W. C. (1991) 'Cloning of the gene conferring resistance to mupirocin in *Staphylococcus aureus*.' *FEMS Microbiology Letters*, 77, 195-198.

ECDC (2012) 'Antimicrobial Resistance.' http://www.ecdc.europa.eu/en/healthtopics/antimicrobial_resistance/Pages/index.aspx. Accessed: 22nd August 2012.

Edwards, D. J., Marquez, B. L., Nogle, L. M., McPhail, K., Goeger, D. E., Roberts, M. A. and Gerwick, W. H. (2004) 'Structure and Biosynthesis of the Jamaicamides, New Mixed Polyketide-Peptide Neurotoxins from the Marine Cyanobacterium *Lyngbya majuscula*.' *Chemistry and Biology*, 11, 817-833.

El-Sayed, A. K., Hothersall, J., Cooper, S. M., Stephens, E., Simpson, T. J. and Thomas, C. M. (2003) 'Characterization of the Mupirocin Biosynthesis Gene Cluster from *Pseudomonas fluorescens* NCIMB 10586 ' *Chemistry and Biology*, 10, 419–430.

El-Sayed, A. K., Hothersall, J. and Thomas, C. M. (2001) 'Quorum-sensing-dependent regulation of biosynthesis of the polyketide antibiotic mupirocin in *Pseudomonas fluorescens* NCIMB 10586.' *Microbiology*, 147, 2127–2139.

Ellman, G. L. (1959) 'Tissue sulfhydryl groups.' *Arch. Biochem. Biophys.*, 82, 70-77.

Eltringham, I. (1997) 'Mupirocin resistance and methicillin-resistant *Staphylococcus aureus* (MRSA).' *Journal of Hospital Infection*, 35, 1-8.

Enne, V. I. (2010) 'Reducing antimicrobial resistance in the community by restricting prescribing: can it be done?' *Journal of Antimicrobial Chemotherapy*, 65, (2): 179-182.

Erol, Ö., Schäberle, T. F., Schmitz, A., Rachid, S., Gurgui, C., Omari, M. E., Lohr, F., Kehraus, S., Piel, J., Müller, R. and König, G. M. (2010) 'Biosynthesis of the Myxobacterial Antibiotic Corallopyronin A.' *Chembiochem*, 11, 1253-1265.

European Centre for Disease Prevention and Control (2012) 'EARS-Net Database.' http://ecdc.europa.eu/en/activities/surveillance/EARS-Net/database. Accessed: 23rd August 2012.

Fabbretti, A., Gualerzi, C. O. and Brandi, L. (2011) 'How to cope with the quest for new antibiotics.' *FEBS Letters*, 585, 1673-1681.

Farmer, T. H., Gilbart, J. and Elson, S. W. (1992) 'Biochemical basis of mupirocin resistance in strains of *Staphylococcus aureus*.' *Journal of Antimicrobial Chemotherapy*, 30, 587-596.

Farnet, C. M., Staffa, A., Zazopoulos, E. and Yang, X. (2009) 'Comparative analyses of the lactimidomycin gene cluster in *Streptomyces amphibiosporus* ATCC53964 and the iso-migrastatin, migrastatin, and dorrigocin gene cluster in *Streptomyces platensis* NRRL18993 unveiling a common pathway for glutarimide-containing polyketide biosynthesis.' http://www.ncbi.nlm.nih.gov/nuccore/GQ274954.1. Accessed: 5th July 2012.

FDA (2012) 'FDA takes steps to protect public health.' http://www.fda.gov/NewsEvents/Newsroom/PressAnnouncements/ucm299802.htm. Accessed: 22nd August 2012.

Feline, T. C., Jones, R. B., Mellows, G. and Phillips, L. (1977) 'Pseudomonic Acid. Part 2. Biosynthesis of Pseudomonic Acid A.' *Journal of the Chemical Society Perkin Transactions I* 309-318.

Fleming, A. (1929) 'On the Antibacterial Action of Cultures of a Penicillium, with Special Reference to their Use in the Isolation of *B. influenzae*.' *British Journal of Experimental Pathology*, 10, (3): 226-236.

Fleming, A. (1945) 'Penicillin.' *Nobel Lecture*.

Flores-Sanchez, I. J. and Verpoorte, R. (2009) 'Plant Polyketide Synthases: A fascinating group of enzymes.' *Plant Physiology and Biochemistry*, 47, 167-174.

Florey, H. W. (1945) 'Penicillin.' *Nobel Lecture*.

Forrest, R. D. (1982) 'Early History of Wound Treatment.' *Journal of the Royal Society of Medicine*, 75, 198-205.

Foster, W. and Raoult, A. (1974) 'Early descriptions of antibiosis.' *The Journal of the Royal College of General Practitioners*, 24, (149): 889-894.

Freire-Moran, L., Aronsson, B., Manz, C., C.Gyssens, I., D.So, A., L.Monnet, D. and Cars, O. (2011) 'Critical shortage of new antibiotics in development against multidrug-resistant bacteria—Time to react is now.' *Drug Resistance Updates*, 14, 118-124.

Fukuda, D., Haines, A. S., Song, Z., Murphy, A. C., Hothersall, J., Stephens, E. R., Gurney, R., Cox, R. J., Crosby, J., Willis, C. L., Simpson, T. J. and Thomas, C. M. (2011) 'A Natural Plasmid Uniquely Encodes Two Biosynthetic Pathways Creating a Potent Anti-MRSA Antibiotic.' *PLoS ONE*, 6, (3): e18031.

Fuller, A. T., Mellows, G., Woolford, M., Banks, G. T., Barrow, K. D. and Chain, E. B. (1971) 'Pseudomonic Acid: an antibiotic produced by *Pseudomonas fluorescens*.' *Nature*, 234,

Funa, N., Ohnishi, Y., Fujii, I., Shibuya, M., Ebizuka, Y. and Horinouchi, S. (1999) 'A new pathway for polyketide synthesis in microorganisms.' *Nature*, 400, 897-899.

Fuqua, W. C., Winans, S. C. and Greenberg, E. P. (1994) 'Quorum Sensing in Bacteria: the LuxR-LuxI Family of Cell Density-Responsive Transcriptional Regulators.' *Journal of Bacteriology*, 176, (2): 269-275.

Gaitatzis, N., Silakowski, B., Kunze, B., Nordsiek, G., Blöcker, H., Höfle, G. and Müller, R. (2002) 'The Biosynthesis of the Aromatic Myxobacterial Electron Transport Inhibitor Stigmatellin Is Directed by a Novel Type of Modular Polyketide Synthase.' *The Journal of Biological Chemistry*, 277, (15): 13082–13090.

Gekko, K. and Timasheff, S. N. (1981) 'Mechanism of Protein Stabilization by Glycerol: Preferential Hydration in Glycerol-Water Mixtures' *Biochemistry,* 20, 4667-4676.

Georgiou, G. and Valax, P. (1996) 'Expression of Correctly Folded Proteins in *Escherichia coli*.' *Current Opinion in Chemical Biology*, 7, 190-197.

Gilbart, J., Perry, C. R. and Slocombe, B. (1993) 'High-Level Mupirocin Resistance in *Staphylococcus aureus*: Evidence for Two Distinct Isoleucyl-tRNA Synthetases.' *Antimicrobial Agents and Chemotherapy*, 37, (1): 32-38.

Gilpin, D. F., Small, S., Bakkshi, S., Kearney, M. P., Cardwell, C. and Tunney, M. M. (2010) 'Efficacy of a standard meticillin-resistant Staphylococcus aureus decolonisation protocol in routine clinical practice.' *Journal of Hospital Infection*, 75, 93-98.

Glaxo Smith Klein (2010) 'Bactroban.' http://public.gsk.co.uk/products/bactroban/. Accessed: August 9th 2010.

Glaxo Smith Klein (2012) 'Bacteria battle: the struggle to find new antibiotics.' http://www.gsk.com/infocus/bacteria-battle.htm. Accessed: 24th August 2012.

Gould, J. C. (1958) 'Environmental penicillin and penicillin-resistant *Staphylococcus aureus*.' *The Lancet*, 271, (7019): 489-493.

Grayson, M. L., Heymann, D., Pittet, D., Grundmann, H., O'Brien, T. F., Stelling, J. M., Cars, O., Heddini, A., Aaerestrup, F. M., Aidara-Kane, A., Cookson, B., Gastmeier, P., Seto, W.-H., Chang, S., So, A., Gerald Dziekan, Jauregui, I. L. and Mathai, E. (2012) 'The evolving threat of antimicrobial resistance. Options for action.' Geneva, World Health Organisation.

Gross, F., Luniak, N., Perlova, O., Gaitatzis, N., Jenke-Kodama, H., Gerth, K., Gottschalk, D., Dittmann, E. and Müller, R. (2006) 'Bacterial type III polyketide synthases: phylogenetic analysis and potential for the production of novel secondary metabolites by heterologous expression in pseudomonads.' *Archives of Microbiology*, 185, 28-38.

Gu, L., Geders, T. W., Wang, B., Gerwick, W. H., Håkansson, K., Smith, J. L. and Sherman, D. H. (2007) 'GNAT-Like Strategy for Polyketide Chain Initiation.' *Science*, 318, 970-974.

Gurney, R., Shields, J. A., Song, Z., Thorpe, H., Haines, A. S., Hothersall, J., Simpson, T. J. and Thomas, C. M. (2012) 'A Tri-functional Edit, Reload, Reduce Protein Crucial for a *Trans*-AT PKS Pathway.' *Manuscript in preparation*.

Gurney, R. and Thomas, C. M. (2011) 'Mupirocin: biosynthesis, special features and applications of an antibiotic from a Gram-negative bacterium.' *Applied Microbiology and Biotechnology*, 90, 11-21.

Haas, D. and Défago, G. (2005) 'Biological control of soil-borne pathogens by fluorescent pseudomonads.' *Nat Rev Micro*, 3, (4): 307-319.

Haines, A. (2012) 'Personal communication.' The University of Birmingham.

Hale, L., Lazos, O., Haines, A. S. and Thomas, C. M. (2010) 'An efficient stress-free strategy to displace stable bacterial plasmids.' *BioTechniques*, 48, (3): 223-228.

Hall, B. G. and Barlow, M. (2004) 'Evolution of the serine β-lactamases: past, present and future.' *Drug Resistance Updates*, 7, (2): 111-123.

Hammond, A. A., Miller, K. G., Kruczek, C. J., Dertien, J., Colmer-Hamood, J. A., Griswold, J. A., Horswill, A. R. and Hamood, A. N. (2011) 'An *in vitro* biofilm model to examine the effect of antibiotic ointments on biofilms produced by burn wound bacterial isolates.' *Burns*, 37, 312-321.

Han, Z., Li, W., Huang, Y. and Zheng, B. (2009) 'Measuring Rapid Enzymatic Kinetics by Electrochemical Method in Droplet-Based Microfluidic Devices with Pneumatic Valves.' *Analytical Chemistry*, 81, 5840-5845.

Haydock, S. F., Aparicio, J. F., Molnár, I., Schwecke, T., Khaw, L. E., König, A., Marsden, A. F. A., Galloway, I. S., Staunton, J. and Leadlay, P. F. (1995) 'Divergent sequence motifs correlated with the substrate specificity of (methyl)malonyl-CoA:acyl carrier protein transacylase domains in modular polyketide synthases.' *FEBS Letters*, 374, 246-248.

He, J. and Hertweck, C. (2005) 'Functional Analysis of the Aureothin Iterative Type I Polyketide Synthase.' *ChemBioChem*, 6, 908-912.

Health Protection Agency (2012) 'Antibiotic Resistance Monitoring & Reference Laboratory (ARMRL).' http://www.hpa.org.uk/ProductsServices/MicrobiologyPathology/LaboratoriesAndReferenceFacilities/AntibioticResistanceMonitoringAndReferenceLaboratory/. Accessed: 22nd August 2012.

Heath, R. J., Rubin, J. R., Holland, D. R., Zhang, E., Snow, M. E. and Rock, C. O. (1999) 'Mechanism of Triclosan Inhibition of Bacterial Fatty Acid Synthesis.' *The Journal of Biological Chemistry*, 274 (16): 11110-11114.

Heddle, J. and Maxwell, A. (2002) 'Quinolone-Binding Pocket of DNA Gyrase: Role of GyrB.' *Antimicrobial Agents and Chemotherapy*, 46, (6): 1805-1815.

Hertweck, C. (2009) 'The Biosynthetic Logic of Polyketide Diversity.' *Angewandte Chemie International Edition*, 48, 4688-4716.

Higgins, A., Lynch, M. and Gethin, G. (2010) 'Can 'search and destroy' reduce nosocomial meticillin-resistant *Staphylococcus aureus* in an Irish hospital?' *Journal of Hospital Infection*, 75, (2): 120-123.

Higgins, D. L., Chang, R., Debabov, D. V., Leung, J., Wu, T., Krause, K. M., Sandvik, E., Hubbard, J. M., Kaniga, K., Jr., D. E. S., Gao, Q., Cass, R. T., Karr, D. E., Benton, B. M. and Humphrey, P. P. (2005) 'Telavancin, a Multifunctional Lipoglycopeptide, Disrupts both Cell Wall Synthesis and Cell Membrane Integrity inMethicillin-Resistant *Staphylococcus aureus*.' *Antimicrobial Agents and Chemotherapy*, 49, (3): 1127-1134.

Hill, A. M. and Staunton, J. (2010) 'Type I Modular PKS.' In: L. M. a. H.-W. Lui (Ed.) 'Comprehensive Natural Products II Chemistry and Biology.' Oxford, Elsevier.

Hiramatsu, K., Cui, L., Kuroda, M. and Ito, T. (2001) 'The emergence and evolution of methicillin-resistant *Staphylococcus aureus*.' *TRENDS in Microbiology*, 9, (10): 486-493.

Hodgson, J. E., Curnock, S. P., Dyke, K. G. H., Morris, R., Sylvester, D. R. and Gross, M. S. (1994) 'Molecular Characterization of the Gene Encoding High-Level Mupirocin Resistance in *Staphylococcus aureus* J2870.' *Antimicrobial Agents and Chemotherapy*, 38, (5): 1205-1208.

Horwich, A. L., Fenton, W. A., Chapman, E. and Farr, G. W. (2007) 'Two Families of Chaperonin: Physiology and Mechanism.' *Annual Review of Cell and Developmental Biology*, 23, 115-45.

Hothersall, J. (2012) 'Unpublished data.' The University of Birmingham.

Hothersall, J., Murphy, A. C., Iqbal, Z., Campbell, G., Stephens, E. R., Wu, J., Cooper, H., Atkinson, S., Williams, P., Crosby, J., Willis, C. L., Cox, R. J., Simpson, T. J. and Thomas, C. M. (2011) 'Manipulation of quorum sensing regulation in *Pseudomonas fluorescens* NCIMB 10586 to increase mupirocin production.' *Applied Microbiology and Biotechnology*, 90, (3): 1017-1026.

Hothersall, J. and Thomas, C. M. (2004) 'Polyketide antibiotics of *Pseudomonas*.' In: J.-L. Ramos (Ed.) 'Pseudomonas.' New York, Kluwer Academic/Plenum Publishers.

Hothersall, J. and Wu, J. 'Unpublished data.' The University of Birmingham.

Hothersall, J., Wu, J. e., Rahman, A. S., Shields, J. A., Haddock, J., Johnson, N., Cooper, S. M., Stephens, E. R., Cox, R. J., Crosby, J., Willis, C. L., Simpson, T. J. and Thomas, C. M. (2007) 'Mutational Analysis Reveals That All Tailoring Region Genes Are Required for Production of Polyketide Antibiotic Mupirocin by *Pseudomonas fluorescens*.' *The Journal of Biological Chemistry*, 282, (21): 15451–15461.

Huang, W., Jia, J., Edwards, P., Dehesh, K., Schneider, G. and Lindqvist, Y. (1998) 'Crystal structure of B-ketoacyl-acyl carrier protein synthase II from *E.coli* reveals the molecular architecture of condensing enzymes.' *The EMBO Journal*, 17, (5): 1183-1191.

Hughes, J. and Mellows, G. (1978) 'Inhibition of Isoleucyl-Transfer Ribonucleic Acid Synthetase in *Escherichia coli* by Pseudomonic Acid.' *Biochemical Journal*, 179, 305-318.

Hughes, V. M. and Datta, N. (1983) 'Conjugative plasmids in bacteria of the `pre-antibiotic' era.' *Nature*, 302, 725-726.

Hurdle, J. G., O'Neill, A. J., Ingham, E., Fishwick, C. and Chopra, I. (2004) 'Analysis of Mupirocin Resistance and Fitness in *Staphylococcus aureus* by Molecular Genetic and Structural Modeling Techniques.' *Antimicrobial Agents and Chemotherapy*, 48, (11): 4366-4376.

Idicula-Thomas, S. and Balaji, P. V. (2005) 'Understanding the relationship between the primary structure of proteins and its propensity to be soluble on overexpression in *Escherichia coli*.' *Protein Science*, 14, 582–592.

Ikeda, H., Nonomiya, T., Usami, M., Ohta, T. and Mura, S. O. (1999) 'Organization of the biosynthetic gene cluster for the polyketide anthelmintic macrolide avermectin in *Streptomyces avermitilis*.' *Proceedings of the National Academy of Sciences of the United States of America*, 96, 9509-9514.

Ikeda, Y., Ban, J., Ishikawa, T., Hashiguchi, S., Urayama, S. and Horibe, H. (2008) 'Stability and Stabilization Studies of TAK-599 (Ceftaroline Fosamil), a Novel N-Phosphono Type Prodrug of Anti-methicillin Resistant *Staphylococcus aureus* Cephalosporin T-91825.' *Chemical and Pharmaceutical Bulletin*, 56, (10): 1406-1411.

Irschik, H., Kopp, M., Weissman, K. J., Buntin, K., Piel, J. and Müller, R. (2010) 'Analysis of the Sorangicin Gene Cluster Reinforces the Utility of a Combined Phylogenetic/Retrobiosynthetic Analysis for Deciphering Natural Product Assembly by *trans*-AT PKS.' *Chembiochem*, 11, 1840-1849.

Ito, T., Katayama, Y. and Hiramatsu, K. (1999) 'Cloning and Nucleotide Sequence Determination of the Entire mec DNA of Pre-Methicillin-Resistant *Staphylococcus aureus* N315.' *Antimicrobial Agents and Chemotherapy*, 43, (6): 1449–1458.

Jagura-Burdzy, G., Kostelidou, K., Pole, J., Khare, D., Jones, A., Williams, D. R. and Thomas, C. M. (1999) 'IncC of broad-host-range plasmid RK2 modulates KorB transcriptional repressor activity *in vivo* and operator binding *in vitro*.' *Journal of Bacteriology*, 181, 2807-2815.

Jenni, S., Leibundgut, M., Boehringer, D., Frick, C., Mikolásek, B. and Ban, N. (2007) 'Structure of Fungal Fatty Acid Synthase and Implications for Iterative Substrate Shuttling.' *Science*, 316, 254-261.

Jensen, K., Niederkrüger, H., Zimmermann, K., Vagstad, A. L., Moldenhauer, J., Brendel, N., Frank, S., Pöplau, P., Kohlhaas, C., Townsend, C. A., Oldiges, M., Hertweck, C. and Piel, J. (2012) 'Polyketide Proofreading by an Acyltransferase-like Enzyme.' *Chemistry and Biology*, 19, 329-339.

Jevons, M. P. (1961) 'Celbenin-resistant *Staphylococci*.' *British Medical Journal*, (Jan 14): 124-125.

Jevons, M. P., Coe, A. W. and Parker, M. T. (1963) 'Methicillin Resistance In *Staphylococci*.' *The Lancet*, 904-907.

Jones, A. C., Gu, L., Sorrels, C. M., Sherman, D. H. and Gerwick, W. H. (2009) 'New tricks from ancient algae: natural products biosynthesis in marine cyanobacteria.' *Current Opinion in Chemical Biology*, 13, 216-223.

Jones, D. T. (1999) 'Protein secondary structure prediction based on position-specific scoring matrices.' *Journal of Molecular Biology*, 292, 195-202.

Josephine, H. R., Kumar, I. and Pratt, R. F. (2004) 'The Perfect Penicillin? Inhibition of a Bacterial DD-Peptidase by Peptidoglycan-Mimetic B-Lactams.' *Journal of the American Chemical Society*, 126, 8122-8123.

Joshi, V. C. and Wakil, S. J. (1971) 'Studies on the Mechanism of Fatty Acid Synthesis. XXVI. Purification and Properties of Malonyl-Coenzyme A-Acyl Carrier Protein Transacylase of *Escherichia coli*.' *Archives of Biochemistry and Biophysics*, 143, 493-505.

Kahne, D., Leimkuhler, C., Lu, W. and Walsh, C. (2005) 'Glycopeptide and Lipoglycopeptide Antibiotics.' *Chemical Reviews*, 105, 425-448.

Kakavas, S. J., Katz, L. and Stassi, D. (1997) 'Identification and Characterization of the Niddamycin Polyketide Synthase Genes from *Streptomyces caelestis*.' *Journal of Bacteriology*, 179, (23): 7515-7522.

Kakirde, K. S., Wild, J., Godiska, R., Mead, D. A., Wiggins, A. G., Goodman, R. M., Szybalski, W. and Liles, M. R. (2010) 'Gram negative shuttle BAC vector for heterologous expression of metagenomic libraries.' *Gene*, 475, (2): 57-62.

Kapur, S., Lowry, B., Yuzawa, S., Kenthirapalan, S., Chen, A. Y., Cane, D. E. and Khosla, C. (2012) 'Reprogramming a module of the 6-deoxyerythronolide B synthase for iterative chain elongation.' *Proceedings of the National Academy of Sciences of the United States of America*, 109, (11): 4110–4115.

Kasbekar, N. (2006) 'Tigecycline: A new glycylcycline antimicrobial agent.' *American Journal of Health-System Pharmacy*, 63, (13): 1235-1243.

Katayama, Y., Ito, T. and Hiramatsu, K. (2000) 'A New Class of Genetic Element, Staphylococcus Cassette Chromosome mec, Encodes Methicillin Resistance in *Staphylococcus aureus*.' *Antimicrobial Agents and Chemotherapy*, 44, (6): 1549–1555.

Keam, S. J. (2008) 'Doripenem. A review of its use in the treatment of bacterial infections.' *Drugs*, 68, (14): 2021-2057.

Keatinge-Clay, A. (2008) 'Crystal Structure of the Erythromycin Polyketide Synthase Dehydratase.' *Journal of Molecular Biology*, 384, 941–953.

Keatinge-Clay, A. T., Shelat, A. A., Savage, D. F., Tsai, S.-C., Miercke, L. J. W., O'Connell, J. D., Khosla, C. and Stroud, R. M. (2003) 'Catalysis, Specificity, and ACP Docking Site of *Streptomyces coelicolor* Malonyl-CoA:ACP Transacylase.' *Structure*, 11, 147-154.

Kelesidis, T., Humphries, R., Uslan, D. Z. and Pegues, D. A. (2011) 'Daptomycin Nonsusceptible *Enterococci*: An Emerging Challenge for Clinicians.' *Clinical Infectious Diseases*, 52, (2): 228-234.

Kellner, R. L. L. (2002) 'Molecular identification of an endosymbiotic bacterium associated with pederin biosynthesis in *Paederus sabaeus* (Coleoptera: Staphylinidae).' *Insect Biochemistry and Molecular Biology*, 32, (4): 389-395.

Kevany, B. M., Rasko, D. A. and Thomas, M. G. (2009) 'Characterization of the Complete Zwittermicin A Biosynthesis Gene Cluster from *Bacillus cereus*.' *Applied and Environmental Microbiology*, 75, (4): 1144–1155.

Kim, S., Kim, S.-H., Chun, S.-G., Park, M.-S., Lim, H. M. and Lee, B. K. (2009) 'An Additional Novel Antimicrobial Resistance Gene Cluster in *Salmonella* Genomic Island 1 of a *Salmonella enterica* Serovar Typhimurium DT104 Human Isolate.' *Foodborne Pathogens and Diease*, 6, (4): 471-479.

Klimek, J. W., Cavallito, C. J. and Bailey, J. H. (1948) 'Induced resistance of *Staphylococcus aureus* to various antibiotics.' *The Lancet*, 55, 139-145.

Knowles, T. J., Finka, R., Smith, C., Lin, Y.-P., Dafforn, T. and Overduin, M. (2009) 'Membrane Proteins Solubilized Intact in Lipid Containing Nanoparticles Bounded by Styrene Maleic Acid Copolymer.' *Journal of the American Chemical Society*, 131, 7484-7485.

Kohanski, M. A., Dwyer, D. J. and Collins, J. J. (2010) 'How Antibiotics Kill Bacteria: from Targets to Networks.' *Nature Reviews Microbiology*, 8, 423-435.

Kopp, M., Irschik, H., Pradella, S. and Müller, R. (2005) 'Production of the Tubulin Destabilizer Disorazol in *Sorangium cellulosum*: Biosynthetic Machinery and Regulatory Genes.' *Chembiochem*, 6, 1277-1286.

Kriebs, J. M. (2008) 'Methicillin-Resistant *Staphylococcus aureus* Infection in the Obstetric Setting.' *Journal of Midwifery & Women's Health*, 53, (3): 247-250.

Kumarasamy, K. K., Toleman, M. A., Walsh, T. R., Bagaria, J., Butt, F. a., Balakrishnan, R., Chaudhary, U., Doumith, M., Giske, C. G., Irfan, S., Krishnan, P., Kumar, A. V., Maharjan, S., Mushtaq, S., Noorie, T., Paterson, D. L., Pearson, A., Perry, C., Pike, R., Rao, B., Ray, U., Sarma, J. B., Sharma, M., Sheridan, E., Thirunarayan, M. A., Turton, J., Upadhyay, S., Warner, M., Welfare, W., Livermore, D. M. and Woodford, N. (2011) 'Emergence of a new antibiotic resistance mechanism in India, Pakistan, and the UK: a molecular, biological, and epidemiological study.' *The Lancet Infectious Diseases*, 10, 597-602.

Kyte, L. (2011) 'Deaths involving *Clostridium difficile*: England and Wales, 2006 to 2010.' Office for National Statistics.

Lal, R., Kumari, R., Kaur, H., Khanna, R., Dhingra, N. and Tuteja, D. (2000) 'Regulation and manipulation of the gene clusters encoding type-I PKSs.' *Trends in Biotechnology*, 18, 264-274.

Lambalot, R. H., Gehring, A. M., Flugel, R. S., Zuber, P., LaCelle, M., Marahiel, M. A., Reid, R., Khosla, C. and Walsh, C. T. (1996) 'A new enzyme superfamily - the phosphopantetheinyl transferases.' *Chemistry and Biology*, 3 (11): 923-936.

Landsberg, H. (1949) 'Prelude to the Discovery of Penicillin.' *Isis*, 40, (3): 225-227.

Larkin, M. (2003) 'Daptomycin approved for skin and skin-structure infections.' *The Lancet*, 3, 677.

Lau, J., Cane, D. E. and Khosla, C. (2000) 'Substrate Specificity of the Loading Didomain of the Erythromycin Polyketide Synthase.' *Biochemistry*, 39, (34): 10514-10520.

Laxminarayan, R. and Powers, J. H. (2011) 'Antibacterial R&D incentives.' *Nature Reviews Drug Discovery*, 10, 727-728.

Lederberg, J. and Tatum, E. L. (1946) 'Gene Recombination in *Escherichia coli*.' *Nature*, 158, 558.

LGC Standards (2010) 'Product Description - *Pseudomonas fluorescens* NCIMB 10586.' http://www.lgcstandards-atcc.org/LGCAdvancedCatalogueSearch/ProductDescription/tabid/1068/Default.aspx?ATCCNum=49323&Template=bacteria. Accessed: August 12th 2010.

Lilie, H., Schwarz, E. and Rudolph, R. (1998) 'Advances in refolding of proteins produced in *E. coli*.' *Current Opinion in Biotechnology*, 9, 497-501.

Lim, S.-K., Ju, J., Zazopoulos, E., Jiang, H., Seo, J.-W., Chen, Y., Feng, Z., Rajski, S. R., Farnet, C. M. and Shen, B. (2009) '*iso*-Migrastatin, Migrastatin, and Dorrigocin Production in *Streptomyces platensis* NRRL 18993 Is Governed by a Single Biosynthetic Machinery Featuring an Acyltransferase-less Type I Polyketide Synthase.' *The Journal of Biological Chemistry*, 284, (43): 29746-29756.

Lindblad, W. J. (2008) 'Review Paper: Considerations for Determining if a Natural Product Is an Effective Wound-Healing Agent.' *The International Journal of Lower Extremity Wounds*, 7, (2): 75-81.

Liu, L., Thamchaipenet, A., Fu, H., Betlach, M. and Ashley, G. (1997) 'Biosynthesis of 2-Nor-6-deoxyerythronolide B by Rationally Designed Domain Substitution.' *Journal of the Americal Chemical Society*, 119, 10553-10554.

Loening, A. (2005) 'Site directed mutagenesis protocol.' www.standford.edu/~loening/protocols.html. Accessed: October 12th 2011.

Logan, R. T. (2012) 'Personal communication.' The University of Birmingham.

Long, P. F., Wilkinson, C. J., Bisang, C. P., Cortés, J., Dunster, N., Oliynyk, M., McCormick, E., McArthur, H., Mendez, C., Salas, J. A., Staunton, J. and Leadlay, P. F. (2002) 'Engineering specificity of starter unit selection by the erythromycin-producing polyketide synthase.' *Molecular Microbiology*, 43, (5): 1215-1225.

Lopanik, N. B., Shields, J. A., Buchholz, T. J., Rath, C. M., Hothersall, J., Haygood, M. G., Håkansson, K., Thomas, C. M. and Sherman, D. H. (2008) '*In Vivo* and *In Vitro Trans*-Acylation by BryP, the Putative Bryostatin Pathway Acyltransferase Derived from an Uncultured Marine Symbiont.' *Chemistry and Biology*, 15, 1175-1186.

Louie, T. J., Emery, J., Krulicki, W., Byrne, B. and Mah, M. (2009) 'OPT-80 Eliminates *Clostridium difficile* and Is Sparing of Bacteroides Species during Treatment of *C. difficile* Infection.' *Antimicrobial Agents and Chemotherapy*, 53, (1): 261-263.

Lugtenberg, B. J. J. and Bloemberg, G. V. (2004) 'Life in the Rhizospere.' In: J.-L. Ramos (Ed.) 'Pseudomonas.' New York, Kluwer Academic/Plenum Publishers.

Lund, P. (1993) 'Unpublished Data.' The University of Birmingham.

Ma, S. M. and Tang, Y. (2007) 'Biochemical characterization of the minimal polyketide synthase domains in the lovastatin nonaketide synthase LovB.' *The FEBS Journal*, 274, 2854-2864.

Macioszek, M. (2009) 'Biosynthesis of mupirocin by *Pseudomonas fluorescens* NCIMB 10586.' PhD Thesis The University of Birmingham, Birmingham.

Madan, D., Lin, Z. and Rye, H. S. (2008) 'Triggering Protein Folding within the GroEL-GroES Complex.' *The Journal of Biological Chemistry*, 283, (46): 32003–32013.

Magnuson, K., Jackowski, S., Rock, C. and John E. Cronan, J. (1993) 'Regulation of Fatty Acid Biosynthesis in *Escherichia coli*.' *Microbiological Reviews*, 57, (3): 522-542.

Maier, T., Leibundgut, M. and Ban, N. (2008) 'The Crystal Structure of a Mammalian Fatty Acid Synthase.' *Science*, 321, 1315-1322.

Marsden, A. F. A., Caffrey, P., Aparicio, J. F., Loughran, M. S., Staunton, J. and Leadlay, P. F. (1994) 'Stereospecific Acyl Transfers on the Erythromycin-Producing Polyketide Synthase.' *Science*, 263, 378-380.

Marsden, A. F. A., Wilkinson, B., Cortés, J., Dunster, N. J., Staunton, J. and Leadlay, P. F. (1998) 'Engineering Broader Specificity into an Antibiotic-Producing Polyketide Synthase.' *Science*, 279, 199-202.

Marston, F. A. O. and Hartley, D. L. (1990) 'Solubilization of Protein Aggregates.' In: M. P. Deutscher (Ed.) 'Guide to Protein Purification.' San Diego, Academic Press INC.

Martin, F. M. and Simpson, T. J. (1989) 'Biosynthetic Studies on Pseudomonic Acid (Mupirocin), a Novel Antibiotic Metabolite of *Pseudomonas fluorescens*.' *Journal of the Chemical Society Perkin Transactions I*, 207-209.

Mattheus, W., Gao, L.-J., Herdewijn, P., Landuyt, B., Verhaegen, J., Masschelein, J., Volckaert, G. and Lavigne, R. (2010) 'Isolation and Purification of a New Kalimantacin/Batumin-Related Polyketide Antibiotic and Elucidation of Its Biosynthesis Gene Cluster.' *Chemistry and Biology*, 17, 149-159.

McDaniel, R., Ebert-Khosla, S., Hopwood, D. A. and Khosla, C. (1993) 'Engineered Biosynthesis of Novel Polyketides.' *Science*, 262, 1546-1550.

McDaniel, R., Ebert-Khosla, S., Hopwood, D. A. and Khosla, C. (1995) 'Rational Design of aromatic polyketide products by recombinant assembly of enzymatic subunits.' *Nature*, 375, 549-554.

McDaniel, R., Thamchaipenet, A., Gustafsson, C., Fu, H., Betlach, M., Betlach, M. and Ashley, G. (1999) 'Multiple genetic modifications of the erythromycin polyketide synthase to produce a library of novel ''unnatural'' natural products.' *Proceedings of the National Academy of Sciences of the United States of America*, 96, 1846–1851.

McGuffin, L. J., Bryson, K. and Jones, D. T. (2000) 'The PSIPRED protein structure prediction server.' *Bioinformatics*, 16, 404-405.

Mdludli, K., Slayden, R. A., Zhu, Y., Ramaswamy, S., Pan, X., Mead, D., Crane, D. D., Musser, J. M. and Barry, C. E. (1998) 'Inhibition of a Mycobacterium tuberculosis b-Ketoacyl ACP Synthase by Isoniazid.' *Science*, 280, 1607-1610.

Medimetriks (2008) 'Products.' http://medimetriks.com/content/blogsection/6/36/. Accessed: August 9th 2010.

Menche, D., Arikan, F., Perlova, O., Horstmann, N., Ahlbrecht, W., Wenzel, S. C., Jansen, R., Irschik, H. and Müller, R. (2008) 'Stereochemical Determination and Complex Biosynthetic Assembly of Etnangien, a Highly Potent RNA Polymerase Inhibitor from the Myxobacterium *Sorangium cellulosum*.' *Journal of the American Chemical Society*, 130, 14234–14243.

Mercer, A. C. and Burkart, M. D. (2007) 'The ubiquitous carrier protein—a window to metabolite biosynthesis.' *Natural Product Reports*, 24, 750-773.

Merck (2005) 'pET System Manual.' (11th Ed) EMD Biosciences.

Migliori, G. B., Besozzi, G., Girardi, E., Kliiman, K., Lange, C., Toungoussova, O. S., Ferrara, G., Cirillo, D. M., Gori, A., Matteelli, A., Spanevello, A., Codecasa, L. R. and Raviglione, M. C. (2007a) 'Clinical and operational value of the extensively drug-resistant tuberculosis definition.' *European Respiratory Journal*, 30, 623-626.

Migliori, G., Iaco, G. D., Besozzi, G., Centis, R. and Cirillo, D. (2007b) 'First tuberculosis cases in Italy resistant to all tested drugs.' *Eurosurveillance*, 12, (20): 3194.

Mochizuki, S., Hiratsu, K., Suwa, M., Ishii, T., Sugino, F., Yamada, K. and Kinashi, H. (2003) 'The large linear plasmid pSLA2-L of *Streptomyces rochei* has an unusually condensed gene organization for secondary metabolism.' *Molecular Microbiology*, 48, (6): 1501-1510.

Moir, A., Lafferty, E. and Smith, D. A. (1979) 'Genetic analysis of spore germination mutants of *Bacillus subtilis* 168: the correlation of phenotype with map location.' *Journal of General Microbiology*, 111, 165-180.

Moore, B. S. and Hopke, J. N. (2001) 'Discovery of a New Bacterial Polyketide Biosynthetic Pathway.' *Chembiochem*, 2, 35-38.

Mootz, H. D., Schwarzer, D. and Marahiel, M. A. (2002) 'Ways of Assembling Complex Natural Products on Modular Nonribosomal Peptide Synthetases ' *Chembiochem*, 3, 490-504.

Moran, L. A., Scrimgeour, K. G., Horton, H. R., Ochs, R. S. and Rawn, J. D. (1994) 'Biochemistry.' London, Prentice-Hall International (UK) Limited.

Moriguchi, T., Ebizuka, Y. and Fujii, I. (2006) 'Analysis of Subunit Interactions in the Iterative Type I Polyketide Synthase ATX from *Aspergillus terreus*.' *Chembiochem*, 7, 1869 – 1874.

Morrissey, I., Hoshino, K., Sato, K., Yoshida, A., Hayakawa, I., Bures, M. G. and Shen, L. L. (1996) 'Mechanism of Differential Activities of Ofloxacin Enantiomers.' *Antimicrobial Agents and Chemotherapy*, 40, (8): 1775-1784.

Morrissey, J. P., Cullinane, M., Abbas, A., Mark, G. L. and O'gara, F. (2004) 'Biosynthesis and regulation of anti-fungal metabolites by Pseudomonads.' In: J.-L. Ramos (Ed.) 'Pseudomonas.' New York, Kluwer Academic/Plenum Publishers.

Moss, S. J., Martin, C. J. and Wilkinson, B. (2002) 'Loss of co-linearity by modular polyketide synthases: a mechanism for the evolution of chemical diversity.' *Natural Product Reports*, 21, 575-593.

Murphy, A. C., Fukuda, D., Song, Z., Hothersall, J., Cox, R. J., Willis, C. L., Thomas, C. M. and Simpson, T. J. (2011) 'Engineered Thiomarinol Antibiotics Active against MRSA Are Generated by Mutagenesis and Mutasynthesis of *Pseudoalteromonas* SANK73390.' *Angewandte Chemie International Edition*, 50, 3271-3274.

Musiol, E. M., Härtner, T., Kulik, A., Moldenhauer, J., Piel, J., Wohlleben, W. and Weber, T. (2011) 'Supramolecular Templating in Kirromycin Biosynthesis: The Acyltransferase KirCII Loads Ethylmalonyl-CoA Extender Onto a Specific ACP of the *trans*-AT PKS.' *Chemistry and Biology*, 18, (4): 438-444.

Musiol, E. M. and Weber, T. (2012) 'Discrete acyltransferases involved in polyketide biosynthesis.' *MedChemComm*, 3, 871-886.

Nagai, K., Davies, T. A., Jacobs, M. R. and Appelbaum, P. C. (2002) 'Effects of Amino Acid Alterations in Penicillin-Binding Proteins (PBPs) 1a, 2b, and 2x on PBP Affinities of Penicillin, Ampicillin, Amoxicillin, Cefditoren, Cefuroxime, Cefprozil, and Cefaclor in 18 Clinical Isolates of Penicillin-Susceptible, -Intermediate, and -Resistant Pneumococci.' *Antimicrobial Agents and Chemotherapy*, 46, (5): 1273-1280.

Nakajima, J., Hitomi, S. and Kurihara, Y. (2011) 'Detection of methicillin-resistant *Staphylococcus aureus* with high-level resistance to mupirocin.' *Journal of Infection and Chemotherapy*, 17, (6): 868-871.

Nakama, T., Nureki, O. and Yokoyama, S. (2001) 'Structural Basis for the Recognition of Isoleucyl-Adenylate and an Antibiotic, Mupirocin, by Isoleucyl-tRNA Synthetase.' *The Journal of Biological Chemistry*, 276, (50): 47387-47393.

Nelson, D. L. and Cox, M. M. (2005) 'Lehninger Principles of Biochemistry.' New York, W. H. Freeman and Company.

Neu, H. C. (1992) 'The Crisis in Antibiotic Resistance.' *Science*, 257, 1064-1073.

Nguyen, T., Ishida, K., Jenke-Kodama, H., Dittmann, E., Gurgui, C., Hochmuth, T., Taudien, S., Platzer, M., Hertweck, C. and Piel, J. (2008) 'Exploiting the mosaic structure of trans-acyltransferase polyketide synthases for natural product discovery and pathway dissection.' *Nature Biotechnology*, 26, (2): 225-233.

O'Hanlon, P. J., Rogers, N. H. and Tyler, J. W. (1983) 'The Chemistry of Pseudomonic Acid. Part 6.' Structure and Preparation of Pseudomonic Acid D.' *The Journal of the Chemical Society Perkins Transactions I*, 2655-2657.

Oefner, C., Henk Schulz, D'Arcy, A. and Dale, G. E. (2006) 'Mapping the active site of *Escherichia coli* malonyl-CoA–acyl carrier protein transacylase (FabD) by protein crystallography.' *Acta Crystallographica Section D Biological Crystallography*, D62, 613-618.

Ohana, R. F., Encell, L. P., Zhao, K., Simpson, D., Slater, M. R., Urh, M. and Wood, K. V. (2009) 'HaloTag7: A genetically engineered tag that enhances bacterial expression of soluble proteins and improves protein purification.' *Protein Expression and Purification*, 68, 110-120.

Oliva, B., O'Neill, A., Wilson, J. M., O'Hanlon, P. J. and Chopra, I. (2001) 'Antimicrobial Properties and Mode of Action of the Pyrrothine Holomycin.' *Antimicrobial Agents and Chemotherapy*, 45, (2): 532-539.

Oliynyk, M., Brown, M. J. B., Cortés, J., Staunton, J. and Leadlay, P. F. (1996) 'A hybrid modular polyketide synthase obtained by domain swapping.' *Chemistry and Biology*, 3, 833-839.

Omer-Bali, A. (2012) 'Personal communications.' The University of Birmingham.

Orrett, F. A. (2008) 'The Emergence of Mupirocin Resistance among Clinical Isolates of Methicillin-Resistant *Staphylococcus aureus* in Trinidad: a First Report.' *Japanese Journal of Infectious Disease*, 61, 107-110.

Otsuka, M., Ichinose, K., Fujii, I. and Ebizuka, Y. (2004) 'Cloning, Sequencing, and Functional Analysis of an Iterative Type I Polyketide Synthase Gene Cluster for Biosynthesis of the Antitumor Chlorinated Polyenone Neocarzilin in "*Streptomyces carzinostaticus*".' *Antimicrobial Agents and Chemotherapy*, 48, (9): 3468-3476.

Oxford Protein Production Facility (2011) http://www.oppf.ox.ac.uk/OPPF/. Accessed: 18th April 2011.

Palleroni, N. J. and Moore, E. R. B. (2004) 'Taxonomy of *Pseudomonas*: Experimental Approaches.' In: J.-L. Ramos (Ed.) 'Pseudomonas.' New York, Kluwer Academic/Plenum Publishers.

Park, S. Y., Kim, S. M. and Park, S. D. (2012) 'The Prevalence, Genotype and Antimicrobial Susceptibility of High- and Low-Level Mupirocin Resistant Methicillin-Resistant *Staphylococcus aureus*.' *Annals of Dermatology*, 24, (1): 32-38.

Partida-Martinez, L. P. and Hertweck, C. (2007) 'A Gene Cluster Encoding Rhizoxin Biosynthesis in "*Burkholderia rhizoxina*", the Bacterial Endosymbiont of the Fungus *Rhizopus microsporus*.' *Chembiochem*, 8, 41-45.

Patel, J. B., Gorwitz, R. and Jernigan, J. A. (2009) 'Mupirocin Resistance.' *Clinical Infectious Diseases*, 49, 935-941.

Patel, U., Yan, Y. P., Frank W. Hobbs, J., Kaczmarczyk, J., Slee, A. M., Pompliano, D. L., Kurilla, M. G. and Bobkova, E. V. (2001) 'Oxazolidinones Mechanism of Action: Inhibition of the First Peptide Bond Formation.' *The Journal of Biological Chemistry*, 276, (40): 37199-37205.

Paulsen, I. T., Brown, M. H. and Skurray, R. A. (1996) 'Proton-Dependent Multidrug Efflux Systems.' *Microbiological Reviews*, 60, (4): 575-608.

Pazirandeh, M., Chirala, S. S. and Wakil, S. J. (1991) 'Site-directed Mutagenesis Studieso n the Recombinant Thioesterase Domain of Chicken Fatty Acid Synthase Expressed in *Escherichia coli.' The Journal of Biological Chemistry*, 266 (35): 20946-20952.

Pegler, K. (2012) 'Deaths Involving *Clostridium difficile*, England and Wales, 2011.' Office for National Statistics.

Pérez-Gil, J., Calisto, B. M., Behrendt, C., Kurz, T., Ignacio Fita and Rodríguez-Concepción, M. (2012) 'Crystal Structure of *Brucella abortus* Deoxyxylulose-5-phosphate Reductoisomerase-like (DRL) Enzyme Involved in Isoprenoid Biosynthesis ' *The Journal of Biological Chemistry*, 287, 15803-15809.

Perez-Roth, E., Kwong, S. M., Alcoba-Florez, J., Firth, N. and Mendez-Alvarez, S. (2010) 'Complete Nucleotide Sequence and Comparative Analysis of pPR9, a 41.7-Kilobase Conjugative *Staphylococcal* Multiresistance Plasmid Conferring High-Level Mupirocin Resistance.' *Antimicrobial Agents and Chemotherapy*, 54, (5): 2252-2257.

Perlova, O., Gerth, K., Kaiser, O., Hans, A. and Müller, R. (2006) 'Identification and analysis of the chivosazol biosynthetic gene cluster from the myxobacterial model strain *Sorangium cellulosum* So ce56.' *Journal of Biotechnology*, 121, 147-191.

Pfizer (2002) 'Pfizer Inc: Exploring Our History 1900-1950.' http://www.pfizer.com/about/history/1900_1950.jsp. Accessed: 15th August 2012.

Piel, J. (2002) 'A polyketide synthase-peptide synthetase gene cluster from an uncultured bacterial symbiont of Paederus beetles.' *Proceedings of the National Academy of Sciences of the United States of America*, 99, (22): 14002-14007.

Piel, J. (2009) 'Metabolites from symbiotic bacteria.' *Natural Product Reports*, 26, 338-362.

Piel, J. (2010) 'Biosynthesis of Polyketides by trans-AT polyketide synthases.' *Natural Product Report*, 27, 996-1047.

Piel, J., Wen, G., Platzer, M. and Hui, D. (2004) 'Unprecedented Diversity of Catalytic Domains in the First Four Modules of the Putative Pederin Polyketide Synthase.' *Chembiochem*, 5, 93-98.

Price, A. C., Zhang, Y.-M., Rock, C. O. and White, S. W. (2004) 'Cofactor-Induced Conformational Rearrangements Establish a Catalytically Competent Active Site and a Proton Relay Conduit in FabG.' *Structure*, 12, 417-428.

Pulsawat, N., Kitani, S. and Nihira, T. (2007) 'Characterization of biosynthetic gene cluster for the production of virginiamycin M, a streptogramin type A antibiotic, in *Streptomyces virginiae*.' *Gene*, 393, 31-42.

Qoronfleh, M. W., Hesterberg, L. K. and Seefeldt, M. B. (2007) 'Confronting high-throughput protein refolding using high pressure and solution screens.' *Protein Expression and Purification*, 55, 209-224.

Racher, K. I., Kalmar, G. B. and Borgford, T. J. (1991) 'Expression and characterization of a recombinant yeast isoleucyl-tRNA synthetase.' *The Journal of Biological Chemistry*, 266, (26): 17158-17164.

Rahman, A. S., Hothersall, J., Crosby, J., Simpson, T. J. and Thomas, C. M. (2005) 'Tandemly Duplicated Acyl Carrier Proteins, Which Increase Polyketide Antibiotic Production, Can Apparently Function Either in Parallel or in Series.' *The Journal of Biological Chemistry*, 280, (8): 6399–6408.

Rahman, M., Noble, W. C. and Cookson, B. (1987) 'Mupirocin-Resistant *Staphylococcus aureus*.' *The Lancet*, 330, (8555): 377-378.

Raja, A., LaBonte, J., Lebbos, J. and Kirkpatrick, P. (2003) 'Daptomycin.' *Nature Reviews Drug Discovery*, 2, 943-944.

Ramsey, M. A., Bradley, S. F., Kauffman, C. A. and Morton, T. M. (1996) 'Identification of Chromosomal Location of mupA Gene, Encoding Low-Level Mupirocin Resistance in *Staphylococcal* Isolates.' *Antimicrobial Agents and Chemotherapy*, 40, (12): 2820-2823.

Rangan, V. S. and Smith, S. (1997) 'Alteration of the Substrate Specificity of the Malonyl-CoA/Acetyl-CoA:Acyl Carrier Protein S-Acyltransferase Domain of the Multifunctional Fatty Acid Synthase by Mutation of a Single Arginine Residue.' *The Journal of Biological Chemistry*, 272, (18): 11975-11978.

Rawlings, M. and Cronan, J. E. (1992) 'The gene encoding *Escherichia coli* acyl carrier protein lies within a cluster of fatty acid biosynthetic genes.' *The Journal of Biological Chemistry*, 267, (9): 5751-4.

Redfield, R. J. (2002) 'Is quorum sensing a side effect of diffusion sensing?' *Trends in Microbiology*, 10, (8): 365-370.

Reed, R., Holmes, D., Weyers, J. and Jones, A. (2003) 'Practical Skills in Biomolecular Sciences.' London, Pearson.

Reeves, C. D., Murli, S., Ashley, G. W., Piagentini, M., Hutchinson, C. R. and McDaniel, R. (2001) 'Alteration of the Substrate Specificity of a Modular Polyketide Synthase Acyltransferase Domain through Site-Specific Mutations.' *Biochemistry*, 40, (51): 15464-15470.

Remold, S. K., Brown, C. K., Farris, J. E., Hundley, T. C., Perpich, J. A. and Purdy, M. E. (2011) 'Differential Habitat Use and Niche Partitioning by *Pseudomonas* Species in Human Homes.' *Microbial Ecology*, 62, 505-517.

Reynolds, R. (2009) 'Antimicrobial resistance in the UK and Ireland.' *Journal of Antimicrobial Chemotherapy*, 64, (suppl 1): i19-i23.

Richardson, M. T., Pohl, N. L., Kealey, J. T. and Khosla, C. (1999) 'Tolerance and Specificity of Recombinant 6-Methylsalicylic Acid Synthase.' *Metabolic Engineering*, 1, 180-187.

Ridley, C. P., Lee, H. Y. and Khosla, C. (2008) 'Evolution of polyketide synthases in bacteria.' *PNAS*, 105, (12): 4595–4600.

Rodier, D. G. (2011) 'European strategic action plan on antibiotic resistance 2011–2016.' In: WHO Regional Committee for Europe, 12-15 September 2011, Baku, Azerbaijan. World Health Organisation.

Rodríguez-Beltrán, J., Elabed, H., Gaddour, K., Blázquez, J. and Rodríguez-Rojas, A. (2012) 'Simple DNA transformation in *Pseudomonas* based on the Yoshida effect.' *Journal of Microbiological Methods*, 89, (2): 95-98.

Rolinson, G. N., Batchelor, F. R., Stevens, S., Wood, J. C. and Chain, E. B. (1960) 'Bacteriological Studies on a New Penicillin - BRL. 1241.' *The Lancet*, (Sept 10): 564-567.

Royer, M., Costet, L., Vivien, E., Bes, M., Cousin, A., Damais, A., Pieretti, I., Savin, A., Megessier, S., Viard, M., Frutos, R., Gabriel, D. W. and Rott, P. C. (2004) 'Albicidin Pathotoxin Produced by *Xanthomonas albilineans* Is Encoded by Three Large PKS and NRPS Genes Present in a Gene Cluster Also Containing Several Putative Modifying, Regulatory, and Resistance Genes.' *Molecular Plant-Microbe Interactions*, 17, (4): 414-427.

Rowe, C. J., Böhm, I. U., Thomas, I. P., Wilkinson, B., Rudd, B. A. M., Foster, G., Blackaby, A. P., Sidebottom, P. J., Roddis, Y., Buss, A. D., Staunton, J. and Leadlay, P. F. (2001) 'Engineering a polyketide with a longer chain by insertion of an extra module into the erythromycin-producing polyketide synthase.' *Chemistry & Biology*, 8, 475-485.

Ruan, X., Pereda, A., Stassi, D. L., Zeidner, D., Summers, R. G., Jackson, M., Shivakumar, A., Kakavas, S., Staver, M. J., Donadio, S. and Katz, L. (1997) 'Acyltransferase Domain Substitutions in Erythromycin Polyketide Synthase Yield Novel Erythromycin Derivatives.' *Journal of Bacteriology*, 179, (20): 6416-6425.

Russo, E. (2003) 'Special Report.' *Nature*, 421, 456-457.

Sambrook, J. and Russell, D. W. (2001) 'Molecular Cloning A Laboratory Manual.' New York, Cold Spring Harbor Laboratory Press.

Schaffer, M. L. and Otten, L. G. (2009) 'Substrate flexibility of the adenylation reaction in the Tyrocidine non-ribosomal peptide synthetase.' *Journal of Molecular Catalysis B: Enzymatic*, 59, 140–144.

Schneider, K., Chen, X.-H., Vater, J., Franke, P., Nicholson, G., Borriss, R. and Süssmuth, R. D. (2007) 'Macrolactin is the Polyketide Biosynthesis Product of the pks2 Cluster of *Bacillus amyloliquefaciens* FZB42.' *Journal of Natural Products*, 70, 1417–1423.

Schneider, T. D. and Stevens, R. M. (1990) 'Sequence Logos: A New Way to Display Consensus Sequences.' *Nucleic Acids Research*, 18, 6097-6100.

Schröder, J., Raiber, S., Berger, T., Schmidt, A., Schmidt, J., Soares-Sello, A. M., Bardshiri, E., Strack, D., Simpson, T. J., Veit, M. and Schröder, G. (1998) 'Plant Polyketide Synthases: A Chalcone Synthase-Type Enzyme Which Performs a Condensation Reaction with Methylmalonyl-CoA in the Biosynthesis of C-Methylated Chalcones.' *Biochemistry*, 37, (23): 8417-8425.

Schujman, G. E. and de Mendoza, D. (2008) 'Regulation of type II fatty acid synthase in Gram-positive bacteria.' *Current Opinion in Microbiology*, 11, 148-152.

Seah, C., Alexander, D. C., Louie, L., Simor, A., Low, D. E., Longtin, J. and Melano, R. G. (2012) 'MupB, a New High-Level Mupirocin Resistance Mechanism in *Staphylococcus aureus*.' *Antimicrobial Agents and Chemotherapy*, 56, (4): 1916-1920.

Serafini, F., Bottacini, F., Viappiani, A., Baruffini, E., Turroni, F., Foroni, E., Lodi, T., Sinderen, D. v. and Ventura, M. (2011) 'Insights into Physiological and Genetic Mupirocin Susceptibility in Bifidobacteria.' *Applied and Environmental Microbiology*, 77, (9): 3141–3146.

Serre, L., Verbree, E. C., Dauter, Z., Stuitje, A. R. and Derewenda, Z. S. (1995) 'The *Escherichia coli* Malonyl-CoA:Acyl Carrier Protein Transacylase at 1.5-Å Resolution.' *The Journal of Biological Chemistry*, 270, (22): 12961-12964.

Shields, J. (2008) 'Biosynthesis of the polyketide antibiotic mupirocin by *Pseudomonas fluorescens* NCIMB 10586.' PhD Thesis. The University of Birmingham, Birmingham.

Shields, J. A., Rahman, A. S., Arthur, C. J., Crosby, J., Hothersall, J., Simpson, T. J. and Thomas, C. M. (2010) 'Phosphopantetheinylation and Specificity of Acyl Carrier Proteins in the Mupirocin Biosynthetic Cluster.' *ChemBioChem*, 11, (2): 248-255.

Shiozawa, H., Kagasaki, T., Kinoshita, T., Haruyama, H., Domon, H., Utsui, Y., Kodama, K. and Takahashi, S. (1993) 'Thiomarinol, A New Hybrid Antimicrobial Antibiotic Produced By A Marine Bacterium.' *The Journal Of Antibiotics*, 46, (12): 1834-1842.

Shiozawa, H., Kagasaki, T., Torikata, A., Tanaka, N., Fujimoto, K., Hata, T., Furukawat, Y. and Takahashi, S. (1995) 'Thiomarinols B and C, New Antimicrobial Antibiotics Produced by a Marine Bacterium.' *THE JOURNAL OF ANTIBIOTICS*, 48, (8): 907-909.

Shiozawa, H., Shimada, A. and Takahashi, S. (1997) 'Thiomarinols D, E, F and G, NewHybrid Antimicrobial Antibiotics Produced by a Marine Bacterium; Isolation, Structure, and Antimicrobial Activity.' *THE JOURNAL OF ANTIBIOTICS*, 50, (5): 449-452.

Silakowski, B., Nordsiek, G., Kunze, B., Blöcker, H. and Müller, R. (2001) 'Novel features in a combined polyketide synthase/non-ribosomal peptide synthetase: the myxalamid biosynthetic gene cluster of the myxobacterium *Stigmatella aurantiaca* Sga15.' *Chemistry & Biology*, 8, (1): 59-69.

Silvian, L. F., Wang, J. and Steitz, T. A. (1999) 'Insights into Editing from an ILe-tRNA Synthetase Structure with tRNAILe and Mupirocin ' *Science*, 285, 1074-1077.

Simon, R., Priefer, V. and Puhler, A. (1983) 'A broad host range mobilisation system for *in vivo* genetic engineering: transposon mutagenesis in Gram-negative bacteria.' In: 'Biotechnology.' pp. 784-791.

Simor, A. E., Stuart, T. L., Louie, L., Watt, C., Ofner-Agostini, M., Gravel, D., Mulvey, M., Loeb, M., McGeer, A., Bryce, E., Matlow, A. and The Canadian Nosocomial Infection Surveillance Program (2007) 'Mupirocin-Resistant, Methicillin-Resistant *Staphylococcus aureus* Strains in Canadian Hospitals.' *Antimicrobial Agents and Chemotherapy*, 51, (11): 3880-3886.

Simunovic, V., Zapp, J., Rachid, S., Krug, D., Meiser, P. and Müller, R. (2006) 'Myxovirescin A Biosynthesis is Directed by Hybrid Polyketide Synthases/Nonribosomal Peptide Synthetase, 3-Hydroxy-3-Methylglutaryl–CoA Synthases, and trans-Acting Acyltransferases.' *Chembiochem*, 7, 1206-1220.

Skarzynski, T., Kim, D. H., Lees, W. J., Walsh, C. T. and Duncan, K. (1998) 'Stereochemical Course of Enzymatic Enolpyruvyl Transfer and Catalytic Conformation of the Active Site Revealed by the Crystal Structure of the Fluorinated Analogue of the Reaction Tetrahedral Intermediate Bound to the Active Site of the C115A Mutant of MurA.' *Biochemistry*, 37, 2572-2577.

Skinner, R., Cundliffe, E. and Schmidt, F. J. (1983) 'Site of Action of a Ribosomal RNA Methylase Responsible for Resistance to Erythromycin and Other Antibiotics.' *The Journal of Biological Chemistry*, 258, (20): 12702-12706.

Skinner, R. H. and Cundliffe, E. (1982) 'Dimethylation of Adenine and the Resistance of *Streptomyces erythrueus* to Erythromycin.' *Journal of General Microbiology*, 128, 2411-2416.

Slocombe, B. and Perry, C. (1991) 'The antimicrobial activity of mupirocin—an update on resistance ' *Journal of Hospital Infection*, 19, (Supp2): 19-25.

Smith, S. and Tsai, S-C. (2007) 'The type I fatty acid and polyketide synthases: a tale of two megasynthases.' *Natural Product Reports*, 24, 1041-1072.

Smith, D. B. and Johnson, K. S. (1988) 'Single-step purification of polypeptides expressed in *Escherichia coli* as fusions with glutathione-*S*-transferase.' *Gene*, 67, (1): 31-40.

Sørensen, H. P. and Mortensen, K. K. (2005) 'Advanced genetic strategies for recombinant protein expression in *Escherichia coli*.' *Journal of Biotechnology*, 115, 113-128.

St-Pierre, B. and Luca, V. D. (2000) 'Chapter 9: Evolution of Acyltransferase Genes: Origin and Diversification of the BAHD Superfamily of Acyltransferases Involved in Secondary Metabolism.' *Recent Advances in Phytochemistry*, 34, 285-315.

Stassi, D. L., Kakavas, S. J., Reynolds, K. A., G.Gunawardana, Swanson, S., Zeidner, D., Jackson, M., Liu, H., Buko, A. and Katz, L. (1998) 'Ethyl-substituted erythromycin derivatives produced by directed metabolic engineering.' *Proceedings of the National Academy of Sciences of the United States of America*, 95, 7305–7309.

Staunton, J. and Weissman, K. J. (2001) 'Polyketide biosynthesis: a millennium review.' *Natural Product Report*, 18, 380-416.

Straight, P. D., Fischbach, M. A., Walsh, C. T., Rudner, D. Z. and Kolter, R. (2007) 'A singular enzymatic megacomplex from *Bacillus subtilis*.' *PNAS*, 104, (1): 305-310.

Sudek, S., Lopanik, N. B., Waggoner, L. E., Hildebrand, M., Anderson, C., Liu, H., Patel, A., Sherman, D. H. and Haygood, M. G. (2007) 'Identification of the Putative Bryostatin Polyketide Synthase Gene Cluster from "*Candidatus* Endobugula sertula", the Uncultivated Microbial Symbiont of the Marine Bryozoan *Bugula neritina*.' *Journal of Natural Products*, 70, (1): 67-74.

Sutherland, R., Boon, R. J., Griffin, K. E., Masters, P. J., Slocombe, B. and White, A. R. (1985) 'Antibacterial Activity of Mupirocin (Pseudomonic Acid), a New Antibiotic for Topical Use.' *Antimicrobial Agents and Chemotherapy*, 27, (4): 495-498.

Swenson, J. M., Wong, B., Simor, A. E., Thomson, R. B., Ferraro, M. J., Hardy, D. J., Hindler, J., Jorgensen, J., Reller, L. B., Traczewski, M., McDougal, L. K. and Patel, J. B. (2010) 'Multicenter Study To Determine Disk Diffusion and Broth Microdilution Criteria for Prediction of High- and Low-Level Mupirocin Resistance in *Staphylococcus aureus*.' *Journal of Clinical Microbiology*, 48, (7): 2469-2475.

Szafranska, A. E., Hitchman, T. S., Cox, R. J., Crosby, J. and Simpson, T. J. (2002) 'Kinetic and Mechanistic Analysis of the Malonyl CoA:ACP Transacylase from *Streptomyces coelicolor* Indicates a Single Catalytically Competent Serine Nucleophile at the Active Site.' *Biochemistry*, 41, (5): 1421-1427.

Takebayashi, Y. (2011) 'Unpublished data.' The University of Birmingham.

Talon, D., Marion, C., Thouverez, M. and Bertrand, X. (2011) 'Mupirocin resistance is not an inevitable consequence of mupirocin use.' *Journal of Hospital Infection*, 79, (4): 366-367.

Tang, G.-L., Cheng, Y.-Q. and Shen, B. (2004b) 'Leinamycin Biosynthesis Revealing Unprecedented Architectural Complexity for a Hybrid Polyketide Synthase and Nonribosomal Peptide Synthetase.' *Chemistry and Biology*, 11, 33-45.

Tang, Y., Chen, A. Y., Kim, C.-Y., Cane, D. E. and Khosla, C. (2007) 'Structural and Mechanistic Analysis of Protein Interactions in Module 3 of the 6-Deoxyerythronolide B Synthase.' *Chemistry and Biology*, 14, 931-943.

Tang, Y., Kim, C.-Y., Mathews, I. I., Cane, D. E. and Khosla, C. (2006) 'The 2.7-Å crystal structure of a 194-kDa homodimeric fragment of the 6-deoxyerythronolide B synthase.' *PNAS*, 103, (30): 11124-11129.

Tang, Y., Lee, T. S., Lee, H. Y. and Khosla, C. (2004a) 'Exploring the biosynthetic potential of bimodular aromatic polyketide synthases.' *Tetrahedron*, 60, 7659–7671.

Tang, Y., Tsai, S.-C. and Khosla, C. (2003) 'Polyketide Chain Length Control by Chain Length Factor.' *Journal of the American Chemical Society*, 125, 12708-12709.

Taubes, G. (2008) 'Collateral Damage: The Rise of Resistant *C. difficile*.' *Science*, 321, 360.

TEVA (2003) 'Press Release - Teva Announces Approval Of Mupirocin Ointment ' http://www.tevapharm.com/pr/2003/pr_421.asp. Accessed: August 9th 2010.

Thomas, C. M. (2012) 'Personal Communications.' The University of Birmingham.

Thomas, C. M., Hothersall, J., Willis, C. L. and Simpson, T. J. (2010) 'Resistance to and synthesis of the antibiotic mupirocin.' *Nature Reviews Microbiology*, 8, 281-289.

Thomas, I., Martin (née Rowe), C. J., Wilkinson, C. J., Staunton, J. and Leadlay, P. F. (2002) 'Skipping in a Hybrid Polyketide Synthase: Evidence for ACP-to-ACP Chain Transfer.' *Chemistry & Biology*, 9, 781-787.

Thomson, K. S. and Moland, E. S. (2000) 'Version 2000: the new B-lactamases of Gram-negative bacteria at the dawn of the new millennium.' *Microbes and Infection*, 2, 1225-1235.

Thornton, M. M., Chung-Esaki, H. M., Irvin, C. B., Bortz, D. M., Solomon, M. J. and Younger, J. G. (2012) 'Multicellularity and Antibiotic Resistance in *Klebsiella pneumoniae* Grown Under Bloodstream-Mimicking Fluid Dynamic Conditions.' *Journal of Infectious Diseases*, 206, (4): 588-595.

Tomaz, A. (1979) 'The Mechanism of the Irreversible Antimicrobial Mechanisms of Penicillins: How the Beta-Lactam Antibiotics Kill and Lyse Bacteria.' *Ann. Rev. Microbiol.*, 33, 113-37.

Torvaldsen, S., Roberts, C. and Riley, T. V. (1999) 'The Continuing Evolution of Methicillin-Resistant *Staphylococcus aureus* in Western Australia.' *Infection Control and Hospital Epidemiology*, 20, (2): 133-135.

Toth, M., Smith, C., Frase, H., Mobashery, S. and Vakulenko, S. (2010) 'An Antibiotic-Resistance Enzyme from a Deep-Sea Bacterium.' *Journal of the American Chemical Society*, 132, (2): 816-823.

Troeschel, S. C., Thies, S., Link, O., Real, C. I., Knops, K., Wilhelm, S., Rosenau, F. and Jaeger, K.-E. (2012) 'Novel broad host range shuttle vectors for expression in *Escherichia coli, Bacillus subtilis* and *Pseudomonas putida*.' *Journal of Biotechnology*, 161, (2): 71-79.

Tsai, F. T. F., Singh, O. M. P., Skarzynski, T., Wonacott, A. J., Weston, S., Tucker, A., Pauptit, R. A., Breeze, A. L., Poyser, J. P., O'Brien, R., Ladbury, J. E. and Wigley, D. B. (1997) 'The High-Resolution Crystal Structure of a 24-kDa Gyrase B Fragment From *E. coli* Complexed With One of the Most Potent Coumarin Inhibitors, Clorobiocin.' *PROTEINS: Structure, Function, and Genetics*, 28, 41-52.

Udo, E. E., Farook, V. S., Mokadas, E. M., Jacob, L. E. and Sanyal, S. C. (1999) 'Molecular Fingerprinting of Mupirocin-Resistant Methicillin-Resistant *Staphylococcus aureus* from a Burn Unit.' *International Journal of Infectious Diseases*, 3, (2): 82-87.

Udo, E. E. and Sarkhoo, E. (2010) 'Genetic analysis of high-level mupirocin resistance in the ST80 clone of community-associated meticillin-resistant *Staphylococcus aureus*.' *Journal of Medical Microbiologu*, 59, 193-199.

Udwadia, Z. F. (2012) 'MDR, XDR, TDR tuberculosis: ominous progression.' *Thorax*, 67, (4): 286-288.

Udwadia, Z. F., Amale, R. A., Ajbani, K. K. and Rodrigues, C. (2012) 'Totally Drug-Resistant Tuberculosis in India.' *CID*, 54, 579-581.

Upton, A., Lang, S. and Heffernan, H. (2003) 'Mupirocin and *Staphylococcus aureus*: a recent paradigm of emerging antibiotic resistance.' *Journal of Antimicrobial Chemotherapy*, 51, 613-617.

van Epps, H. L. (2006) 'René Dubos: unearthing antibiotics.' *The Journal of Experimental Medicine*, 203, (2): 259.

van Rijen, M. M. L., Van Keulen, P. H. and Kluytmans, J. A. (2008) 'Increase in a Dutch Hospital of Methicillin-Resistant *Staphylococcus* aureus Related to Animal Farming.' *Clinical Infectious Diseases*, 46, (2): 261-263.

van Trijp, M. J. C. A., D. C. Melles., W. D. H. Hendriks, G. A. Parlevliet, M. Gommans and A. Ott (2007) 'Successful Control of Widespread Methicillin-Resistant *Staphylococcus aureus* Colonization and Infection in a Large Teaching Hospital in The Netherlands.' *Infection Control and Hospital Epidemiology*, 28, (8): 970-975.

Vasquez, J. E., Walker, E. S., Franzus, B. W., Overbay, B. K., Reagan, D. R. and Sarubbi, F. A. (2000) 'The Epidemiology of Mupirocin Resistance Among Methicillin-Resistant *Staphylococcus aureus* at a Veterans Affairs Hospital.' *Infection Control and Hospital Epidemiology*, 21, (7): 459-464.

Velayati, A. A., Masjedi, M. R., Farnia, P., Tabarsi, P., Ghanavi, J., ZiaZarifi, A. H. and Hoffner, S. E. (2009) 'Emergence of New Forms of Totally Drug-Resistant Tuberculosis BacilliSuper Extensively Drug-Resistant Tuberculosis or Totally Drug-Resistant Strains in Iran.' *CHEST Journal*, 136, (2): 420-425.

Vernet, E., Kotzsch, A., Voldborg, B. and Sundström, M. (2011) 'Screening of genetic parameters for soluble protein expression in *Escherichia coli*.' *Protein Expression and Purification*, 77, 104-111.

Wagner, S., Klepsch, M. M., Schlegel, S., Appel, A., Draheim, R., Tarry, M., Hogbom, M., Wijk, K. J. v., Slotboom, D. J., Persson, J. O. and Gier, J.-W. d. (2008) 'Tuning *Escherichia coli* for membrane protein over expression.' *PNAS*, 105, (38): 14371-14376.

Walsh, C. (2003a) 'Antibiotics. Actions, Origins, Resistance.' Washington, D.C., ASM Press.

Walsh, C. (2003b) 'Where will new antibiotics come from?' *Nature Reviews Microbiology*, 1, 65-70.

Walsh, C. T., Fisher, S. L., Park, I.-S., Prahalad, M. and Wu, Z. (1996) 'Bacterial resistance to vancomycin: five genes and one missing hydrogen bond tell the story.' *Chemistry and Biology*, 3, 21-28.

Wang, J., Soisson, S. M., Young, K., Shoop, W., Kodali, S., Galgoci, A., Painter, R., Parthasarathy, G., Tang, Y. S., Cummings, R., Ha, S., Dorso, K., Motyl, M., Jayasuriya, H., Ondeyka, J., Herath, K., Zhang, C., Hernandez, L., Allocco, J., Basilio, A., Tormo, J. R., Genilloud, O., Vicente, F., Pelaez, F., Colwell, L., Lee, S. H., Michael, B., Felcetto, T., Gill., C., Silver, L. L., Hermes, J. D., Bartizal, K., Barrett, J., Schmatz, D., Becker, J. W., Cully, D. and Singh, S. B. (2006) 'Platensimycin is a selective FabF inhibitor with potent antibiotic properties.' *Nature*, 44, 358-361.

Watson, A. A., Alm, R. A. and Mattick, J. S. (1996) 'Construction of improved vectors for protein production in *Pseudomonas aeruginosa*.' *Gene*, 172, (1): 163-164.

Weber, T., Laiple, K. J., Pross, E. K., Textor, A., Grond, S., Welzel, K., Pelzer, S., Vente, A. and Wohlleben, W. (2008) 'Molecular Analysis of the Kirromycin Biosynthetic Gene Cluster Revealed b-Alanine as Precursor of the Pyridone Moiety.' *Chemistry and Biology*, 15, 175-188.

Wenzel, S. C., Kunze, B., Höfle, G., Silakowski, B., Scharfe, M., Blöcker, H. and Müller, R. (2005) 'Structure and Biosynthesis of Myxochromides S_{1-3} in Stigmatella aurantiaca: Evidence for an Iterative Bacterial Type I Polyketide Synthase and for Module Skipping in Nonribosomal Peptide Biosynthesis.' *ChemBioChem*, 6, 375-385.

Wertheim, H. F. L., Vos, M. C., Boelens, H. A. M., Voss, A., Vandenbroucke-Grauls, C. M. J. E., Meester, M. H. M., Kluytmans, J. A. J. W., van Keulen, P. H. J. and Verbrugh, H. A. (2004) 'Low prevalence of methicillin-resistant *Staphylococcus aureus* (MRSA) at hospital admission in the Netherlands: the value of search and destroy and restrictive antibiotic use.' *Journal of Hospital Infection*, 56, (4): 321-325.

Wesener, S. R., Potharla, V. Y. and Cheng, Y.-Q. (2011) 'Reconstitution of the FK228 Biosynthetic Pathway Reveals Cross Talk between Modular Polyketide Synthases and Fatty Acid Synthase.' *APPLIED AND ENVIRONMENTAL MICROBIOLOGY*, 77, (4): 1501-1507.

Whatling, C., Hodgson, J. E., Burnham, M. K. R., Clarke, N. J., Franklin, C. H. and Thomas, C. M. (1995) 'Identification of a 60kb region of the chromosome of *Pseudomonas fluorescens* NCIB 10586 required for the biosynthesis of pseudomonic acid (mupirocin).' *Microbiology*, 141, 973-982.

Whitmore, L. and Wallace, B. A. (2004) 'DICHROWEB, an online server for protein secondary structure analyses from circular dichroism spectroscopic data.' *Nucleic Acids Research*, 32, (Web Server): W668-W673.

Whitmore, L. and Wallace, B. A. (2008) 'Protein Secondary Structure Analyses from Circular Dichroism Spectroscopy: Methods and Reference Databases.' *Biopolymers*, 89, (5): 392-400.

Wilkinson, B., Foster, G., Rudd, B. A. M., Taylor, N. L., Blackaby, A. P., Sidebottom, P. J., Cooper, D. J., Dawson, M. J., Buss, A. D., Gaisser, S., Böhm, I. U., Rowe, C. J., Cortés, J., Leadlay, P. F. and Staunton, J. (2000) 'Novel octaketide macrolides related to 6-deoxyerythronolide B provide evidence for iterative operation of the erythromycin polyketide synthase.' *Chemistry & Biology*, 7 (2): 111-117.

Wine, Y., Cohen-Hadar, N., Freeman, A. and Frolow, F. (2007) 'Elucidation of the mechanism and end products of glutaraldehyde crosslinking reaction by X-ray structure analysis.' *Biotechnology and Bioengineering*, 98, (3): 711-718.

Wong, F. T., Chen, A. Y., Cane, D. E. and Khosla, C. (2010) 'Protein-Protein Recognition Between Acyltransferases and Acyl Carrier Proteins in Multimodular Polyketide Synthases.' *Biochemistry*, 49, 95-102.

Wong, F. T., Jin, X., Mathews, I. I., Cane, D. E. and Khosla, C. (2011) 'Structure and Mechanism of the trans-Acting Acyltransferase from the Disorazole Synthase.' *Biochemistry*, 50, 6539-6548.

Wright, G. D. (2010) 'Q&A: Antibiotic resistance: where does it come from and what can we do about it?' *BMC Biology*, 8, 123-128.

Wu, J., Cooper, S. M., Cox, R. J., Crosby, J., Crump, M. P., Hothersall, J., Simpson, T. J., Thomas, C. M. and Willis, C. L. (2007) 'Mupirocin H, a novel metabolite resulting from mutation of the HMG-CoA synthase analogue, *mupH* in *Pseudomonas fluorescens*.' *Chemical Communications*, 2040–2042.

Wu, J., Hothersall, J., Mazzetti, C., O'Connell, Y., Shields, J. A., Rahman, A. S., Cox, R. J., Crosby, J., Simpson, T. J., Thomas, C. M. and Willis, C. L. (2008) '*In vivo* Mutational Analysis of the Mupirocin Gene Cluster Reveals Labile Points in the Biosynthetic Pathway: the "Leaky Hosepipe" Mechanism.' *Chembiochem*, 9, 1500-1508.

Wuite, J., Davies, B. I., Go, M., Lambers, J., Jackson, D. and Mellows, G. (1983) 'Pseudomonic Acid: A New Topical Antimicrobial Agent.' *The Lancet*, 322, (8346): 394.

Xue, Y., Zhao, L., Liu, H.-W. and Sherman, D. H. (1998) 'A gene cluster for macrolide antibiotic biosynthesis in *Streptomyces venezuelae*: Architecture of metabolic diversity.' *Proceedings of the National Academy of Sciences of the United States of America*, 95, 12111-12116.

Yadav, G., Gokhale, R. S. and Mohanty, D. (2003) 'Computational Approach for Prediction of Domain Organisation and Substrate Specificity of Modular Polyketide Synthases.' *Journal of Molecular Biology*, 328, 335-363.

Yanagisawa, T. and Kawakami, M. (2003) 'How Does *Pseudomonas fluorescens* Avoid Suicide from Its Antibiotic Pseudomonic Acid?' *The Journal of Biological Chemistry*, 278, (28): 25887-25894.

Yanagisawa, T., Lee, J. T., Wu, H. C. and Kawakami, M. (1994) 'Relationship of Protein Structure of Isoleucyl-tRNA Synthetase with Pseudomonic Acid Resistance of *Escherichia coli*.' *The Journal of Biological Chemistry*, 269, (39): 24304-24309.

Yong, D., Toleman, M. A., Giske, C. G., Cho, H. S., Sundman, K., Lee, K. and Walsh, T. R. (2009) 'Characterization of a New Metallo-β-Lactamase Gene, bla_{NDM-1}, and a Novel Erythromycin Esterase Gene Carried on a Unique Genetic Structure in *Klebsiella pneumoniae* Sequence Type 14 from India.' *Antimicrobial Agents and Chemotherapy*, 53, (12): 5046–5054.

Yoshida, H., Bogaki, M., Nakamura, M. and Nakamura, S. (1990) 'Quinolone Resistance-Determining Region in the DNA Gyrase gyrA Gene of *Escherichia coli*.' *Antimicrobial Agents and Chemotherapy*, 34, (6): 1271-1272.

Zhao, C., Coughlin, J. M., Ju, J., Zhu, D., Wendt-Pienkowski, E., Zhou, X., Wang, Z., Shen, B. and Deng, Z. (2010) 'Oxazolomycin Biosynthesis in *Streptomyces albus* JA3453 Featuring an "Acyltransferase-less" Type I Polyketide Synthase That Incorporates Two Distinct Extender Units.' *The Journal of Biological Chemistry*, 285, (26): 20097–20108.

Xue, Y. And Sherman, D. H. (2000) 'Alternative modular polyketide synthase expression controls macrolactone structure.' *Nature*, 403, 571-575.